Finite element analyses for structures subjected to time-varying and non-uniform temperatures for linear and non-linear creep

Cheng, Yuk Fai

FINITE ELEMENT ANALYSES FOR STRUCTURES SUBJECTED TO TIME-VARYING AND NON-UNIFORM TEMPERATURES FOR LINEAR AND NON-LINEAR CREEP

By

Yuk Fai CHENG, B.Sc (Eng.)

King's College London

Submitted to the University of London
for
the Degree of Doctor of Philosophy.

1990

ABSTRACT

This thesis is related to the study of stress redistributions brought about by differential thermal creep in non-uniformly heated concrete and non-concrete structures subjected to either raised sustained or to cylically varying temperatures using finite element methods. Constitutive laws are formulated as differential equations utilising the 'pseudo-time' concept. The emphasis is on an engineering theory of creep for heated structures with a strong reliance on experimental data.

The complementary power theory presented permits stresses to be evaluated in both the transient creep phase and in the limiting steady-state condition from a power minimisation procedure in conjuction with a Ritz process. The nature of the Ritz expression and its automatic generation is explored in detail. The procedure is extended to general two and three dimensional continua utilising iso-parametric finite elements. Cost and efficiency comparisons are made between a conventional two and three dimensional step-by-step algorithm using constant strain finite elements. It is concluded that this procedure is superior to the time-step algorithm as it may be used at the early design stage in a crude form, at low cost; and then in a refined form, which is still more economical than the time-step algorithm, for the final evaluation of a firm design.

Extension of the power minimisation procedure to include delayed elastic strain, namely the analogous Burgers model which is able to describe the concrete material behaviour more closely, is investigated. A second order matrix differential equation is obtained and methods of solving it are discussed. It is found that no new Ritz expression is necessary to approximate the time-dependent stress distributions throughout the structural continuum.

A flexibility method of creep analysis for steady-state stresses in continuous prestressed concrete beam structures subjected to cyclically varying temperatures is presented. Several conclusions are drawn and some modifications of the current Code of Practice are recommended.

Attention is turned to the analysis of structures which exhibit non-linear creep behaviour using a step-by-step method. A multi-axial creep law is derived from an analogous flow rule approach and criteria for pseudo-time step size are deduced.

Finally, computer programs resulting from the present study are documented as internal reports and are available for the engineering community to use. Some publications which have been prepared during the course of this work are also listed in the appendix.

CONTENTS

ACKNOWLEDGMENT

The author gratefully acknowledges the encouragement and most valuable advice given by Professor G.L. England who has supervised this research.

The financial support of the Nuclear Installation Inspectorate for this research project is also gratefully acknowledged.

Computer calculations were carried out on VAX 11/780, CDC 7600, CRAY 1 and IBM mainframe computers.

To Wai Ying

NOMENCLATURE

[ ]	Matrix.
{ }	Vector.
| |	Determinant of a matrix.
A	Strain or strain rate.
B	Curvature or curvature rate.
D	Elastic modulus or analogous elastic modulus.
E_R	Elastic moduli ratio.
E_m	Elastic modulus or Maxwell's spring constant.
E_k	Kelvin's spring constant.
E_{eff}	Effective modulus.
EXP	Exponential function.
H_i, H_j, H_m	Gauss quadrature weighting factors.
I_2	Second invariant of the strain tensor.
J_2	Second invariant of the stress tensor.
K_c	Constant relating real and pseudo-time.
M	Beam bending moment.
M_o	Beam bending moment caused by applied loading.
N	Beam axial force.
N_i	Ith shape function.
P_e	Applied external load.
R_s	Support reactions.
S_{ij}	Stress deviator tensor.
T	Temperature.
T_i	Temperature at phase i of a temperature cycle.
T_a	weighted average temperature over a temperature cylce.
T_d	Datum temperature.
$\dot{U}_e$	Displacement rate of applied load.
$\dot{U}_s$	Displacement rate of support reactions.
V^e	Elemental volume.
a_i	Time-dependent weighting coefficients.
a'_i	Shape function interpolation coefficents.
b'_i	Shape function interpolation coefficents.
c	Pseudo-time.
c_i	Ith phase length of a temperature cylce in pseudo-time.
c'_i	Shape function interpolation coefficents.
d'_i	Shape function interpolation coefficents.

k	Ratio of phase lengths in pseudo-time.
k_t	Ratio of phase lengths in real-time.
r,z	Cylindrical coordinate system.
r',z'	Centroidal coordinate of a axi-symmetric ring element.
r_a	Arithematic progression ratio.
r_b	Geometric progression ratio.
t	Real time.
t'	Thickness.
t_i	Ith phase length of a temperature cylce in real time.
u',v',w'	Nodal displacements in x,y,z directions.
v	Elastic Poisson's ratio.
v_c	Creep Poisson's ratio.
x,y,z	Cartesian Coordinate system.
x_i,y_i,z_i	x,y,z coordinates of the ith node.
$\{F\}$	Global force vector
$\{F^e\}$	Elemental nodal force vector.
$\{F^e_{\varepsilon o}\}$	Elemental force vector associated with initial strain.
$\{F^e_{\sigma o}\}$	Elemental force vector associated with initial stress.
$\{F^e_p\}$	Elemental force vector associated with body force.
$\{F^e_q\}$	Elemental force vector associated with surface traction.
$\{F^e\}_i$	Force vector associated with free strain at ith step.
$\{X\}$	Vector of redundancies.
$\{Z\}$	Force vector.
$\{a\}$	Vector of time-dependent weighting coefficients.
$\{a'\}$	Displacement vector.
$\{a^e\}$	Nodal displacement vector.
$\{m\}$	Vector of unit moments.
$\{p\}$	Vector of body force per unit volume.
$\{q\}$	Vector of applied surface traction.
$[B]$	Strain matrix.
$[C]$	Beam flexibility matrix.
$[D]$	Elasticity matrix.
$[I]$	Identity matrix.
$[J]$	Jacobian matrix.
$[K]$	Global stiffness matrix.
$[K^e]$	Element stiffness matrix.
$[L]$	Lower triangular of a matrix.
$[N]$	Shape function matrix.
$[P],[Q],\{s\}$	Coefficients of Maxwellian creep differential equation.
$[P_b],[Q_b]$	Coefficients of Burgers creep differential equation.

$[R_b], \{s_b\}$	Coefficients of Burgers creep differential equation.
$[U]$	Upper triangular of a matrix.
$[V]$	Matrix of elastic Poisson's ratio.
$[V_c]$	Matrix of creep Poisson's ratio.
∇, ∇^2	Pseudo-time differential operator.
$\Phi(T)$	Maxwell temperature normalisation function.
$\Phi_b(T)$	Burgers temperature normalisation function.
Λ	Area of an triangular element.
$\int$	Integration.
Ω	Global energy functional.
Ω^e	Elemental energy functional.
∂	Partial differentiation operator.
Σ	Summation.
ΔT	Temperature difference.
Δc	Pseudo-time increments.
$\Delta\Delta c$	First pseudo-time step size.
∞	Infinity.
α	Coefficients of thermal expansion.
$\phi_{k,ij}$	Basis function.
ε	Strain rate.
ε_e	Uniaxial strain.
ε_o	Initial strain.
$\dot{\varepsilon}_o$	Initial strain rate.
$\dot{\varepsilon}_a$	Average strain rate.
ε_c	Creep strain.
ε_r	Recoverable strain.
$\dot{\varepsilon}_{ss}$	Steady-state strain rate.
$\dot{\varepsilon}_i$	Strain rate at phase i.
ε_{ij}	Strain tensor.
$\dot{\varepsilon}_{ij}$	Strain rate tensor.
$\{\dot{\varepsilon}\}$	Strain rate vector.
$\{\varepsilon_o\}$	Initial strain vector.
$\{\varepsilon_f\}$	Free strain vector.
$\{\varepsilon\}_i$	Strain vector at increment i.
λ	Factor of proportionality.
η_k	Kelvin's dashpot constant.
κ	Roots of an auxilliary equation.
ω, μ	Creep power index.
γ	A constant.

σ	Stress.
$\dot{\sigma}$	Stress rate.
σ'_e	Elastic stress.
σ_e	Uniaxial stress.
σ_{eff}	Effective stress.
σ_i	Stress at phase i of a temperature cycle.
σ_T	Thermal stress.
σ_{Ti}	Thermal stress at phase i of a temperature cycle.
σ_{eTi}	Thermo-elastic stress at phase i of a temperature cycle.
σ_r	Reference stress.
σ_{ss}	Steady-state stress.
σ_{ssc}	Cyclic-steady-state stress.
σ_o	Thermo-elastic stress.
σ_{Tf}	Fictitious thermal stress.
σ_{ij}	Stress tensor.
σ_{kk}	Direct stress tensor.
$\{\sigma_o\}$	Stress vector in equilibrium with boundary load.
$\{\sigma_i\}$	Self-equilibrating stress vector.
$\{\sigma\}_i$	Stress vector of the ith time-step.
$\{\dot{\sigma}\}$	Stress rate vector.
$[\sigma]$	Self-equilibrating stress matrix.
ξ,η,ζ	Local curvilinear coordinate.
δ	Variation Operator.
δ_{ij}	Kronecker delta.
$\{\delta\}$	Global displacement vector.
π	Pi.
τ_{xy}	Shear stress.
γ_{xy}	Shear strain.

Note: A Glossary is given in Appendix D.

CHAPTER ONE

INTRODUCTION

1.1 General

Where a structure is designed for service at temperatures where creep effects are negligible, a rigorous assessment can be made of the factors which affect integrity, safety and satisfactory performance. Many of the more advanced design codes, such as BS 5400, BS 5500 and section III of the ASME pressure vessel and boiler code, provide a sound basis for doing this. The necessary stress analysis methods are available, and the basic properties of the commonly used materials are well established, under both static and dynamic loading. When we come to structures operating at time-varying and non-uniform temperatures (Burrow 1978 and Derrington 1978), this is no longer true.

Until recently very little has been known about the factors which affect the time-varying and non-uniform temperature performance of concrete structures of complex shape. Design has largely been dictated by experience and by the knowledge that certain components gave satisfactory service. Such experience cannot, by its nature, be extrapolated with certainty to structures of different shape, or of different size, or in a different material, or subjected to a different operating regime. Any significant advance in design requirement is therefore accompanied by the risk of either poor structural or uneconomic design or both. The assurances of structural integrity and serviceability are not forthcoming.

Fortunately, there has been growing interest, at a research level, during the past decades, into the understanding of structural concrete performance under multi-axial stress states (Jordan 1969) and non-isothermal conditions (Sanders 1973). Furthermore, the powerful mathematical modelling techniques, notably the finite element method, together with those modern super-computers, such as Cray XMP and Cyber 205, have provided the engineer with computing power undreamt of by its predecessors. Engineer is now able to extract precise information on the stress and strain history in a structure and thus provided a rational basis for design.

1.2 Status of Finite Element Analysis

The finite element method of structural analysis has become well established for the solution of both static and dynamic linear elastic problems. Solutions can be obtained accurately and inexpensively even for relatively complex three dimensional geometry and loading conditions.

The solution of time-dependent structural response under cyclic thermal and mechanical loading conditions where creep must be taken into account is less well established. Previous use of the finite element technique for solving plane stress creep problems was presented by Padlog, Hull and Holloway (1960) and has been summarised by Gallagher et al (1962). The inclusion of creep behaviour in a finite element approach is handled by using an incremental algorithm and treating the creep strains as initial strains. Mendelson (1959) used this method in the solution of rotating disks and included an iteration method to improved the solution for each time increment. Zienkiewicz et al (1968), Greenbaum (1968), Rashid (1970) and Haisler et al (1979) adopted similar incremental algorithm for different types of problems.

Many general purpose finite element systems that are in use and have the capability of performing creep analysis have been summarised by Nickell (1974), Dhalla and Gallagher (1980) and Yamada and Nagato (1979). Some of those widely used today are shown in Table 1.2.2.

As far as creep is concerned, all but ADINA use the initial strain approach. All of these programs have means of setting the convergence of the creep analysis except WECAN. Obviously these programs have extensive capabilities in the analysis of different types of problems that might arise in creep analysis of solids and structures. The main difficulty with the general purpose finite element programs is that they are too expensive to use for creep analysis. Published works (Dhalla 1975 and Barsoum 1976) indicated that the human resources and level of engineering expertise required to perform such an analysis would virtually prohibit the use of three dimensional continuum modelling for routine design calculations.

The engineer thus faces a dilemma. On the one hand he is required to produce economic designs, on the other hand he must satisfy himself that structural integrity and safety are not impaired. Is is possible to strike a compromise between cost and precision of solutions? The answer is affirmative. Direct solutions are scarce but do exist for some classes of problem. The work reported here is aimed at the development of cost-effective and sufficiently accurate predictive methods of analysis using finite element techniques.

1.3 Brief Description of Work

The theory of creep is a section of the mechanics of deformable solids which has been developed in recent years and takes its place alongside the theories of elasticity and plasticity. Creep theory is concerned with a much more complicated set of phenomena than elasticity or even plasticity and has not reached the same level of logical perfection as have the theories of elasticity or of ideal plasticity. The field of study is diverse and complex. There is not as yet a unified theory of creep that is applicable to all materials and the author considers that such a theory is inherently impossible.

The study involved here is concerned with the distribution of stresses caused by the combined effects of creep and time-varying non-uniform temperatures in concrete structures. Strains are discussed in terms of elastic, recoverable creep and flow components. The structures considered are subjected to either raised non-uniform sustained temperatures or to non-uniform temperatures which may vary periodically and in a step-wise manner in time between defineable limits. It is assumed for this latter type that temperature transients are of short duration compared to the 'hold' periods at steady-state temperatures between successive changes. Theories developed and analyses presented here are mainly concerned with concrete structures.

However, the theory is quite general and may be applied to creep analysis of non-concrete structures provided they exhibit similar creep-temperature behaviours.

Assumptions regarding the effect of temperature on material behaviour are deduced and their validity discussed in Chapter 2. The concept of 'pseudo-time' is introduced and used in the theoretical analyses which

follow. A non-homogeneous steady-state creep-temperature theory is presented and different methods of structural analysis are reviewed.

Chapter 3 describes the theoretical development and computer implementation of a flexibility method of creep analysis for steady-state stresses in continuous prestressed concrete beam structures subjected to cyclically varying temperatures. A Fortran program 'FCREEP' is developed and applied to a two span continuous beam with realistic temperature data. Several conclusions are drawn and some modifications of the current Code of Practice BS 5400 are recommended.

In Chapter 4, a finite element step-by-step linear creep algorithm is developed. A computer code 'SSCREEP' is written and applied to some benchmark problems to enable an engineering and economic evaluation of the algorithm to be made.

The historical time-step algorithm described in Chapter 4 and the other incremental formulations used in the software industry are capable of predicting the variation of stresses and strains, but require many time steps if accuracy of solution is to be maintained throughout the life-span of the structure. In consequence, this type of procedure is often expensive to used. Chapter 5 describes a direct finite element solution algorithm, namely a Power Minimisation Procedure. Utilising this procedure and adopting an analogous Maxwell model representation, a 'VPCREEP' program is written and applied to various problems. It is demonstrated that the procedure is more economic than the time-step techniques.

Extension of the Power Minimisation Procedure to include delayed elastic strain, namely the analogous Burgers model representation, is investigated in Chapter 6. A second order matrix differential equation is obtained and the methods of solving it are discussed. Comparison between solutions of the Burgers model and for the Maxwell model are made and some conclusions are reached.

In Chapter 7, extension of the step-by-step algorithm to include the non-linear, μ-th power, creep law is studied. A multi- axial creep law is derived from an analogous flow rule approach and criteria for pseudo-time step size are deduced.

Chapter 8 concludes the present study and some suggestions for future research are made.

Program	Originator
ADINA	K.J. Bathe, MIT, U.S.A.
ANSYS	Swanson Analysis Systems, Inc., U.S.A.
MARC	MARC Analysis Research Corp., U.S.A.
NEPSAP	D.N. Yates, Lockheed Miss. and Space Co., U.S.A.
NASTRAN	National Aeronautics and Space administration, U.S.A.
WECAN	Anon., Westinghouse Research and Development Centre, U.S.A.
ASAS	R.K. Henrywood, Atkins Research and Development, U.K.
BERSAFE	T.K. Hellen, CEGB, U.K.
FESS	O.C. Zienkiewicz, University of Wales, Swansea, U.K.
PAFEC	R.D. Henshell, University of Nottingham, U.K.
ASKA	J.H. Argyris, Institut fur Statik und Dynamik der Luft-und-Raumfahrtkonstruktionen, Germany.
ASTUC	Y. Yokouchi et al, University of Electro-Communications, Japan.
MINAT-X	K. Nagato and A. Minato, Kawasaki Heavy Industries, Japan.
PCRAP	T. Mori and T. Murakami, Toshiba Corp., Japan.
SATEPIC	M. Ueda and M. Tanikawa, Hitachi Shipbuilding and Engineering Co., Japan.

Table 1.2.1 : List of major finite element systems that have the capability of performing creep analysis.

Capability	Program				
	ADINA	ANSYS	MARC	NEPSAP	WECAN
Type of Analysis:					
Small deformation (inelastic)	x	x	x	x	x
Creep buckling	x	x	x	x	0
Large strain	x	0	0	x	0
Heat transfer	x	x	x	0	x
Creep Equations:					
Equation of state (strain hardening)	x	x	x	x	x
Auxiliary rules for stress reversal	x	x	x	0	x
User supplied creep equations	0	0	x	0	x
Temperature dependent properties	x	x	x	x	x
Orthotropic properties	x	x	x	x	x

Table 1.2.2: Comparison of programs with creep analysis capability.

x - indicates that the program has a given capability.
0 - indicates that it does not.

CHAPTER TWO

THE NON-HOMOGENEOUS CREEP THEORY: ASSUMPTIONS AND VALIDITY

Summary

The effects of temperature and stress on creep are reviewed. Constitutive equations for certain classes of material in which creep-temperature plays an essential role are formulated as differential equations utilizing the pseudo-time concept. The emphasis is on an engineering theory of creep for heated concrete structures with a strong reliance on experimental data. Extension to non-concrete materials in which non-linear behaviour predominates is also discussed.

2.1 Preliminary

Creep effects under variable stress and varying temperature are observed in most materials. There is a vast body of literature describing experimental and analytical work regarding creep in heated concrete structures (Ross 1958, Hannah 1961, Arutyunyan 1966, Clarke 1978, England et al 1962-83 and Wittmann 1982), in metals (Sully 1949, Hoff 1954, Finnie 1959, Hult 1966, Boley et al 1967, Boley 1968, Robotnov 1969, Kovalenko 1969, Smith et al 1971, Penny 1971, Johnson 1973, Odquist 1974, Gittus 1975, Kraus 1981 and Boyle et al 1983). The field of study is diverse and complex and it is in a stage of rapid development with considerable uncertainty concerning the physical characteristics which need to be incorporated and the corresponding mathematical formulations of the constitutive relations. This uncertainty far transcends that in the analysis of non-linear visco-elasticity which still presents many open questions concerning adequate formulation of constitutive relations in order to predict material response to general loading histories.

In view of the breadth and the unsettled nature of the subject, the author considers that it is impractical to make a completely general study of it and thus require concentration on a particular area. In this thesis particular attention is devoted to the creep of heated

concrete structures with which the author happens to be familiar. The principles described are however fairly general and maybe applied to creep analysis of non-concrete structures provided they satisfy the criteria described herein.

2.2 The Effects of Temperature and Stress on Creep

It is generally agreed that as the temperature is raised for a given stress, or stress is increased at a given temperature, the creep rate increases. While creep in concrete structures is directly proportional to the applied stress provided it does not exceed 50% of the ultimate strength (Lorman 1940, Ross 1958 and Fluck 1958), creep in metallic structures is predominately non-linear (Andrade 1910, McVetty 1943, Griffiths 1948, Rabotnov 1969 and Odquist 1974).

The relationship between creep of concrete and temperature was investigated by Hannant (1968), Illston et al (1973), England et al (1962-83), Vyas et al (1979), Nasser et al (1967), Hansen (1960) and Browne (1968) in the temperature range from $0^{o}C$ to $140^{o}C$ for sealed, semi-sealed or unsealed concrete. They all agreed that creep is approximately directly proportional to the temperature for the temperature range $20^{o}C$ to $80^{o}C$.

To provide a detailed description of the influence of temperature on creep of metal, it would be necessary to study the temperature dependence of all the parameters in any creep equations that satisfactorily describe the shape of the creep curve. Unfortunately, there are too many creep equations and the test results are too scattered. However Dorn (1955) observed that creep curves obtained at different temperatures for a given stress approximate to geometric similarities of each other.

Little is known about the creep of concrete when it reaches a new temperature level for the first time. Arthanari and Yu (1967) observed an increase in the creep rate when a new level of temperature was attained. This phenomenon was also reported by Hansen and Erikson (1966). Sanders (1973) concluded that this was a transitional phenomenon which was completed within 5 days after the change in temperature.

The influence of sudden temperature change on creep metallic structures was investigated by Nishihara (1958), Ivanova (1958) and Taira et al (1960). They found that if the temperature was raised rapidly during a creep test at first, the deformation increased more rapidly than was to be expected. On the other hand, if the temperature was lowered, creep was temporarily delayed. During cyclic temperature variations these two effects compensated for each other and overall the influence was likely to be small.

Various investigators (Sanders 1973, Freudental 1958, Arthanari 1966 and Jordan et al 1977) agreed that concrete creep recovery is proportional to stress, independent of temperature and tends to a limiting value which does not vary with age of concrete at which the change of load takes place and is related to the current rate of flow. Temperature has no effect on the rate of creep recovery.

2.3 Variation of Elastic Modulus and Creep Poisson's Ratio

Most researchers agreed that the creep Poisson's ratio of concrete should be taken as the same as the elastic Poisson's ratio (England et al 1962-83, Hannant 1968 and Jordan et al 1969).

Many investigateors observed that the elastic modulus of concrete increases with age (Roll 1964, Ross et al 1965 and Hannant 1967). At high temperature this increase could partially compensate an initial fall in the value due to heating. They also reported that a temperature increase leads to a reduction in the elastic modulus (England 1961 and Theuer 1937). Richmond et al (1977) suggested the following relation holds:

$$E_R = 1.05 - \frac{T}{400} \qquad (2.3.1)$$

where E_R is the ratio between the elastic modulus at T^oC to that at 20^oC.

2.4 The Pseudo-time Concept

The time-dependent creep strain ε_c is a function of stress σ and

temperature, for any practical analysis this relationship must be known. Figure 2.4.1 shows how creep data from experiments at constant stress and temperature maybe manipulated into a conventional form for use in analysis (Ross 1958 and England 1966). A single curve maybe readily obtained by normalising with respect to stress raised to some power 'ω' as shown in Figure 2.4.1 (a). A further and similar normalisation is possible with respect to temperature for a suitable function $\Phi(T)$ as shown in Figure 2.4.1(b). This is possible because the creep curves obtained at different stresses and temperatures approximate to geometric similarities of each other (vide section 2.2). By combining these two a single curve of normalised specific creep maybe obtained as shown in Figure 2.4.1(c) viz.

$$c = \frac{\varepsilon_c}{\sigma^{\omega}\Phi(T)} \qquad (2.4.1)$$

This quantity 'c' may then be used as a pseudo-time parameter in creep analysis and the curve shown in Figure 2.4.1(c) used to give real time when required. The units of 'c' being strain per unit stress (raised to the power 'ω') per degree centigrade. The form of $\Phi(T)$ and the values of 'ω' are properties of a material. Existing creep data indicates that the temperature function maybe represented adequately by a simple polynomial expression of the form:

$$\Phi(T) = b'_0 + b'_1 T + b'_2 T^2 + b'_3 T^3 + ... \qquad (2.4.2)$$

Creep in concrete is linear in the working range, with $\omega=1$, and for normal temperature (vide section 2.2), the temperature function maybe taken as:

$$\Phi(T) = T + b'_0 \qquad (2.4.3)$$

where b'_0, b'_1 ... are constants.

The creep normalisation process is modified slightly when the elastic strain, or recoverable creep strain ε_r is to be featured in the analysis. As far as concrete is concerned, experiments revealed that this recoverable strain to be stress dependent but essentially temperature independent (vide section 2.2). It is therefore necessary

to deduct the recoverable strain portion from the total time-dependent strains before normalising with respect to temperature. When this is done, a different temperature function results, $\Phi_b(T)$, Figure 2.4.2 and the resulting normalised creep curve of c against real time t is obtained, Figure 2.3.2(c), and c is then defined, for that particular model, as:

$$c = \frac{\varepsilon_c - \varepsilon_r}{\sigma^{\omega}\Phi_b(T)} \qquad (2.4.4)$$

The application of pseudo-time has the advantage that calculations maybe carried out entirely in the pseudo-time domain without the need to have knowledge of overall creep capacity and with greater ease than when the explicit relationship between real time t and pseudo-time c is incorporated in the analysis.

The relationship between real time t and pseudo-time c is of the form:

$$c = K_c \log_{10}(1+t) \qquad (2.4.5)$$

where K_c is a constant. For a high grade concrete, such as would be used in a prestressed concrete reactor pressure vessel (Hannant 1968), a creep capacity of about 2×10^{-6} per N/mm^2 per ^oC is anticipated. For a low grade structural concrete, a high creep capacity of about 20×10^{-6} per N/mm^2 per ^oC is suggested. This is similar to that in the CEB code (1970).

The nature of temperature cycling investigated is of the constant phase type with step changes due to sudden changes in temperature, Figure 2.4.3. If k is the ratio between lengths of second and first parts of a cycle in pseudo-time, i.e.:

$$k = c_2/c_1 \qquad (2.4.4)$$

and k_t is the ratio in real time, i.e.:

$$k_t = t_2/t_1 \qquad (2.4.5)$$

It can be shown that:

$$\frac{k}{k_t} = \frac{t_1 \log_{10} D_1}{t_2 \log_{10} D_2} \qquad (2.4.6)$$

where $D_1 = (1 + t_1 + t_2 + t)/(1 + t_1 + t)$ and $D_2 = (1 + t_1 + t)/(1 + t)$.

In the development to follow, all mathematical operations will be in the pseudo-time domain unless stated otherwise. Thus differentiation is with respect to pseudo-time and denoted by a superscript dot.

2.5 The Description and Prediction of Creep Behaviour

The object of creep theory is to relate measured values of stress, deformation, temperature and time by an equation or system of equations of universal character. The equations maybe represented in terms of a superposition integral (Boltzmann 1874 and Volterra 1930) or in terms of differential equations (Hinton and Clements 1964). In connexion with the differential equation approach, rheological (spring and dashpot) models have been extensively used as a heuristic device.

These two different approaches are, of course, mathematically related to each other (Gross 1953), but in practice, each has its own peculiar advantages and disadvantages (Hinton and Clement 1964). It would seem that from the point of view of a stress analyst, concerned with the practical solution of boundary-value problems, the most convenient representation would be the one requiring the least amount of computational effort, a minimum of experimental data, and has the ability to allow sufficient freedom for each of the strain components to respond individually to variable stress and varying temperature. From this stand-point, the most efficient formulation appears to be the differential equation form of the lowest order which represents the behaviour of the real material with sufficient accuracy.

To proceed with the differential equation approach, we assume at the outset an uniaxial constitutive law of the form:

$$\dot{\varepsilon} = \frac{\dot{\sigma}}{E_m} + \sigma^{\omega} \Phi(T) \qquad (2.5.1)$$

where ε, σ,σ, E_m, $\Phi(T)$ represents strain rate, stress rate, stress, Young's modulus and temperature normalisation function respectively. The differentiation is with respect to pseudo-time c and is denoted by a superscript dot. In particular, the constitutive law for concrete being:

$$\dot{\varepsilon} = \frac{\dot{\sigma}}{E_m} + \sigma\Phi(T) \qquad (2.5.2)$$

Equation 2.5.2 is analogous to the strain rate in a Maxwell model in which $\Phi(T)$ takes place of the reciprocal of the viscosity of the dashpot and pseudo-time replaces real time (Figure 2.5.1).

If allowance is made for recovery strains when stresses decline, an analogous Burgers representation, Figure 2.5.2, (England and Jordan 1975) maybe more appropriate. It has the advantages over the simpler Maxwell approach, equation 2.5.2, in that it is capable of predictiong, with good engineering accuracy, the major strain features associated with stressed concrete (Illston 1965). The constitutive relationship for uniaxial stress and strain is given by equation 2.5.3:

$$\ddot{\varepsilon} + \left\{\frac{E_k}{\eta_k}\right\}\dot{\varepsilon} = \left\{\frac{(E_m + E_k)}{\eta_k E_m} + \Phi(T)\right\}\dot{\sigma} + \frac{\ddot{\sigma}}{E_m} + \left\{\frac{E_k\Phi(T)}{\eta_k}\right\}\sigma \qquad (2.5.3)$$

Here E_k and η_k refer to the elastic and viscous parameters of the Kelvin component and the differentiation is with respect to pseudo-time. L'Hermite (1969) found that concrete creep recovery was about 18% of the elastic and hence:

$$E_k = 5E_m \qquad (2.5.4)$$

The subsequent investigations which follow have utilised equation 2.5.2 (Chapter 2 to Chapter 5), equation 2.5.3 (Chapter 6) for concrete structures. Equation 2.5.1 has been investigated and discussed in detail in Chapter 7 for non-concrete structures.

2.6 The Existence of a Steady-State

Under the effect of sustained non-uniform temperatures and loads, stress redistribution takes place within the structure due to creep until they reach their stationary values known as 'steady-state stresses' (England 1966). With $\dot{\sigma} = 0$, equation 2.5.2 reduces to:

$$\sigma_{ss} = \frac{\dot{\varepsilon}_{ss}}{\Phi(T)} \qquad (2.6.1)$$

where σ_{ss} and $\dot{\varepsilon}_{ss}$ are the stresses and strain rates at the steady-state respectively. Comparing equation 2.6.1 with the elastic stress-strain relationship reveals an analogy in which $1/\Phi(T)$ replaces Young's modulus and $\dot{\varepsilon}_{ss}$ replaces existing strains. This elastic analogy can be used to obtain directly the steady-state stresses by just replacing the elastic modulus by $1/\Phi(T)$ in an ordinary elastic calculation.

When temperature vary in cyclic manner between two sets of fixed values T_1 and T_2 and with phase length k_1 and k_2 respectively, Figure 2.4.3, the steady-state cyclic stresses during one cycle maybe represented to a good degree of approximation by a pair of stress distributions which differ by the thermal stress, σ_T, corresponding to the change in temperature. Let σ_1 be the steady-state cyclic stress at T_1. This phase will be known as the reference phase and is, of course, an arbitrary choice. The steady-state cyclic stress at T_2 is then $(\sigma_1-\sigma_T)$. The strain rate in the first part of the temperature cycle will be:

$$\dot{\varepsilon}_1 = \sigma_1 T_1 \qquad (2.6.2)$$

and that in the second phase it will be:

$$\dot{\varepsilon}_2 = (\sigma_1 - \sigma_T) T_2 \qquad (2.6.3)$$

An average strain rate over one temperature cycle is defined as:

$$\dot{\varepsilon}_a = \frac{k_1\dot{\varepsilon}_1 + k_2\dot{\varepsilon}_2}{k_1 + k_2} \qquad (2.6.4)$$

On re-arrangement, this becomes:

$$\dot{\varepsilon}_a = \frac{(k_1T_1 + k_2T_2)\sigma_1}{k_1 + k_2} - \frac{k_2T_2\sigma_T}{k_1 + k_2} \qquad (2.6.5)$$

Thus,

$$\sigma_1 = \frac{1}{T_a}\{\varepsilon_a + \frac{k_2T_2\sigma_T}{k_1 + k_2}\} \qquad (2.6.6)$$

where $T_a = (k_1T_1 + k_2T_2)/(k_1 + k_2)$ is the average weighted temperature over the cycle.

Comparing equation 2.6.6 with the general elastic stress-strain relation of the initial strain type viz.

$$\sigma = E(\varepsilon - \varepsilon_o) \qquad (2.6.7)$$

An analogous elastic modulus for cyclic temperature creep analysis of $1/T_a$ is abserved together with an 'analogous initial strain' (actually an initial strain rate) of the form:

$$\dot{\varepsilon}_o = -(k_2T_2\sigma_T)/(k_1 + k_2) \qquad (2.6.8)$$

Generalising the theory to a temperature cycle with m discrete parts, with part r taken as the reference temperature state, the analogous quantities become:

$$\sigma_{Ti} = \sigma_r - \sigma_i \qquad (2.6.9)$$

$$T_a = (\Sigma k_iT_i)/(\Sigma k_i) \qquad (2.6.10)$$

$$\dot{\varepsilon}_o = -(\Sigma k_iT_i\sigma_{Ti})/(\Sigma k_i) \qquad (2.6.11)$$

2.7 Method of Structural Analysis

Numerical procedures, related to the investigations reported here, maybe classified into three categories within the framework of the finite element method:

I. One Step Procedure in conjunction with an effective modulus, E_{eff}, approach - By this procedure, time-dependent stresses are calculated directly by using an effective space varying elastic modulus, E_{eff}, of the value:

$$E_{eff} = E_m/(1 + E_m\Phi(T)c) \qquad (2.7.1)$$

This procedure neither takes account of stress history nor of creep recovery. It is unreliable as a guide to the rate of decay of thermal stresses and was also described by Ross (1958), in solutions at uniform temperatures, as being 'theoretically unsound'.

II. Time-step Procedure in conjunction with an analogous Maxwell constitutive law (vide equation 2.5.2) or a non-linear creep law - This is a historical step-by-step procedure (England 1967) which is capable of predicting the variations of stresses and strains with time, but require many time-steps if accuracy of the solution is to be maintained throughout the life-span of the structure. In consequence, this type of procedure is often expensive. Nevertheless it is a valuable numerical algorithm when used in conjunction with a non-linear creep law as depicted in equation 2.5.1 (vide Chapter 7).

III. Power Minimisation Procedure in conjunction with a Ritz process - This is a direct procedure based on England's Principle of the Minimum of The Total Complementary Power (1968), which states:

'The total complementary power at any instant has a stationary value with respect to small variations of stress from the true equilibrium state.'

Consider the body shown in Figure 2.7.1, it is acted upon by a set of external loads P_e and rests on an arbitrary number of statically determinate or indeterminate supports with reactions R_s. The loads are

prescribed and do not vary with time, which the reactions for the redundant support condition will be time-varying quantities. The displacement rates of the applied loads and the support reactions are denoted respectively by U_e and U_s, these quantities being positive when measured in the direction of the force.

The rate of working of the external loads and reactions is the sum of the products of the loads and reactions and their respective displacement rates taken in the direction of these forces. Internally, a similar quantity maybe formulated from consideration of the stresses , σ , and strain rates, $\dot{\varepsilon}$, throughout the whole volume of the body. The internal rate of working includes the rate of change of stored energy which results from stress redistribution and the rate at which energy is dissipated from the body. Because the total rate of working at any instant, internal and external, must be zero as depicted by the principle of conservation of energy, thus:

$$\int \sigma_{ij}\dot{\varepsilon}_{ij}\, dV = P_e\dot{U}_e + R_s\dot{U}_s \qquad (2.7.2)$$

Here the dot denotes differentiation with respect to pseudo-time and the integration is taken over the volume of the body. By applying simultaneous small variations to the stresses, strain rates, surface displacement rates at the load points and the reactive forces and neglecting the second-order terms, it maybe established that:

$$\int\dot{\varepsilon}_{ij}\delta\sigma_{ij}dV + \int\sigma_{ij}\delta\dot{\varepsilon}_{ij} = P_e\delta\dot{U}_e + \dot{U}_e\delta P_e + \dot{U}_s\delta R_s \qquad (2.7.3)$$

When the prescribed loads are not subjected to variation, it follows that the variational set of stresses together with the variations of the reactions constitute a self-equilibrating stress system. Thus with $\delta P_e = 0$, equation 2.7.3 maybe rearranged to give:

$$\int\dot{\varepsilon}_{ij}\delta\sigma_{ij}dV - \dot{U}_s\delta R_s = -\{\int\sigma_{ij}\delta\dot{\varepsilon}_{ij}dV - P_e\delta\dot{U}_e\} \qquad (2.7.4)$$

The left hand side of equation 2.7.4 shows the strain and displacement rates which correspond to the true stress system, i.e. the compatible system of strain rates by the variational set of stresses which themselves are a self-equilibrating system without the external loads.

On multiplying equation 2.7.4 by Δc, the work rates are transformed into actual work quantities during the pseudo-time interval Δc. Then by the principle of virtual work the modified left hand side of equation 2.7.4 must vanish since this statement is true for all c it follows that:

$$\int \dot{\varepsilon}_{ij} \delta\sigma_{ij} \, dV - \dot{U}_s \delta R_s = 0 \qquad (2.7.5)$$

This equation is similar in form to the variational principle which is developed in elasticity from the theory of complementary energy. Here strain rates and displacement rates replace strains and displacements of the complementary energy theory. By analogy of form, therefore, equation 2.7.5 is referred to as the variation of the total complementary power and is defined by:

$$\delta(\psi_I + \psi_E) = 0 \qquad (2.7.6)$$

When equation 2.7.5 represents the variation of a definable function ψ_I and ψ_E are respectively the contributions from the internal stresses and external reactions as given in equation 2.7.5.

Similar argument reveals a second variation principle from equation 2.7.4.:

$$\int \sigma_{ij} \delta\dot{\varepsilon}_{ij} dV - P_e \delta\dot{U}_e = 0 \qquad (2.7.7)$$

This variational principle is analogous in form to the variational principle development in elasticity and known as the minimum of the total potential. It will not be discussed in detail in this thesis.

When a structure is at all times in equilibrium with the specified loading and compatible with respect to both internal strains and external geometrical constraints, with $\dot{U}_s = 0$, equation 2.7.5 may be rewritten in matrix form:

$$\int \{\dot{\varepsilon}\}^T \{\delta\sigma\} \, dV = 0 \qquad (2.7.8)$$

Equation 2.7.8 maybe used in conjunction with a Ritz process in which the state of stress is specified as a series of terms as given in equation 2.7.9 for which the spatial stress distributions $\{\sigma_i\}$ are

specified. The problem becomes one of identifying the time functions {a} associated with each stress distribution to give the best match to the exact solutions at all times as dictated by the Complementary Power Principle viz, equation 2.7.8, thus:

$$\{\sigma\} = \{\sigma_o\} + a_1\{\sigma_1\} + \ldots. a_n\{\sigma_n\}$$
$$= \{\sigma_o\} + \{a\}^T[\sigma] \qquad (2.7.9)$$

Where $\{\sigma_o\}$ represents any set of stresses which are in equilibrium with the boundary loading, and $[\sigma]$ constitutes self-equilibrating internal stress distributions. The application of the Complementary Power Principle to creep problems will be discussed in detail in Chapter 5.

2.8 Discussion and Concluding Remarks

In developing methods of calculating creep and applying them to the study of real objects the fairly considerable scatter of creep test results must be taken into account. A difference of 10% between the deformation found in creep curves taken at the same stress and temperature on specimens of material of a single source is not considered excessive. It is therefore hardly worthwhile to attempt very accurate analytical description of creep curves and approximating expressions are usually selected on grounds of practicality.

The author who has been concerned with the development of an engineering creep theory has used the hypothesis of similarity of creep curves (vide section 2.5) from which the pseudo-time concept is derived. The hypothesis of similarity of creep curves is fairly well justified in problems involving moderate strains and temperatures.

Constitutive equations are formulated as differential equations utilising the pseudo-time concept. As far as concrete is concerned, it has been shown that for situations where unloading is unlikely or its effect is insignificant, the analogous Maxwell rheological body is an appropriate material model, whereas when creep recovery is more important the analogous Burgers model is more suitable.

In cases where linear creep analysis is not wholly satisfactory for

non-concrete materials, a non-linear creep law is adopted.

Structures considered are subjected to either raised non-uniform temperatures or to non-uniform temperatures which may vary periodically and in a step-wise manner in time between definable limits. It is assumed that for this latter type problem, temperature transients are of short duration compared to the 'hold' periods between successive changes.

The modulus of elasticity is assumed temperature and time invariant. However, the modulus of elasticity variation will affect the time-dependent stresses but not the conclusions drawn or the theoretical procedures developed. The variation in the modulus maybe incorporated readily in the creep calculations.

Creep Poisson's ratio for concrete is assumed to exist and to be of a value equal to that of the elastic Poisson's ratio, thus:

$$v_c = v \qquad (2.8.1)$$

Equation 2.8.1 is a convenient simplification but if another value for creep Poisson's ratio was found to be more appropriate this would not invalidate any of the conclusions drawn, or the theoretical procedures used.

Finally, the normalisation temperature function, $\Phi(T)$, is assumed, unless stated otherwise, to be:

$$\Phi(T) = T^{o}C \qquad (2.8.2)$$

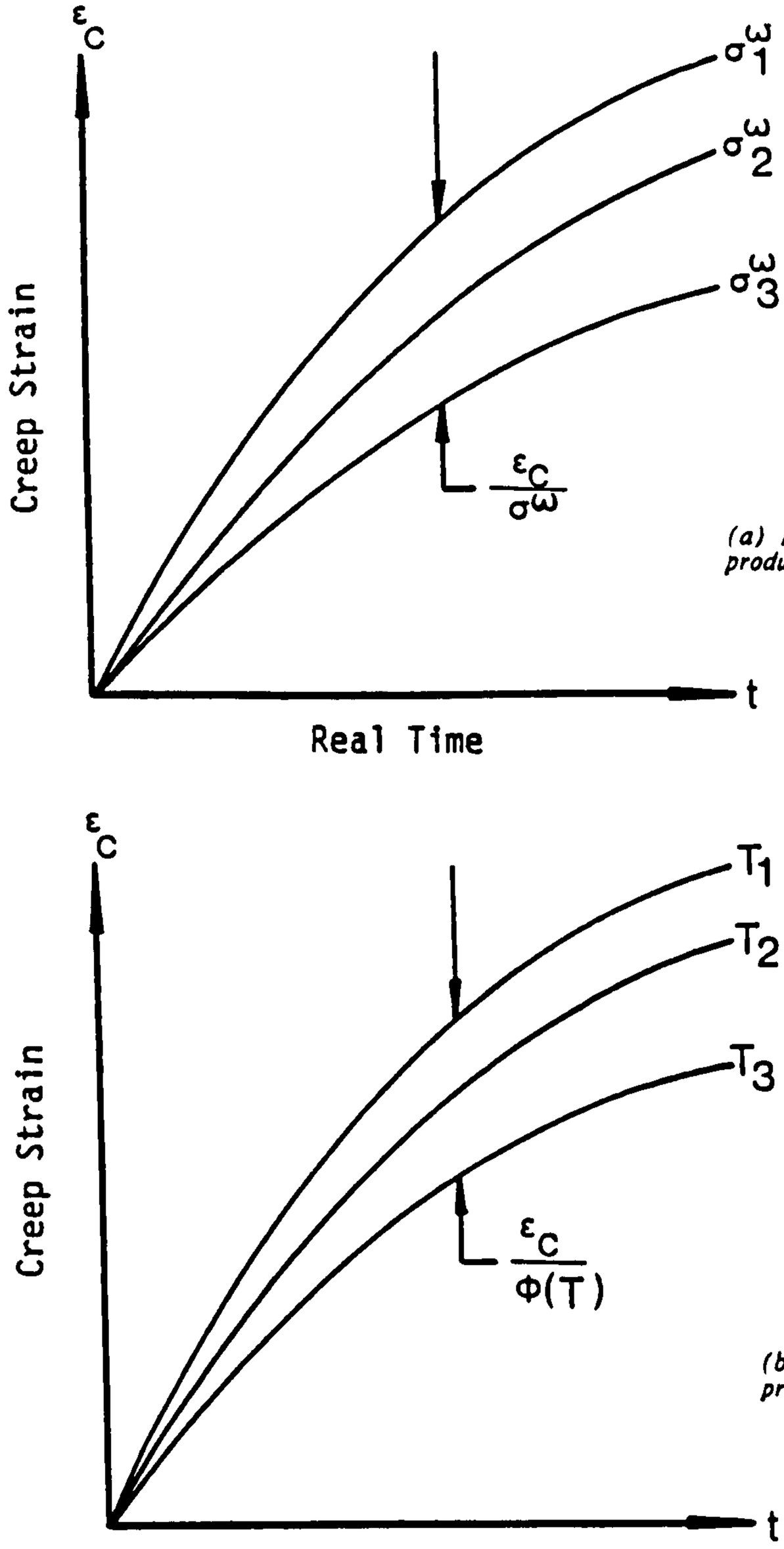

(a) Normalization of creep curves plotted for various stresses produces a single curve for each temperature

(b) Further normalization with respect to temperature produces the single curve shown in (c)

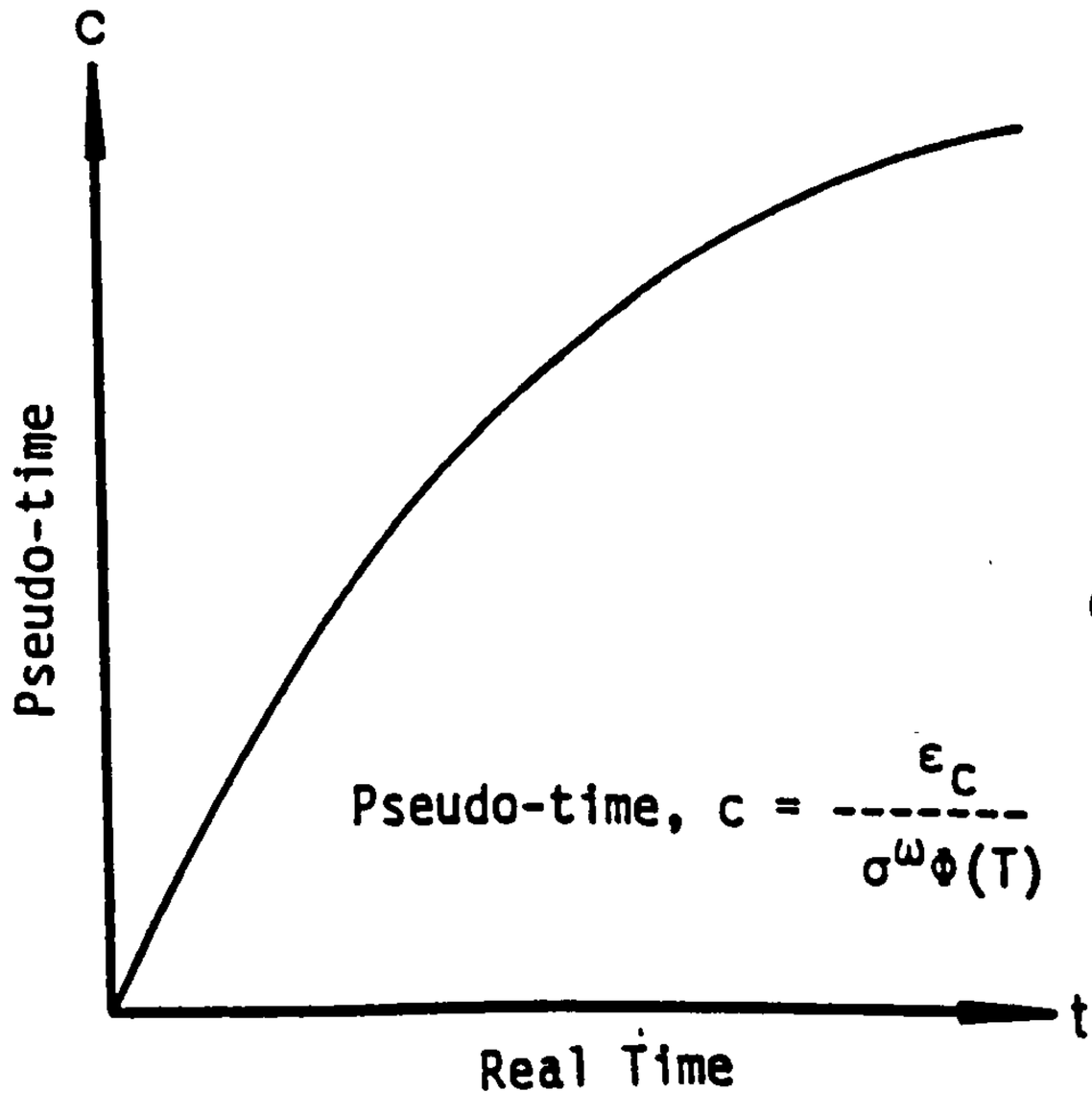

(c) Normalized creep or pseudo-time, c

Figure 2.4.1: Determination of pseudo-time for Maxwell model.

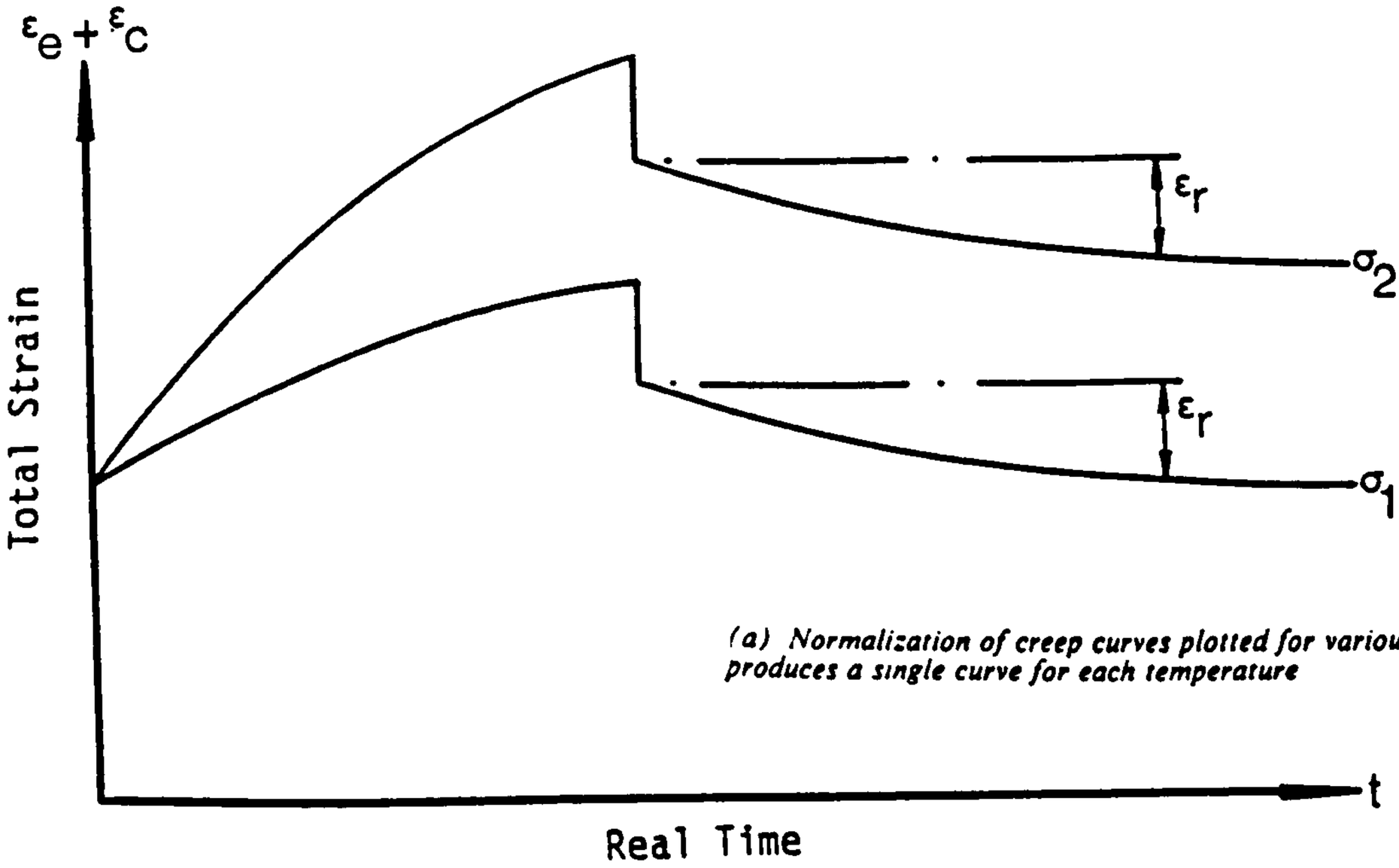

(a) Normalization of creep curves plotted for various stresses produces a single curve for each temperature

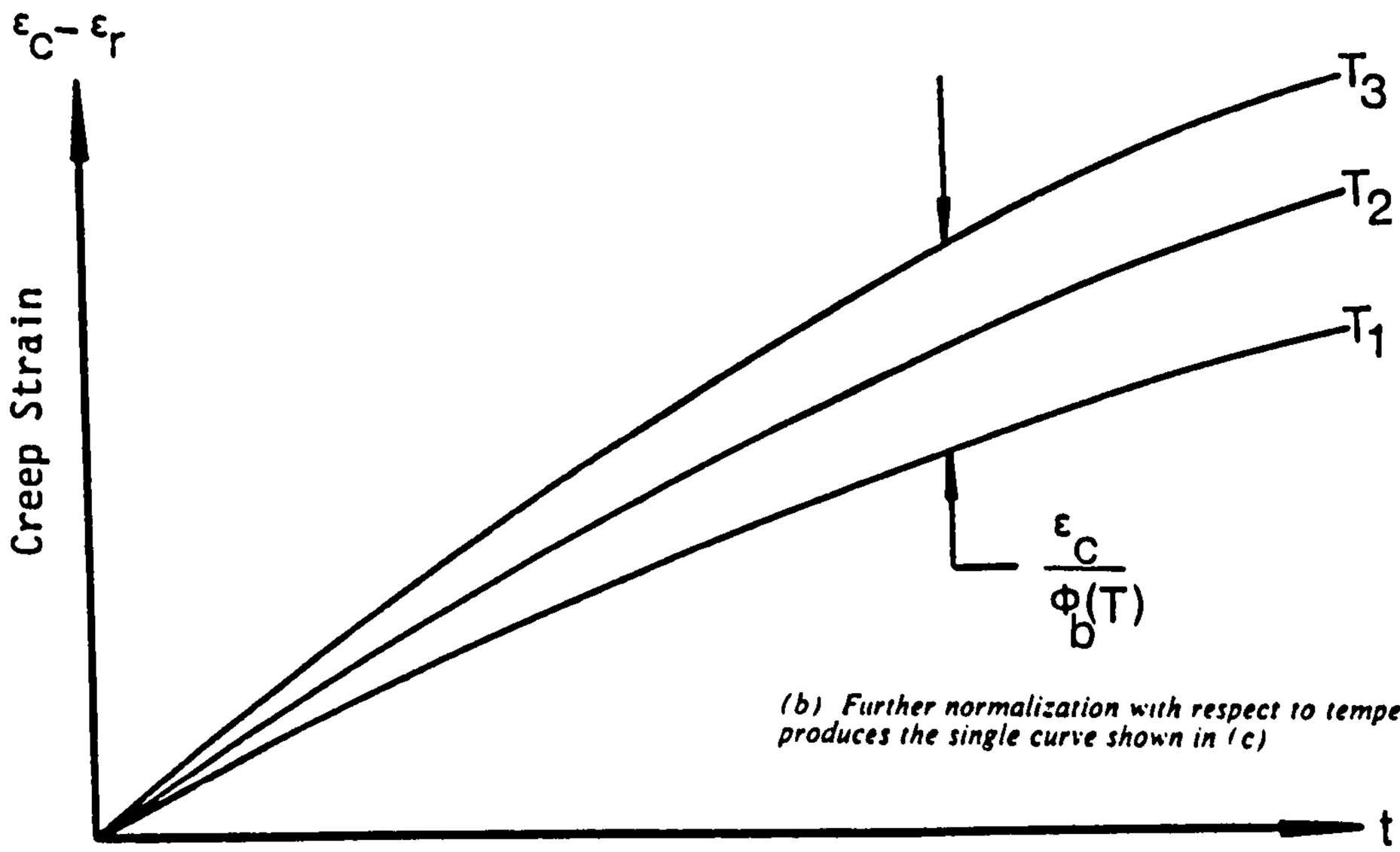

(b) Further normalization with respect to temperature produces the single curve shown in (c)

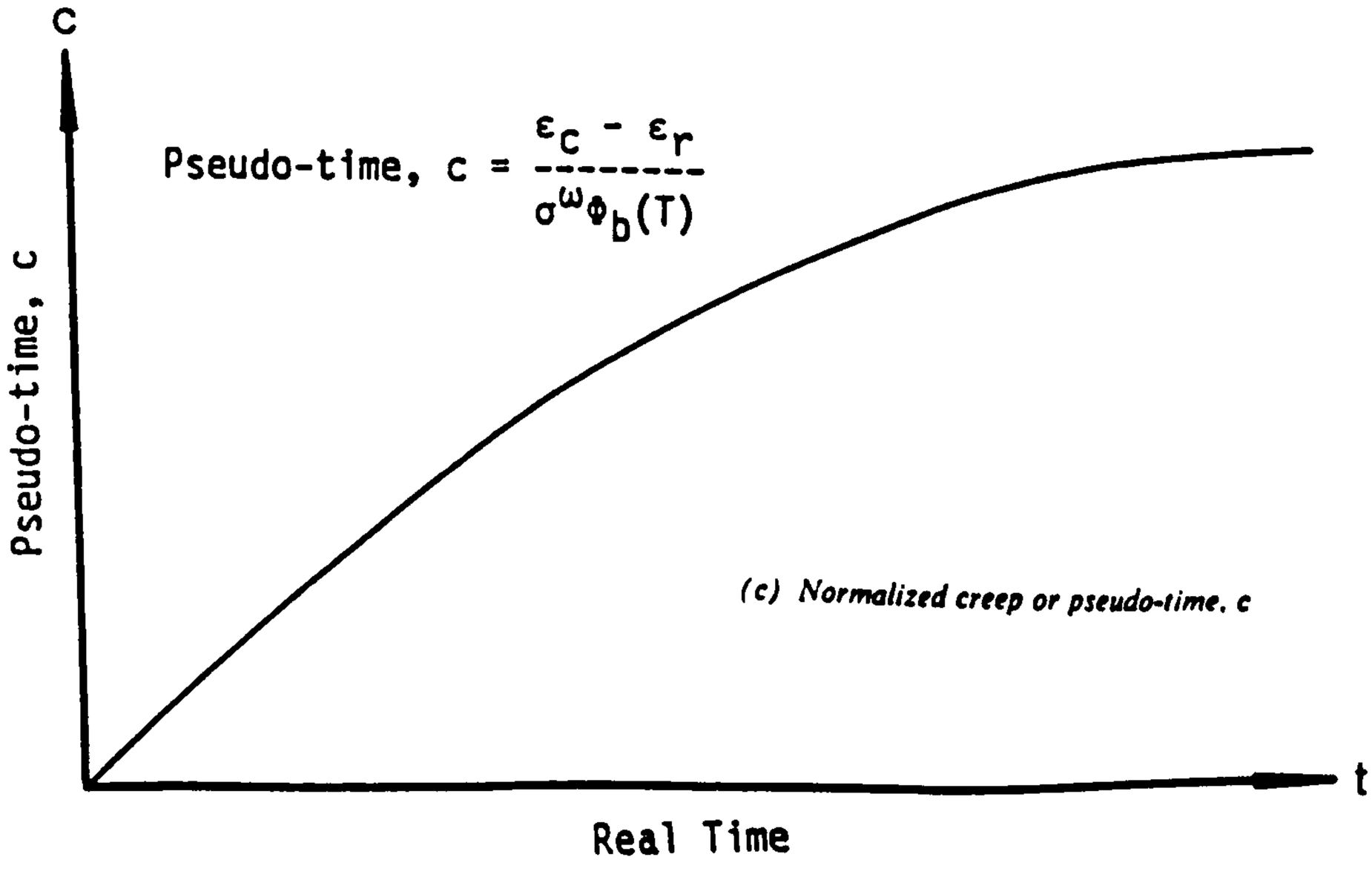

(c) Normalized creep or pseudo-time, c

Figure 2.4.2: Determination of pseudo-time for Burgers model.

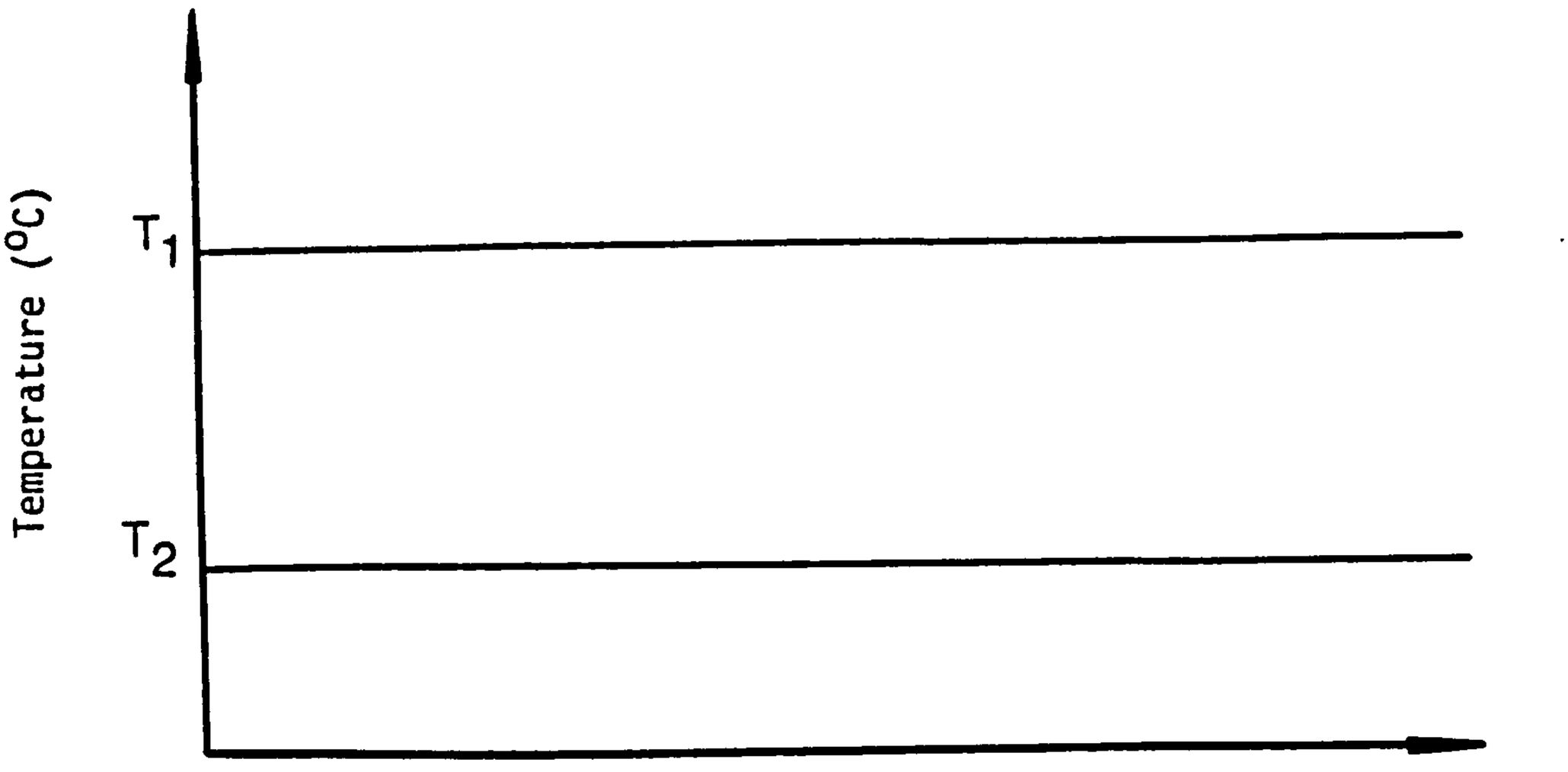

(a) Sustained temperature.

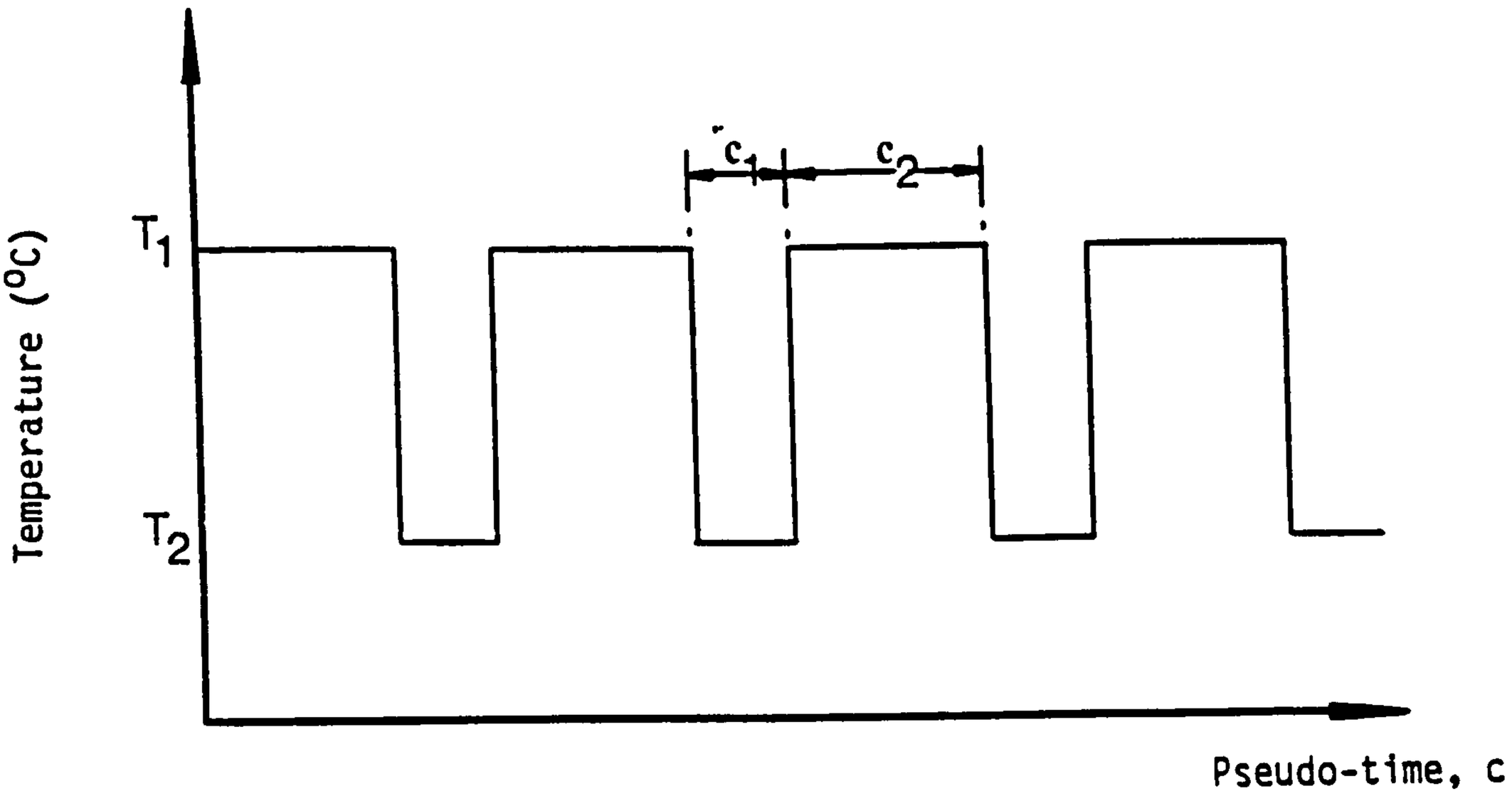

(b) Reversible cyclic temperature.

$$k = \frac{c_1}{c_2}$$

Figure 2.4.3: Nature of temperature cycling.

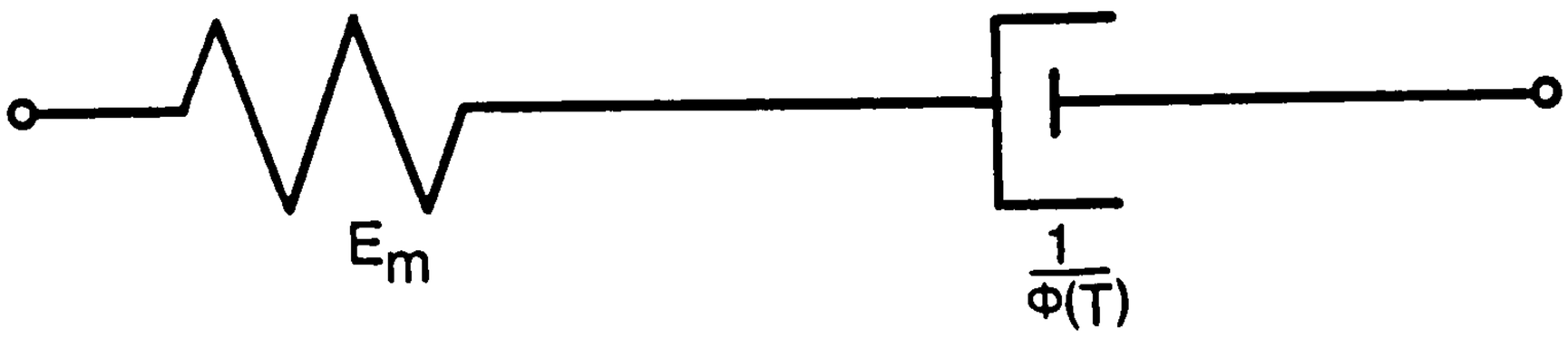

Figure 2.5.1: An analogous Maxwell model.

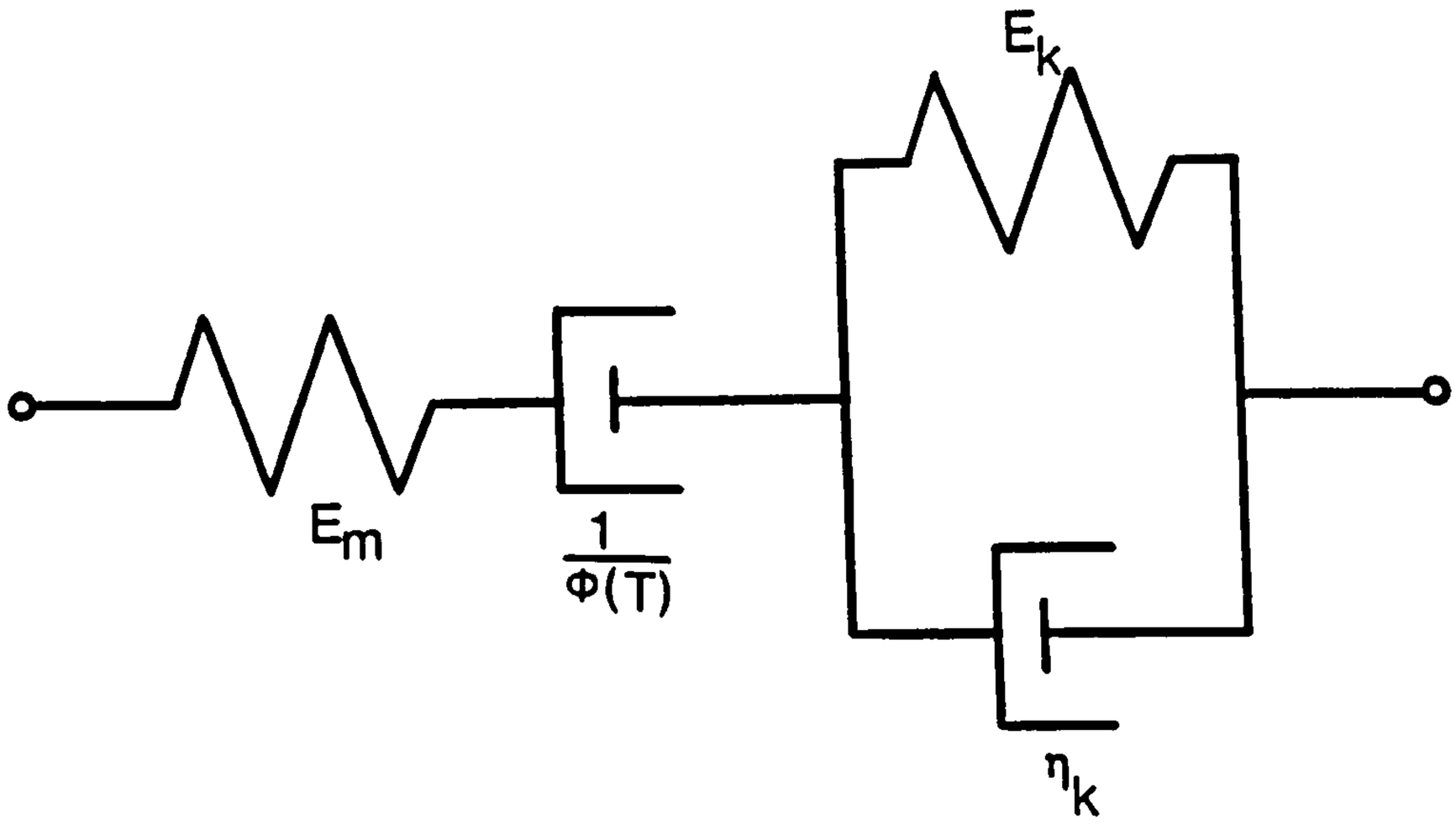

Figure 2.5.2: An analogous Burgers model.

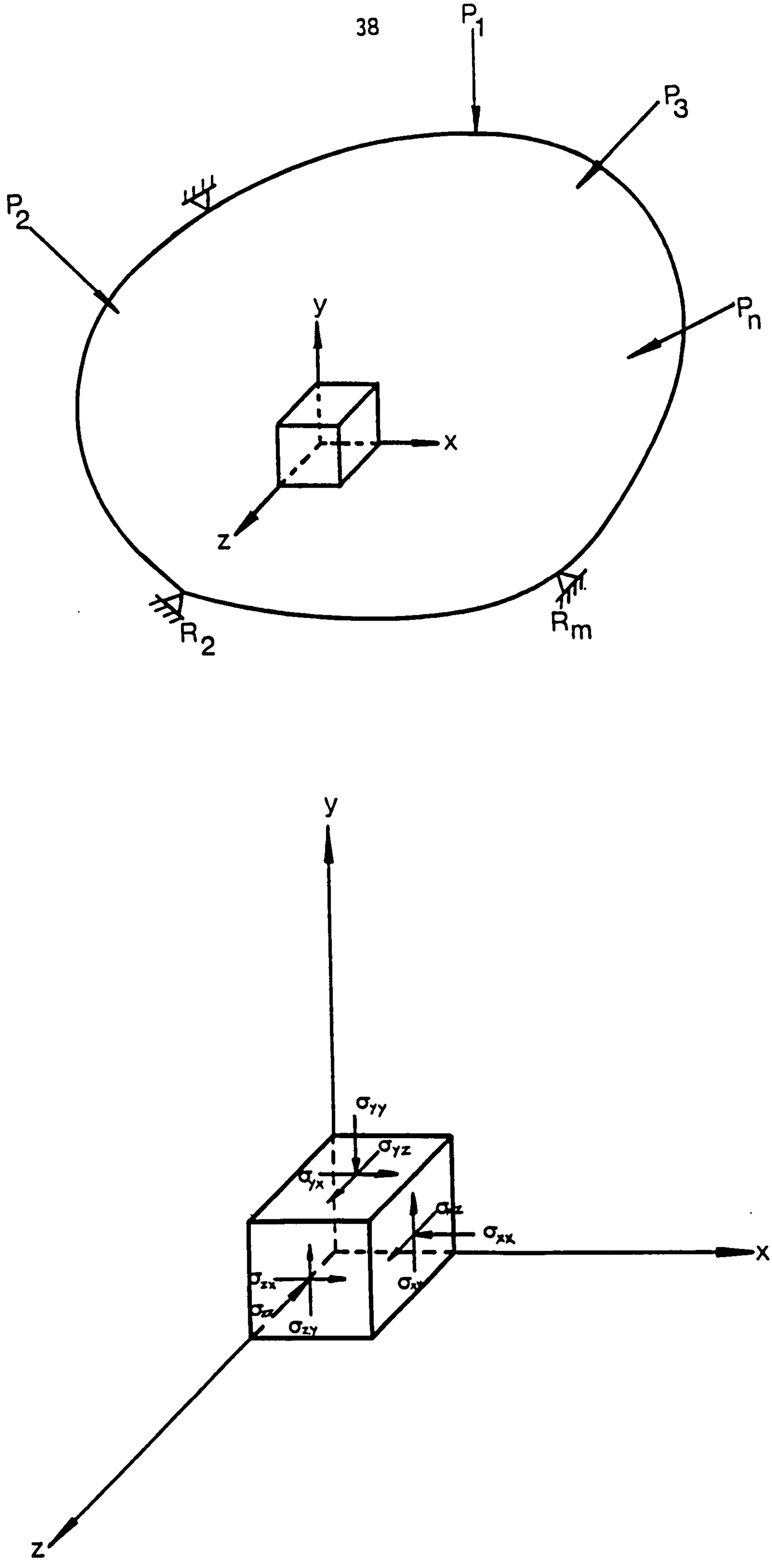

Figure 2.7.1: A general body under applied loadings.

CHAPTER THREE

APPLICATION OF THE STEADY-STATE THEORY TO STRUCTURAL ANALYSIS OF CONTINUOUS PRESTRESSED CONCRETE BEAM PROBLEMS: A FLEXIBILITY APPROACH

Summary

This chapter describes the theoretical development and computer implementation of the flexibility method of creep analysis for steady-state stresses in continuous prestressed concrete beam structures subjected to cyclically varying temperatures. A creep theory for beams is developed and is shown to be analogous to a beam theory of non-homogeneous elasticity. Use is then made of elastic analysis procedures to generate creep solutions. A Fortran program is developed and applied to a two span continuous beam with realistic temperature data.

It is concluded that combined influence of creep and cyclic temperatures cause significant changes to the working stresses which should be accounted for in design. It is also recommended that the Codes of Practice BS 5400 should include explicit information relating to average temperature for different seasons and different times of day, together with theory and information on temperature-dependence of creep to enable designers to perform creep temperature calculations.

3.1 Preliminary

Prestressed concrete beams are used widely in road and motorway construction and their serviceable life will often be expected to exceed 100 years. They are often subjected to continuous heating and cooling from the environment and solar radiation. This may cause undesirable deformations and stresses.

The design of concrete bridges for temperature fluctuations has traditionally been a simple matter. Longitudinally movements induced by the maximum expected average temperature changes, typically ±20 ^{o}C are accommodated by provision of sliding joints, bearing

displacements, or by a flexible pier design. Effects due to non-linear differential temperature distributions have normally been considered only in connection with bridges of unusual span and cross-section.

However, in recent years there has been growing awareness (Emerson 1976-77, Narucks et al 1957, Bryant et al 1974, Leonhardt et al 1965, Churchward et al 1981 and Priestly 1972) throughout the world, in the effects of non-linear differential temperature distributions on all types of concrete bridge structures. The results of research into temperature effects have been introduced into design standards (BS 5400 1978, German design standard 1953, Krishnamarthy 1971 and CEP-FIP 1978) and have often resulted in a reassessment of the importance of temperature effects in the design process.

Unfortunately, few realised that the behaviour of concrete structures subjected to spatially varying temperatures cannot be predicted reliably from an elastic analysis because creep is temperature dependent. Experimental work carried out at King's College London has revealed that significant changes to the working stresses and bending moments in prestressed continuous beams can occur during the operational life time of many beam structures. Not only do stresses exhibit time-dependent changes, with attendant changes being observed in bending moments also, but bending moments can at some locations change sense.

In the long term, a steady-state of stress is reached, when temperature are time-invariant, and a quasi steady-state is reached, when temperature is repeated cyclic manner with time. The combined influence of creep and cyclic temperatures on the long term serviceability and integrity of concrete bridges can be considerable. Design should therefore be based on both an appreciation of the elastic and thermo-elastic states in early life and the steady-state at large times.

This chapter describes a method of analysis for continuous prestressed concrete beams which is capable of evaluating section bending moments and stresses for the separate effects of mechanical loading and temperature from elastic analyses, and the corresponding sets of quantities relating to the combined influence of creep and temperature in the long term for cyclically varying temperatures.

3.2 Statement of the Problem

The problem is that of a long prestressed continuous concrete beam on any finite number of co-linear supports, Figure 3.2.1 (a). Prestressed forces are applied at the centroid of each cross-section and longitudinal restraints are not permitted except at one end support which maybe fixed or hinged. In other respects the problem is specified through knowledge of the applied loading and cyclical temperature states to which the structure is subjected. The following assumptions are made:

a. A continuous temperatures variation with time over one cycle is approximated to series of discrete temperature states, Figure 3.2.1 (b).

b. For the cyclic temperature problem, a steady-state is defined as that state which corresponds to the existence of repeating stresses in any part of the structure, at corresponding times in successive temperature cycles. Within any one cycle there will exist several stress states and these will differ from each other by states of thermal stresses of the same magnitude as in the thermo-elastic solution (vide Chapter 2).

c. Each span of the continuous beam is subjected to the same temperature cycling.

d. Temperature varies only with depth although variations between spans are permitted. The distribution of temperature across a vertical section maybe non-linear within any part of the temperature cycle.

e. Beams are prismatic and of constant cross-section in each span, width may vary with depth, Figure 3.2.2 (a).

f. Non-homogeneous elastic properties maybe specified in each span, as a variation with depth only.

g. Thermal stresses can be considered independently of stress or strain imposed by other loading conditions (i.e. the principle of

superposition applies). The thermal expansion behaviour is homogeneous.

h. Plane sections remain plane after bending and during creep, i.e. at all times (i.e. small displacement theory is applied), see Figure 3.2.2.

The aim of the analysis is to determine the limiting steady-state moments, forces and stresses. To do this a flexibility type of analysis is adopted for the solution of the redundant support bending moments of the continuous beam.

For the elastic solution, virtual work equations are set up and these incorporate product of the true curvatures with successive sets of bending moments corresponding to unit values of the redundancies taken in turn, Figure 3.3.1.

For the creep solution, virtual power equations are constructed for the evaluation of the long-term limiting steady-state stresses. In this part of the analysis curvature rates in the steady-state replace curvatures of the elastic solution.

3.3 Theoretical Basis and Flexibility Formulation

The theory is based on the elastic analogies described in section 2.6 in which the cyclic temperature creep problem is analogous to a non-homogeneous elastic initial strain problem for which the analogous initial strains are related to the true thermal stresses of the thermo-elastic problem, Table 3.3.1. Consider a section of a general non-homogeneous beam subjected to a bending moment M(sagging positive) and an axial force N(compressive positive) applied at the centroid of the cross-section, assumption h (vide section 3.2) implies that:

$$\sigma = D(A + Bz - \varepsilon_0) \qquad (3.3.1)$$

The interpretations of σ, D, A, B, z, ε_0, depend on the problem in hand, Table 3.3.1. Equilibrium of the cross-section requires that:

$$\int \sigma b \, dz = N \qquad (3.3.2)$$

$$\int \sigma b z dz = M \qquad (3.3.3)$$

where $\int$ denotes integration is taken over the section of beam with the geometrical centroid as the origin and b is the width of the section which vary with depth (assumption e).

Substitution of equation 3.3.1 in equation 3.3.2 and equation 3.3.3 results:

$$N = \int bDAdz + \int bDBzdz + \int -bD\varepsilon_o \, dz \qquad (3.3.4)$$

$$M = \int bDAzdz + \int bDBz^2dz + \int -bDz\varepsilon_o \, dz \qquad (3.3.5)$$

or simply,

$$N = AI_1 + BI_2 + I_4 \qquad (3.3.6)$$

$$M = AI_2 + BI_3 + I_5 \qquad (3.3.7)$$

The interpretations of integrals I_1 to I_5 are shown in Table 3.3.2.

Equations 3.3.6 and 3.3.7 maybe represented in matrix form, thus:

$$\begin{Bmatrix} N \\ M \end{Bmatrix} = \begin{bmatrix} I_1 & I_2 \\ I_2 & I_3 \end{bmatrix} \begin{Bmatrix} A \\ B \end{Bmatrix} + \begin{Bmatrix} I_4 \\ I_5 \end{Bmatrix} \qquad (3.3.8)$$

Equation 3.3.8 maybe rewritten as:

$$\begin{Bmatrix} A \\ B \end{Bmatrix} = \begin{bmatrix} I_1 & I_2 \\ I_2 & I_3 \end{bmatrix}^{-1} \begin{Bmatrix} N - I_4 \\ M - I_5 \end{Bmatrix} \qquad (3.3.9)$$

From which the following equation representing either the curvature of the section for the elastic problem or the steady-state curvature rate in creep problem is obtained:

$$B = aM + bN + d \qquad (3.3.10)$$

d is an initial curvature or curvature rate and there is an inherent coupling between axial and bending effects in this general representation. The parameters a, b, and d relate to five integrals, I_1 to I_5,

and are given in Table 3.3.2. It is observed that 'a' and 'b' of equation 3.3.10 are constants for no variation of temperature along the beam. However, d is a linear function of the horizontal co-ordinate.

The continuity equations at the sections of the redundant moments maybe written as:

$$\int B\{m\}\, dV = 0 \qquad (3.3.11)$$

where

$$\{m\} = \{m_1, \ldots. m_i \ldots m_n\}^T \qquad (3.3.12)$$

n is the number of redundancies in the problem and m_i represents the set of bending moments relating to unit value of the ith redundancy applied to the statically determinate released structure and the integration is performed over the entire structure, Figure 3.3.1.

The actual bending moments are specified in the form:

$$M = M_o + \{X\}^T\{m\} \qquad (3.3.13)$$

where

$$\{X\} = \{X_1, \ldots. X_i \ldots X_m\}^T \qquad (3.3.14)$$

M_o is the set of bending moments caused by the specified loading applied to the released structure; X_i is the ith redundancy and m_i is as before.

Combinations of equations 3.3.10, 3.3.11 and 3.3.13 leads to a set of algebraic equations of the form:

$$\int [a(M_o + \{X\}^T\{m\}) + bN + d]\{m\}\, dV = 0 \qquad (3.3.15)$$

In matrix form the equations become:

$$[C]\{X\} = \{Z\} \qquad (3.3.16)$$

where [C] is an n x n flexibility matrix and {Z} is an n x 1 vector. The general terms of equation 3.3.15 are:

$$C_{rs} = \int am_r m_s \, dV \tag{3.3.17}$$

$$Z_r = - \int (U_r + V_r + W_r) \tag{3.3.18}$$

$$U_r = \int aM_o m_r \, dV \tag{3.3.19}$$

$$V_r = F \int bm_r \, dV \tag{3.3.20}$$

$$W_r = \int dm_r \, dV \tag{3.3.21}$$

The solution of equation 3.3.16 reveals the redundant moments from which section moments maybe evaluated by linear interpolation and superposition (assumption g). In the case of thermal problems, equation 3.3.16 reduces to:

$$[C]\{X\} = -\{W\} \tag{3.3.22}$$

Because no variation of axial force is induced by temperature effects (vide section 3.2).

For elastic solutions (mechanical loading only), equation 3.3.16 collapses to:

$$[C]\{X\} = -\{U\} \tag{3.3.23}$$

3.4 Determination of Section Stresses

For the general case of a non-homogeneous elastic analogous elastic beam, D = D(z), with initial strain or analogous initial strain (rate), $\varepsilon_o = \varepsilon_o(z)$, equation 3.3.1 can be rewritten in matrix form as:

$$\sigma = D(\{1 \; z\}\{A \; B\}^T - \varepsilon_o) \tag{3.4.1}$$

Substitution of equation 3.3.9 into equation 3.4.1 leads to:

$$\sigma = D\left(\{1 \; z\} \begin{bmatrix} I_1 & I_2 \\ I_2 & I_3 \end{bmatrix}^{-1} \begin{Bmatrix} N-I_4 \\ M-I_5 \end{Bmatrix} - \varepsilon_o\right) \tag{3.4.2}$$

where the parameters have the meaning defined in Table 3.3.1 and Table 3.3.2. N and M are section actions - longitudinal compressive force at the centroid and bending moment.

The distribution of elastic stress through a particular cross-section is then:

$$\sigma'_e = E_m(\{1\ z\} \begin{bmatrix} I_1 & 0 \\ 0 & I_3 \end{bmatrix}^{-1} \begin{Bmatrix} N \\ M \end{Bmatrix}) \qquad (3.4.3)$$

In the case of thermal stress distribution that arise by changing the temperature from uniform datum temperature to a particular phase, equation 3.4.2 reduces to:

$$\sigma_{Ti} = E_m(\{1\ z\} \begin{bmatrix} I_1 & I_2 \\ I_2 & I_3 \end{bmatrix}^{-1} \begin{Bmatrix} -I_4 \\ M-I_5 \end{Bmatrix} - \alpha\Delta T) \qquad (3.4.4)$$

The thermo-elastic stress, σ_{eTi}, distribution through a cross-section for temperature phase i in a temperature cycle can be obtained simply by superposing the thermal stress and the elastic stress viz:

$$\sigma_{eTi} = \sigma_e + \sigma_{Ti} \qquad (3.4.5)$$

The cyclic steady-state stress distribution for the reference temperature T_r can be expressed as (vide equation 3.4.2):

$$\sigma_r = \frac{1}{T_a} (\{1\ z\} \begin{bmatrix} I_1 & I_2 \\ I_2 & I_3 \end{bmatrix}^{-1} \begin{Bmatrix} N-I_4 \\ M-I_5 \end{Bmatrix} - \varepsilon_o) \qquad (3.4.6)$$

Thus the cyclic steady-state stress distribution for temperature phase T_i maybe obtained via the principle of superposition (vide section 3.2) viz:

$$\sigma_i = \sigma_r - \sigma_{Ti} \qquad (3.4.7)$$

3.5 Flexibility Equation Solution Scheme

Consider the direct solution of the set of flexibility equation given by (vide equation 3.3.16):

$$[C]\{X\} = \{Z\} \tag{3.5.1}$$

It is obvious that for this structure and the release system chosen, the flexibility matrix [C] contains many zero terms. In fact, the C_{rs} terms of the matrix only exist for the condition r-s<1 and C_{rs}=0 when r-s >1. Thus [C] is a nicely banded symmetric, positive definite and square coefficient matrix. The flexibility matrix can be written as the product of a lower triangular matrix with unit diagonals and an upper triangular matrix, i.e.

$$[C] = [L][U] \tag{3.5.2}$$

where

$$[L] = \begin{bmatrix} 1 & 0 & \cdots\cdots\cdots\cdots \\ \cdot & & \\ \cdot & & \\ L_{21} & 1 & 0 \\ \cdot & \cdot & \cdot \\ \cdot & \cdot & \cdot \\ L_{n1} & \cdot & \cdots\cdots\cdots 1 \end{bmatrix} \tag{3.5.3}$$

and

$$[U] = \begin{bmatrix} U_{11} & U_{12}\cdots\cdots\cdots\cdots\cdots U_{1n} \\ 0 & \cdot & \cdots\cdots\cdots\cdots \\ 0 & 0 & U_{33} & U_{3n} \\ 0 & 0 & 0\cdots\cdots\cdots & \\ \cdots\cdots\cdots\cdots\cdots\cdots & & & \\ \cdots\cdots\cdots\cdots\cdots\cdots\cdots & U_{nn} & & \end{bmatrix} \tag{3.5.4}$$

This is called the triangular decomposition of [C] and is accomplished using a compact Crout's method which is a variation on Gaussian elimination (Zienkeiwicz 1982). the operations necessary for the decomposition of an nxn matrix is then, Figure 3.5.1:

$$U_{11} = C_{11} \; ; \; L_{11} = 1 \tag{3.5.5}$$

For each active zone, from 2 to n,

$$L_{j1} = C_{j1}/U_{11} \; ; \; U_{1j} = C_{1j} \tag{3.5.6}$$

Then

$$L_{ji} = (C_{ji} - \Sigma \; L_{jm}U_{mi})/U_{ii} \tag{3.5.7}$$

$$U_{ij} = C_{ij} \; - \Sigma \; L_{im}U_{mj} \tag{3.5.8}$$

and finally,

$$L_{ij} = 1 \; ; \; U_{jj} = C_{jj} - \Sigma \; L_{jm}U_{mj} \tag{3.5.9}$$

For i = 1, 2,....j-1. The Σ is over the range m = 1, 2, ... i-1.

Since [C] is symmetric,

$$U_{ij} = L_{ji} \; U_{ii} \tag{3.5.10}$$

Thus it is not necessary to store the entire coefficient array. It is sufficient to store only those coefficients above (or below) the principle diagonal and use equation 3.5.10 to construct the missing part. It is possible to reduce the storage and computational effect still further by storing the necessary parts of the upper triangular portion of the flexibility matrix by columns, Figure 3.5.2 (Zienkiewicz 1982). Now it is necessary to store and compute only within the non-zero profile of the equations. This method of storage has the advantages that it always requires less storage than the ordinary banded matrix solver and furthermore it is very easy to use vector dot product routines to effect the triangular decomposition and forward reduction.

Once the triangular decomposition of a coefficient matrix is completed and the solution to the equations can now be obtained by solving the following pair of equations:

$$[L]\{Y\} = \{Z\} \tag{3.5.11}$$

and

$$[U]\{X\} = \{Y\} \qquad (3.5.12)$$

where {Y} is introduced to facilitate the separation. In terms of the elements of the equations the solution is:

$$Y_1 = Z_1 \qquad (3.5.13)$$

$$Y_i = Z_i - \Sigma\ L_{ij}Y_j \qquad (3.5.14)$$

For i = 2, 3,....n. The Σ is over the range j = 1, 2, ... i-1.

and

$$X_n = Y_n/U_{nn} \qquad (3.5.15)$$

$$X_i = (Y_i - \Sigma\ U_{ij}X_j)/U_{ii} \qquad (3.5.16)$$

For i = n-1, n-2, ... 1. The Σ is over the range j = i+1, i+2 ..... n.

Equation 3.5.11 is called 'forward reduction' and Equation 3.5.12 is termed 'back substitution'.

3.6 Programming Remarks

A computer code 'FCREEP' or Flexibility creep analysis program, (with approximately 3000 Fortran statements) has been developed utilising the flexibility formulation in such a manner that the elastic and creep solutions are obtained from the same computer routines, the different solutions corresponding simply to different information to the routines. The following remarks can be made:

a. To solve the equation system the compact Crout's algorithm (vide section 3.5) together with a non-zero profile storage scheme is utililised (Zienkiewicz 1982 and Jennings 1966).

b. The flexibility matrices are formed and reduced only once for elastic (mechanical loading only) and thermal (temperature only) problems.

c. Dynamic field length allocation is implemented, i.e. small problems need less field length and will therefore be treated with a higher priority and lower costs in multiple programming mainframes, such as Cray at ULCC.

d. Single-subscript arrays are used throughout the program to enable vector dot product routines to be incorporated and thus improve the efficiency of the program.

e. Machine Independence - FCREEP is written in Fortran and maybe installed on a variety of machines ranging from mini-computers to super-computers.

f. All the section and volume integrals are evaluated numerically using Simpson's rule.

g. There is no limitation imposed on the size of the problems.

h. Stress profile plotting facilities are also available.

The operation of FCREEP program maybe considered in five distinct phases and these are illustrated diagrammatically in Figure 3.6.1. Further details of the program will be shown in a separate internal report (vide Appendix C).

3.7 Application of FCREEP Program

The two-span prestressed concrete beam, shown in Figure 3.7.1 together with beam dimensions, properties and loading, is used to illustrated the application of FCREEP program to various types of temperature cycling data:

a. Creep analysis with linear temperature distribution

The beam is subjected to an n-part temperature cycle of equal duration within the limits of two temperature states T_1 and T_2, Figure 3.7.2. These n-part discrete temperature states are used to approximate a continuous sinusoidal change of temperature from T_1 to T_2. Observations of the results indicate that adequate accuracy maybe obtained

with n=8, Figure 3.7.3. A cost study is also carried out and the results, Table 3.7.1, show that the cost is small for carrying out a creep analysis.

Stress distributions of the beam subjected to a 4-part temperature cycle of equal phase length at various sections are plotted to illustrated the long-term influence of creep and cyclic temperature on prestressed concrete beam structures, Figure 3.7.4 to Figure 3.7.7., and it can be observed that the effect can be dramatic. In some cases the stresses at the uppermost fibre can change from compressive to tensive, Figure 3.7.6.

b. Creep analysis with TRRL temperature cycle data

Section temperature distributions, based on field measurements and on approximate annual temperature cycle extracted from information in BS 5400, are obtained from computer generated data supplied by Miss M. Emerson (1980) of the Transport and Road Research Laboratory (TRRL). Typical 24 hour temperature cycles were provided for spring, summer, autumn and winter days. Temperatures at thirty-one equal spaced points along the vertical axis of a rectangular section at twenty minute intervals were generated.

The program run uses only those temperature distributions at 0200, 0800, 1400 and 2000 hours for a typical spring day. Each distribution is assumed to be constantly applied during a six hour phase of the cycle, Figure 3.7.8.

Stress distributions from the thermo-elastic and creep analyses at various section of the beam are plotted in Figure 3.7.9 to Figure 3.7.12. It can be observed that in the uppermost fibre of the beam, the stress change in phase 2 of the cycle from 3 MN/m^2 compressive in the initial thermo-elastic condition to 0.004 MN/m^2 compressive in the steady-state, Figure 3.7.11. Since the temperature cycle imposed does not exhibit particularly severe change in temperature gradient, the effect is significant.

3.8 Concluding Remarks and Recommendations

A creep-temperature flexibility formulation for beams is presented and a Fortran program 'FCREEP' has been developed based on the above theory and maybe utilised, with minimal cost, for design or analysis. FCREEP maybe run on microcomputers, minicomputers or mainframes.

It is concluded that creep in prestressed concrete structures under daily or seasonal fluctuations of temperature has a significant effect on their working stresses and they should be accounted for in design.

It is therefore recommended that the Codes of Practice BS 5400 should include explicit information relating to temperatures for different seasons and different times of day, together with theory and information on temperature-dependence of creep to enable designers to perform creep-temperature calculations.

Symbol	Thermo-elastic problem	Cyclic creep problem
α	Coefficients of thermal expansion.	Coefficient of thermal expansion.
T_d	Datum temperature.	Datum temperature.
T_i	ith temperature phase within a cycle.	ith temperature phase within a cycle.
$\Delta T(>0)$	$T_i - T_d$	$T_i - T_d$
σ_i	Thermo-elastic stress at ith phase.	steady-state stress at ith phase.
D	Elastic modulus E.	Analogous elastic modulus $T_a = \Sigma k_i T_i / \Sigma k_i$
A	Strain.	Strain rate.
B	Curvature.	Curvature rate.
ε_o	Initial strain: $\varepsilon_o = -\alpha \Delta T$	Analogous elastic initial strain (rate): $\varepsilon_o = -(\Sigma k_i T_i \sigma_{Ti}) / \Sigma k_i$ for $\sigma_{Ti} = \sigma_r - \sigma_i$
z	Upward coordinate with origin at centroid.	Upward coordinate with origin at centroid.

Table 3.3.1: Notations and their definitions.

Integral	Thermo-elastic problem	Cyclic creep problem
I_1	$\int bE\,dz$	$\int b/T_a\,dz$
I_2	$\int bEz\,dz$	$\int bz/T_a\,dz$
I_3	$\int bEz^2\,dz$	$\int bz^2/T_a\,dz$
I_4	$\int bE\epsilon_o\,dz$	$\int b\epsilon_o/T_a\,dz$
I_5	$\int bE\epsilon_o z\,dz$	$\int b\epsilon_o z/T_a\,dz$
p	$I_1I_3 - I_2^2$	$I_1I_3 - I_2^2$
a	I_1/p	I_1/p
b	$-I_2/p$	$-I_2/p$
d	$(I_2I_4 - I_1I_5)/p$	$(I_2I_4 - I_1I_5)/p$

Table 3.3.2: Integrals for flexibility formulation

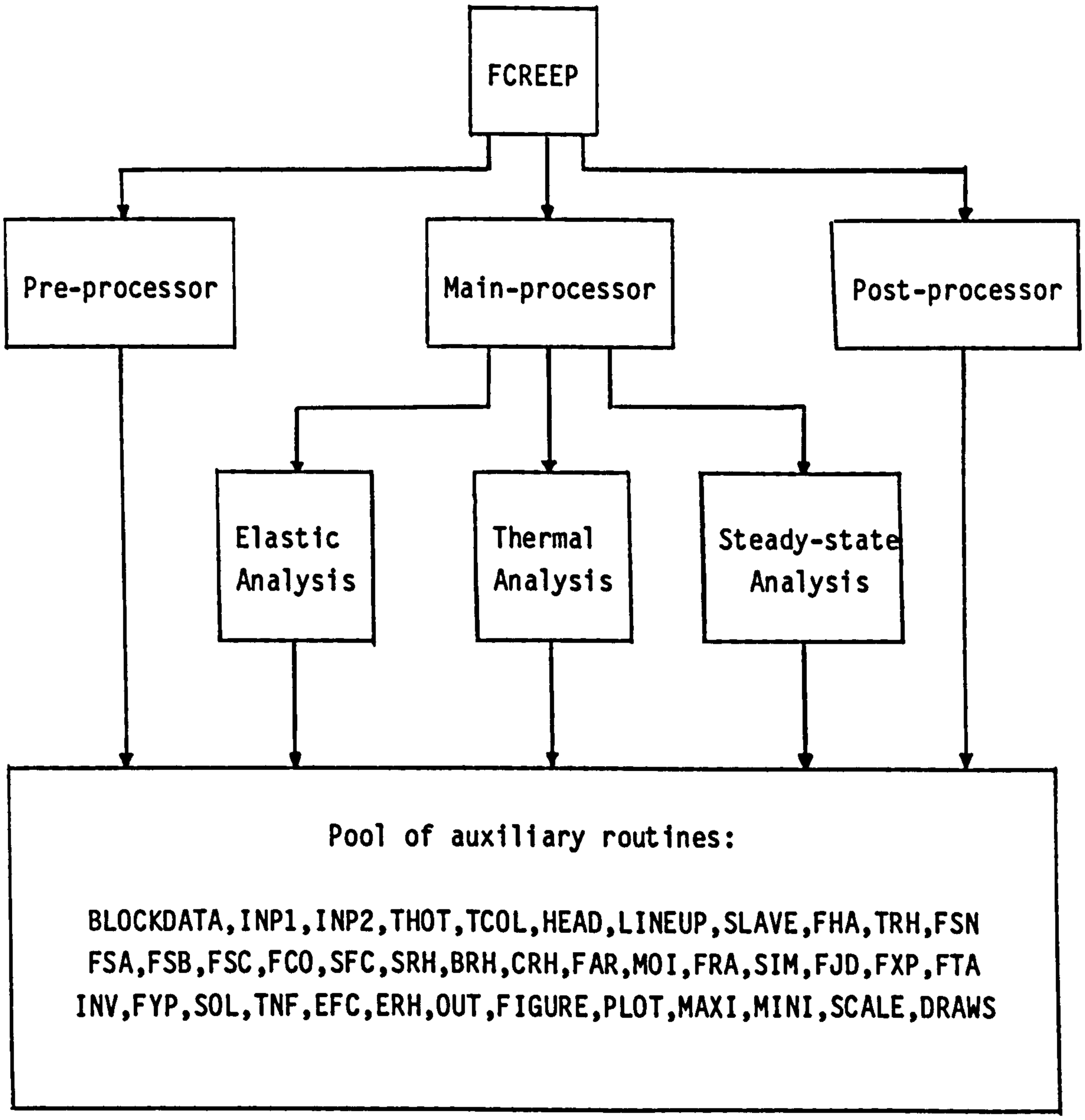

Figure 3.6.1: Macro flow chart for FCREEP

Solution Type	CP time (seconds)	Ratio = Other/Elastic sol
Pre-processing	2.2521	3856
Elastic	6.5380 x 10-3	1
Thermal per phase	3.5100 x 10-3	5.37
Steady-state per phase	8.8150 x 10-3	1.35
Post-processing	1.588	2429

Table 3.7.1: Cost comparison for a steady-state creep analysis

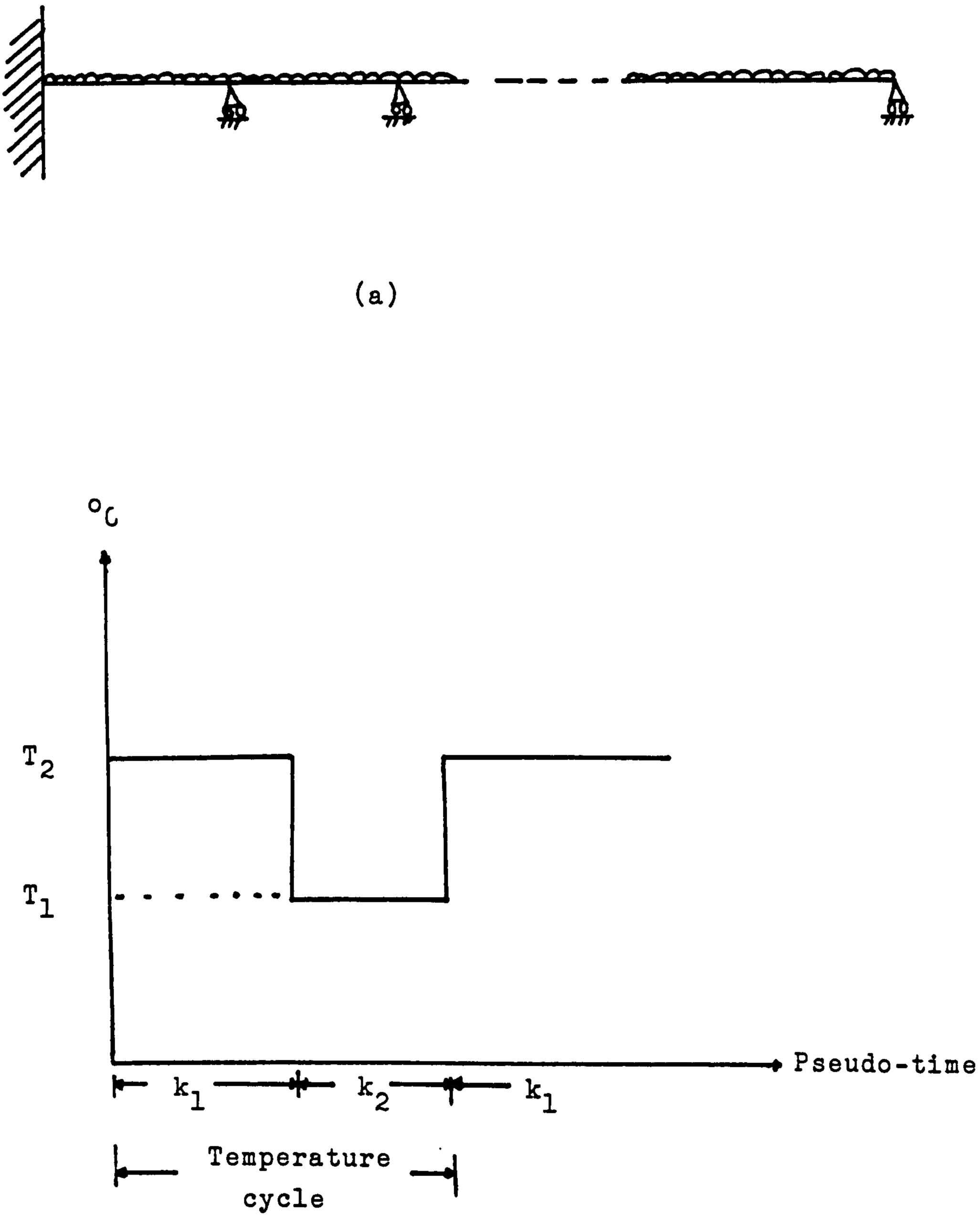

Figure 3.2.1: (a) A Beam on Co-linear Support
(b) Temperature cycle at a typical point within a cyclically heated structure

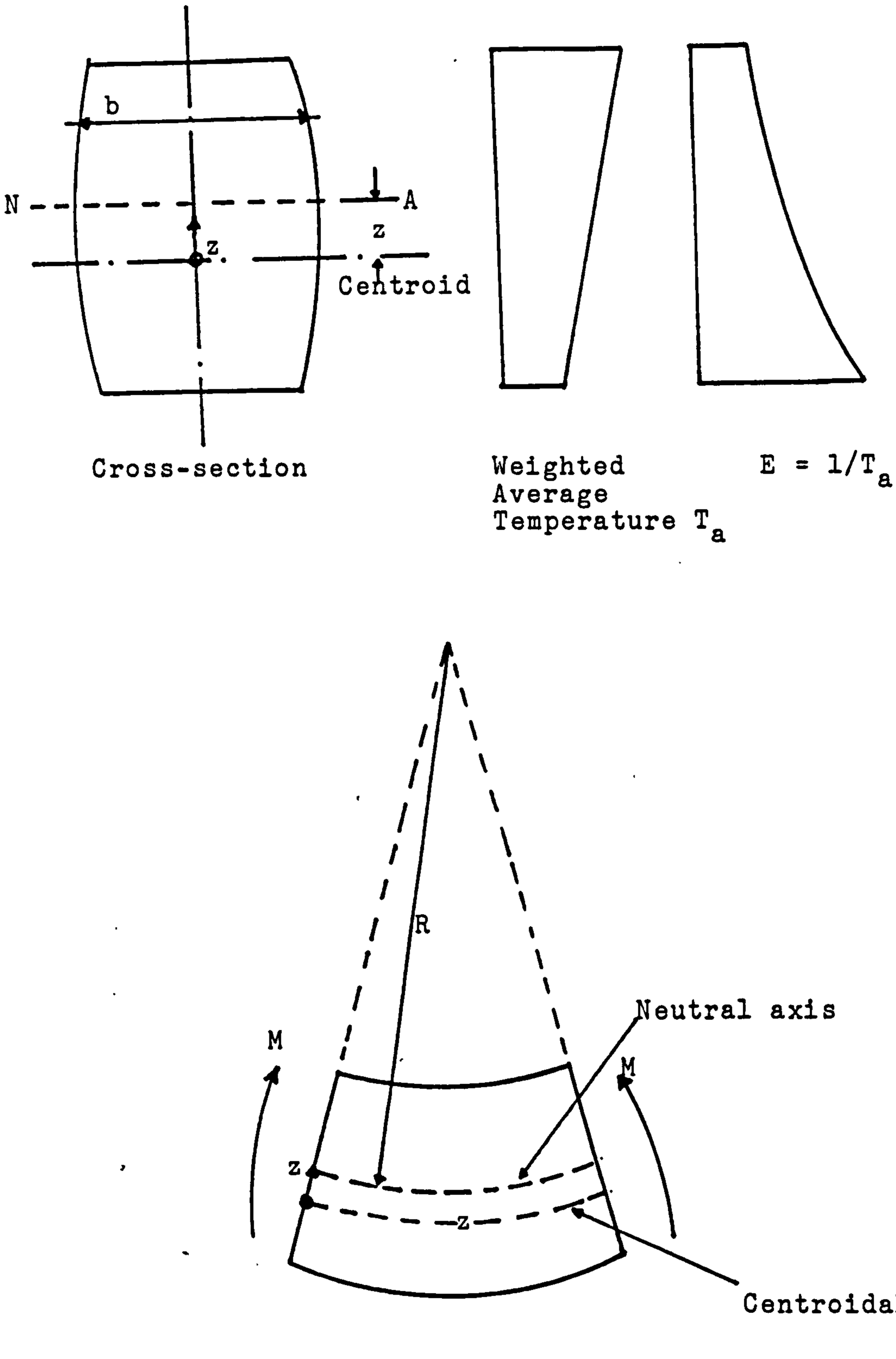

Figure 3.2.2 : A Non-Homogeneous Beam
(a) Cross-section and temperature details
(b) Section of beam in pure bending

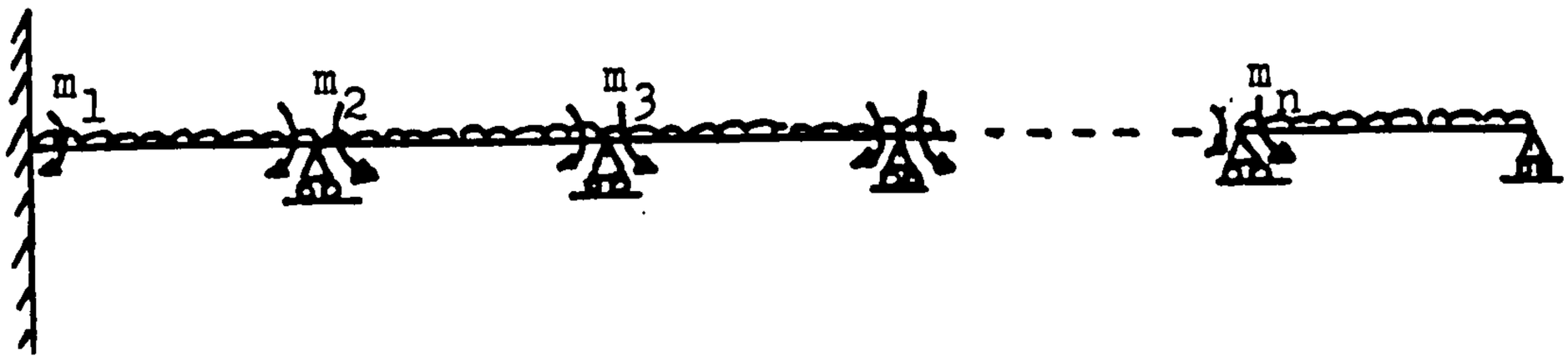

(a) Moments at the support are chosen as redundancies.

(b) M_0 diagram

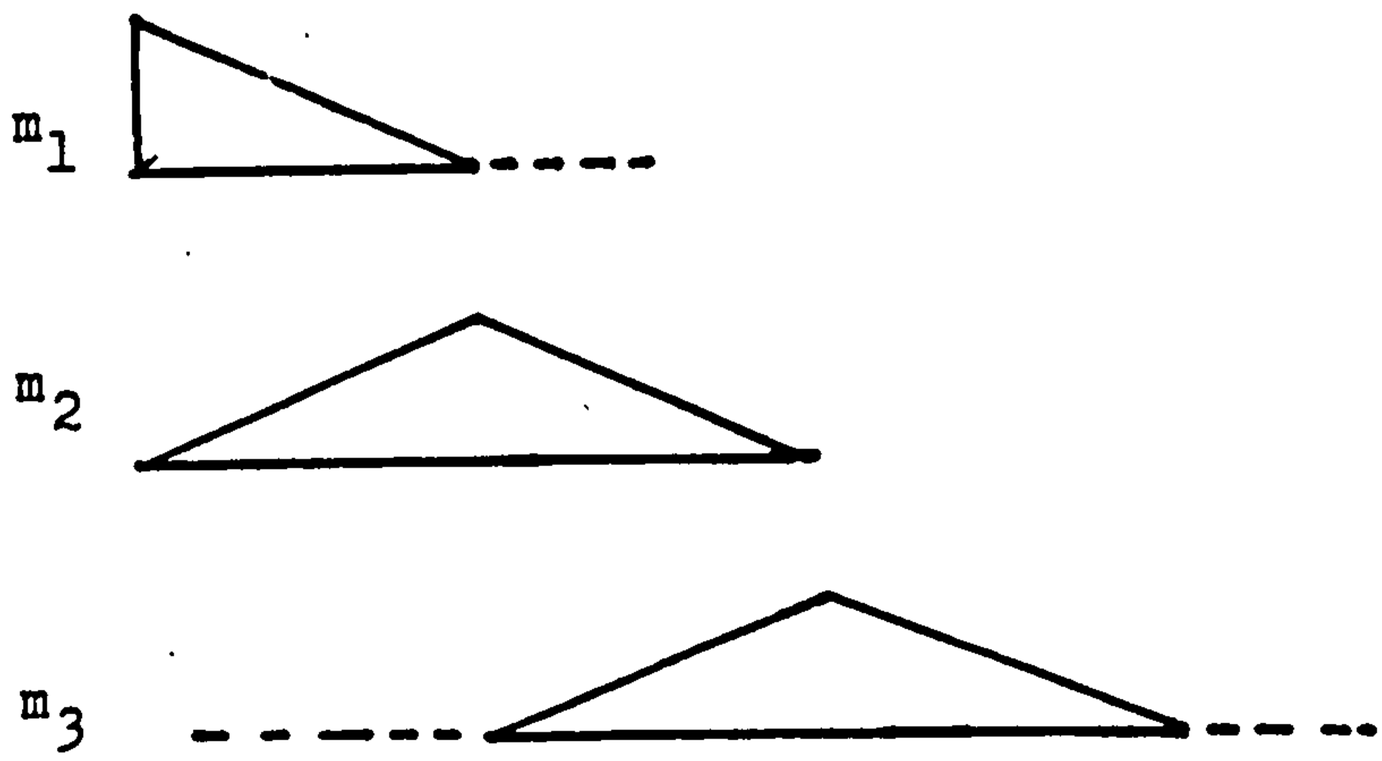

(c) m diagram

Figure 3.3.1: Release system.

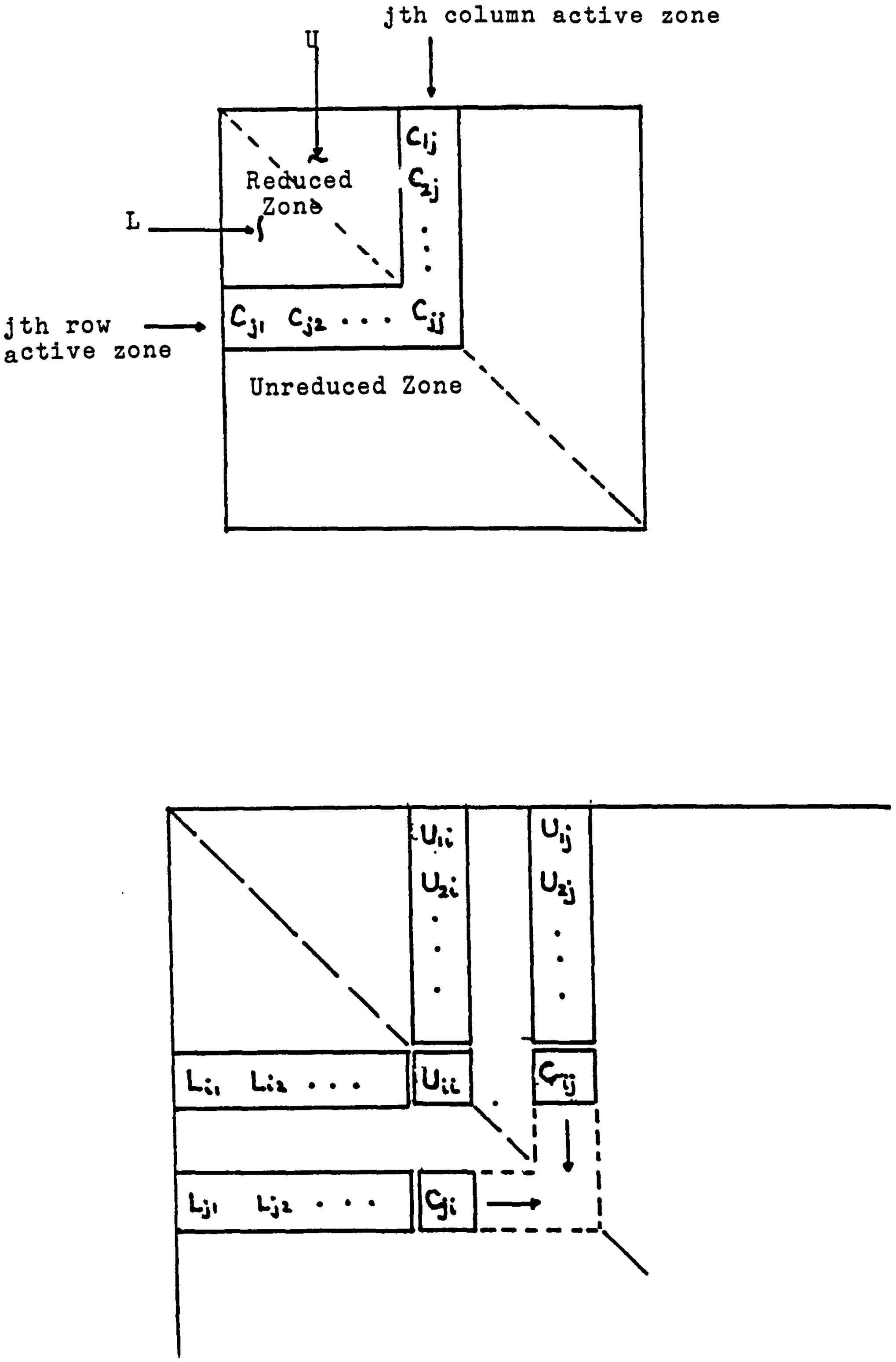

Figure 3.5.1: Triangular decomposition of the flexibility matrix.

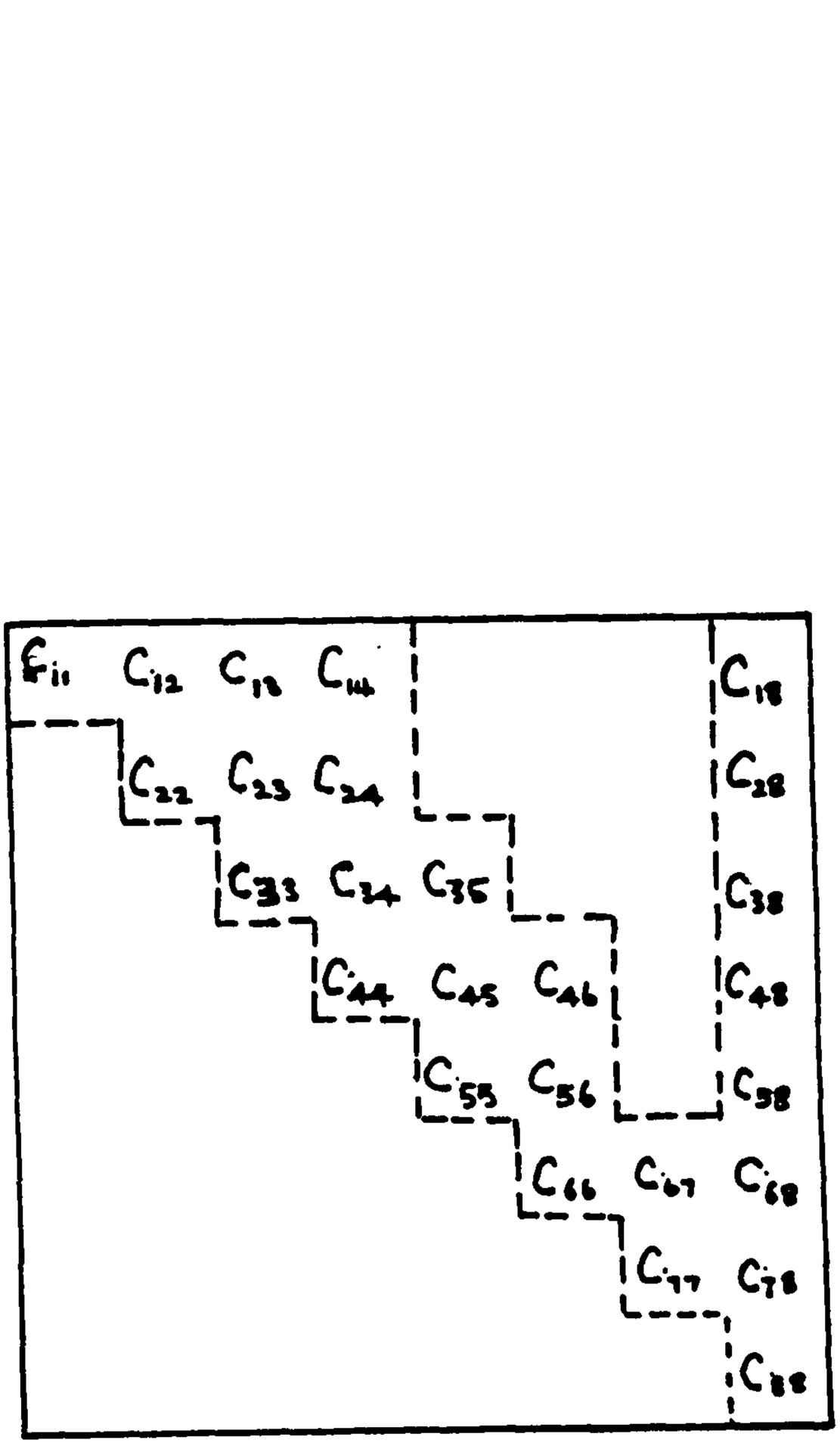

Flexibility Matrix

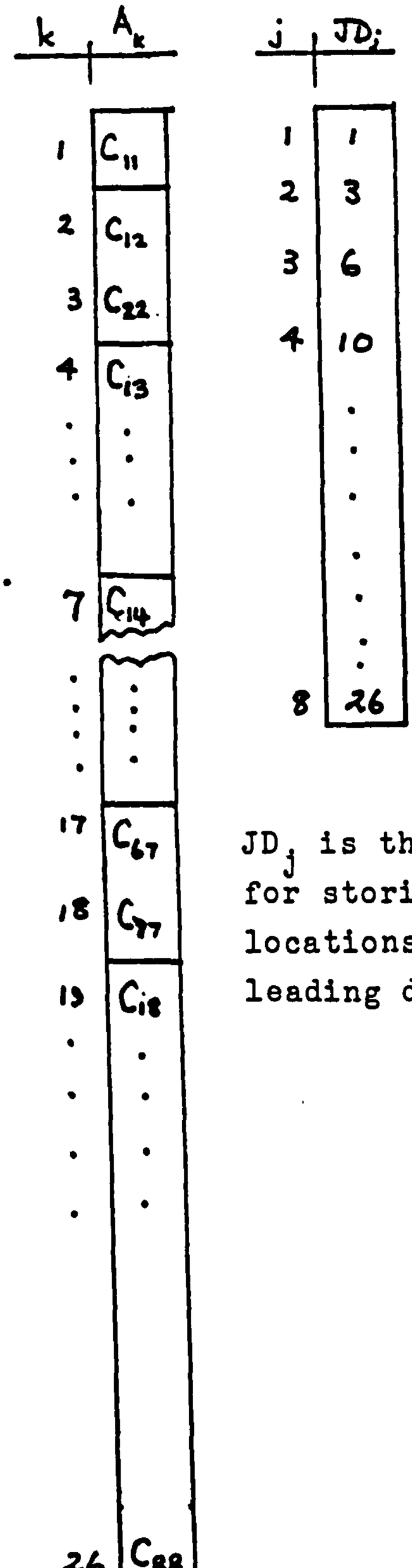

JD_j is the vector for storing the locations of the leading diagonals

A_k is the vector for storing the coefficients.

Figure 3.5.2: Profile storage scheme

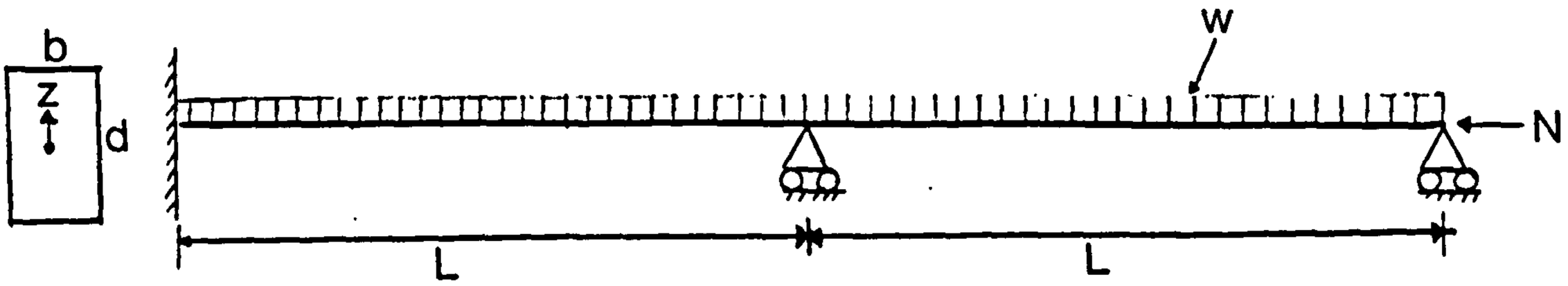

$w = 5.10^{-3}$ MN/m ; L = 10 m ; N = 1.5 MN_2; $\alpha = 12 \times 10^{-6}\ ^{o}C$
b = 0.3 m ; d = 0.5 m ; $E_m = 40000\ MN/m^2$

Figure 3.7.1: A two span beam

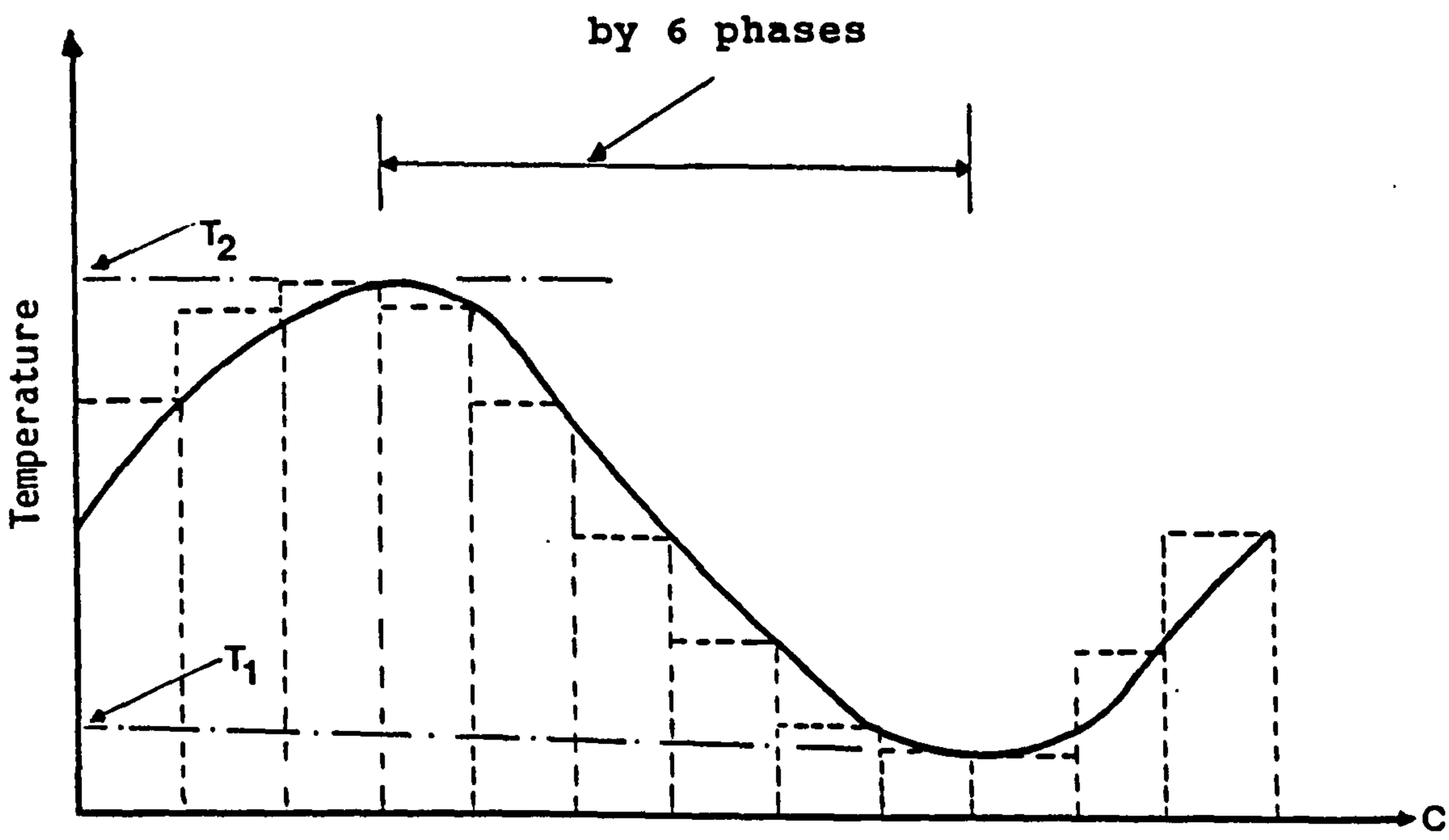

Figure 3.7.2: Approximation of a sinusoidal temperature cycle into discrete phases

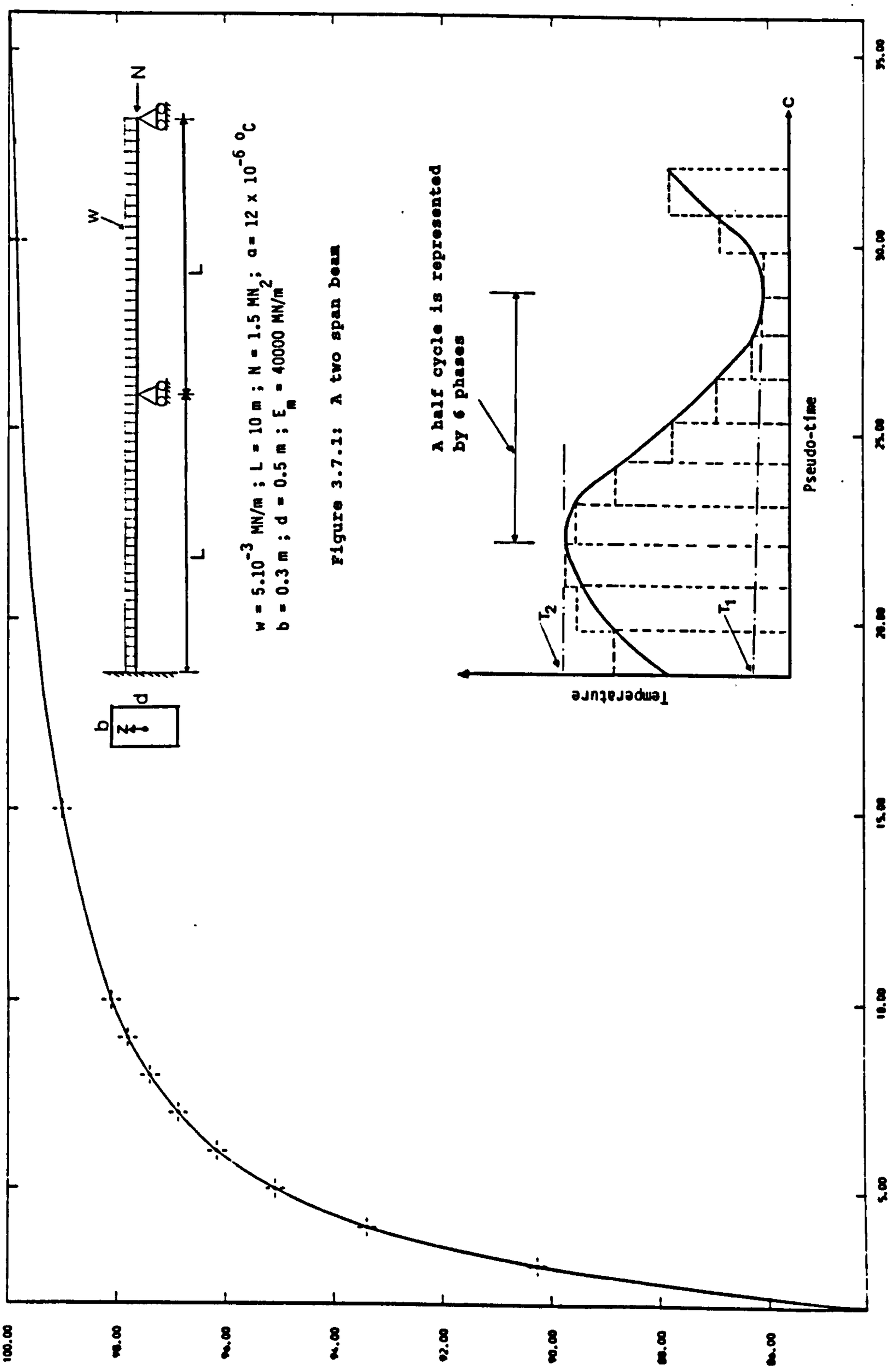

Figure 3.7.1: A two span beam

Figure 3.7.3: A solution accuracy vs degree of approximation plot

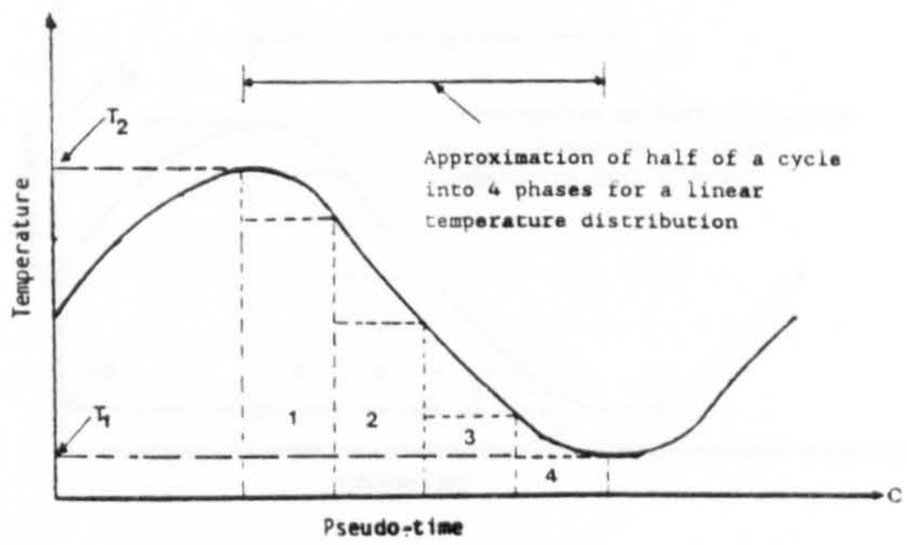

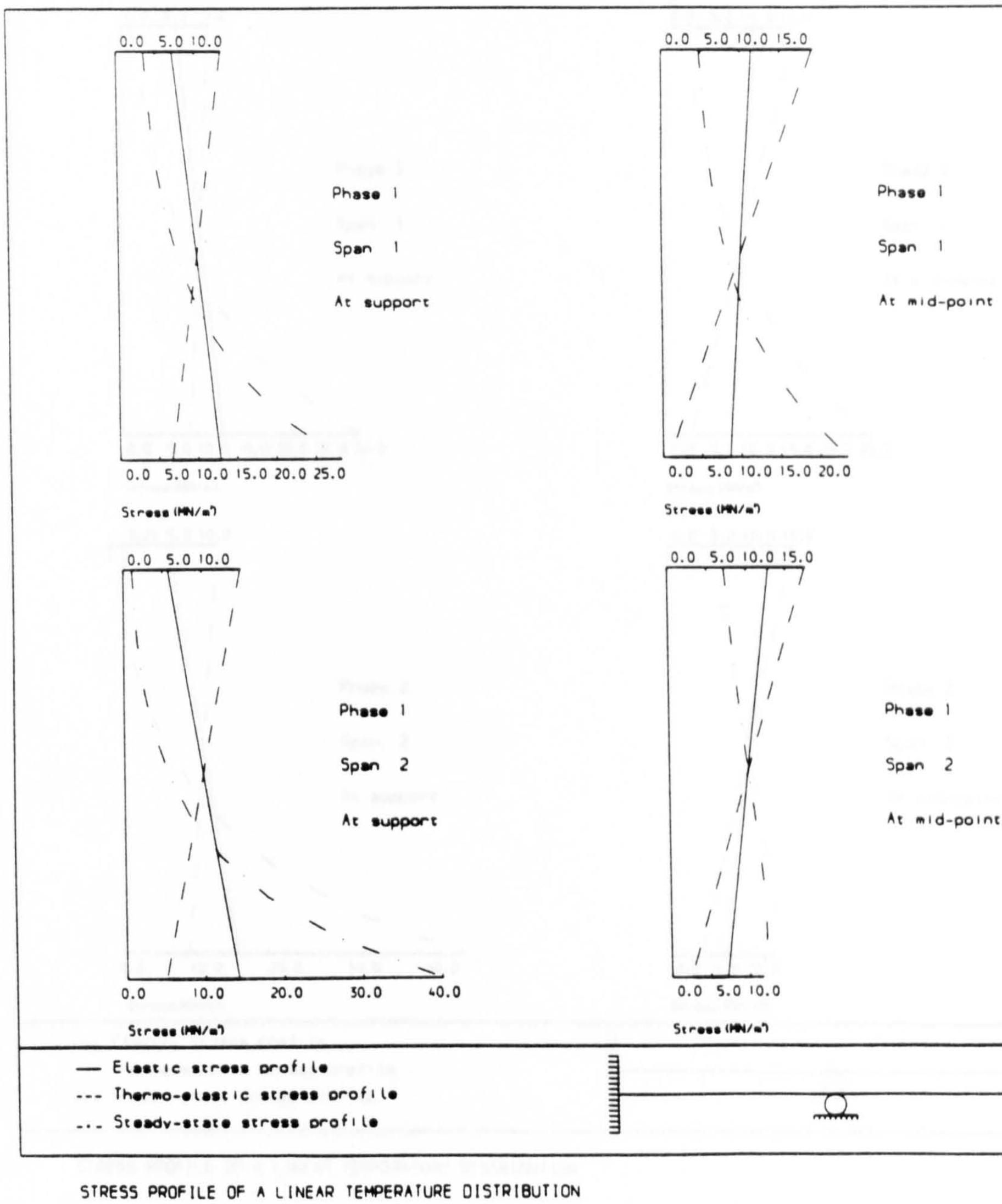

STRESS PROFILE OF A LINEAR TEMPERATURE DISTRIBUTION

Figure 3.7.4: Stress profile for linear temperature - phase 1 (n=4)

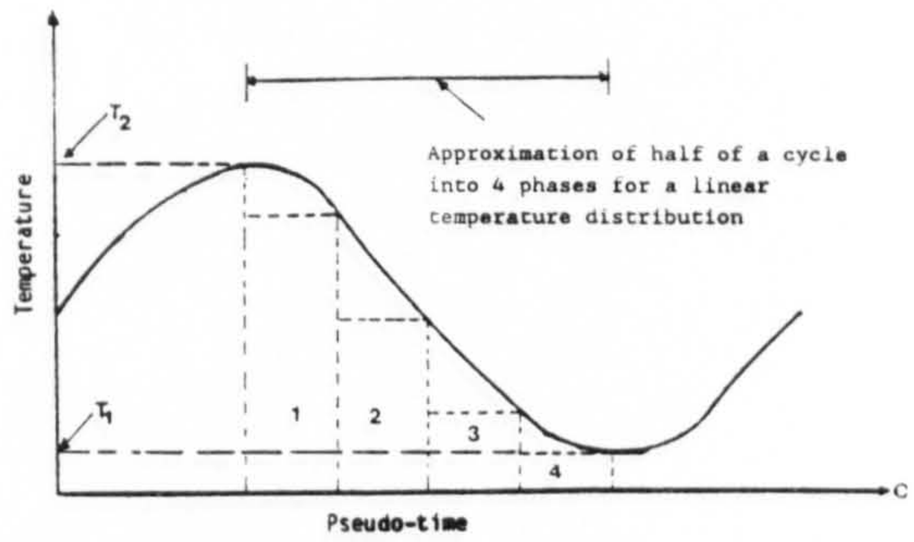

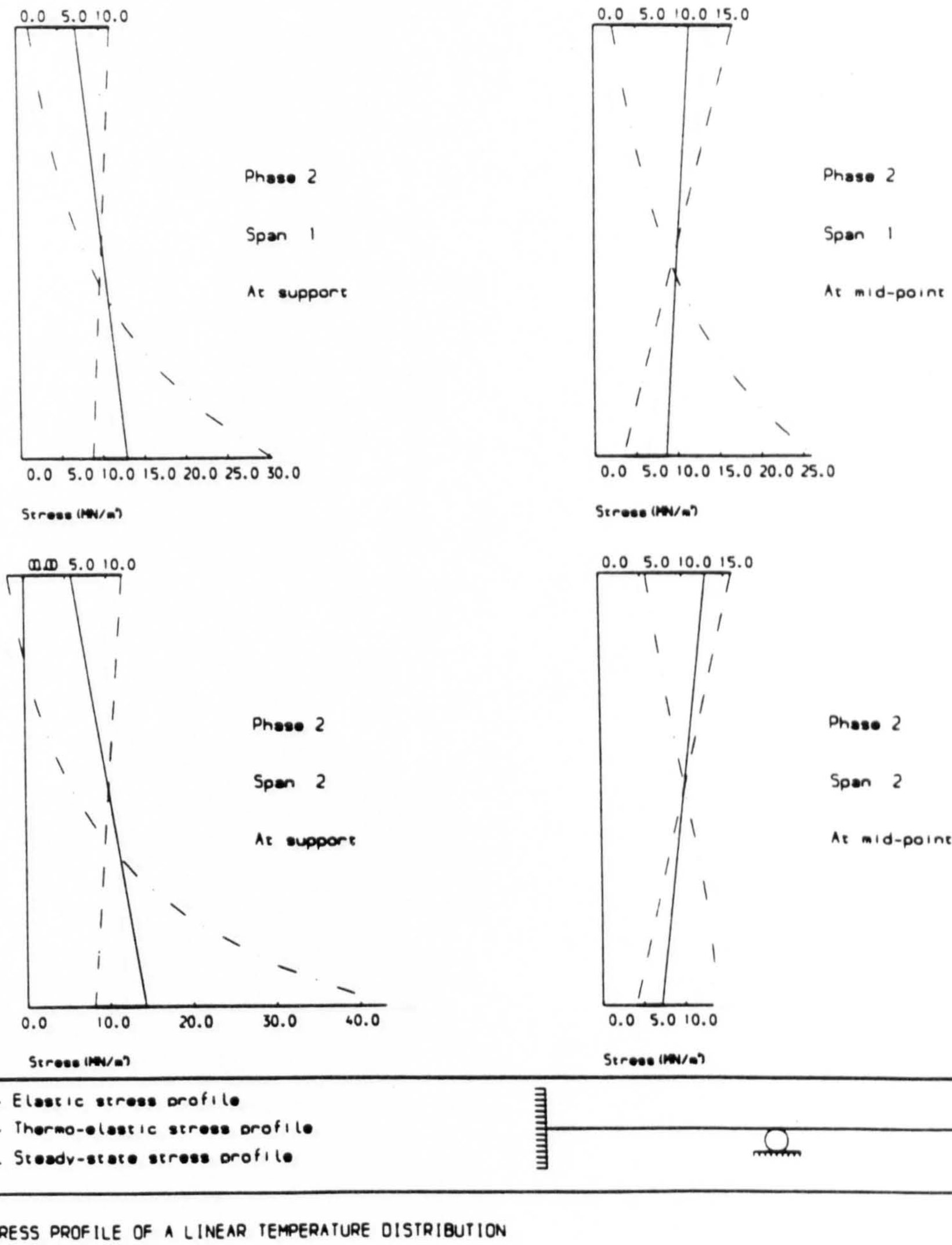

STRESS PROFILE OF A LINEAR TEMPERATURE DISTRIBUTION

Figure 3.7.5: Stress profile for linear temperature - phase 2 (n=4)

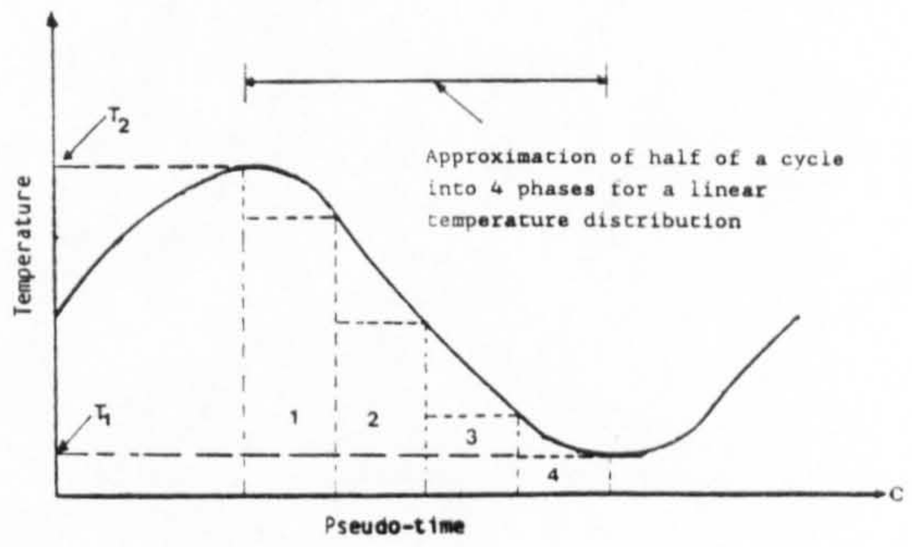

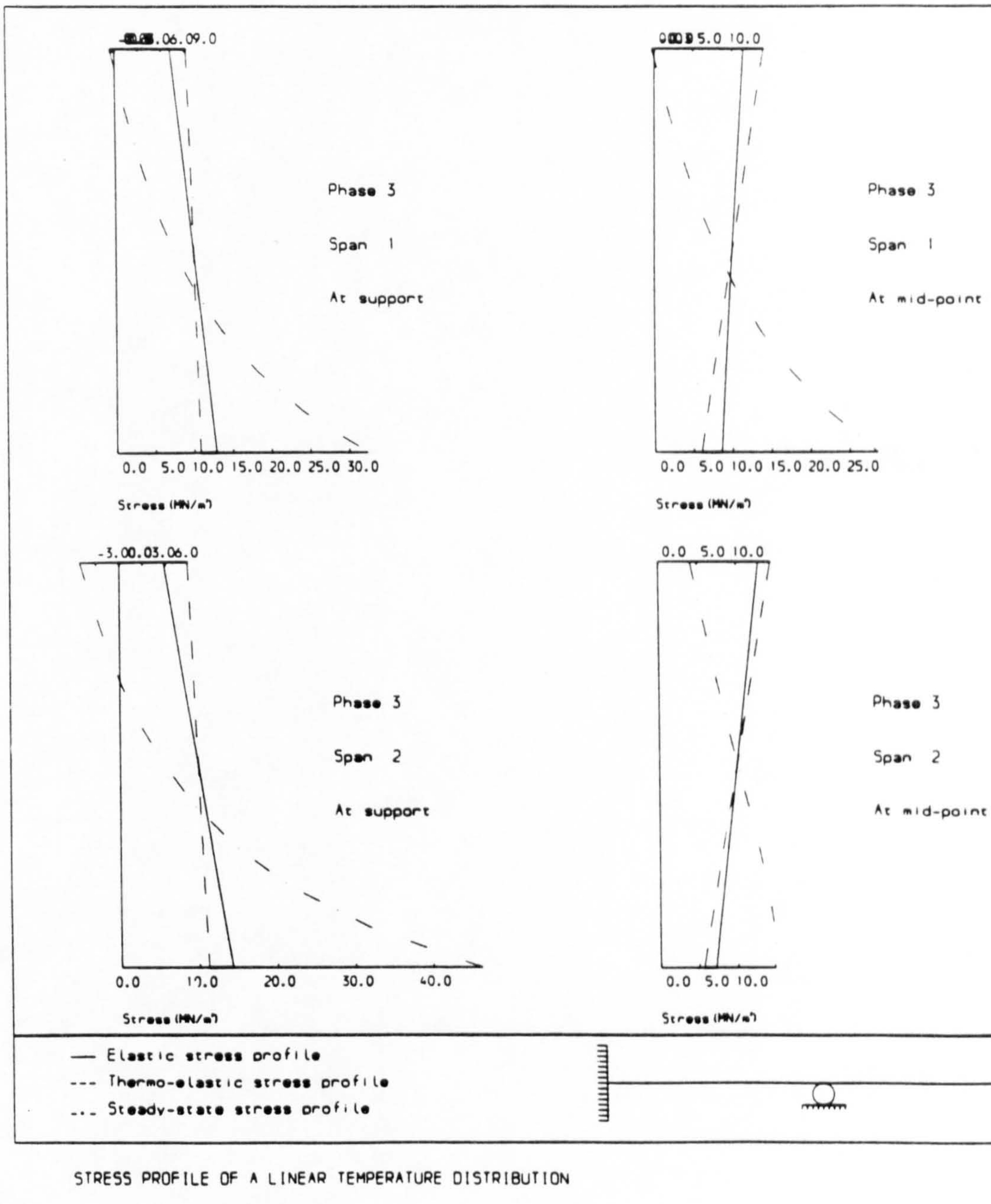

STRESS PROFILE OF A LINEAR TEMPERATURE DISTRIBUTION

Figure 3.7.6: Stress profile for linear temperature - phase 3 (n=4)

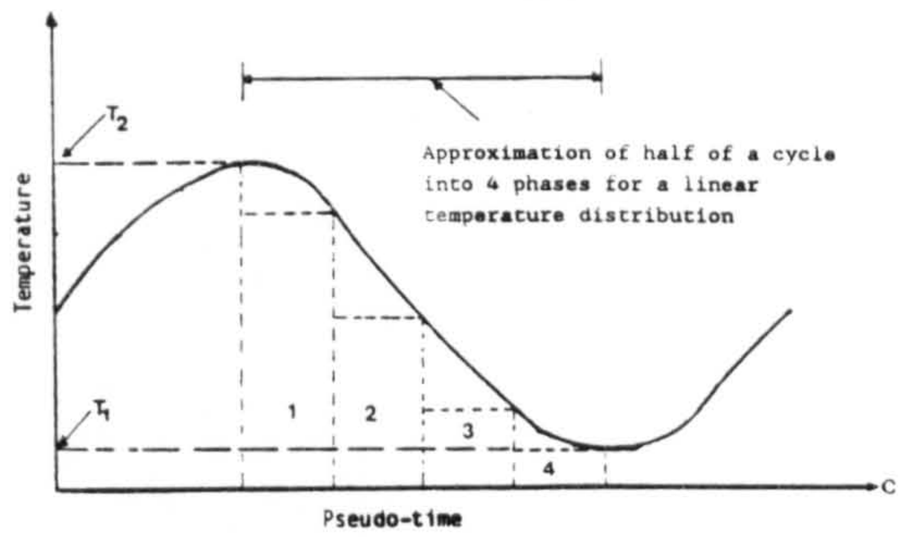

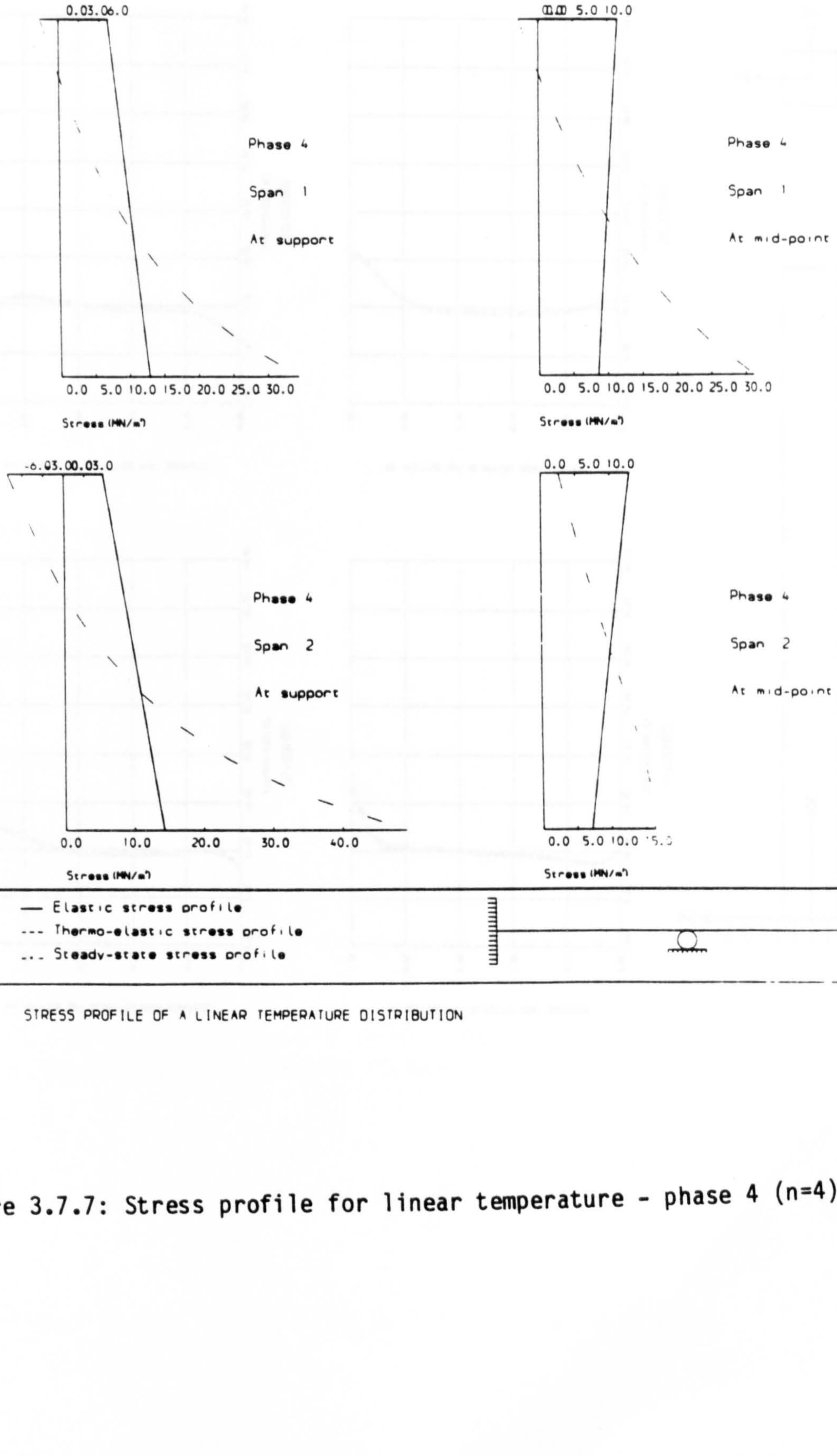

Figure 3.7.7: Stress profile for linear temperature - phase 4 (n=4)

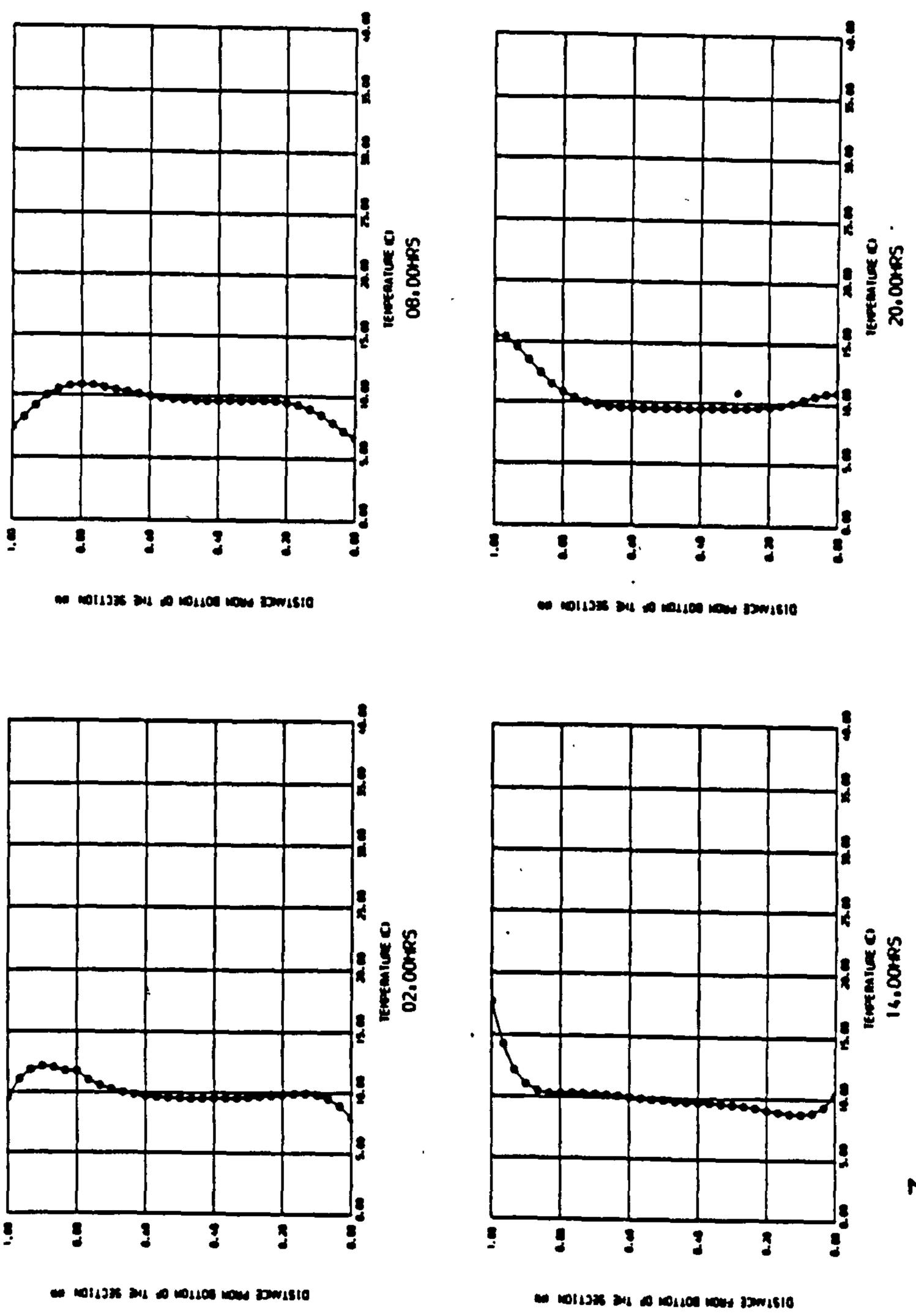

Figure 3.7.8: Temperature profile of a typical spring day (TRRL data)

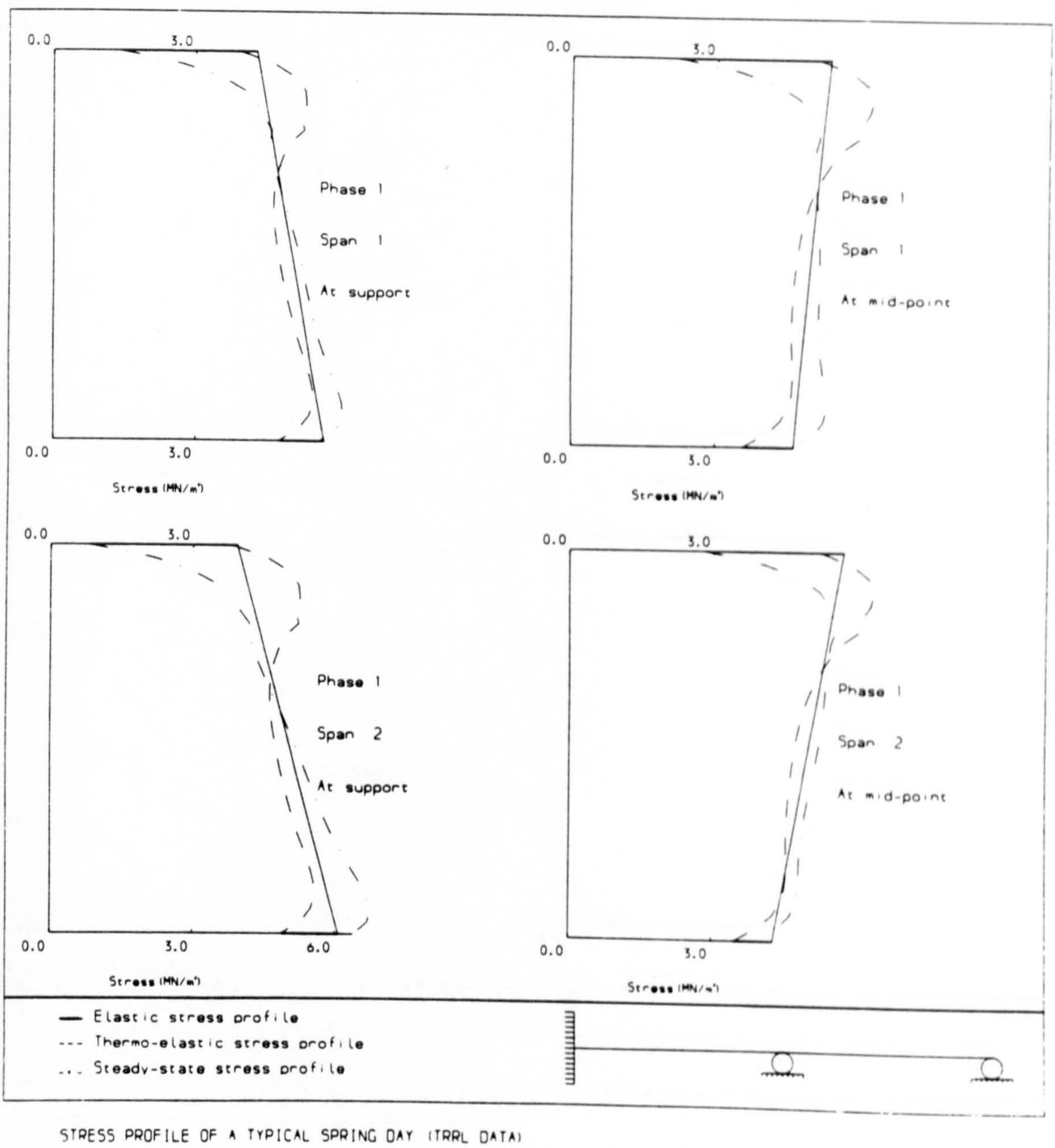

Figure 3.7.9: Stress profile for TRRL data - phase 1

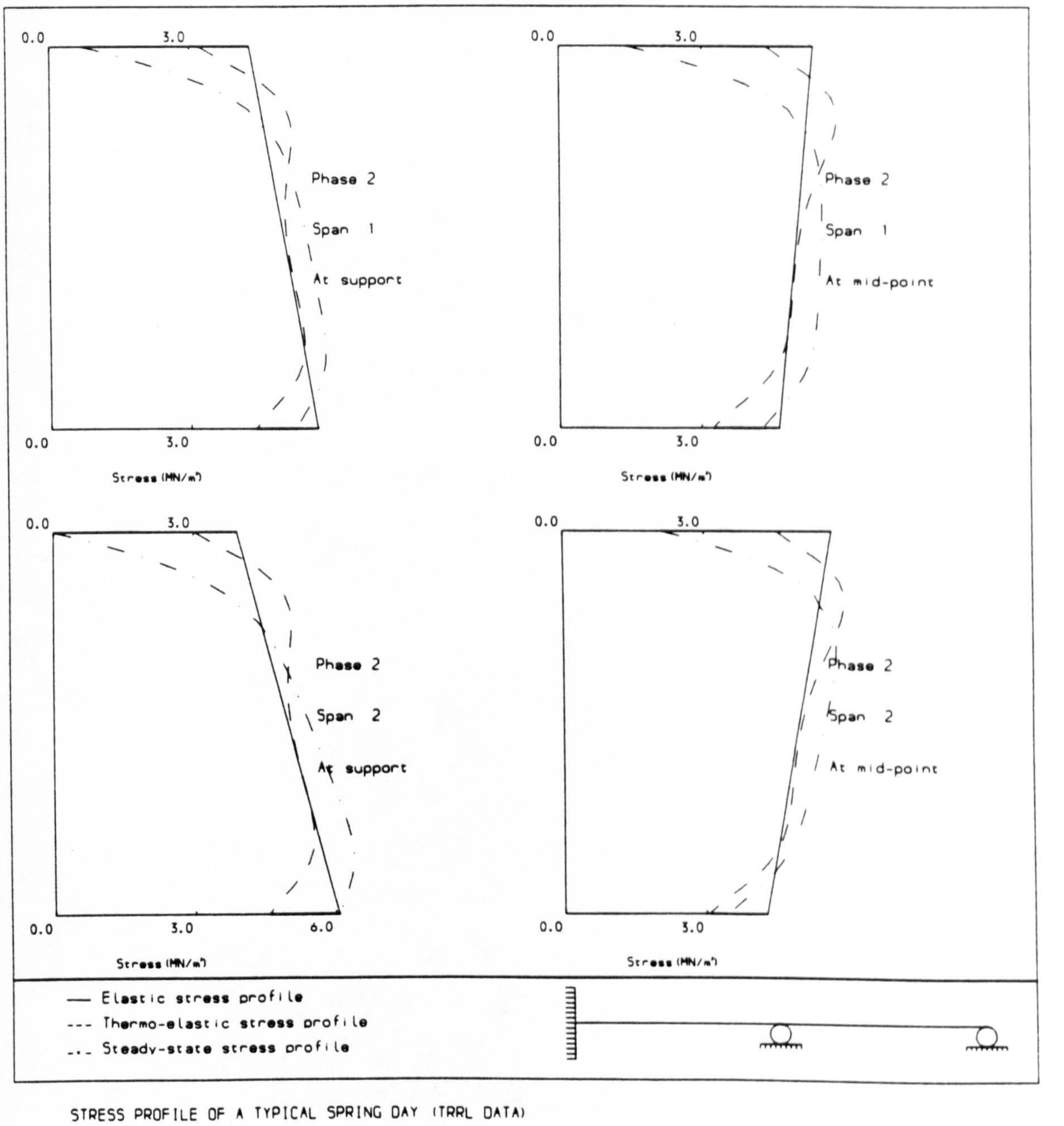

Figure 3.7.10: Stress profile for TRRL data - phase 2

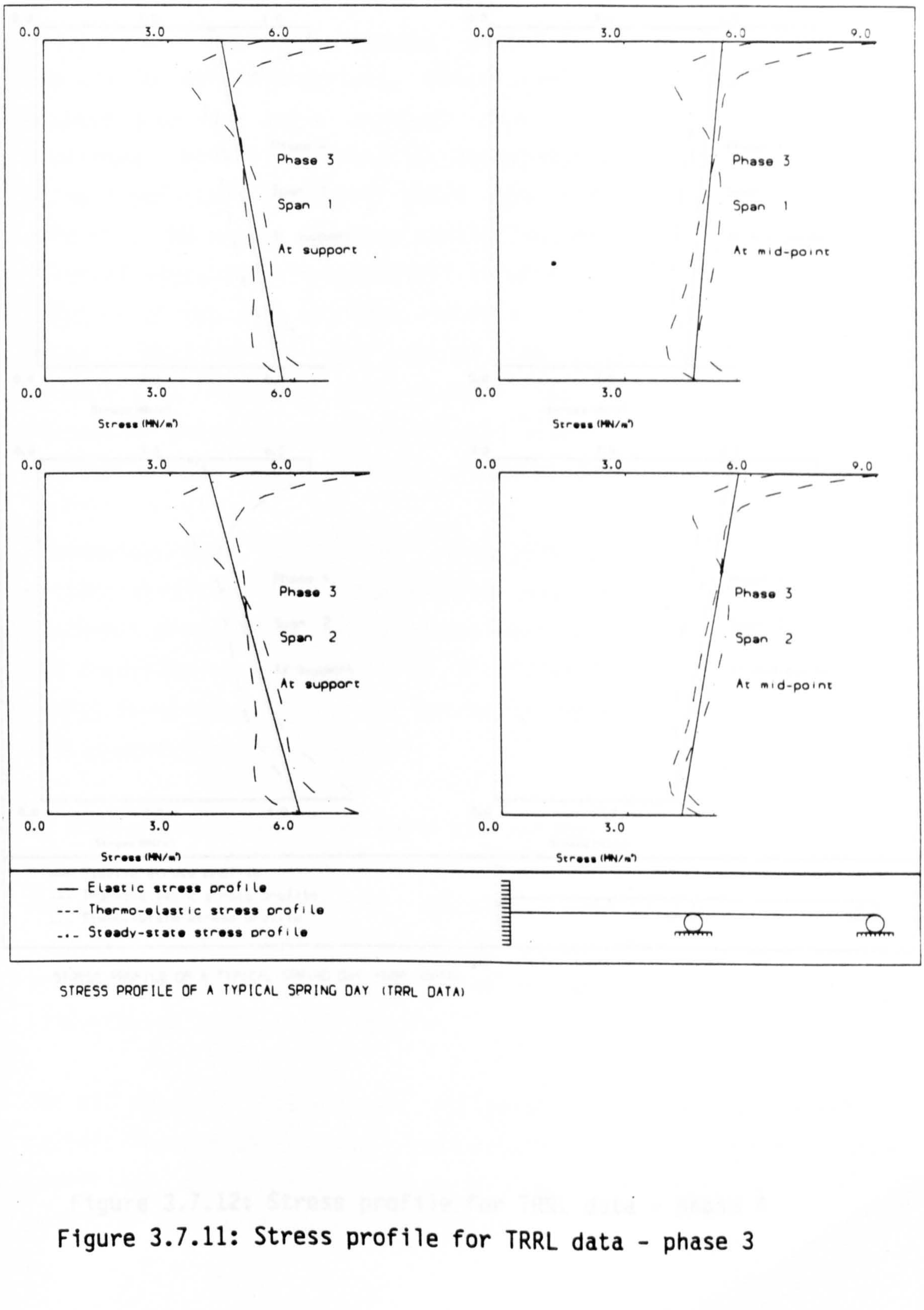

STRESS PROFILE OF A TYPICAL SPRING DAY (TRRL DATA)

Figure 3.7.11: Stress profile for TRRL data - phase 3

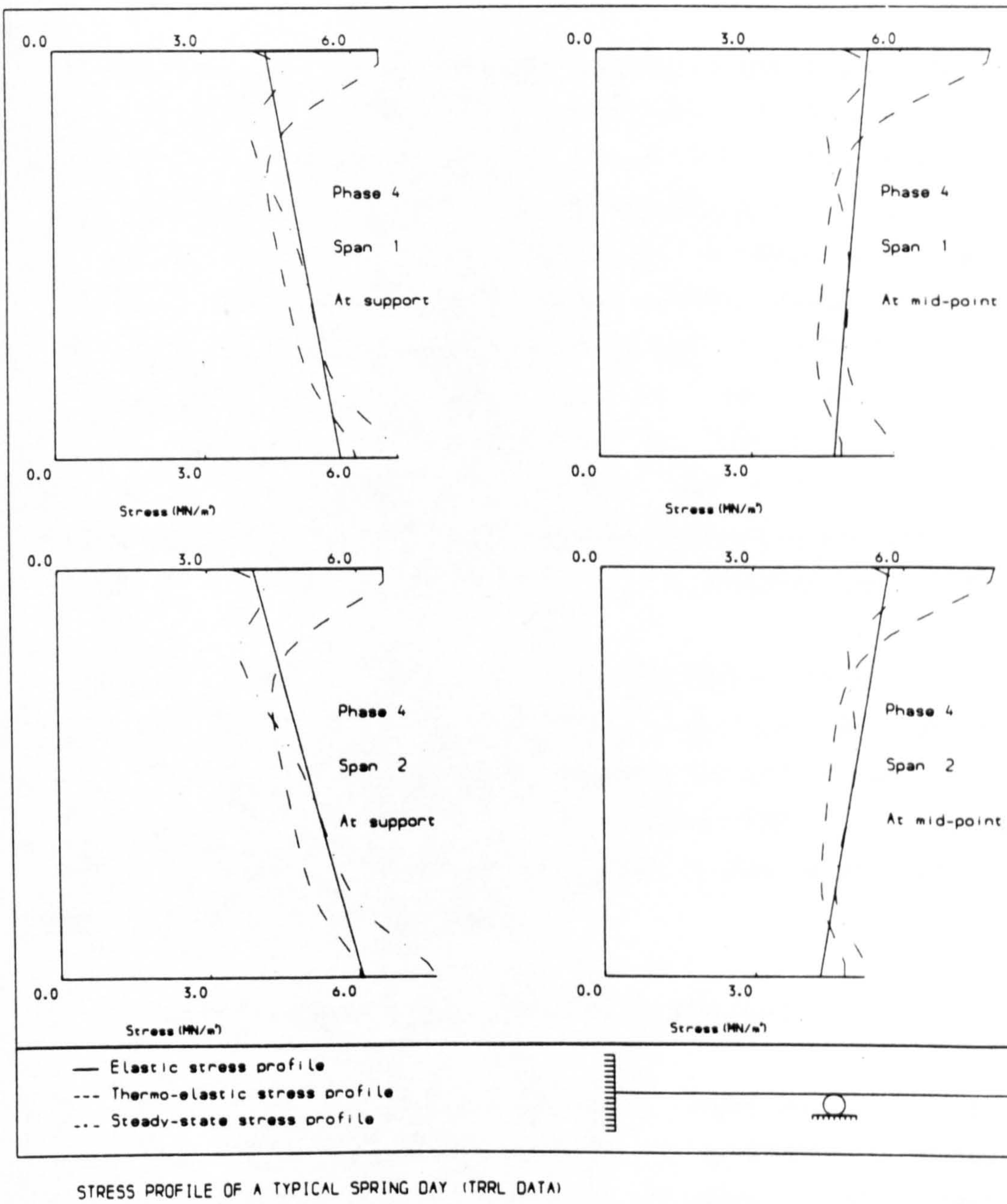

STRESS PROFILE OF A TYPICAL SPRING DAY (TRRL DATA)

Figure 3.7.12: Stress profile for TRRL data - phase 4

CHAPTER FOUR

THREE DIMENSIONAL FINITE ELEMENT STEP-BY-STEP ANALYSIS FOR LINEAR CREEP PROBLEMS

Summary

Principles of the finite element method in the displacement formulation are briefly summarised. Description of a step-by-step finite element algorithm and a computer code for linear creep problems is presented. The full solution is accomplished in a step-by-step manner using time intervals during which the stresses are taken to remain constant. The change of creep strain taking place during such a time interval leads to an incompatibility which is corrected by an elastic solution at the end of each interval. The elastic solution at any stage is obtained by the use of the finite element method. The procedure is repeated until either the final solution sought is reached or until steady-state stress distributions are obtained. The constant strain finite element is used to discretised the continuum.

A computer code 'SSCREEP' or Step-by-Step CREEP analysis program is written utilising the step-by-step algorithm and applied to some benchmark problems to enable an engineering and economic evaluation of the algorithm to be made. It is concluded that while the algorithm is useful in general, it can be extremely expensive and overtax even the most powerful modern computers.

4.1 A Brief Description of the Finite Element Method

The finite element method of solution reported here for the development of a creep program represents a systematic procedure for the implementation of the Principle of Minimum Total Potential Energy (Zienkiewicz 1982) which states:

'Of all possible displacement configurations a body can assume which satisfy compatibility and the constraints or kinematic boundary conditions, the configuration satisfying equilibrium makes the total potential energy assumes a minimum value.'

Consider a general three dimensional continuum, the potential energy, Ω, is given as the sum of the internal strain energy and work contributions of body forces and distributed surface loads viz:

$$\Omega = \tfrac{1}{2}\int \{\sigma\}^T\{\varepsilon\}dV - \int \{a'\}^T\{p\}dV - \int \{a'\}^T\{q\}dS \quad (4.1.1)$$

where $\{\sigma\}$ and $\{\varepsilon\}$ are stress and strain vectors respectively, $\{a'\}$ are displacements at any point, $\{p\}$ are body forces per unit volume and $\{q\}$ are applied surface tractions.

In the finite element displacement method, the displacement is assumed to have unknown values only at nodal points, so that the variation within any element, $\{a'\}$, is described in terms of nodal values by means of interpolation functions:

$$\{a'\} = [N]\{a^e\} \quad (4.1.2)$$

where $[N]$ is the set of interpolation functions termed the shape functions and $\{a^e\}$ is the vector of nodal displacements of the element. Thus

$$\{a^e\} = \{\{a'_1\} \ldots \{a'_n\}\}^T$$
$$\{a'_i\} = \{u'_i\ v'_i\ w'_i\}^T \quad (4.1.3)$$

Where n is the number of nodes per element. Strains within the element can be expressed in terms of element nodal displacements as:

$$\{\varepsilon\} = [[B_1], [B_2], \ldots\ldots [B_n]]\{a^e\} \quad (4.1.4)$$

where $[B]$ is the strain matrix generally composed of shape function derivatives viz:

$$[B_i] = \begin{bmatrix} \partial N_i/\partial x & 0 & 0 \\ 0 & \partial N_i/\partial y & 0 \\ 0 & 0 & \partial N_i/\partial z \\ \partial N_i/\partial y & \partial N_i/\partial x & 0 \\ 0 & \partial N_i/\partial z & \partial N_i/\partial y \\ \partial N_i/\partial z & 0 & \partial N_i/\partial x \end{bmatrix} \quad (4.1.5)$$

Finally stresses $\{\sigma\}$ maybe related to strains by use of an elasticity matrix [D] as follows:

$$\{\sigma\} = [D](\{\varepsilon\} - \{\varepsilon_o\}) + \{\sigma_o\} \qquad (4.1.6)$$

with complete anisotropy, the [D] matrix relating six stress components to strain components can contain 21 independent constants (Zienkiewicz 1982). Although no difficulty presents itself in computation when dealing with such materials, since the multiplication will never be carried out explicitly, it is convenient to recapitulate here the [D] matrix for an isotropic material. In terms of elastic modulus E and Poisson's ratio v, [D] can be written as:

$$[D] = v3\begin{bmatrix} 1 & v1 & v1 & 0 & 0 & 0 \\ v1 & 1 & v1 & 0 & 0 & 0 \\ v1 & v1 & 1 & 0 & 0 & 0 \\ 0 & 0 & 0 & v2 & 0 & 0 \\ 0 & 0 & 0 & 0 & v2 & 0 \\ 0 & 0 & 0 & 0 & 0 & v2 \end{bmatrix} \qquad (4.1.7)$$

where v1=v/v4 ; v2=v6/2v4 ; v3=(Ev4)/(v5v6)
v4=(1-v) ; v5=(1+v) ; v6=(1-2v)

And $\{\varepsilon_o\}$ and $\{\sigma_o\}$ are initial strain and stress vectors respectively.

Provided the element shape functions have been chosen so that no singularities exist in the integrands of the functional, the total potential energy of the continuum will be the sum of energy contributions of individual elements. Thus,

$$\Omega = \Sigma\ \Omega^e \qquad (4.1.8)$$

where Ω^e represents the total potential energy of element e which, on use of equation 4.1.1 can be written as:

$$\Omega^e = -\tfrac{1}{2}\int \{a^e\}^T[B]^T[D][B]\{a^e\}\ dV$$

$$- \int \{a^e\}^T[N]^T\{p\}dV - \int \{a^e\}^T[N]^T\{q\}dS \qquad (4.1.9)$$

where dV is the integration over the element volume and dS is the

integration over the loaded element surface area. Minimisation for element e with respect to the nodal displacements $\{a^e\}$ for the element results:

$$\frac{\partial \Omega^e}{\partial a^e} = \int [B]^T[D][B]\{a^e\}dV - \int [N]^T\{p\}dV - \int [N]^T\{q\}dS \qquad (4.1.10)$$

Utilising equation 4.1.5, equation 4.1.10 can be written in a general form:

$$\frac{\partial \Omega^e}{\partial a^e} = \int [B]^T[D][B]\{a^e\}dV - \int [N]^T\{p\}dV - \int [N]^T\{q\}dS - \int [B]^T[D]\{\varepsilon_o\}dV + \int [B]^T\{\sigma_o\}dV \qquad (4.1.11)$$

$$= [K^e]\{a^e\} - (\{F_q{}^e\} + \{F_p{}^e\} + \{F_{\varepsilon o}{}^e\} - \{F_{\sigma o}{}^e\})$$

$$= [K^e]\{a^e\} - \{F^e\} \qquad (4.1.12)$$

$\{F^e\}$ is termed the equivalent nodal forces vector for the element and $[K^e]$ is called the element stiffness matrix. Summation of terms in equation 4.1.12 over all elements, when equated to zero as dictated by the Principle of Minimum Total Potential, results in a system of equilibrium equations for the complete continuum viz:

$$[K]\{\delta\} = \{F\} \qquad (4.1.13)$$

The equations are often solved by any standard technique (vide section 4.4) to yield nodal displacements. Basic steps for deriving a finite element solution to an structural problem can be summarised as shown in Figure 4.1.1.

4.2 Element Characteristics

In this chapter the simplest type of elements, namely the constant

strain family (Zienkiewicz 1982) over which strains are assumed to be constant, is implemented.

a. Two dimensional analysis:

Figure 4.2.1 shows a typical two-dimensional element implemented, with nodes i, j, m numbered in an anti-clockwise manner. The shape function [N] is a linear one viz:

$$\begin{Bmatrix} u' \\ v' \end{Bmatrix} = [N]\{a^e\}$$

$$= [[I]N_i, [I]N_j, [I]N_m]\{a^e\} \qquad (4.2.1)$$

where [I] is a 2x2 identity matrix and typically,

$$N_i = (a'_i + b'_i x + c'_i y)/2\Lambda \qquad (4.2.2)$$

Where a'_i, b'_i, c'_i are interpolation constants and Λ is the area of the elementary triangle, i.e.:

$$2\Lambda = \begin{vmatrix} 1 & x_i & y_i \\ 1 & x_j & y_j \\ 1 & x_m & y_m \end{vmatrix} \qquad (4.2.3)$$

and

$$\begin{aligned} a'_i &= x_i y_m - x_m y_j \\ b'_i &= y_j - y_m \\ c'_i &= x_m - x_j \end{aligned}$$

with N_j, N_m and other coefficients obtained by a cyclic permutation of subscripts in the order i, j, m.

b. Axisymmetric analysis:

In the case of axisymmetric analysis, the element used is that defined by a torus of triangular sections with nodes i, j, m shown in Figure 4.2.2. By symmetry, two components of displacements in any plane

section of the body along its axis of symmetry define completely the state of strain and, therefore the state of stress. Indeed the situation is two-dimensional and the same displacements functions described in section 4.2(a) can be used to define displacements within the triangular element i, j, m shown. The volume of material associated with an element is now that of a body of revolution and all integrations have to refer to this. It should be noted that the strain matrix becomes:

$$[B_i] = \begin{bmatrix} \partial N_i/\partial r & 0 \\ 0 & \partial N_i/\partial z \\ N_i/r & 0 \\ \partial N_i/\partial r & \partial N_i/\partial z \end{bmatrix} \qquad (4.2.5)$$

c. Three dimensional analysis:

In practice situations arise in which a full three dimensional analysis is required. A suitable three dimensional element is a tretrahedron which has four nodal corners i, j, m, p in space defined by the x, y, z coordinates, Figures 4.2.3 and 4.2.4. The displacement functions can be written as:

$$\begin{Bmatrix} u' \\ v' \\ w' \end{Bmatrix} = [[I]N_i, [I]N_j, [I]N_m, [I]N_p]\{a^e\} \qquad (4.2.6)$$

where [I] is a 3x3 identity matrix and with shape functions defined as:

$$N_i = (a'_i + b'_i x + c'_i y + d'_i z)/6V^e \qquad (4.2.7)$$

where a'_i, b'_i, c'_i, d'_i are interpolation constants, and the value V^e represents the volume of the tetrahedron:

$$6V^e = \begin{vmatrix} 1 & x_i & y_i & z_i \\ 1 & x_j & y_j & z_j \\ 1 & x_m & y_m & z_m \\ 1 & x_p & y_p & z_p \end{vmatrix} \qquad (4.2.8)$$

By expanding other relevant determinants into their cofactors we have:

$$a'_i = \begin{vmatrix} x_j & y_j & z_j \\ x_m & y_m & z_m \\ x_p & y_p & z_p \end{vmatrix}$$

$$b'_i = -\begin{vmatrix} 1 & y_j & z_j \\ 1 & y_m & z_m \\ 1 & y_p & z_p \end{vmatrix}$$

(4.2.9)

$$c'_i = \begin{vmatrix} x_j & 1 & z_j \\ x_m & 1 & z_m \\ x_p & 1 & z_p \end{vmatrix}$$

$$d'_i = -\begin{vmatrix} x_j & y_j & 1 \\ x_m & y_m & 1 \\ x_p & y_p & 1 \end{vmatrix}$$

With other constants defined by cyclic interchange of subscripts in the order p, i, j, m. The ordering of nodal numbers p, i, j, m must follow a 'right-hand' rule. In this the first three nodes are numbered in an anti-clockwise manner when viewed from the last one.

4.3 The Element Stiffness and Nodal Forces Due to Initial Strain

a. Two-dimensional analysis:

The stiffness matrix of a typical element (vide section 4.2(a)) is given simply as:

$$[K^e] = [B]^T[D][B]t'\Lambda \qquad (4.3.1)$$

where t' is the thickness of the element. Nodal forces due to initial strains are given as:

$$\{F^e\} = -[B]^T[D]\{\varepsilon_o\}t'\Lambda \qquad (4.3.2)$$

where Λ is the area of the triangle as defined in section 4.2.

b. Axisymmetric analysis:

The simplest approximate integration procedure is to evaluate [B] for a centroidal point (vide section 4.2(b)):

$$r' = (r_i + r_j + r_m)/3 \; ; \; z' = (z_i + z_j + z_m)/3 \qquad (4.3.3)$$

Thus we have the element stiffness matrix as:

$$[K^e] = 2\pi[B]^T[D][B]r'\Lambda \qquad (4.3.4)$$

Similarly, nodal forces due to initial strains are:

$$\{F^e\} = -2\pi[B]^T[D][B]\{\varepsilon_o\}r'\Lambda \qquad (4.3.5)$$

where Λ is the area of the triangle as defined in section 4.2.

c. Three dimensional analysis:

Similarly, the stiffness matrix of a typical tetrahedron (vide section 4.2(c)) is given as:

$$[K^e] = [B]^T[D][B]V^e \qquad (4.3.6)$$

Nodal forces due to initial strains become:

$$\{F^e\} = -[B]^T[D]\{\varepsilon_o\}V^e \qquad (4.3.7)$$

4.4 The Step-By-Step Algorithm

The step-by-step algorithm can be summarised as follows:

a. Elastic solution:

At pseudo-time c = 0, the stresses $\{\sigma\}_o$ are determined from solving (vide section 4.1):

$$[K]\{a'\} = \{F\} \qquad (4.4.1)$$

b. First time step:

The stresses obtained at c = 0 are assumed to remain constant during a small pseudo-time increment, Δc; and creep strain increment $\{\Delta\varepsilon_c\}$ are calculated utilising the rate creep law (vide equation 2.5.2) viz:

$$\{\Delta\varepsilon_c\}_1 = \Phi(T)[V_c]\{\sigma\}_0\Delta c \qquad (4.4.2)$$

Where $[V_c]$ is the creep Poisson's matrix and is defiend as:

$$[V_c]=\begin{bmatrix} 1 & -v_c & -v_c & 0 & 0 & 0 \\ -v_c & 1 & -v_c & 0 & 0 & 0 \\ -v_c & -v_c & 1 & 0 & 0 & 0 \\ 0 & 0 & 0 & 2(1+v_c) & 0 & 0 \\ 0 & 0 & 0 & 0 & 2(1+v_c) & 0 \\ 0 & 0 & 0 & 0 & 0 & 2(1+v_c) \end{bmatrix} \qquad (4.4.3)$$

The corresponding initial strain $\{\varepsilon\}_1$ is given as:

$$\{\varepsilon\}_1 = \{\varepsilon_f\} - \{\Delta\varepsilon_c\}_1 \qquad (4.4.4)$$

where $\{\varepsilon_f\}$ is the free strain vector and its associated nodal force vector is then:

$$\{F_\varepsilon\}_1 = -\int [B]^T[D]\{\varepsilon\}_1 \, dV \qquad (4.4.5)$$

Equation 4.4.1 now becomes:

$$[K]\{a'\} = \{F\} + \{F_\varepsilon\}_1 \qquad (4.4.6)$$

where $\{F\}$ is a global vector at c = 0 and $\{F_\varepsilon\}_1$ is the global load vector associated with the initial strain vector $\{\varepsilon\}_1$.

Equation 4.4.6 can be solved and new stresses evaluated. The new stress distributions are then used to obtain the solution for the next time increment.

c. m-th time step:

Similarly, for the m-th time-step, the creep strain increment is given

as:

$$\{\Delta\varepsilon_c\}_m = \Phi(T)[V]\{\varepsilon\}_{m-1} \tag{4.4.7}$$

and the initial strain is:

$$\{\varepsilon\}_m = \{\varepsilon_f\}_{m-1} - \{\Delta\varepsilon_c\}_m \tag{4.4.8}$$

and its associated nodal load vector is:

$$\{F_\varepsilon\}_m = -\int [B]^T[D]\{\varepsilon\}_m \, dV \tag{4.4.9}$$

and equilibrium equations are again given by:

$$[K]\{a'\} = \{F\} + \{F_\varepsilon\}_m \tag{4.4.10}$$

from which $\{\sigma\}_m$ maybe obtained.

For cyclic temperature problems, the only difference from the above mentioned procedure is that the free strains vector (vide equation 4.4.4) must be altered at the end of each part of the cycle by appropriate values corresponding to each temperature change.

4.5 The Choice of the Pseudo-time Step Increment

The choice of the pseudo-time step increment is crucial for the success of the step-by-step procedure. If the increment is too large, solution instability may result. On the other hand an increment which is too small will render the solution costly. Also, since the redistribution of stresses is slower at larger values of pseudo-time, it is possible to change the pseudo-time step increment to larger values as time increases. In the case of cyclic temperature problems the upper bound value of pseudo-time step increment is given as the highest common factor of all the phase length in pseudo-time within a cycle if a single pseudo-time step increment is used throughout the analysis. Again the pseudo-time step increment maybe varied from phase to phase and even from cycle to cycle. For sustained temperature problems, the variable pseudo-time step increment is implemented in the SSCREEP program in the form either:

a. Arithmetic progression type increments, viz:

$$\Delta c_i = i r_a \Delta\Delta c \qquad (4.5.1)$$

where Δc_i is the i-th pseudo-time step increment and r_a is a constant multiplier and $\Delta\Delta c$ is the first pseudo-time step increment.

b. Geometric progression type increments viz:

$$\Delta c_i = r_a r_b{}^i \Delta\Delta c \qquad (4.5.2)$$

where r_b is the geometric ratio.

c. User supplied variable pseudo-time step increments.

From experience $\Delta\Delta c$ is usually taken as 1×10^{-8} MN/m^2 per ^oC.

4.6 The Sequential Frontal Linear Equation Solver

The number of simultaneous equations (vide equation 4.1.13) to be solved in the use of the finite element displacement method can be very large for engineering structures. This is because of the need to represent the body with a relatively large number of elements to obtain an accurate stress distribution. Moreover, in the step-by-step solution algorithm (vide section 4.4.1) the right-hand side of these equations changes for each time increment. Therefore the method adopted for equation solution is a major factor influencing the efficiency of any finite element program. In SSCREEP a Frontal solving scheme with re-solution capability is implemented (Hinton and Owen 1977).

The Frontal method, produced by Irons (1970) can be considered as a particular technique for first assembling finite element stiffness and nodal forces into a global stiffness matrix and load vector and then solving for unknown displacements by means of a Gaussian elimination and back-substitution process. The main idea of the frontal solution is to assemble equations and eliminate variables at the same time. As soon as coefficients of one equation are completely assembled from contributions of all relevant elements, the corresponding variables can be eliminated. Therefore, the complete structural stiffness matrix

[K] is never formed as such, since after elimination the reduced equation is immediately transferred to back-up storage.

The computer core contains, at any given instant, the upper triangular part of a square matrix containing equations which are being formed at that particular time. Theses equations, their corresponding nodes and degrees of freedom are termed the 'front'. The number of unknowns in the front is the the 'frontwidth' whose length generally changes continually during the assembly/reduction process. The maximum size of problem which can be solved is governed by the maximum frontwidth and the maximum computer core requirement is given as:

$$\text{Core requirement} = (\text{Max. frontwidth} + 1) \times (\text{Max. frontwidth})/2 \qquad (4.6.1)$$

Equations, nodes and degrees of freedom belonging to the front are termed active; those which are yet to be considered are inactive; those which have passed through the front and have been eliminated are said to be deactivated.

During the assembly/elimination process, elements are considered each in turn according to a prescribed order. Whenever a new element is called in, its stiffness coefficients are read from disc file and summed either into existing equations, if nodes are already active, or into new equations which have to be included in the front if nodes are being activated for the first time. If some nodes are appearing for the last time, the corresponding equations can be eliminated and stored away on disc file and are thus deactivated. In so doing they free spaces in the front which can be employed during assembly of the next element. The operation of the sequential frontal linear equation solver is shown schemetically in figure 4.6.1.

For the economic processing of variable load vector cases the inclusion of an equation re-solution facility is essential. In this the reduced equations are stored in their eliminated form and a second and subsequent solution merely necessitates the reduction of right hand side load terms. Thus saving are made in two ways. Firstly, the computation of the element stiffness is unnecessary and secondly, the element assembly and reduction phase is avoided. From experience, solution for each time increment in the step-by-step algorithm can be

obtained in the order of 25% of the time required for a single elastic analysis for large problems.

4.7 The Computer Program

The SSCREEP computer code, or step-by-step CREEP analysis program, is a medium size program (with approximately 5000 Fortran statements) and the following capabilities:

a. It can be used to carry out plane stress, plane strain, axisymmetric and three dimensional continuum analysis.

b. Either raised sustained or cyclic temperature problems maybe handled (vide chapter 2) .

c. To solve the equilibrium equation, the sequential frontal solving scheme with re-solution capability is implemented.

d. Dynamic computer memory allocation, i.e. small problems need less memory and will therefore be treated with a higher priority and lower costs in mainframe computer.

e. The two and three dimensional mesh generation preprocessor in SSCREEP saves the user a lot of time for preparing data. (vide chapter 5).

f. Diagnostic preprocessor is also built in for error detection and early warning before entering the main solution processor.

g. SSCREEP is written in Fortran 77 and maybe installed on a variety of machines. In fact SSCREEP has been run on machines ranging from CRAY mainframe to mini-computers such as VAX 11/780.

Figures 4.7.1 and 4.7.2 show a simplified block diagram illustrating the operation of the program. Further details of SSCREEP will be found in a separate internal report (see Appendix C).

4.8 Numerical Examples

4.8.1 Benchmark problems

It is instructive, when testing a method of analysis, to use a simple structure for which alternative solutions can be obtained. Thus England's (England 1962) classical flexurally restrained beam was used as a benchmark problem and solved as one, two and three dimensional models, Figure 4.8.1 shows the details of boundary conditions and loadings. Two types of temperature variations were investigated:

(a) Sustained temperature field, see Figure 4.8.1(b), for one, two and three dimensional models.

(b) Unidirectional cyclic temperature field with Δc_1 = 9.0E-8 and Δc_2 = 40.0E-8, see Figure 4.8.1(c), for one and two dimensional models only.

The one dimensional analysis was handled by a step-by-step rate of creep method (England 1967), Figures 4.8.2 and 4.8.3.

The two and three dimensional analyses were performed using SSCREEP. For the two dimensional analysis, the beam was analysyed as a plane stress problem, Figure 4.8.4. A total of 60 triangular elements was used to model the beam.

Although strictly unnecessary for solving the problem, a three dimensional version of the beam was considered in order to test the ability of SSCREEP for solving three dimensional problems. The beam was modeled using 250 tetrahedra, Figures 4.8.5 and 4.8.6.

The arithmetic progression type pseudo-time incremental strategy, with r_a=1.0 and $\Delta\Delta c$=0.25E-08, was used (vide section 4.5). The solution was terminated at c=3.99E-06 due to computer cost considerations. The total number of time steps used was 58. The Young's modulus, Poisson's ratio and coefficient of thermal expansion were taken as 34500 MN/m^2, 0.3 and 0.12xE-04 $/^oC$ respectively. Stresses are expressed in MN/m^2.

Results for the above analyses are given in Tables 4.8.1 to 4.8.3 for sustained temperature problems. For unidirectional cyclic temperature

problems, the results are shown in Tables 4.8.4 to 4.8.6. All results are given in terms of the x-ordinate used in the one dimensional analysis (Figure 4.8.2).

It is seen from Tables 4.8.1 to 4.8.6 that for practical purposes, the solutions are in close agreement with one another.

4.8.2 Allen's rectangular plate with parabolic edge loading

A finite element solution to a rectangular plate of aspect ratio of 3 was obtained by Allen (England et al 1971). The plate is subjected to a sustained temperature gradient and an inplane edge parabolic loading. A quarter of the plate was modeled using a finite element mesh of 25x9 rectangular elements. An analytical solution was also dervied based on a minimization principle approach.

The same problem was analysed utilising SSCREEP using a 60 triangular element mesh, Figure 4.8.7. The following data was used (Smith 1981):

Young's modulus	= 41400 MN/m^2
Poisson's ratio	= 0.2
Coefficient of thermal expansion	= 0.0000135 per ^oC
Reference temperature	= 20.0 ^oC

The logitudinal stresses at x=0 for inner and outer faces obtained was compared with those given by Allen and Smith, Figure 4.8.8. It is observed that a close match of solutions was obtained.

More detailed pictures of the transient longitudinal stresses distribution, in the form of stress contour diagrams over the structure, are shown in Figures 4.8.9 to 4.8.11. The stresses plotted were obtained by first extrapolating elemental stresses to nodal points using a nodal stress averaging technique and then interpolated inside the element using a predictor-corrector contour tracing algorithm as described in next chapter.

4.9 Economic Assessment of the Algorithm

In the above analyses, the computer time required by the two dimensional model was 0.2 seconds per increment and for the three

dimensional model it was 0.8 seconds per increment on an IBM 3081 KX3 mainframe computer. Both the pseudo-time step size and the mesh size were finely tuned to minimize computer cost and to achieve an accurate solution at the edge far from the loaded edge of the model. The models analysed are relatively simple in comparison with real structures both in terms of loading and geometry, and therefore fine tuning the step size was relatively easy. If stresses were required nearer to the loaded edge, more elements must be used in the longitudinal direction.

The optimal choice of pseudo-time step size, incremental strategy and mesh refinement required a lot of practical analysis experience and probably some trials and errors. For an inexperienced or occasional user, he might be tempted to choose a single pseudo-time step size of say, 1.0E-08, and a finite element mesh consists of 600 triangular elements for the two-dimensioanal model. In order to achieve a steady-state solution, the analysis probably has to proceed until c=4.0E-6. The total computer time accrued is then:

$$\text{Time} = \frac{10 \times 0.2 \times 4.0\text{E-}06}{1.0\text{E-}08} = 800 \text{ seconds.}$$

A lot of stresses output would also be generated too. This is rather costly, both in terms of computer and human resources required, for a small problem.

4.10 Concluding Remarks

A computer program SSCREEP is written utilising the step-by-step algorithm and applied to a restrained beam problem analysed as a plane stress problem. From the results obtained it is revealed that while the algorithm itself is easy to implement, it is very expensive to use even for a small problem. A greater disadvantage is the large amount of information generated from such an analysis and consequently the large human resources which maybe required for the interpretation of results.

In the case of sustained temperature problems, the situation maybe

improved by using a variable pseudo-time step increment approach albeit solution accuracy is sacrificed. In the case of cyclic temperature problems, the choice of pseudo-time step increment is restricted because it must not be bigger than the largest temperature phase length within a cycle. Consequently the analysis is often expensive.

It is concluded that while the algorithm is useful in general, it can be extremely expensive and overtax even the most powerful modern computers and thus other ways of solving the problem must be sought and this forms the subject the next chapter.

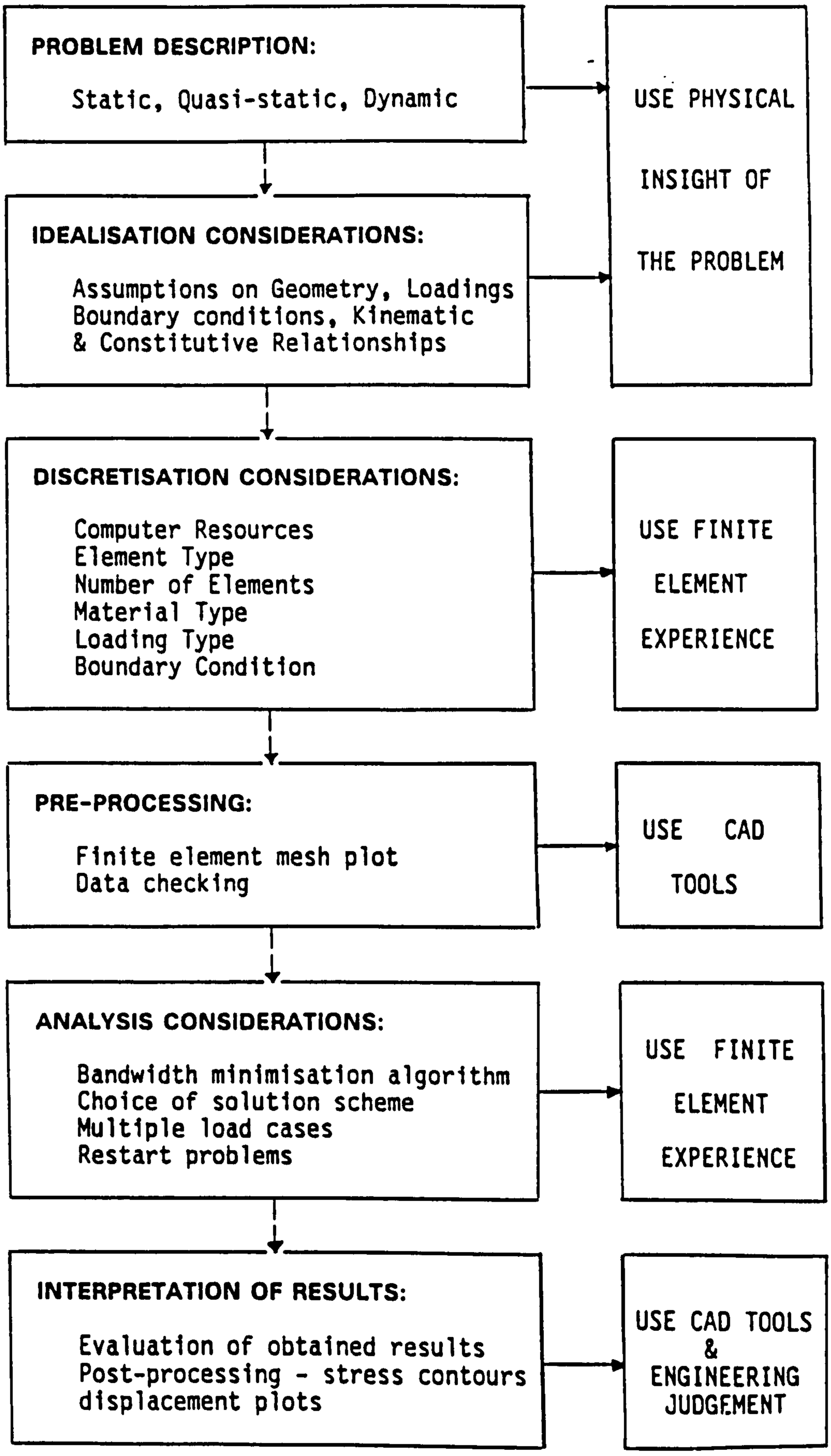

Figure 4.1.1: Tackling a structural problem using the finite element method

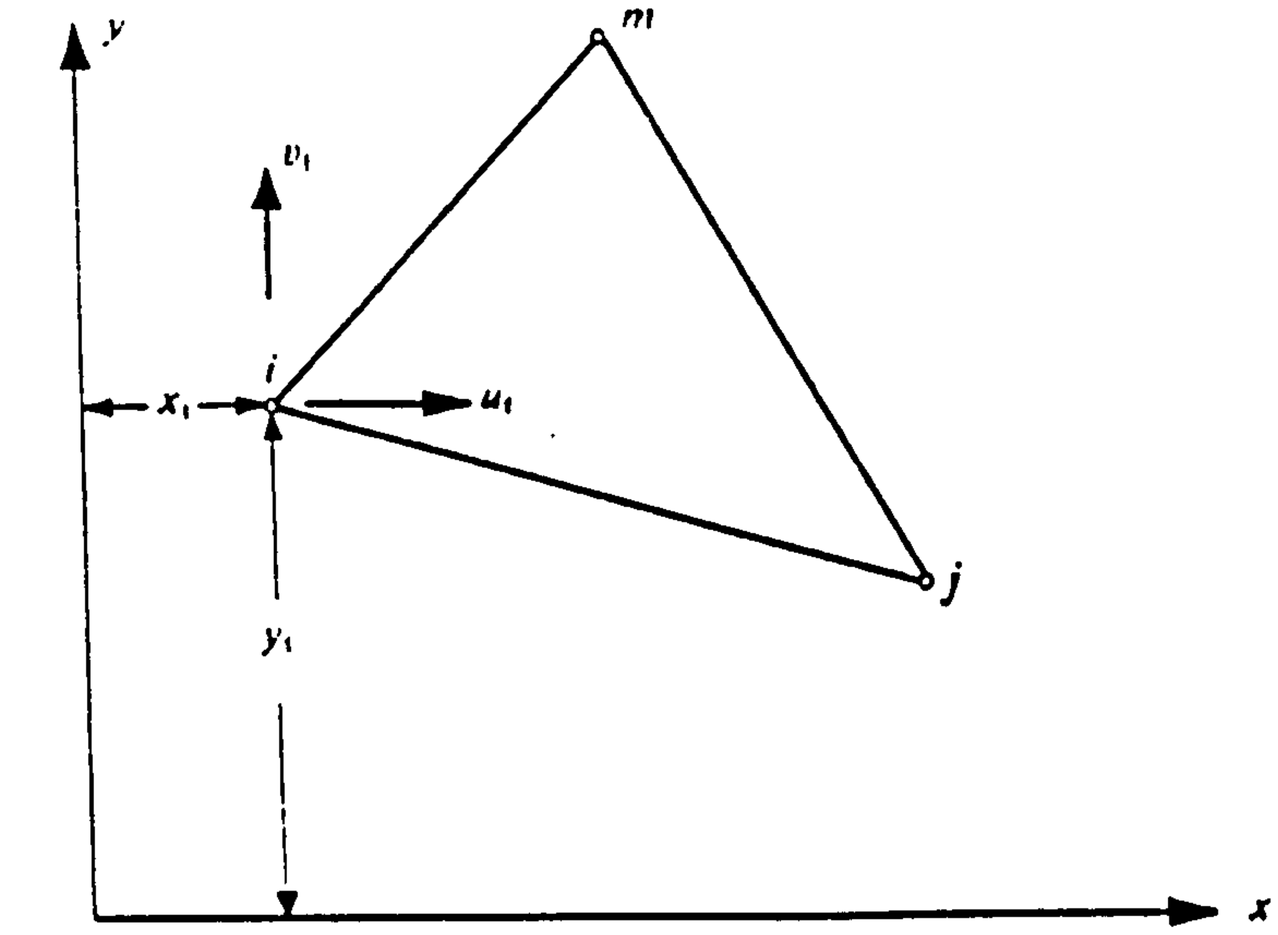

(a) An element of a continuum in plane stress or plane strain

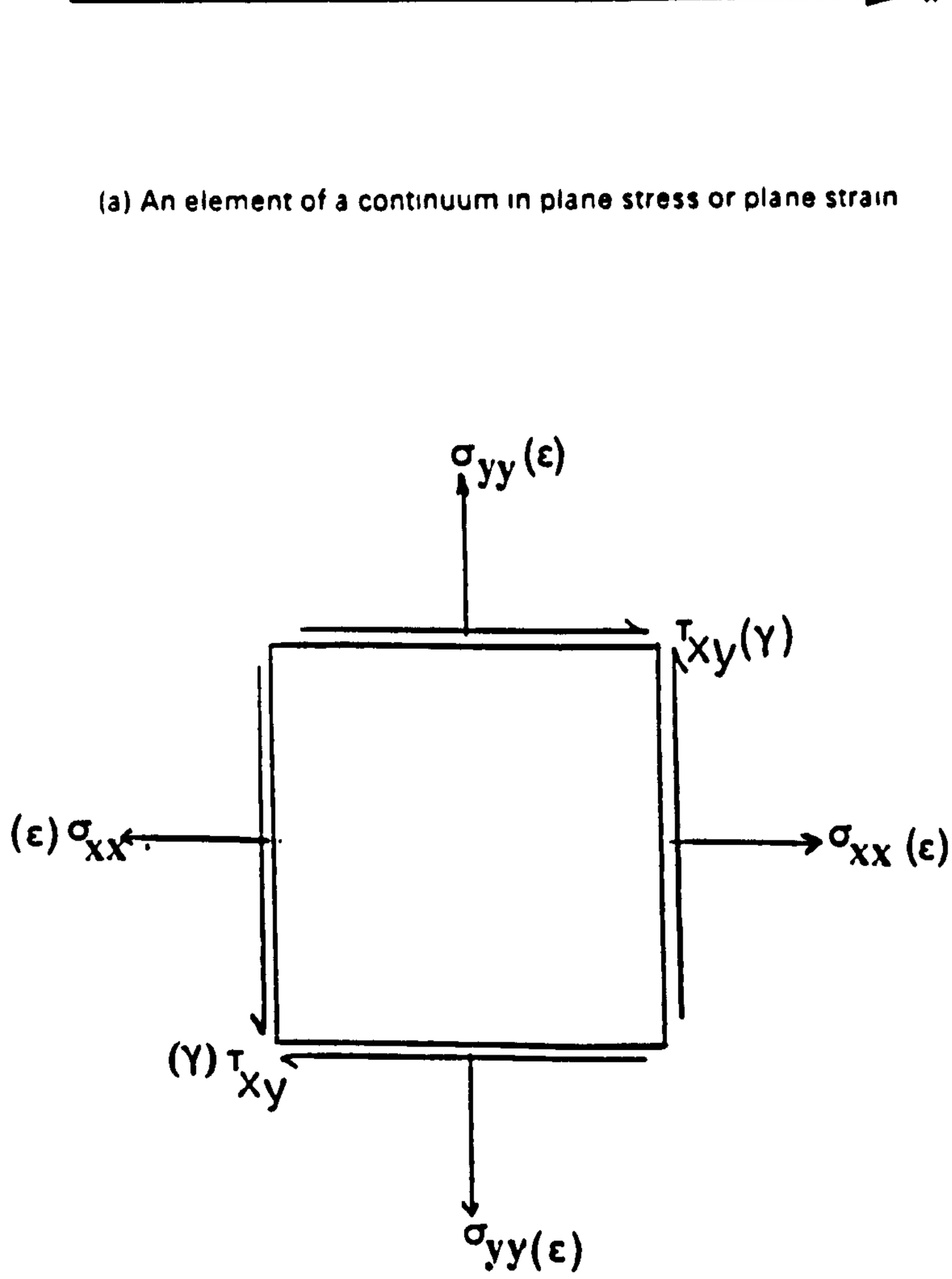

(b) Strains and stresses involved in the analysis of plane problems

Figure 4.2.1: The constant strain triangular element

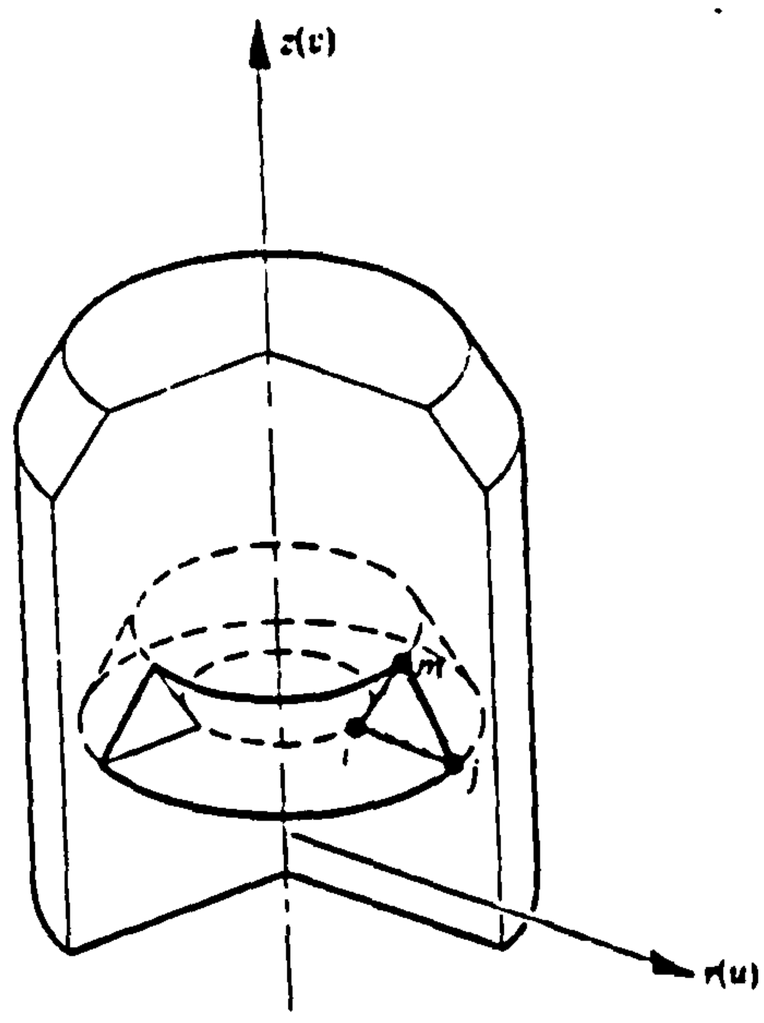

(a) Element of an axisymmetric solid

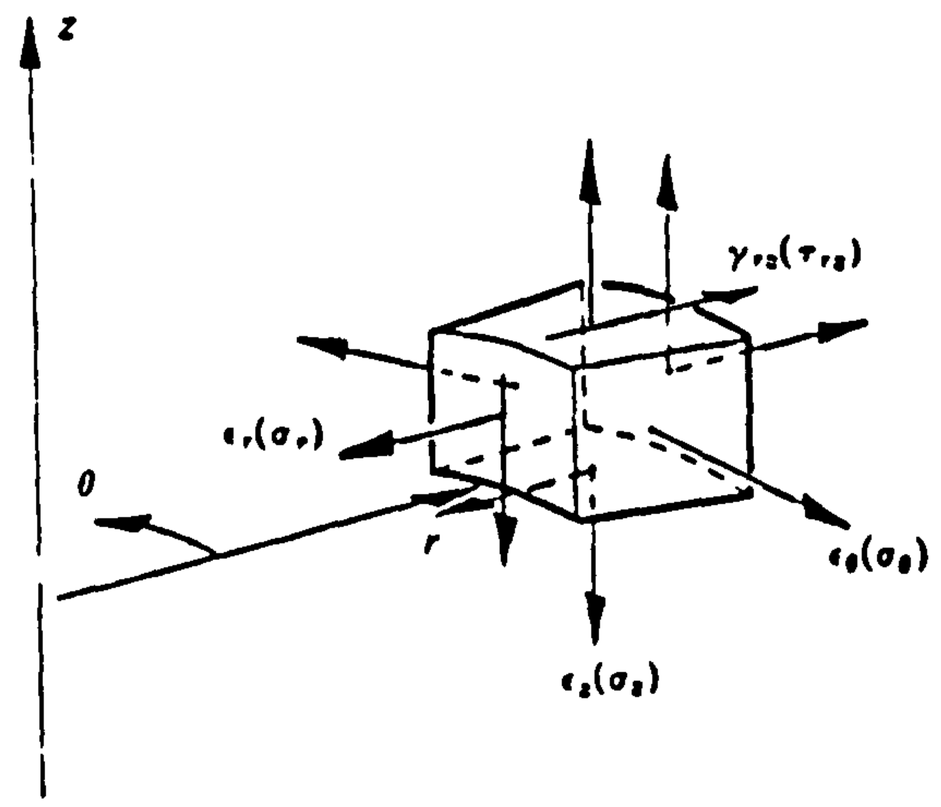

(b) Strains and stresses involved in the analysis of axisymmetric problems

Figure 4.2.2: The constant strain axisymmetric solid element

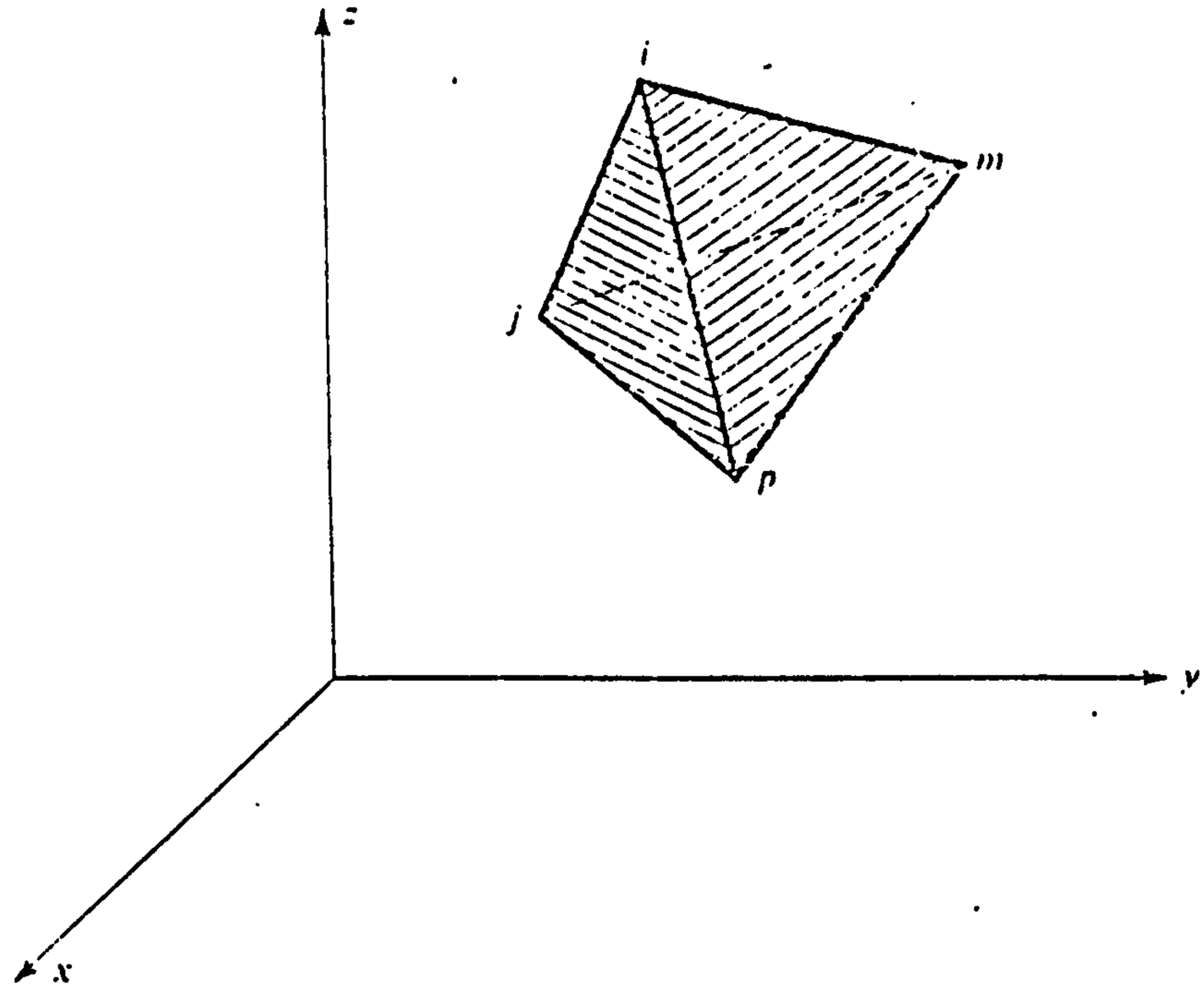

(a) A tetrahedron element

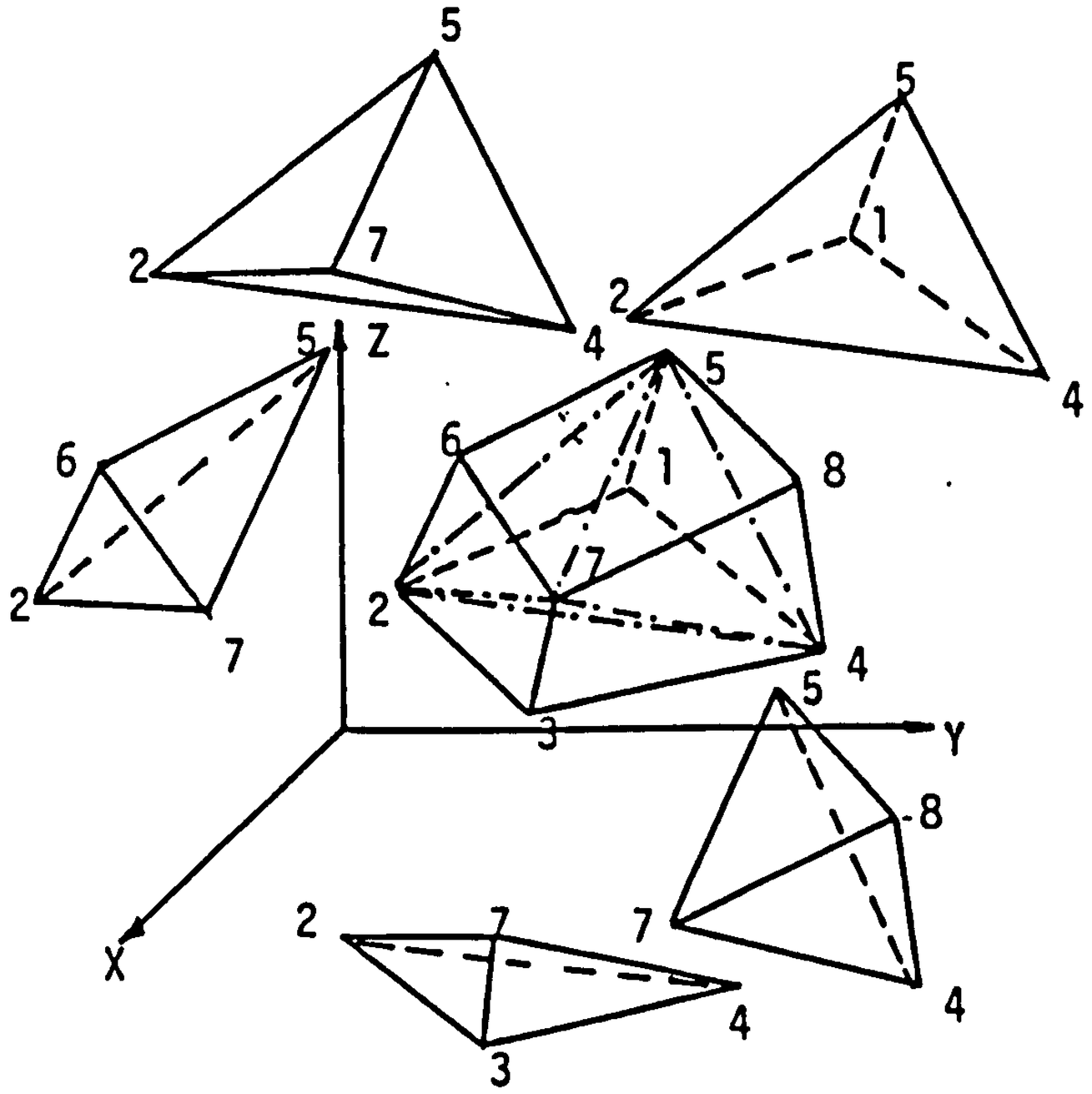

(b) Composite element with eight nodes and its systematic way programmed for subdividing into five tetrahedra

Figure 4.2.3: The constant strain tetrahedron element

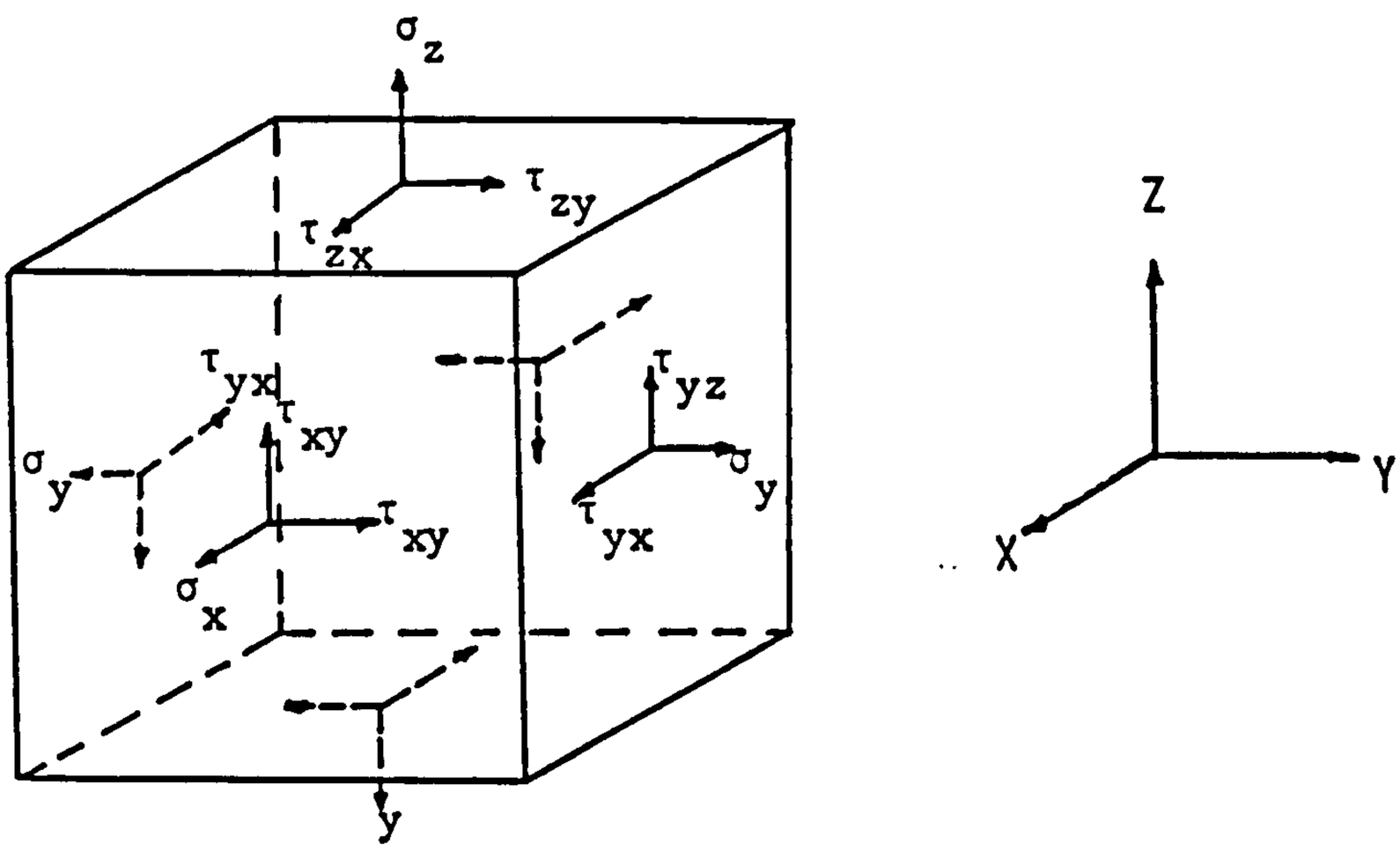

Figure 4.2.4: Components of stresses in cartersian coordinates

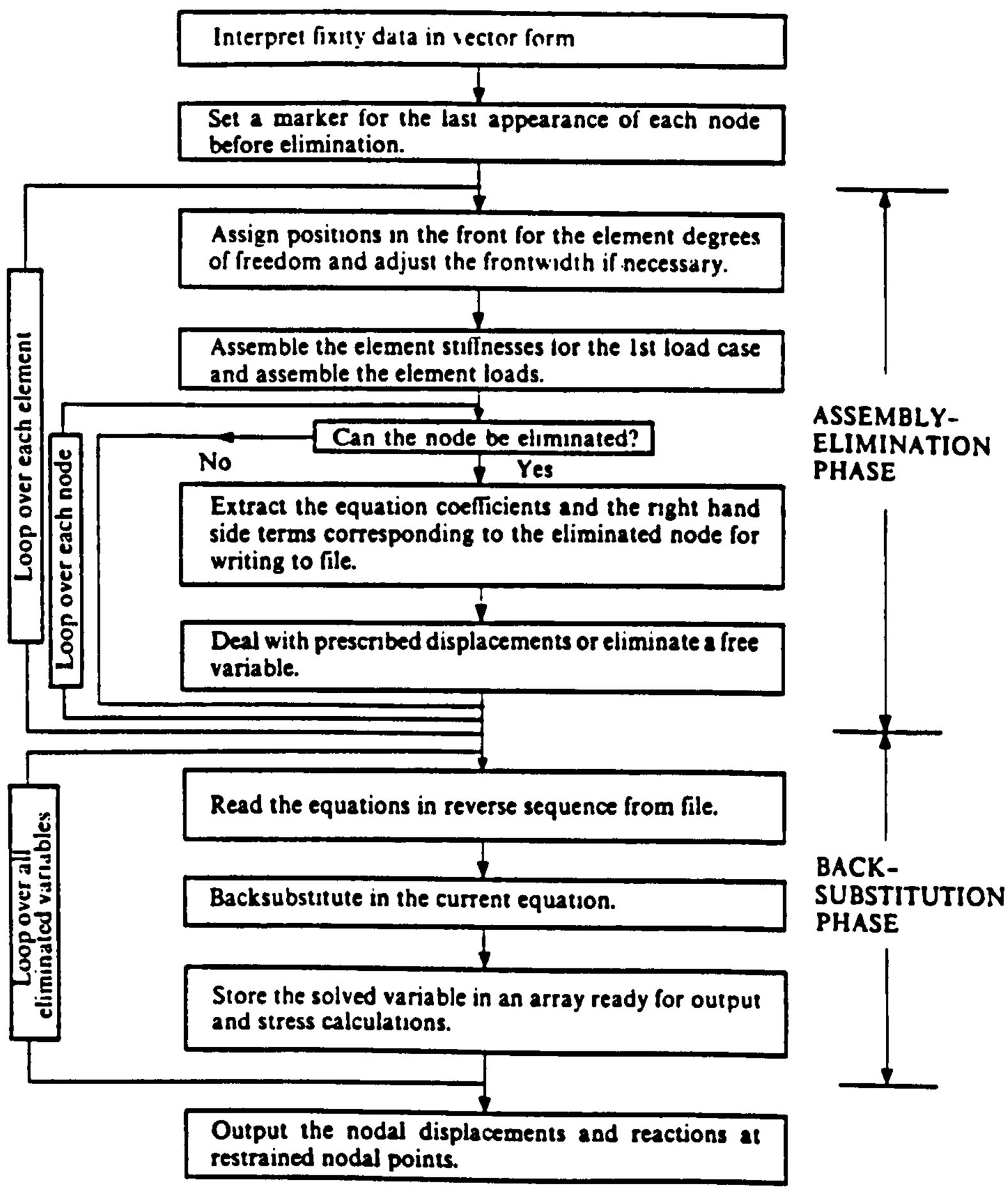

Figure 4.6.1: Operation sequence for the Sequential Frontal Solver

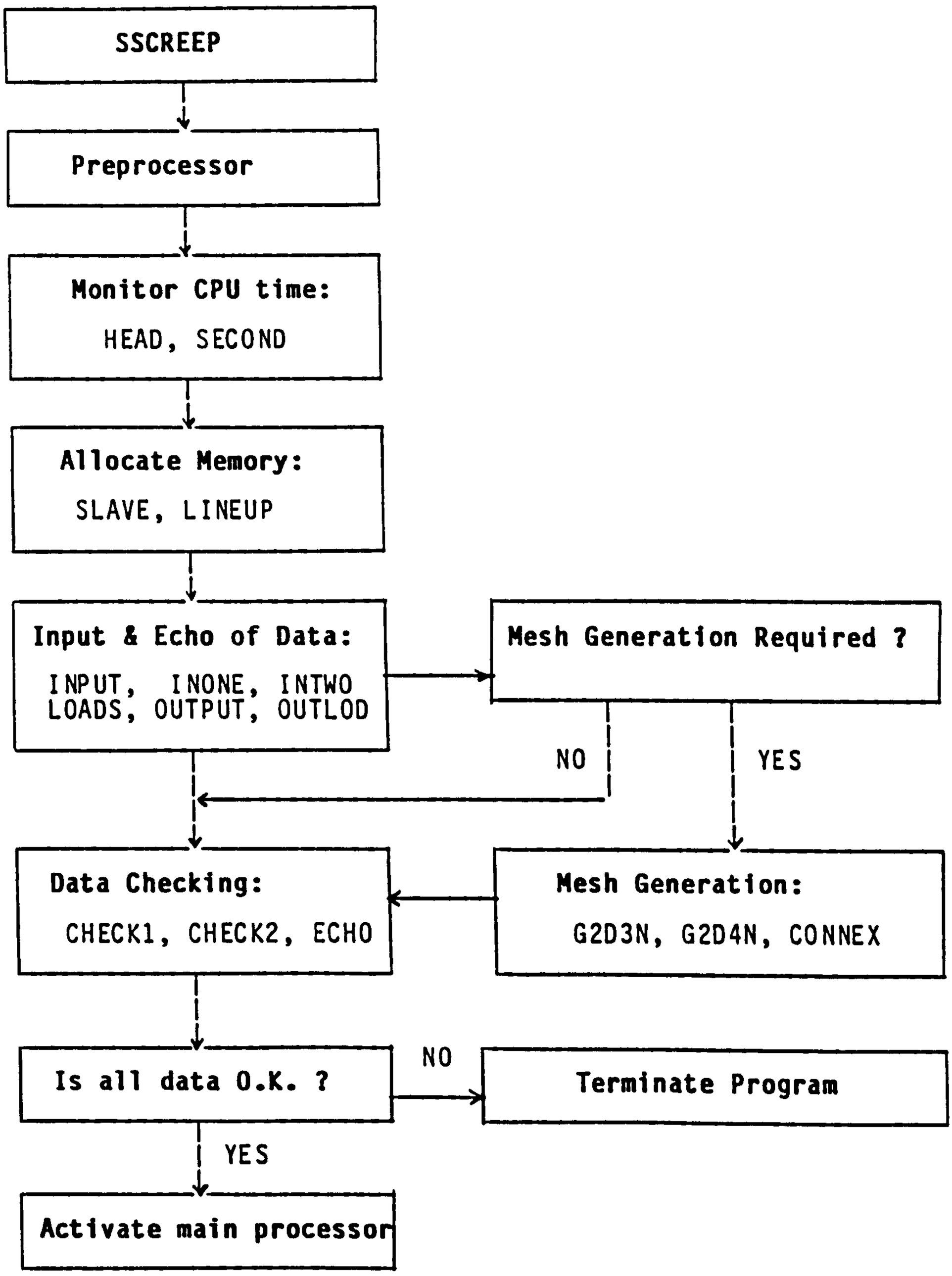

Figure 4.7.1: Macro flow chart for SSCREEP preprocessor

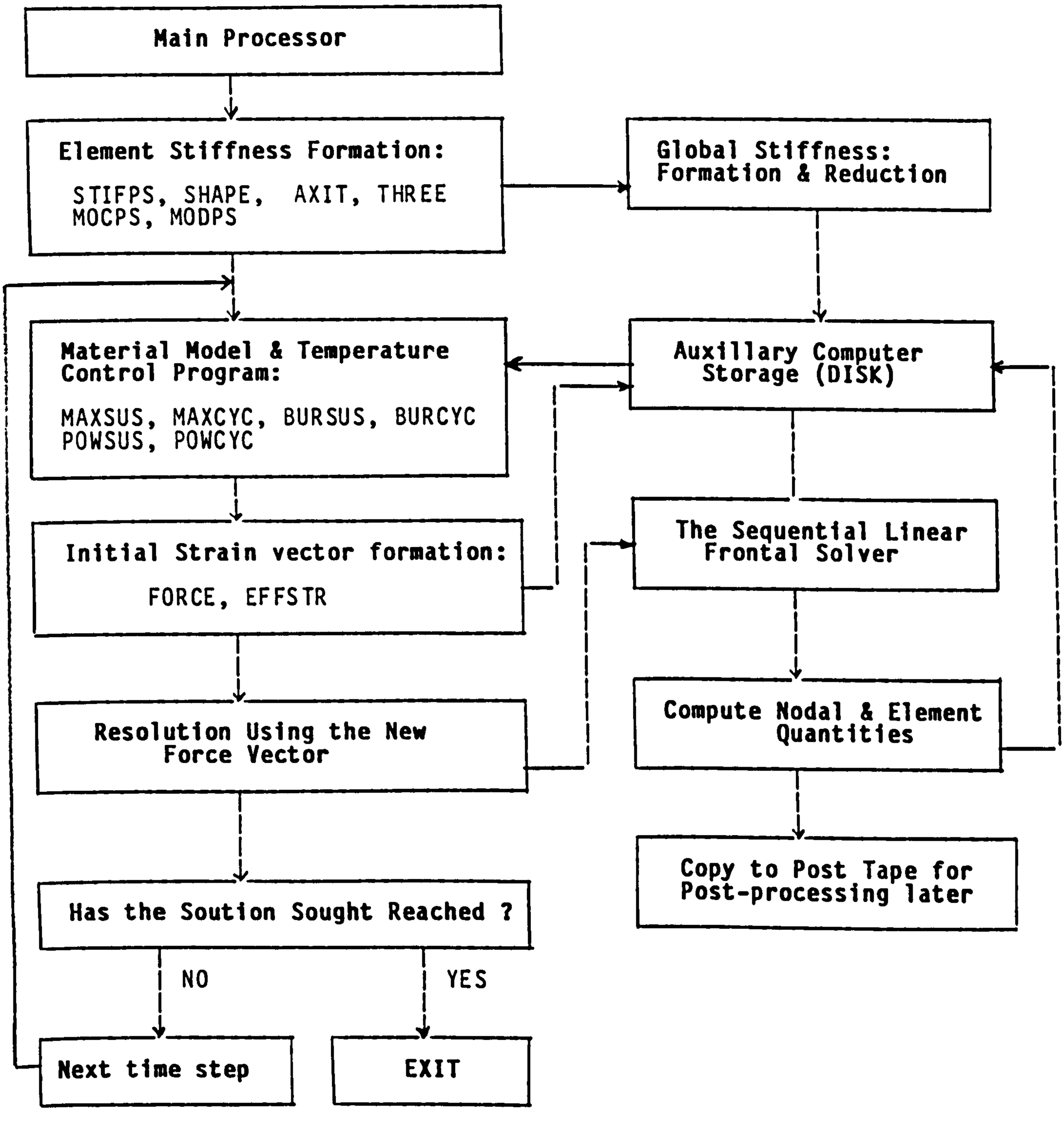

Figure 4.7.2: Macro flow chart for SSCREEP main processor

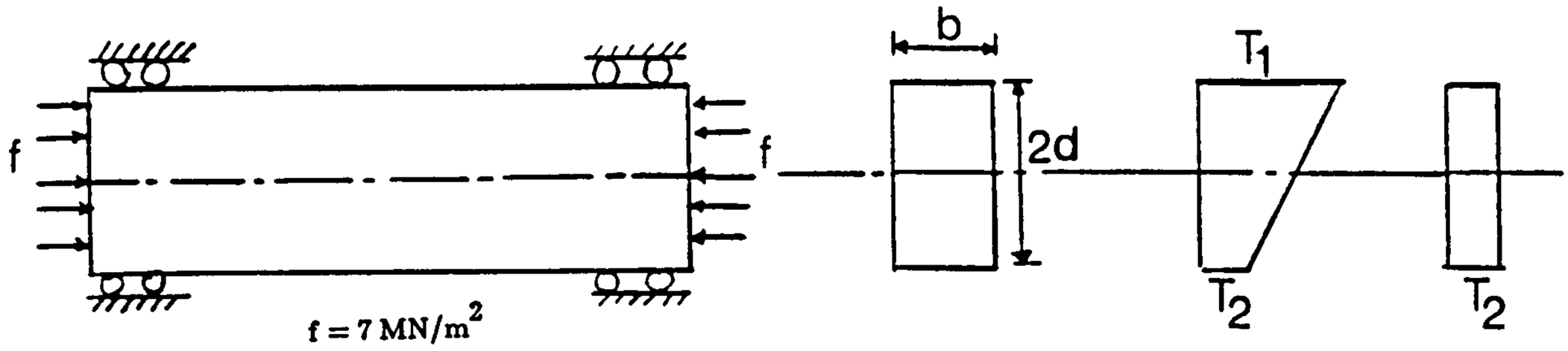

(a) Prestressed flexurally restrained beam

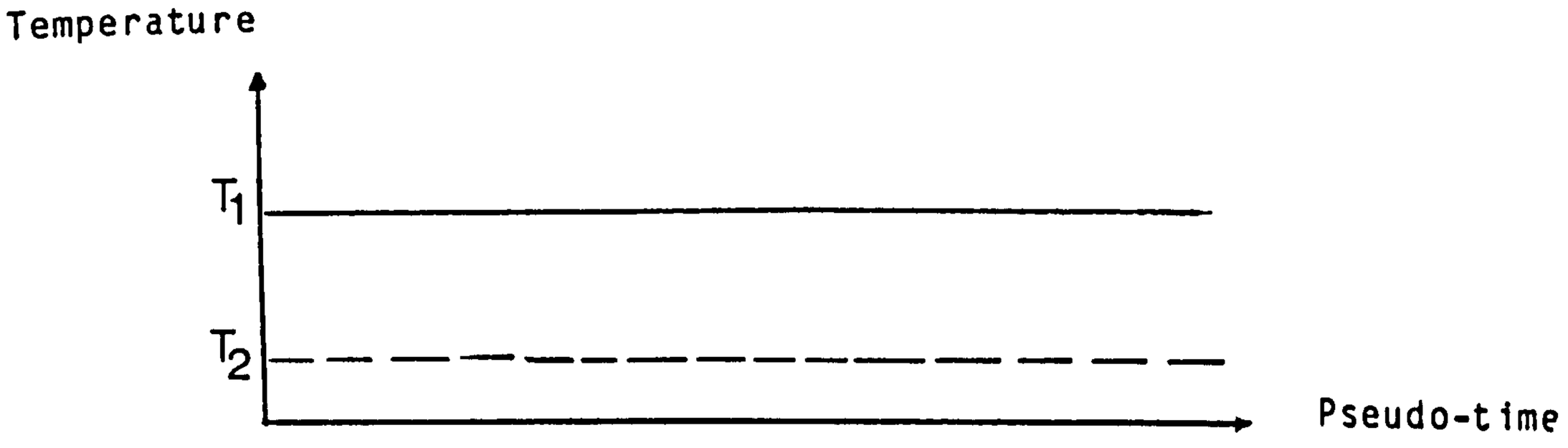

(b) Sustained temperatue field

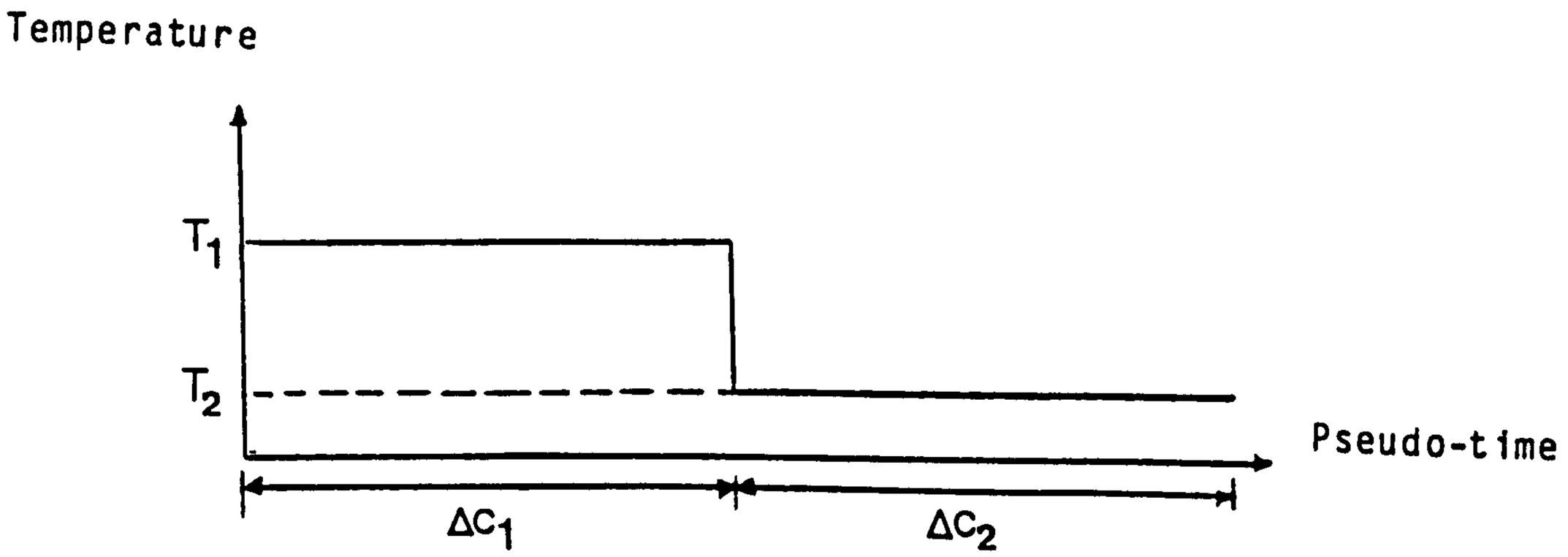

(c) Unidirectional cyclic temperature field

Figure 4.8.1: The beam and nature of temperature fields

Divide the beam into n strips each with thickness d/n and it is subjected to an average 'follow up' prestress of f = N/bd and a linear temperature field T= α + βX, see figure 4.8.3.

↓

Compute the thermo-elastic stresses:

$$\sigma = f + E\bar{\alpha}\beta X$$

↓

The incremental creep strain for the short time interval ΔΔc is given as:

$$\Delta\varepsilon_c = \sigma\Phi(T)\ \Delta\Delta c$$

↓

Calculate a new set of free strains (initial strains) for the time increment:

$$\varepsilon_{f(new)} = \varepsilon_{f(old)} + \Delta\varepsilon_c$$

↓

To enforce compatibility & equilibrium, the actual strain ε_o has to be recalculated:

$$F = Ebd/n\ \Sigma\ (\varepsilon_f - \varepsilon_o)$$
$$\varepsilon_o = 1/n\ \Sigma\ \varepsilon_f - f/E$$

↓

Thus the stresses at the end of time step is given as:

$$\sigma = E(\varepsilon_f - \varepsilon_o)$$

↓

Solution sought reached ?

YES → STOP

NO → (return to the incremental creep strain step)

Figure 4.8.2: Macro flow chart for one dimensional step by step rate of creep analysis for a beam problem

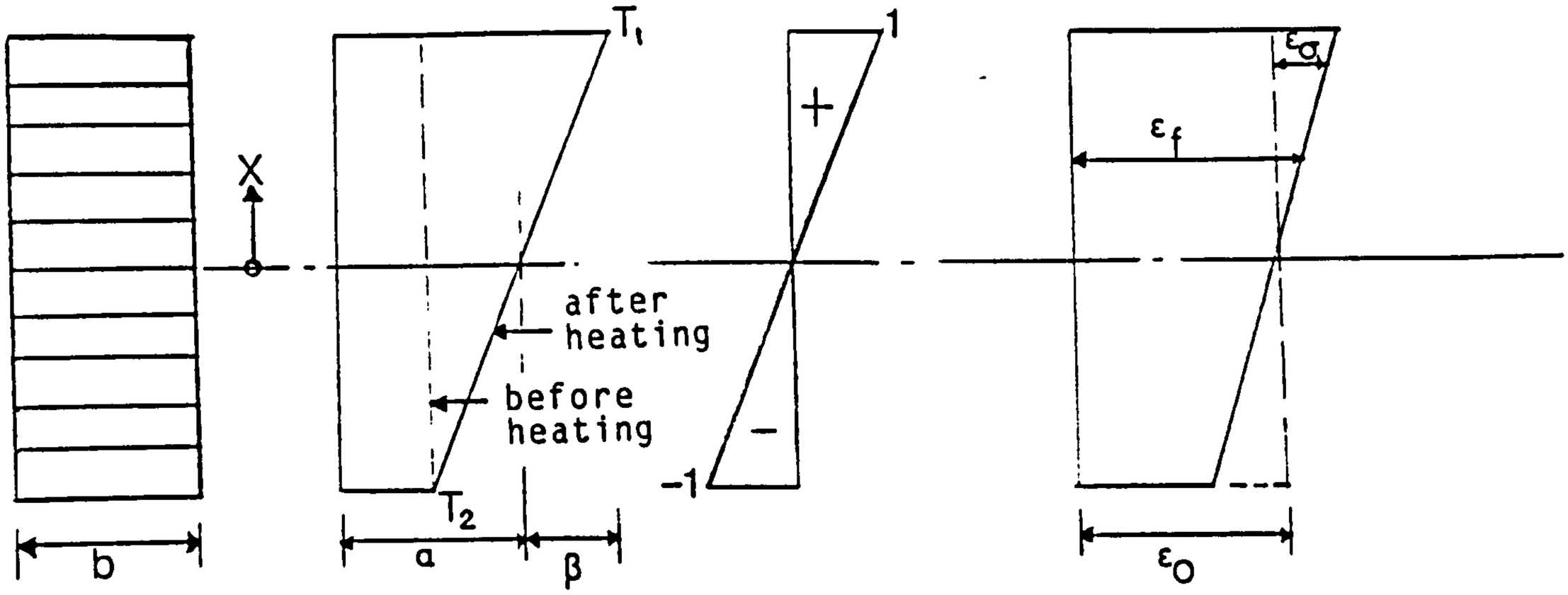

x-section | Temperature $T = \alpha + \beta X$ | X diagram | observable ε

intial free strain
$\varepsilon_f = \bar{\alpha}\Delta T$

$\varepsilon_\sigma = \bar{\alpha}\beta X$

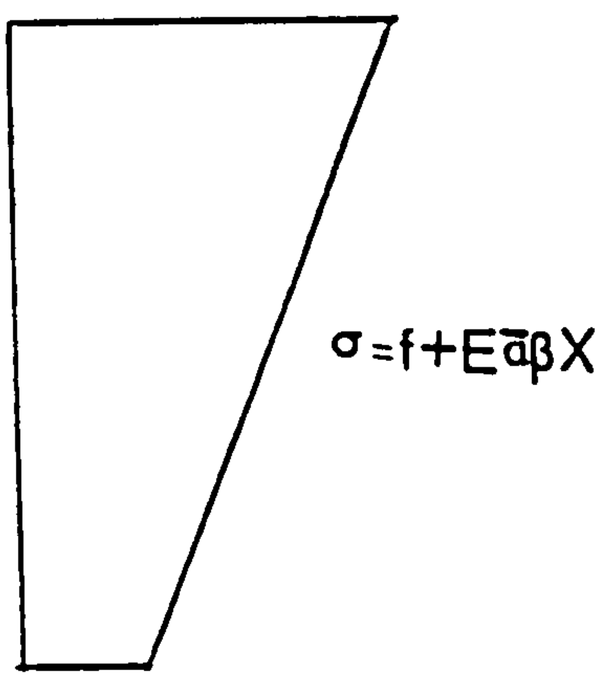

$\sigma = f + E\bar{\alpha}\beta X$

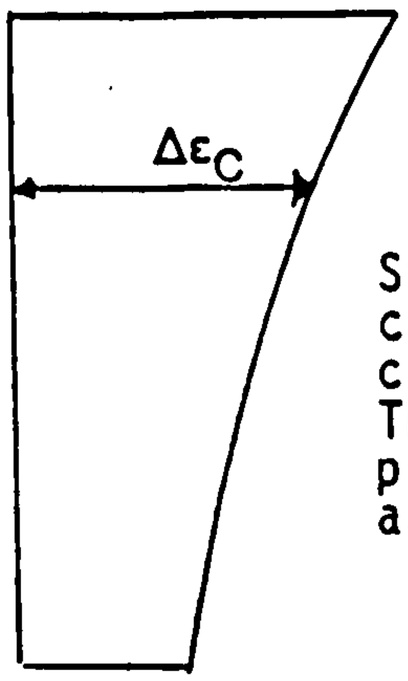

Strain at end of a time interval creep strain which destroy compatibility during a step. These are added to $_f$ of previous step and the analysis repeats.

Total stresses at loading

Figure 4.8.3: One dimensional step by step analysis by the rate of creep method for a flexurally restrained beam.

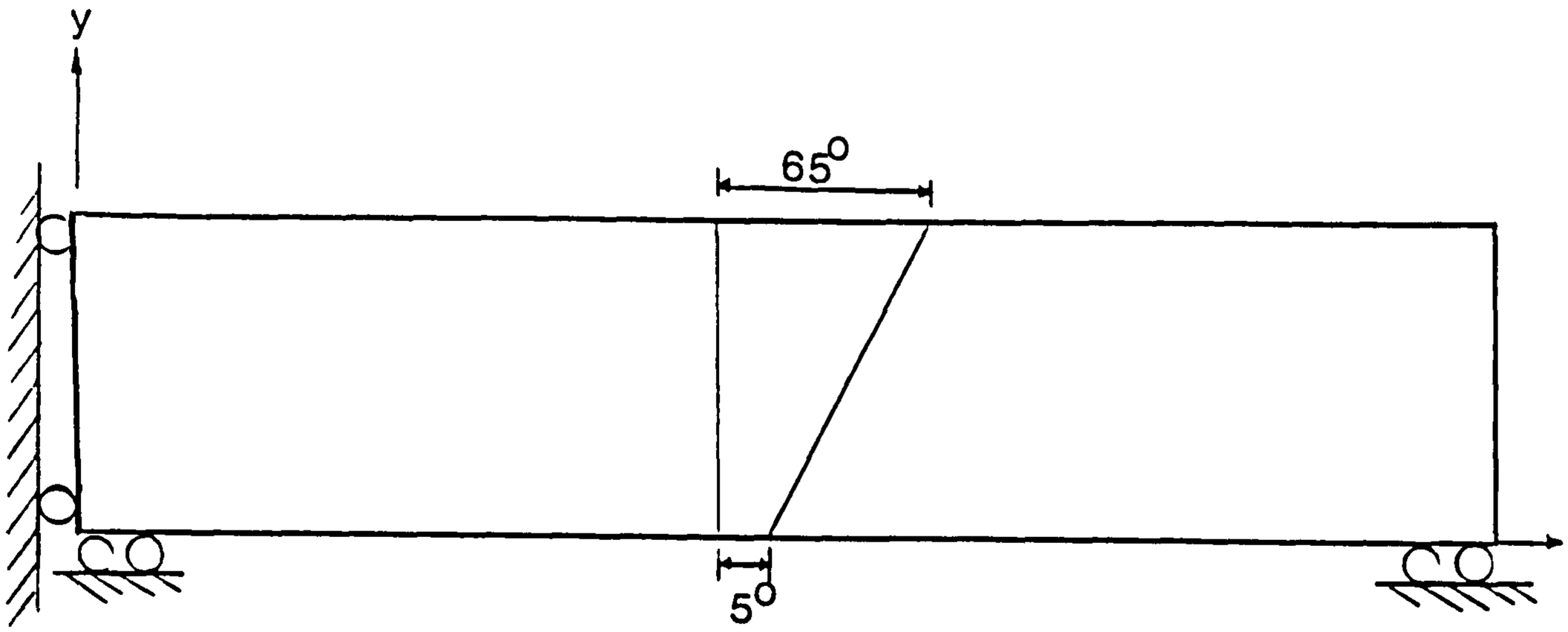

Applied axial stress = 7 MN/m^2

(a) The beam model

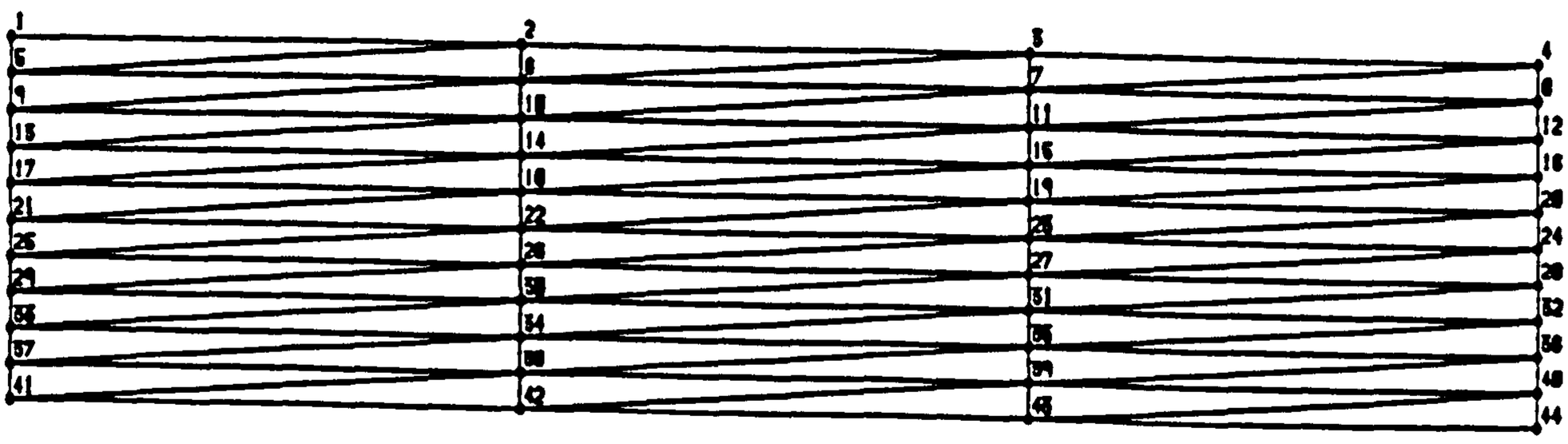

(b) Finite element idealisation

Figure 4.8.4: The finite element model for the flexurally restrained beam problem

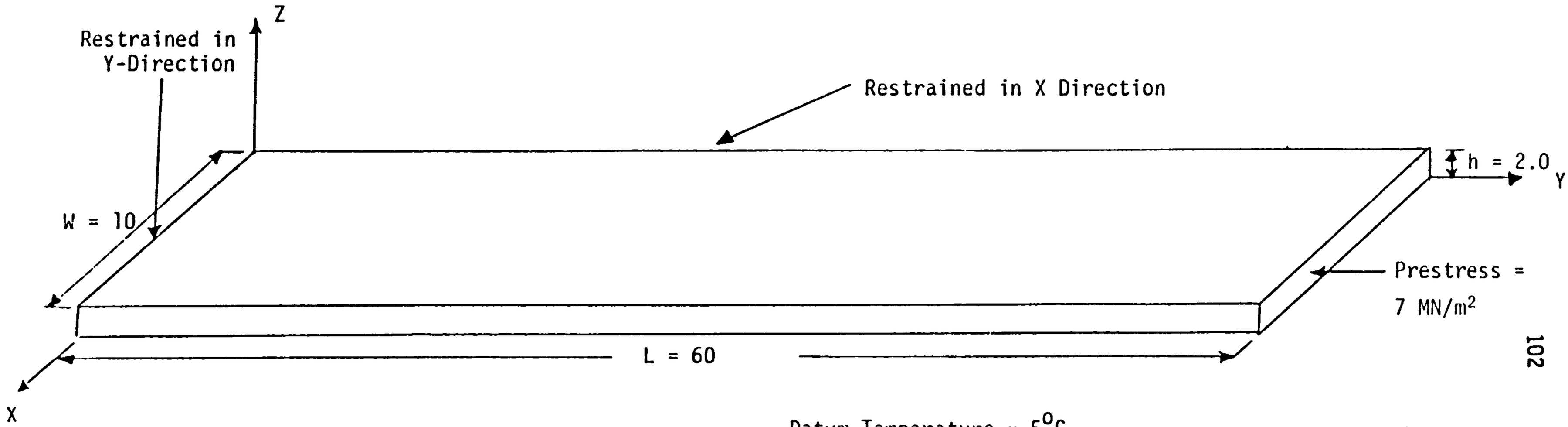

Figure 4.8.5: The three dimensional finite element model for the flexurally restrained beam problem

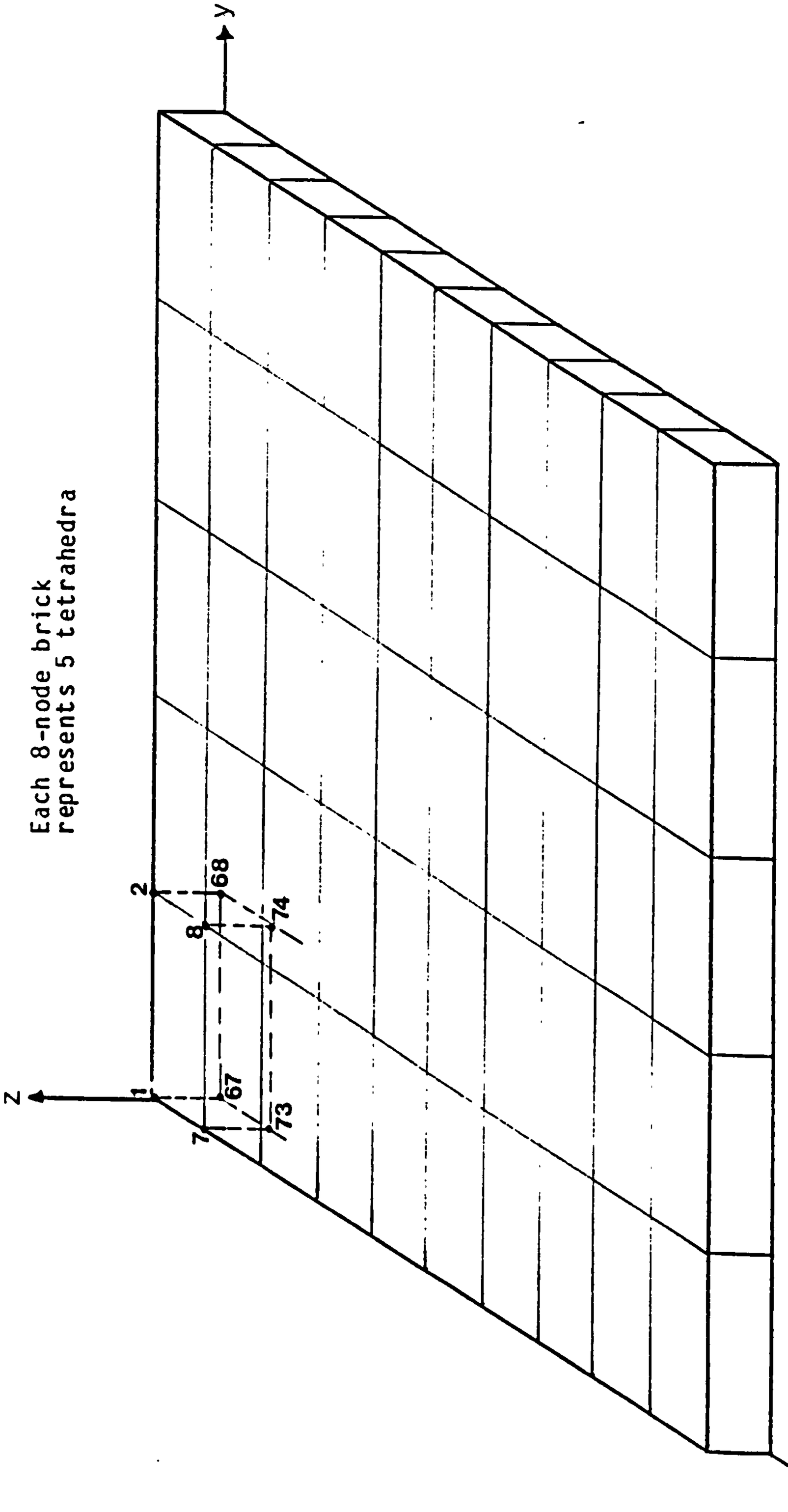

Figure 4.8.6: The three dimensional finite element mesh for the flexurally restrained beam problem

Time	0.0			0.900E-07		
X	1-D	2-D	3-D	1-D	2-D	3-D
0.9	-18.016	-18.180	-18.350	-15.879	-15.980	-16.126
0.7	-15.568	-15.700	-15.712	-14.109	-14.200	-14.214
0.5	-13.120	-13.210	-13.208	-12.267	-12.340	-12.334
0.3	-10.672	-10.730	-10.722	-10.349	-10.400	-10.396
0.1	-8.224	-8.241	-8.240	-8.355	-8.378	-8.380
-0.1	-5.776	-5.755	-5.758	-6.283	-6.278	-6.283
-0.3	-3.328	-3.270	-3.276	-4.129	-4.094	-4.102
-0.5	-0.880	-0.784	-0.792	-1.893	-1.825	-1.834
-0.7	1.568	1.701	1.711	0.428	0.532	0.540
-0.9	4.016	4.187	4.348	2.835	2.979	3.135

Note:

(a) Stresses are expressed with reference to one dimensional problem and is in terms of MN/m^2.
(b) For one dimension model (1-D), stresses location is in terms of x.
(c) For two dimension model (2-D), stresses were extracted at x=0, x in the table should be read as y.
(d) For three dimension model (3-D), stresses are extracted at y=0 and the stresses were calculated as an average of five tetrahedra.
(e) See page 86 for details.

Table 4.8.1: Longitudinal stress comparisons for England's flexurally restrained beam (Sustained temperatures). (Benchmark problem)

Time / X	1.015E-06			2.050E-06		
	1-D	2-D	3-D	1-D	2-D	3-D
0.9	-6.003	-5.799	-5.832	-3.722	-3.627	-3.636
0.7	-6.451	-6.286	-6.303	-4.178	-4.078	-4.087
0.5	-6.887	-6.769	-6.783	-4.728	-4.631	-4.641
0.3	-7.286	-7.221	-7.235	-5.391	-5.304	-5.316
0.1	-7.612	-7.603	-7.617	-6.181	-6.116	-6.131
-0.1	-7.816	-7.862	-7.877	-7.103	-7.077	-7.095
-0.3	-7.831	-7.925	-7.942	-8.145	-8.172	-8.193
-0.5	-7.564	-7.695	-7.711	-9.253	-9.344	-9.367
-0.7	-6.894	-7.041	-7.042	-10.295	-10.450	-10.464
-0.9	-5.658	-5.792	-5.663	-11.003	-11.200	-11.104

Note:

(a) Stresses are expressed with reference to one dimensional problem and is in terms of MN/m^2.
(b) For one dimension model (1-D), stresses location is in terms of x.
(c) For two dimension model (2-D), stresses were extracted at x=0, x in the table should be read as y.
(d) For three dimension model (3-D), stresses are extracted at y=0 and the stresses were calculated as an average of five tetrahedra.
(e) See page 86 for details.

Table 4.8.2: Longitudinal stress comparison for England's flexurally restrained beam (Sustained temperatures). (Benchmark problem)

Time / X	3.062E-06			3.990E-06		
	1-D	2-D	3-D	1-D	2-D	3-D
0.9	-3.155	-3.116	-3.118	-2.952	-2.936	-2.935
0.7	-3.525	-3.477	-3.480	-3.283	-3.263	-3.262
0.5	-3.990	-3.933	-3.938	-3.700	-3.673	-3.673
0.3	-4.585	-4.522	-4.529	-4.238	-4.203	-4.206
0.1	-5.360	-5.295	-5.304	-4.934	-4.911	-4.917
-0.1	-6.377	-6.322	-6.337	-5.936	-5.889	-5.889
-0.3	-7.716	-7.689	-7.711	-7.320	-7.279	-7.298
-0.5	-9.459	-9.488	-9.518	-9.307	-9.297	-9.328
-0.7	-11.648	-11.760	-11.790	-12.163	-12.220	-12.264
-0.9	-14.184	-14.400	-14.340	-16.147	-16.330	-16.308

Note:

(a) Stresses are expressed with reference to one dimensional problem and is in terms of MN/m^2.
(b) For one dimension model (1-D), stresses location is in terms of x.
(c) For two dimension model (2-D), stresses were extracted at x=0, x in the table should be read as y.
(d) For three dimension model (3-D), stresses are extracted at y=0 and the stresses were calculated as an average of five tetrahedra.
(e) See page 86 for details.

Table 4.8.3: Longitudinal stress comparisons for England's flexurally restrained beam (Sustained temperatures). (Benchmark problem)

Time	0.0 (phase 1)			0.900E-07 (phase 1)		
X	1-D	2-D	3-D	1-D	2-D	3-D
0.9	-18.016	-18.180	---	-15.879	-15.980	---
0.7	-15.568	-15.700	---	-14.109	-14.200	---
0.5	-13.120	-13.210	---	-12.267	-12.340	---
0.3	-10.672	-10.730	---	-10.349	-10.400	---
0.1	-8.224	-8.241	---	-8.355	-8.378	---
-0.1	-5.776	-5.755	---	-6.283	-6.278	---
-0.3	-3.328	-3.270	---	-4.129	-4.094	---
-0.5	-0.880	-0.784	---	-1.893	-1.825	---
-0.7	1.568	1.701	---	0.428	0.532	---
-0.9	4.016	4.187	---	2.835	2.979	---

Note:

(a) Stresses are expressed with reference to one dimensional problem and is in terms of MN/m^2.
(b) For one dimension model (1-D), stresses location is in terms of x.
(c) For two dimension model (2-D), stresses were extracted at x=0, x in the table should be read as y.
(d) No three dimension analysis were performed for computer cost considerations.
(e) See page 86 for details.

Table 4.8.4: Longitudinal stress comparisons for England's flexurally restrained beam (Cyclic temperatures). (Benchmark problem)

Time / X	1.015E-06 (phase 2)			2.050E-06 (phase 2)		
	1-D	2-D	3-D	1-D	2-D	3-D
0.9	-5.157	-5.089	---	-5.456	-5.404	---
0.7	-5.740	-5.693	---	-5.944	-5.908	---
0.5	-6.261	-6.233	---	-6.381	-6.359	---
0.3	-6.719	-6.707	---	-6.764	-6.755	---
0.1	-7.110	-7.112	---	-7.093	-7.094	---
-0.1	-7.435	-7.449	---	-7.364	-7.375	---
-0.3	-7.690	-7.714	---	-7.578	-7.596	---
-0.5	-7.875	-7.907	---	-7.733	-7.757	---
-0.7	-7.987	-8.024	---	-7.827	-7.855	---
-0.9	-8.025	-8.066	---	-7.859	-7.890	---

Note:

(a) Stresses are expressed with reference to one dimensional problem and is in terms of MN/m^2.
(b) For one dimension model (1-D), stresses location is in terms of x.
(c) For two dimension model (2-D), stresses were extracted at x=0, x in the table should be read as y.
(d) No three dimension analysis were performed for computer cost considerations.
(e) See page 86 for details.

Table 4.8.5: Longitudinal stress comparisons for England's flexurally restrained beam (Cyclic temperatures). (Benchmark problem)

Time / X	3.062E-06 (phase 2)			3.990E-06 (phase 2)		
	1-D	2-D	3-D	1-D	2-D	3-D
0.9	-5.699	-5.622	---	-5.900	-5.861	---
0.7	-6.111	-6.085	---	-6.241	-6.221	---
0.5	-6.479	-6.462	---	-6.555	-6.542	---
0.3	-6.802	-6.794	---	-6.831	-6.825	---
0.1	-7.078	-7.078	---	-7.067	-7.066	---
-0.1	-7.307	-7.314	---	-7.262	-7.267	---
-0.3	-7.487	-7.500	---	-7.416	-7.425	---
-0.5	-7.617	-7.634	---	-7.527	-7.539	---
-0.7	-7.697	-7.717	---	-7.595	-7.609	---
-0.9	-7.723	-7.746	---	-7.617	-7.634	---

Note:

(a) Stresses are expressed with reference to one dimensional problem and is in terms of MN/m^2.
(b) For one dimension model (1-D), stresses location is in terms of x.
(c) For two dimension model (2-D), stresses were extracted at x=0, x in the table should be read as y.
(d) No three dimension analysis were performed for computer cost considerations.
(e) See page 86 for details.

Table 4.8.6: Longitudinal stress comparisons for England's flexurally restrained beam (Cyclic temperatures). (Benchmark problem)

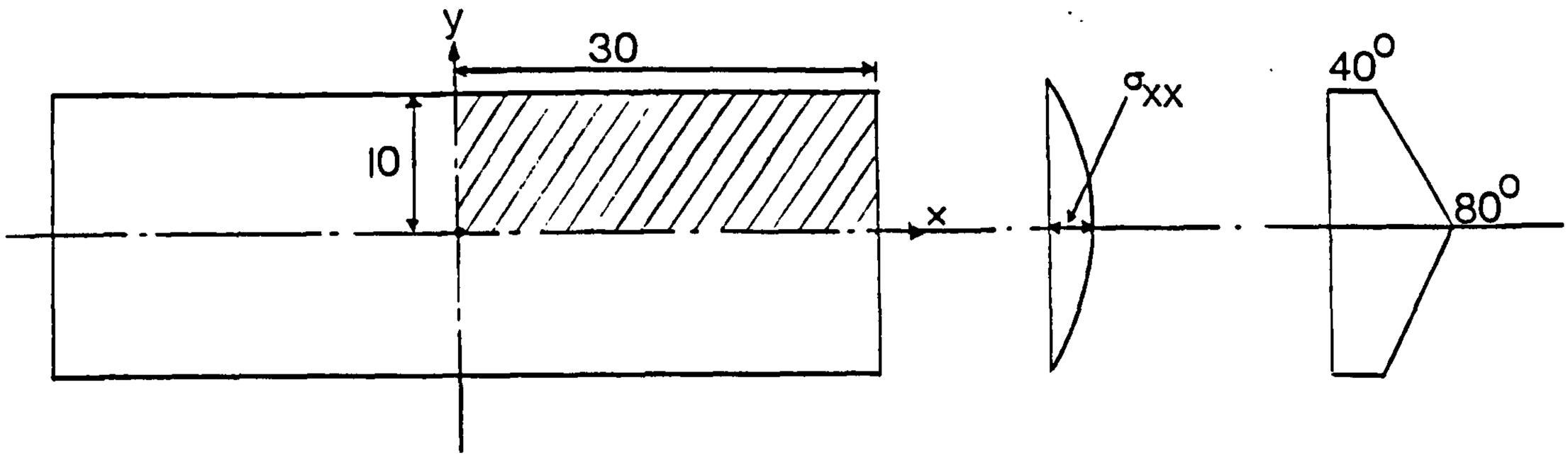

Aspect ratio = 3

Compressive edge pressure
$\sigma_{xx}=13.79(1-y^2)$ MN/m^2

Temperature
T=T(y)

(a) The Allen's plate subjected to parabolic edge loading

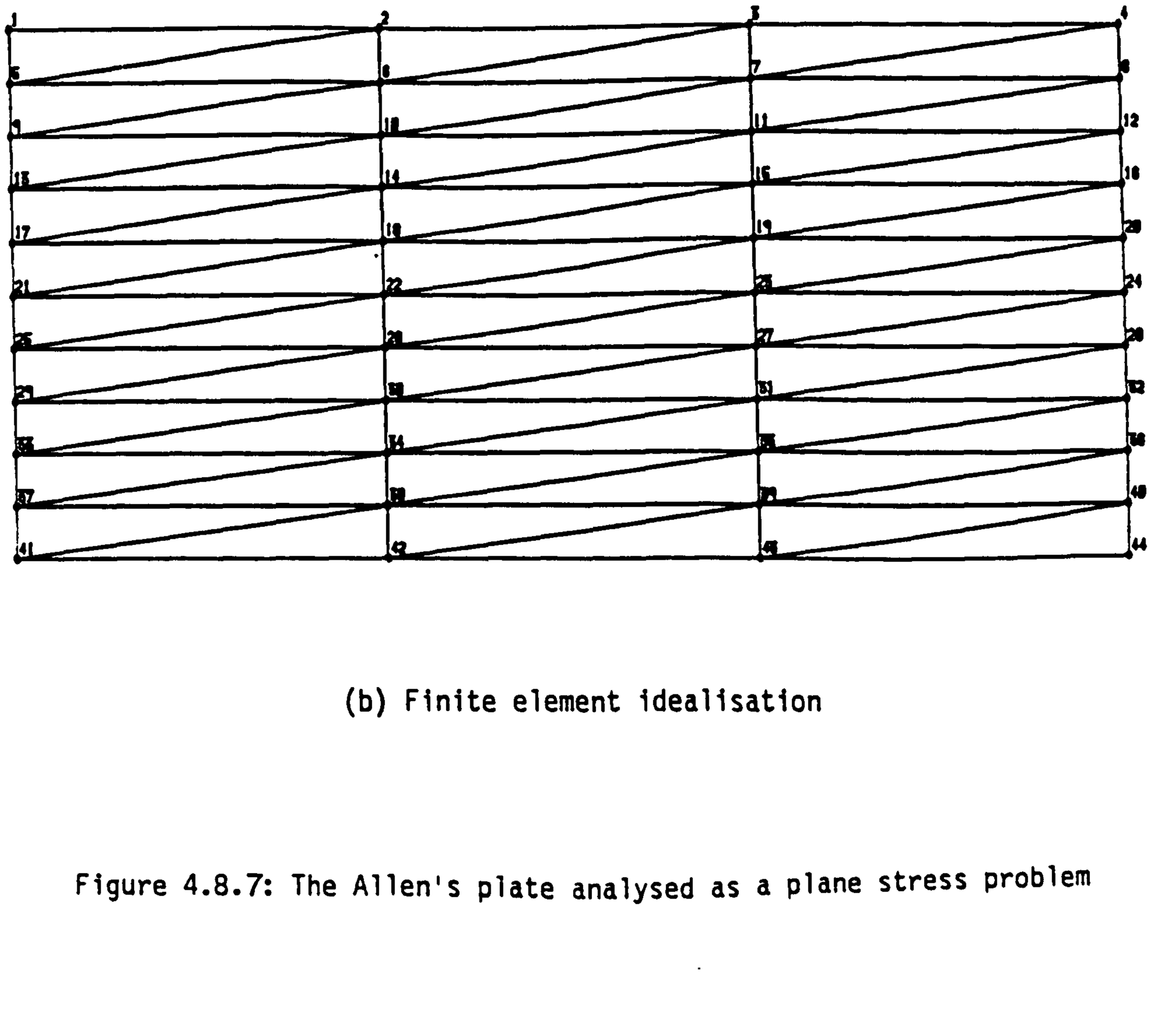

(b) Finite element idealisation

Figure 4.8.7: The Allen's plate analysed as a plane stress problem

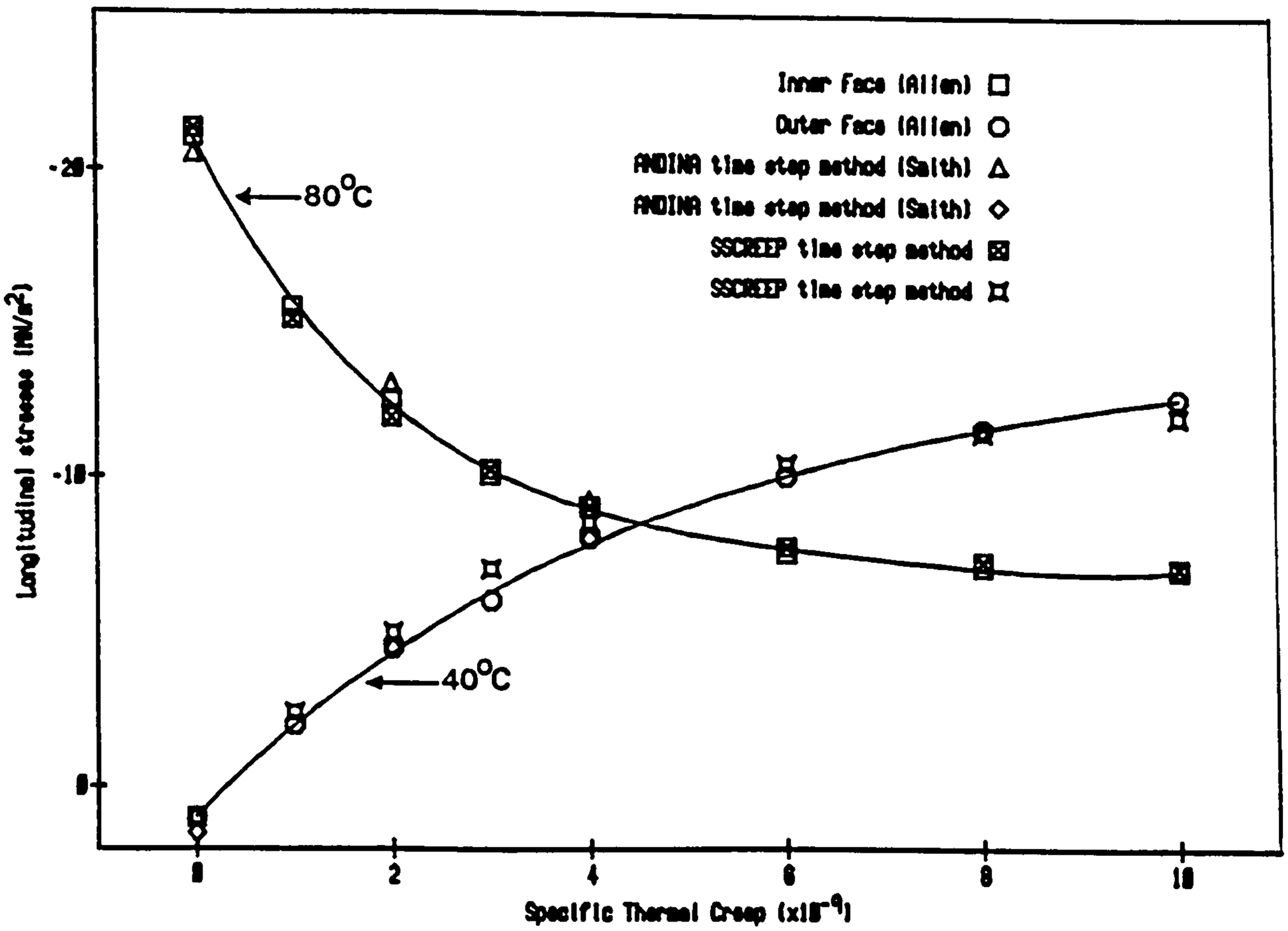

Note:

(a) Units for specific thermal creep is microstrain per lb/in^2 per ^oC.

(b) Allen's results was obtained using an analytical approach using stress functions

(c) Smith's results were obtained using a general purpose finite element program called ANDINA.

Figure 4.8.8 Stress contours for Allen's flat plate problem

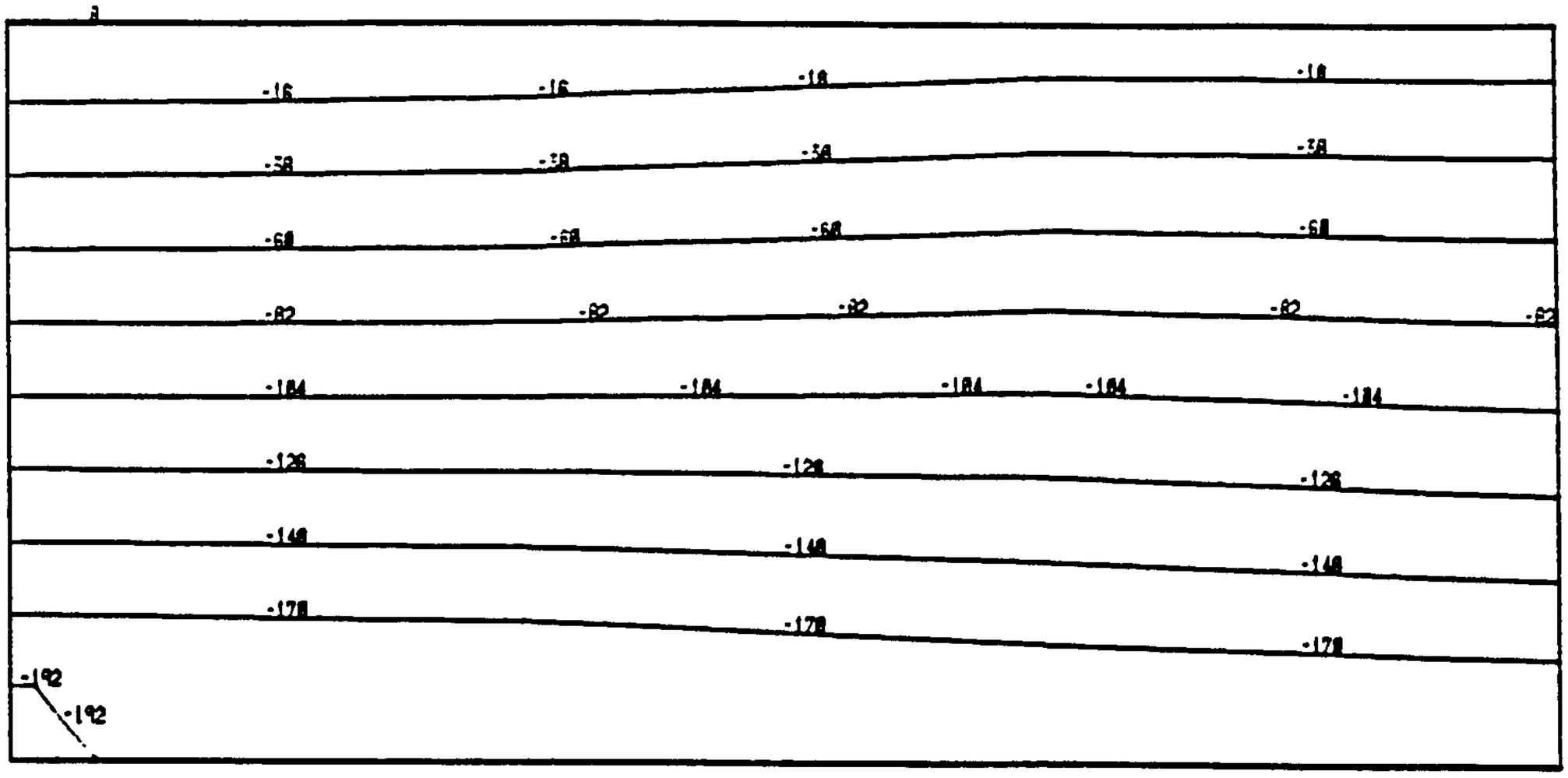

(a) σ_{xx} (x10) at c = 0.0

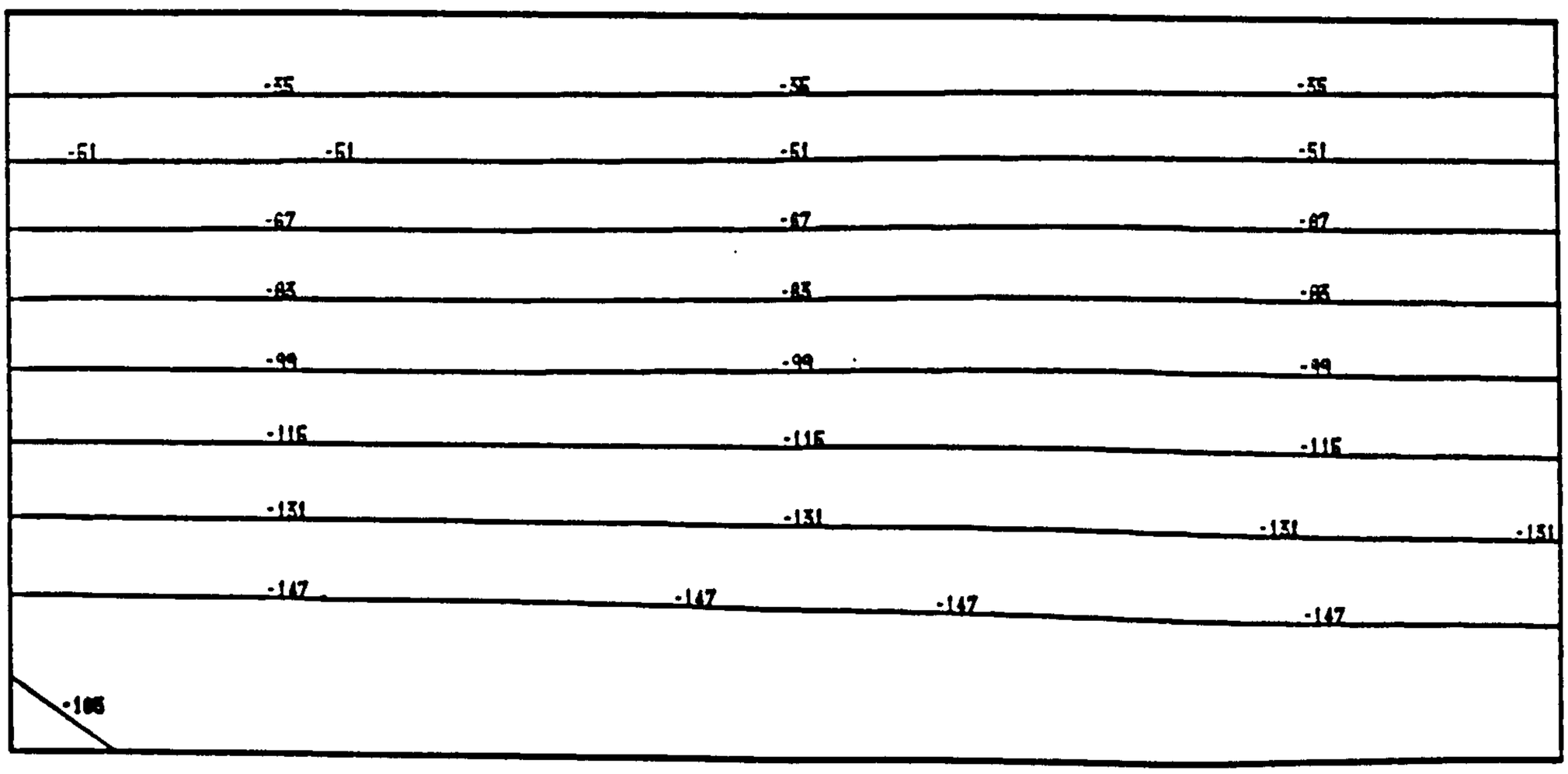

(b) σ_{xx} (x10) at c = 9.0E-08

Figure 4.8.9 Stress contours for Allen's flat plate problem

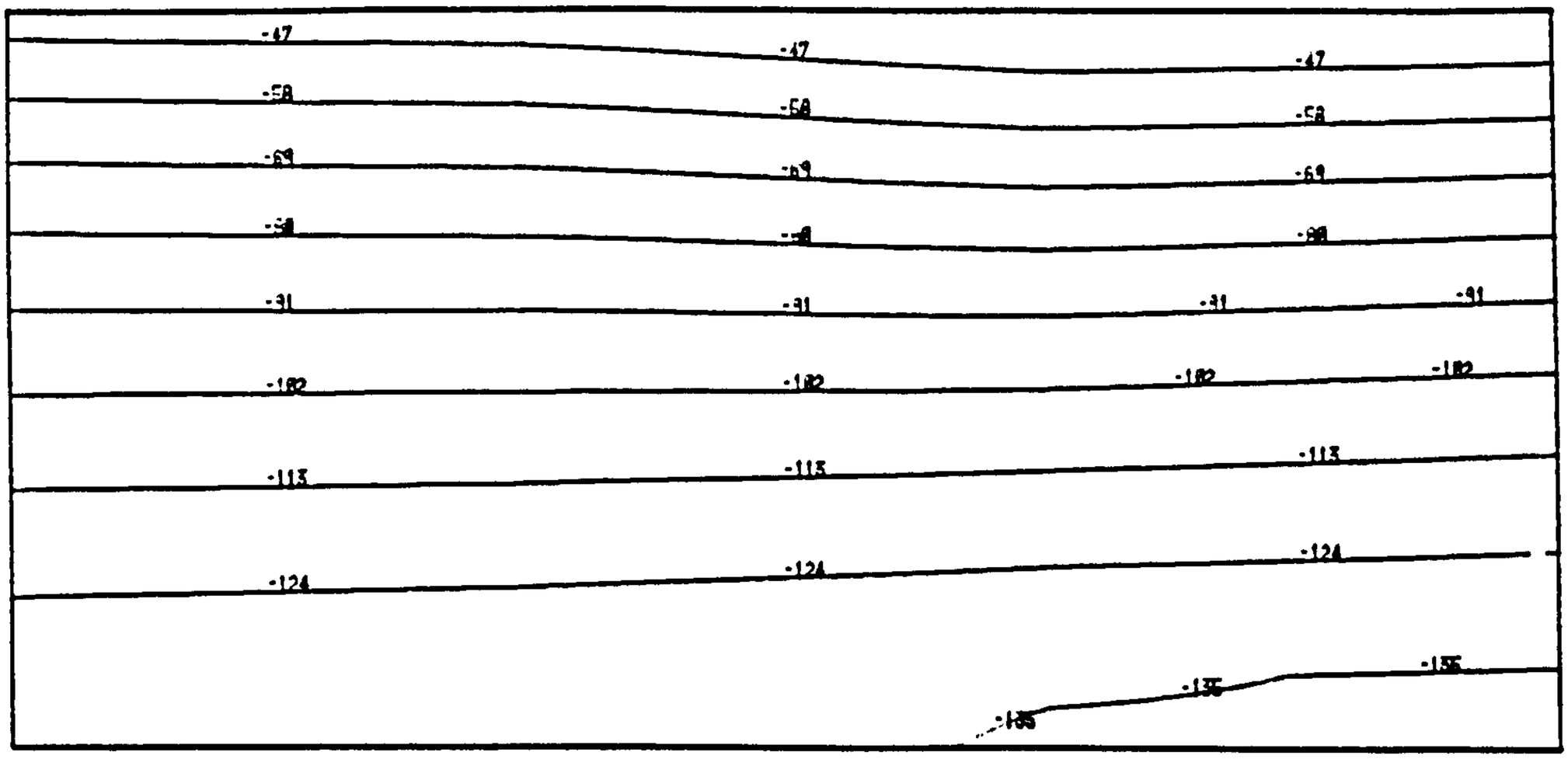

(a) σ_{xx} (x10) at c = 2.275E-07

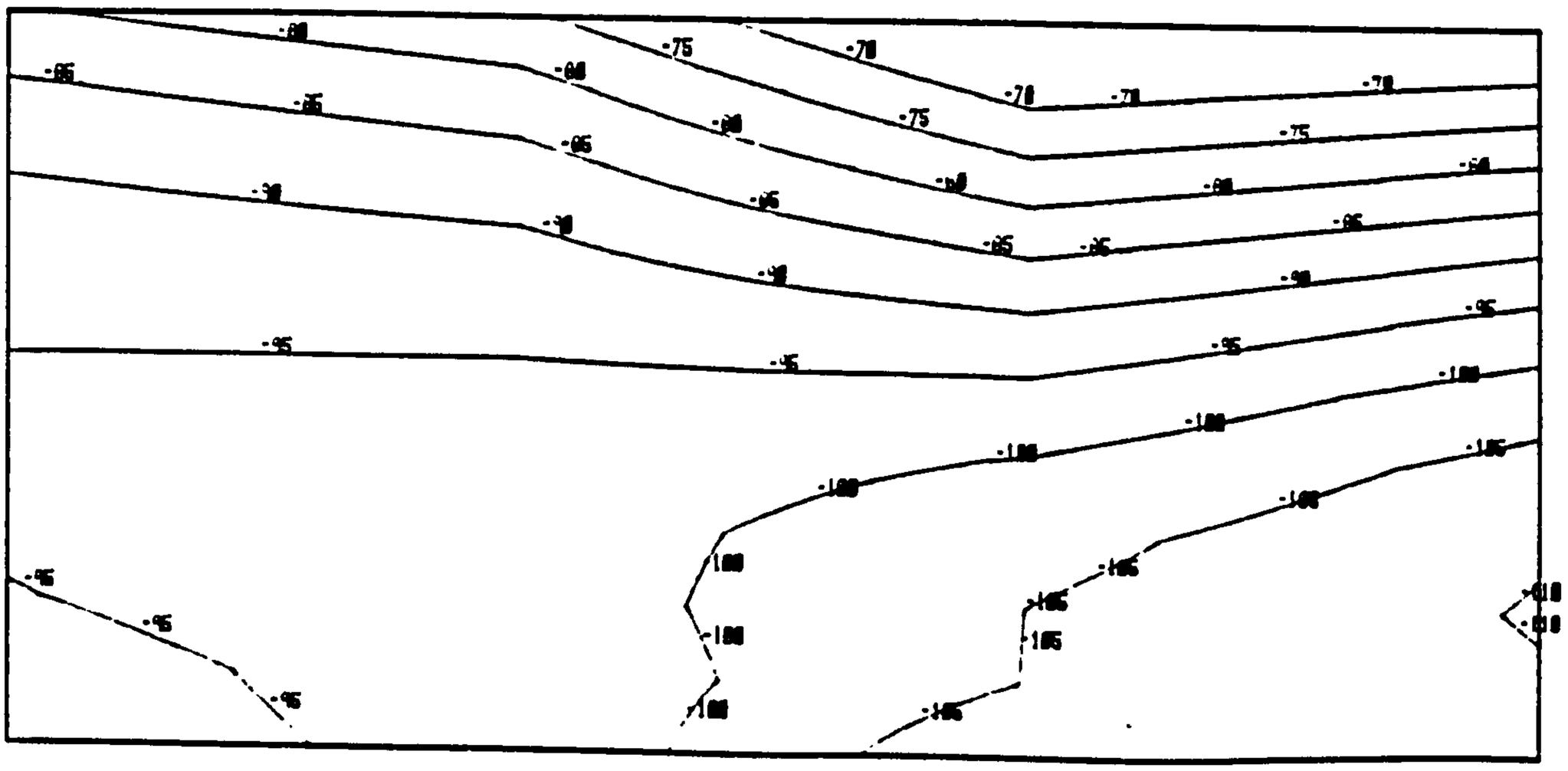

(b) σ_{xx} (x10) at c = 5.25E-07

Figure 4.8.10 Stress contours for Allen's flat plate problem

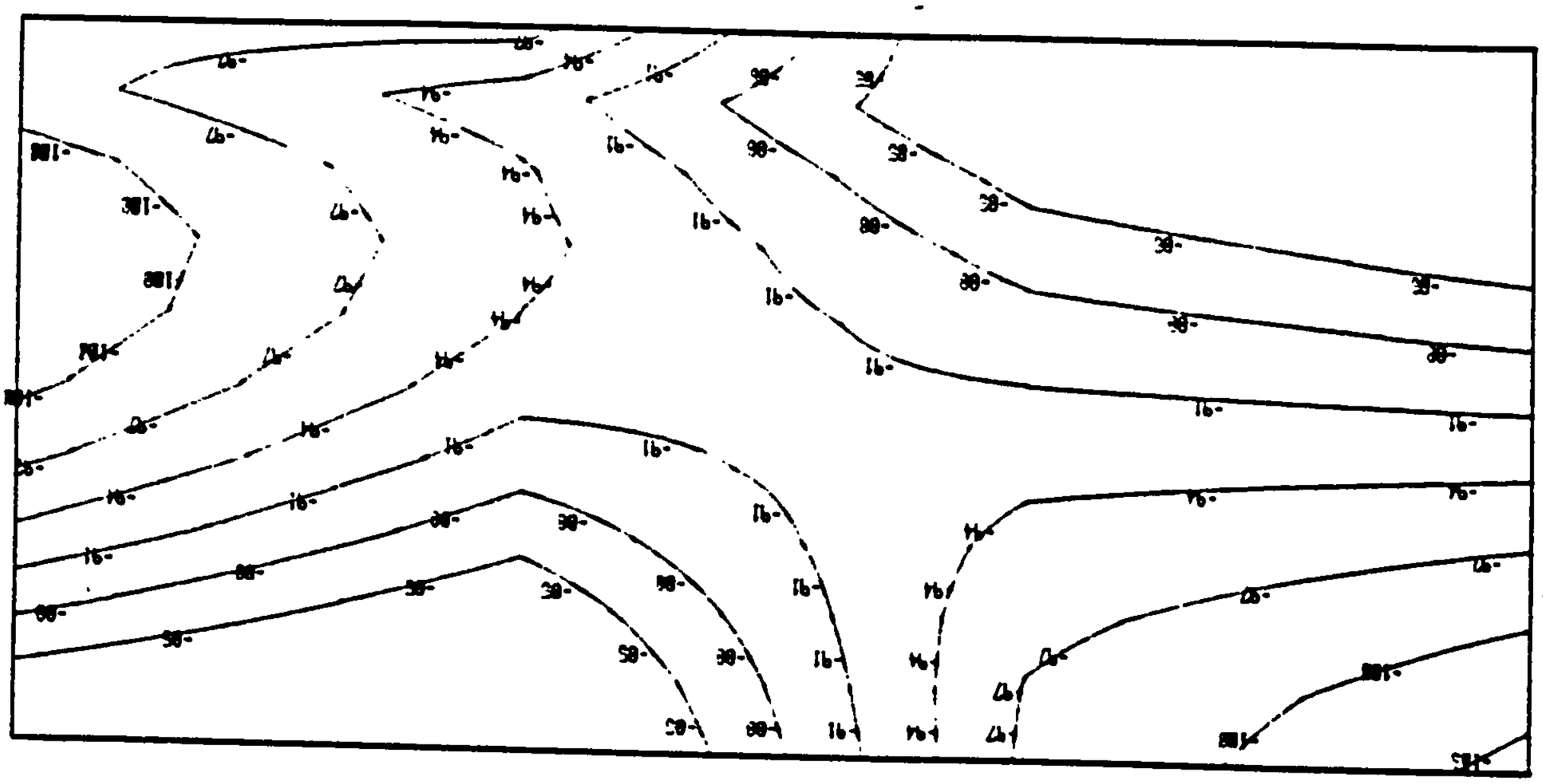

(a) σ_{xx} (x10) at c = 8.775E-07

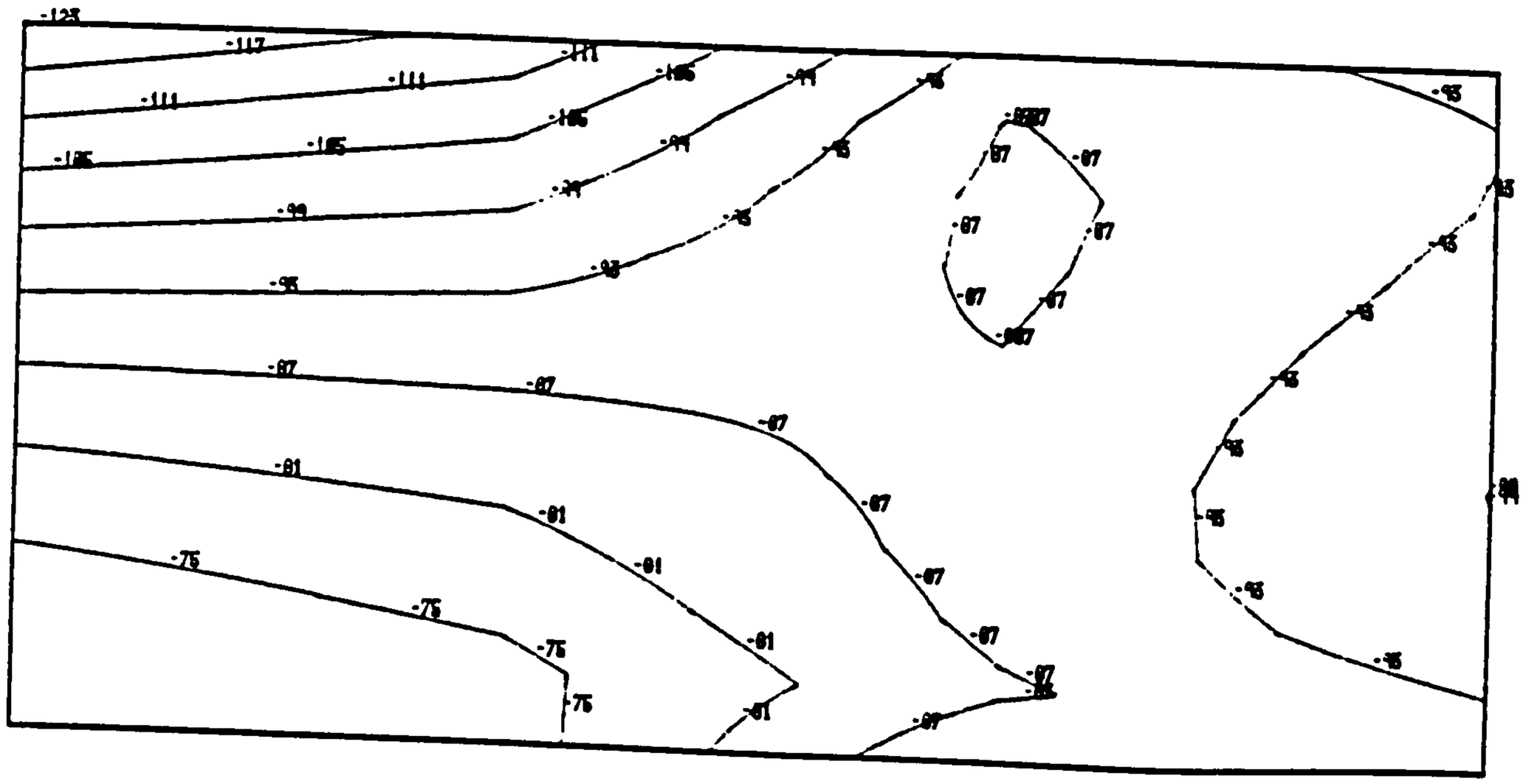

(b) σ_{xx} (x10) at steady-state

Figure 4.8.11 Stress contours for Allen's flat plate problem

CHAPTER FIVE

A DIRECT THREE DIMENSIONAL SOLUTION ALGORITHM BASED ON THE PRINCIPLE OF MINIMUM COMPLEMENTARY POWER

Summary

The Complementary Power Theory is presented. It permits stresses to be evaluated in both the transient creep phase and in the limiting steady state condition from a Power Minimisation Procedure in conjunction with a Ritz process. This Procedure has the advantage that it maybe used in the form of exact or approximate analysis and is more economic than the conventional time-step algorithms. The nature of the Ritz's expression together with its automatic generation is explored in detail.

The Power Minimisation Procedure is extended to general two and three dimensional continua utilising the finite element technique. A computer program VPCREEP in which isoparametric elements of the serendipity family is used as the finite element model is developed based on the Procedure and applied to some benchmark problems to validate the accuracy and efficiency of the Procedure.

5.1 The Power Minimisation Procedure

The Power Minimisation Procedure utilised the Principle of the Minimum of the Total Complementary Power depicted in section 2.7. Where a structure at all times in equilibrium with the specified loading and compatible with respect to both internal strains and external geometrical constraints, the Complementary Power Principle states:

$$\int \{\dot{\varepsilon}\}^T\{\delta\sigma\}\, dV = 0 \qquad (5.1.1)$$

In a Ritz type representation, the state of stress $\{\sigma\}$ is specified as a series of terms as given in equation 5.1.2, for which the spatial stress distributions $\{\sigma_i\}$ are specified. The problem becomes one of identifying the time functions $\{a_i\}$ associated with each stress distribution. These functions represent the preferred weighting of each spatial stress distribution to give the best match to the exact

solutions at all times as dictated by the Complementary Power Principle, viz equation 5.1.1. Thus

$$\{\sigma\} = \{\sigma_o\} + a_1\{\sigma_1\} + \ldots + a_n\{\sigma_n\}$$

$$= \{\sigma_o\} + \{a\}^T[\sigma] \qquad (5.1.2)$$

where $\{\sigma_o\}$ represents any set of stresses which are in equilibrium with the boundary loading and $[\sigma]$ constitutes self-equilibrating internal stress distributions.

In an analogous Maxwell representation, the strain rate vector $\{\dot{\varepsilon}\}$ is given as, (vide equation 2.5.2):

$$\{\dot{\varepsilon}\} = \frac{1}{E_m}[V]\{\dot{\sigma}\} + \Phi(T)[V_c]\{\sigma\} \qquad (5.1.3)$$

where $[V]$ and $[V_c]$ are matrices of the elastic and creep Poisson's ratio respectively, viz:

$$[V] = \begin{bmatrix} 1 & -v & -v & 0 & 0 & 0 \\ -v & 1 & -v & 0 & 0 & 0 \\ -v & -v & 1 & 0 & 0 & 0 \\ 0 & 0 & 0 & 2(1+v) & 0 & 0 \\ 0 & 0 & 0 & 0 & 2(1+v) & 0 \\ 0 & 0 & 0 & 0 & 0 & 2(1+v) \end{bmatrix} \qquad (5.1.4)$$

$$[V_c] = \begin{bmatrix} 1 & -v_c & -v_c & 0 & 0 & 0 \\ -v_c & 1 & -v_c & 0 & 0 & 0 \\ -v_c & -v_c & 1 & 0 & 0 & 0 \\ 0 & 0 & 0 & 2(1+v_c) & 0 & 0 \\ 0 & 0 & 0 & 0 & 2(1+v_c) & 0 \\ 0 & 0 & 0 & 0 & 0 & 2(1+v_c) \end{bmatrix} \qquad (5.1.5)$$

Experimental evidence (vide section 2.3) suggests that creep Poisson's ratio v_c and elastic Poisson's ratio v can be taken as identical at working stress levels. Thus

$$[V] = [V_c] \qquad (5.1.6)$$

Therefore equation 5.1.3 maybe recast as:

$$\{\dot{\varepsilon}\} = (\nabla + \Phi(T))[V]\{\sigma\}/E_m \qquad (5.1.7)$$

where ∇ is the differential operator in pseudo-time, $\nabla = d/dc$.

The strain rate vector $\{\dot{\varepsilon}\}$ of equation 5.1.1 maybe represented in terms of the stresses of equation 5.1.2 through equation 5.1.7 and noting that:

$$\{\delta\sigma\} = \frac{\partial\{\sigma\}}{\partial a_i}\,\delta a_i = \{\sigma_i\}\delta a_i \qquad (5.1.8)$$

We have then,

$$\{\dot{\varepsilon}\} = (\nabla + \Phi(T))[V]\{\sigma\}$$

$$= \frac{1}{E_m}[V][\sigma]\{\dot{a}\} + \Phi(T)[V][\sigma]\{a\} + \Phi(T)[V]\{\sigma_o\} \qquad (5.1.9)$$

From equation 5.1.2 and equation 5.1.8 we obtain:

$$\int \{\dot{\varepsilon}\}\{\delta\sigma\} = \int [\sigma]^T\{\dot{\varepsilon}\}\,dV = 0 \qquad (5.1.10)$$

After substitution of $\{\dot{\varepsilon}\}$ from equation 5.1.9, equation 5.1.10 leads to the following matrix differential equation for the time functions $\{a\}$; thus,

$$[Q]\{\dot{a}\} + [R]\{a\} + \{s\} = \{0\} \qquad (5.1.11)$$

where

$$Q_{rs} = \int \frac{1}{E_m}\{\sigma_r\}^T[V]\{\sigma_s\}\,dV$$

$$R_{rs} = \int \Phi(T)\{\sigma_r\}^T[V]\{\sigma_s\}\,dV \qquad (5.1.12)$$

$$s_r = \int \Phi(T)\{\sigma_r\}^T[V]\{\sigma_0\}\, dV$$

Equation 5.1.11 has the solution:

$$\{a\} = EXP(-[Q]^{-1}[R]c)\{s\} - [R]^{-1}\{s\} \qquad (5.1.13)$$

where {s} is a vector of coefficients determined from the initial condition. This equation maybe evaluated readily for any values of pseudo-time c, to give the weighting functions {a} at these times.

When temperature varies in a cyclic manner in time, the time-dependent stresses can be evaluated by the varying coefficients method. Analysis by this method proceeds by evaluating stresses using equation 5.1.11 with appropriate [Q] and [R] matrices. Then after each change in temperature an initial value problem arises where the vector {s} has to be re-evaluated. It is apparent that this requires the evaluation of the vector {a} at the end and at the start of each phase, i.e. immediately before and after each change of temperature. After each change there is a change in thermal stresses which is reflected in a definable change in the vector {a}.

5.2 The Finite Element Characteristics

In this chapter iso-parametric elements of the serendipity family (Zienkiewicz 1982) are implemented. The iso-parametric elements are those elements having the same shape function for defining geometry and displacements. In terms of performance, the iso-parametric elements have been demonstrated to be distinctly superior to any other types of elements for continuum stress analysis, both with regard to the individual element properties and also in application to idealised structural systems. In addition, the iso-parametric element have the advantage of isotropy (i.e. their stiffnesses are identical along their axis).

a. Two dimensional analysis:

Figure 5.2.1 shows a typical quadratic (8 nodes) iso-parametric element defined in local coordinates with axis (ξ,η). For corner nodes, the shape function N_i (vide section 4.1) defined in local coordinates (ξ,η) is:

$$N_i = \tfrac{1}{4}(1 + \xi_o)(1 + \eta_o)(\xi_o + \eta_o - 1) \qquad (5.2.1)$$

and for the mid-side nodes:

$$N_i = \tfrac{1}{2}(1 - \xi^2)(1 + \eta_o) \ , \quad \xi_i = 0$$
$$N_i = \tfrac{1}{2}(1 + \xi_o)(1 - \eta^2) \ , \quad \eta_i = 0 \qquad (5.2.2)$$

where

$$\xi_o = \xi_i\xi \quad ; \quad \eta_o = \eta_i\eta \qquad (5.2.3)$$

b. Axisymmetric analysis:

The problem of stress analysis of solids of revolution under axisymmetric loads is of practical importance (vide section 4.2). The element used for modelling solids of revolution is the axisymmetric ring element having an 8-nodes iso-parametric cross-section. The shape function being the same as those in two dimensional analysis (Figure 5.2.2).

c. Three dimensional analysis:

The three dimensional 20-node iso-parametric brick elements is used for three dimensional modelling. The shape function for corner nodes being:

$$N_i = \tfrac{1}{8}(1 + \xi_o)(1 + \eta_o)(1 + \zeta_o)(\xi_o + \eta_o\zeta_o + 2) \qquad (5.2.4)$$

and for typical mid-side nodes:

$$\xi_i = 0 \ , \ \eta_i = \pm 1 \ , \ \zeta_i = \pm 1$$
$$N_i = \tfrac{1}{4}(1 - \xi^2)(1 + \eta_o)(1 + \zeta_o) \qquad (5.2.5)$$

Again, the shape function is expressed in terms of local coordinates, Figure 5.2.3.

5.3 Numerical Computation of Element Matrices by Gauss-Legendre Quadrature

To perform finite element analysis using the iso-parametric elements, element stiffness matrices (vide section 4.1) viz:

$$[K^e] = \int [B]^T[D][B]\, dV \qquad (5.3.1)$$

and associated load vectors (vide section 4.1) viz:

$$\{F^e\} = \int [N]^T\{q\}\, dS \qquad (5.3.2)$$

must be evaluated. To evaluate such matrices, two transformations are necessary. In the first place as N_i is defined in terms of local curvilinear coordinates, it is necessary to devise some means of expressing the global derivatives in terms of local derivatives. In the second place, the element of volume (or surface) over which the integration has to be carried out needs to be expressed in terms of the local coordinates with appropriate change limits of integration.

The derivatives in a typical matrix $[B_i]$ (vide equation 4.1.4) maybe evaluated by applying the 'chain rule' of partial differential as follows:

$$\begin{Bmatrix} \partial N_i/\partial \xi \\ \partial N_i/\partial \eta \\ \partial N_i/\partial \zeta \end{Bmatrix} = \begin{bmatrix} \partial x/\partial \xi & \partial y/\partial \xi & \partial z/\partial \xi \\ \partial x/\partial \eta & \partial y/\partial \eta & \partial z/\partial \eta \\ \partial x/\partial \zeta & \partial y/\partial \zeta & \partial z/\partial \zeta \end{bmatrix} \begin{Bmatrix} \partial N_i/\partial x \\ \partial N_i/\partial y \\ \partial N_i/\partial z \end{Bmatrix}$$

$$= [J] \begin{Bmatrix} \partial N_i/\partial x \\ \partial N_i/\partial y \\ \partial N_i/\partial z \end{Bmatrix} \qquad (5.3.4)$$

In the above, the left hand side can be evaluated as the functions N_i are specified in local coordinates (vide section 5.2). Furthermore as x, y, z are explicitly given by the relation defining the curvilinear coordinates (vide equation 4.1.2), the Jacobian matrix [J] can be found explicitly in terms of the local coordinates. To find the global derivatives we invert [J]; thus

$$\begin{Bmatrix} \partial N_i/\partial x \\ \partial N_i/\partial y \\ \partial N_i/\partial z \end{Bmatrix} = [J]^{-1} \begin{Bmatrix} \partial N_i/\partial \xi \\ \partial N_i/\partial \eta \\ \partial N_i/\partial \zeta \end{Bmatrix} \qquad (5.3.5)$$

[J] maybe written in terms of the shape function viz:

$$[J] = \begin{bmatrix} \partial N_1/\partial \xi & \partial N_2/\partial \xi & \dots & \partial N_i/\partial \xi \\ \partial N_1/\partial \eta & \partial N_2/\partial \eta & \dots & \partial N_i/\partial \eta \\ \partial N_1/\partial \zeta & \partial N_2/\partial \zeta & \dots & \partial N_i/\partial \zeta \end{bmatrix} \begin{bmatrix} x_1 & y_1 & z_1 \\ x_2 & y_2 & z_2 \\ x_3 & y_3 & y_3 \\ . & . & . \\ . & . & . \\ x_i & y_i & z_i \end{bmatrix} \qquad (5.3.6)$$

Since matrix [B] is expressed in local coordinates, it is necessary to carry out the integration in equation 5.3.1 in local coordinates too, using the relationship:

$$dV = dxdydz = \det[J]\, d\xi d\eta d\zeta \qquad (5.3.7)$$

Thus equation 5.3.1 maybe written as:

$$[K^e] = \iiint [B]^T[D][B] \det[J]\, d\xi d\eta d\zeta \qquad (5.3.8)$$

The integration is carried out within a prism (vide Figure 5.2.3) with limits between 1 and -1, not in the complicated distorted shape, hence accounting for the simple integration limits. Typically, the expressions for evaluating the contributions of surface tractions (vide equation 5.3.2) are:

$$\{F^e\} = \int [N]^T\{q\}\, dS \qquad (5.3.9)$$

The element dS will generally lie on the surface where one of the coordinates is constant. It is convenient to consider dS as vector orientated in the direction normal to the surface. For three dimensional problems the following vector cross products gives dS:

$$dS = \begin{Bmatrix} \partial x/\partial \xi \\ \partial y/\partial \xi \\ \partial z/\partial \xi \end{Bmatrix} X \begin{Bmatrix} \partial x/\partial \eta \\ \partial y/\partial \eta \\ \partial z/\partial \eta \end{Bmatrix} \qquad (5.3.10)$$

for ζ=constant and on substitution integrate within a domain $\xi>1, \eta<1$.

In order to integrate equation 5.3.8 efficiently the Gauss-Legendre Quadrature is utilised viz:

$$I = \iiint f(\xi, \eta, \zeta)\, d\xi d\eta d\zeta \qquad (5.3.11)$$

$$= \Sigma\Sigma\Sigma\, H_i H_j H_m\, f(\xi_i, \eta_j, \zeta_m) \qquad (5.3.12)$$

The limit of integration is bewteen -1 and 1. The Σ is over the indices i, j, m for i = 1, 2, ... n; j = 1, 2,... n; m=1, 2 ... n.

where n is the order of integration rule used and H_i, H_j, H_m are the weighting coefficients, Table 5.3.1. It should be noted that an n-th order rule integrates any polynomial of degree (2n-1), or less exactly. It is of interest to note that the sampling positions of the Gauss-Legendre Quadrature (ξ_i, η_j, ζ_m) coincide with roots of the Legendre polynomials. For quadratic elements, a 3-order Gauss point integration is adequate. Typically, the element stiffness is given as:

$$[K^e] = \Sigma\Sigma\Sigma\, H_i H_j H_m\, [B]^T[D][B]\det[J] \qquad (5.3.13)$$

where [B], [J] are evaluated at Gauss sampling points (ξ_i, η_j, ζ_m).

5.4 Evaluation of [Q], [R] and {s}

Likewise the matrix coefficients [Q], [R] and {s} (vide equation 5.1.11) maybe conveniently evaluated exactly as before. Let

$$\Psi(\sigma) = ([\sigma]^T[V][\sigma] \det [J])$$

and

$$\Psi(\sigma_o) = ([\sigma]^T[V]\{\sigma_o\} \det [J])$$

$$[Q] = \Sigma\Sigma\Sigma\Sigma\ H_i H_j H_m (\Psi(\sigma)/E_m) \qquad (5.4.1)$$

where $\Sigma\Sigma\Sigma\Sigma$ is the summation over the body volume and $[\sigma]$ are evaluate at the sampling point (ξ_i, η_j, ζ_m). Similarly,

$$[R] = \Sigma\Sigma\Sigma\Sigma\ H_i H_j H_m\ (\Phi(T)\Psi(\sigma)) \qquad (5.4.2)$$

$$\{s\} = \Sigma\Sigma\Sigma\Sigma\ H_i H_j H_m\ (\Phi(T)\Psi(\sigma_o)) \qquad (5.4.3)$$

Again $\Phi(T)$ and $\{\sigma_o\}$ are the values evaluated at sampling points. Typically,for a 20-nodes element, $\Phi(T(\xi_i,\eta_j,\zeta_m))$ are given as:

$$\Phi(T(\xi_i,\eta_j,\zeta_m))=\Sigma N_k(\xi_i,\eta_j,\zeta_m)\Phi(T(x_k,y_k,x_k)) \qquad (5.4.4)$$

For k=1, 2, ... n which represents the number of nodes per element.

5.5 Solution of Matrix Differential Equations

The resulting equilibrium equations are to be solved by the Partition Frontal Scheme as described in next section.

The matrix differential equation 5.1.11 maybe solved by a variety of methods, e.g. Runge-Kutta, and since the equation is first order it maybe solved explicitly viz:

$$\{a\} = EXP(-[Q]^{-1}[R]c)\{s\} - [R]^{-1}\{s\} \qquad (5.5.1)$$

Thus the time-dependent coefficients {a} maybe obtained by exponential series expansion of the first term in the right hand side viz:

$$EXP([\Gamma]) = [I] + [\Gamma] + \frac{1}{2!}[\Gamma]^2 + \ldots + \frac{1}{p!}[\Gamma]^p \qquad (5.5.2)$$

by writing $[\Gamma] = -[Q]^{-1}[R]c$. Let

$$[\Gamma_o] = [I]\ ;\ [\Gamma_r] = ([\Gamma][\Gamma_{r-1}])/r$$

Then the sums

$$[S_0] = [\Gamma_0]$$

$$[S_r] = [S_{r-1}] + [\Gamma_r] \ , \ r=1, 2, \ldots p \text{ and } p \to \infty. \tag{5.5.4}$$

give approximations to EXP([Γ]). Sometimes it is convenient to evaluate the sum of equation 5.5.2 for a small value of $c = \Delta c$, and then obtain the solution of other times such as $2c$, $4c$ ... $2^r c$ by successively squaring the result for $c=\Delta c$, r is a positive integer. Experiences indicates that $\Delta c = 10^{-8}$ MN/m^2 per ^oC is an optimal value.

However, the proportion of the central processing time (cp time) required to solve equation 5.5.1 is likely to be insignificant when it is embedded within a finite element program. Indeed this is one of the main reason why the Power Minimisation Procedure is distinctly superior to conventional time-step procedure.

5.6 The Partition Frontal Linear Equation Solver

In the sequential frontal solver (vide section 4.6), at any time during the elimination of the coefficients, only those equations corresponding to the degrees of freedom that have had their first appearance and not yet their last appearance, in terms of element by element processing, needed to be in core. This set of degrees of freedom constitutes the current front. Consequently, the front size will vary as the solution moves through the structure element by element processing deactivating certain degrees of freedom and activating others.

Such a scheme is efficiently used for the solution of structures in which the front size can be accommodated in-core throughout the processing of the coefficient matrix.

In cases where either the computer core required for the storage of the front equations exceeds the maximum in-core storage available in the computer or a small portion of the elements in the structural discretisation forms a 'spike' for which the front size is much larger than the mean front size for the entire structure, the front

can be partitioned into different sets, Figure 5.6.1. Since the order for processing eliminnation effects is immaterial, each column set can be loaded into central computer core when required, processed and then unloaded again to auxillary storage.

The partitioning of the frontal column is completely internal to the assembly and elimination phases of frontal solution method. In VPCREEP the partitioning process is completely automatic and is summarised in Figures 5.6.2.

5.7 Nature of Ritz's Representation

In a Ritz process mentioned in section 5.1, a set of basis functions is selected and constructed to an approximated solution of the form:

$$\sigma_{ij}(x,y,z,c)= \sigma_{ij}(x,y,z,0) + \Sigma\ a_k\Phi_{k,ij}(x,y,z) \qquad (5.7.1)$$

In the context of present work, these basis functions $\Phi_{k,ij}$ are known as self-equilibrating stress functions and they must at least satisfy the following conditions:

a. $\Phi_{k,ij}$ must satisfy the prescribed boundary conditions under no load conditions.

b. $\Phi_{k,ij}$ must be self-equilibrium.

c. $\Phi_{k,ij}$ must be linearly independent.

and if $\Phi_{k,ij}$ forms an orthogonal set, numerical stability is assured. These self-equilibrating stress distributions maybe defined by closed form functions such as Legendre polynomials, Airy stress functions and Finzi stress functions for one, two and three dimensional problems respectively. Despite many trials of great complexity, these analytic functions are often either difficult or impossible to solve except for structures of the simplest shape.

A possible way round this is the use of numerically defined self-equilibrating stress distributions which are generated from displacement finite element analyses which forms the subject of discussion in the next section.

5.8 Automatic Generation of Self-Equilibrating Stress Distributions

There are various possibilities exist for generating the self-equilibrating distributions. At least two methods are readily available in any creep problem:

1. An elastic analysis for a structure subjected to initial strain. The initial strain could be due to a temperature variation in space. The resulting stress distributions could be self-equilibrium.

2. The difference between two elastic solutions for the same boundary loads and with spatial variation of the elastic modulus.

In VPCREEP the following types of self-equilibrating stress distributions maybe generated:

a. The actual thermal stress distribution:

This arises from the temperature field under which the structure is operating.

b. Effective modulus type distributions:

It has been stated that in chapter 2 that by the effective modulus method, one step calculation of transient stresses is possible using a non-homogeneous elastic modulus throughout the structure defined by:

$$E_{eff} = \frac{E_m}{(1 + E_m \Phi(T) c)} \qquad (5.8.1)$$

where E_m is the Young's modulus of elasticity, $\Phi(T)$ is the normalising creep function, T is the sustained temperature at the point considered and c is the pseudo-time at which the transient stresses σ_{eff} are required. This approach is known to provide inaccurate creep solution. However, this method could be beneficial in obtaining self-equilibrating stress distributions by subtracting the stresses obtained from the thermo-elastic stresses. It is also possible to generate more than

one distribution by this way corresponding to solutions at different values of pseudo-time, and the self-equilibrating stress distribution becomes $(\sigma_o - \sigma_{eff})$.

c. True steady-state type distributions:

The steady-state stresses required for this distribution are obtained by making use of the analogy that exists between conventional elastic theory and the direct calculation of steady-state stresses caused by creep (vide section 2.6).

By this analogy, the steady-state stresses in a structure subjected to a sustained temperature distribution, σ_{ss}, maybe obtained from a stiffness analysis by replacing the elastic modulus with the reciprocal of $\Phi(T)$ and the self-equilibrating stress distribution becomes $(\sigma_o - \sigma_{ss})$.

In the case of temperature varying in a cyclic manner between two sets of fixed values T_1 and T_2 and with phase length k_1 and k_2 respectively, the steady-state cyclic stresses σ_{ssc} can be obtained readily through a single elastic procedure (vide section 2.6). In these procedures the modulus of elasticity is replaced by an equivalent spatially varying modulus of the value:

$$E_m = \frac{(1 + k)}{\Phi(T_1) + \Phi(T_2)k} \qquad (5.8.2)$$

where $k = k_2/k_1$ and at the same time the structure is subjected to analogous initial strains $\{\varepsilon_o\}$ of the value,

$$\{\varepsilon_o\} = \frac{-[V]\{\sigma_T\}k\Phi(T_2)}{(1+k)} \qquad (5.8.3)$$

and the self-equilibrating stress distribution becomes $(\sigma_o - \sigma_{ssc})$.

d. Fictitious temperature fields type distributions:

This type of stress distributions, σ_{Tf}, is based on suitable choice of spatially varying temperature fields for the structure being considered.

5.9 The VPCREEP Program

5.9.1 General Remarks

The VPCREEP computer code, or Virtual Power CREEP analysis program, is designed as a special purpose finite element program for the analysis of two and three dimensional concrete structures subjected to the combined influence of creep and temperature utilising the Power Minimisation Procedure as described earlier in this chapter. It evaluates the time variation of stresses for two classes of problems, for which cracking does not occur:

(i) Sustained temperature and loads.
(ii) Sustained loads and cyclically varying temperatures; between any two states.

VPCREEP is a self-contained and medium size program (approximately 8000 Fortran statements). It can perform both elastic and thermal creep analyses. The program is capable of handling plane stress, plane strain, axisymmetric and three dimensional problems. A data input interpreter is utilised for a format-free style of data entry.

5.9.2 Data checking

In the analysis of large structures, it is important to be able to check the data read and generated by the program. For this purpose, a diagnostic pre-processor is built in to identify any potential errors before entering the main solution phase. The resulting error messages are printed out in plain language.

5.9.3 Dynamic computer memory management

To solve the resulting system of linear equations, a partition frontal

solver is implemented. It has been shown that the frontal algorithm is not only efficient but also natural to the finite element system (Abbas 1980).

Dynamic computer memory management is implemented in that the program calculates automatically the amount of work space needed and allocates core memory dynamically in such a way that minimum disc access is required during execution time. The program determines whether the frontwidth is small enough to fit into the available computer memory. If the frontwidth is too large, then the frontal column will be partitioned automatically.

5.9.4 The restart facility

The restart facility enables the user to enter the program at any significant point for data checking and additional solutions.

In linear elastic analysis, it allows for the economic processing of multiple load cases in that the reduced global stiffness matrix is stored in their reduced form, and a second or subsequent solutions merely necessitate the reduction of the right hand side load vector. Thus the computation of element stiffness, the global assembly and reduction of stiffness can be avoided.

In creep analysis, the restart facility allows for multiple generation of self-equilibrating stresses in different runs and the multiple creep solutions at different pseudo-times.

5.9.5 Mesh generation, stress smoothing and contouring

The subjects of finite element pre-processing and post-processing are vast and they belong to a multi-million pounds computer aided design (CAD) industry. A selected list of publications related to these subjects are shown in appendix A. Some CAD packages are shown in Table 5.9.1. In cases where such packages are not available, companion programs, namely SBSPOST for SSCREEP and VPCPOST for VPCREEP, are provided. However they are not intended for competing with such CAD packages which obviously provide extensive facilities.

5.9.5.1 Mesh generation

For many practical problems, thousands of elements and nodes are involved and the task of preparing the data becomes extremely lengthy and tedious. Moreover, during the preparation of thousands of data cards some human error maybe introduced and remain undetected in spite of checks which are usually made. The presence of such errors will inevitably bring about incorrect results and if detected at that stage it would mean another run on the computer after correcting the data, which is tiresome and costly, although not disastrous. However, if the errors remain undetected and such incorrect results are used for making decisions and judgements, there maybe series repercussions. It is therefore important to eliminate such data errors, and this can be achieved to a large extent by automatic mesh generation, in which nodal numbers and their nodal connection order are prepared automatically by the computer as input data using the minimal amount of information necessary to describe the geometry of the structure and the desired fineness of the mesh.

In recent years considerable effort has been made in developing mesh generating algorithms. Buell and Bush (1973) reviewed the pre-1973 literature and Thacker (1980) published an extensive bibliography in 1980. Ho-Le (1988) identified seven classes of mesh generation methods as shown in Figure 5.9.1.

In VPCRREP the iso-parametric mapped element approach is utilised (Zienkiewicz 1971). The mapping functions are 8-node for two dimensional elements and 20-nodes for three dimensions. The method is best illustrated by considering the process of generating a 8-node parabolic mesh. A single domain shown in Figure 5.9.2 maybe regarded as one large iso-parametric element and the topology is adequately defined by the eight master nodes. A suitable 8-node iso-parametric mesh is then obtained by using lines of constant ξ and η to divide the large master element into m elements in ξ-direction and n elements in the η-direction. The coordinates of any point j are given as:

$$x_j = \Sigma N_i(\xi_j,\eta_j)x_i$$

$$y_j = \Sigma N_i(\xi_j,\eta_j)y_i \qquad (5.9.1)$$

where N_i are the shape functions for the parabolic iso-parametric elements and are used as mapping functions (vide section 5.2). Similarly, for three dimensional meshes the coordinates of any generated point j are given as:

$$x_j = \Sigma\ N_i(\xi_j,\eta_j,\zeta_j)x_i$$

$$y_j = \Sigma\ N_i(\xi_j,\eta_j,\zeta_j)y_i \qquad (5.9.2)$$

$$z_j = \Sigma\ N_i(\xi_j,\eta_j,\zeta_j)z_i$$

Again, (x_i,y_i,z_i) are the coordinates of the master mesh, (ξ_j,η_j,ζ_j) are the generated coordinates of node j in local (ξ,η,ζ) coordinates. The Σ is over the number of nodes per master element.

Although better fitting is possible by using the blending functions interpolation procedure (Gordon et al 1973) or any other methods as shown in Figure 5.9.1, experiences have shown that the fit of quadratic iso-parametric elements to fairly complex boundaries is reasonable.

5.9.5.2 Stress smoothing

In the displacement method, the stresses are discontinuous between elements because of the nature of the assumed displacement variation. A typical stress distribution is shown in Figure 5.9.3. In analysis involving numerically integrated elements such as isoparametric elements, experience has shown that the integration points are the best stress sampling points. The nodes, which are the most useful output locations for stresses, appear to be the worst sampling points. It is well known that interpolation functions tend to behave badly near the extremities of the interpolation region. It is therefore reasonable to expect that shape functions derivatives, and hence stresses, sampled in the interior of the elements would be more accurate than those sampled on the element periphery. The analyst is therefore faced with the problem of interpreting quantities which are histogram-type distributions. Often the subjective eye of the experienced analyst may be quite successful in interpreting such information; equally, it may easily be prejudiced and such an interpretation may lack consistency and rationality. It is therefore

crucial that some rational and consistent procedures for the interpretation of discontinuous functions be adopted. One of such procedure is termed stress smoothing. If the stress smoothing is carried out over the whole of the finite element domain, it is referred to as global smoothing. Otherwise the smoothing process performed separately over each individual element is called local smoothing.

In the constant strain family of elements, such as those used in the SSCREEP program (vide chapter 4), an economic and simple global stress smoothing procedure utilised is to take nodal averages of stresses, that is the average of the nodal stresses of all elements meeting at a common node. No local stress smoothing is applied for this family of elements.

In the isoparametric elements of the serendipity family, such as those used in the VPCREEP program, a local stress smoothing is carried out in that the stress values at the integration points are dispersed to nodal points first. If a second order integration rule is used, the local smoothing is carried out using a least squares method (Hinton and Campbell 1974). If a third order rule is used, the local smoothing is carried out using a blending functions technique (Gordon et al 1973). Examples of the two approaches for a 8-node iso-parametric element are shown in Figures 5.9.4 and 5.9.5.

The local stress smoothing is followed by a global stress smoothing technique as applied to the constant strian elements to give a global view of stresses.

5.9.5.3 Stress contouring

After the nodal stresses are obtained, it can be presented in the form of a stress contour plot. Contouring in two and three dimensional spaces is of great importance and is a subject of intense research in both the academic and the industrial world.

In VPCPOST and SBSPOST, an iso-parametric inverse mapping coupled with a predictor-corrector approach advanced by Gray and Akin (1979), is adopted.

Consider any iso-parametric element formulated in local coordinates as shown in Figure 5.9.6. At any local point the value of stress is:

$$V(\xi,\eta) = [N(\xi,\eta)]\{V_e\} \qquad (5.9.3)$$

Where [N] and $\{V_e\}$ denote the shape functions and the nodal values, respectively. If a contour of V can be defined in local space, then can be converted to the global space.

Assume that the contour is given by V=k, where k is a known constant, and also assume that the local coordinates (ξ_o,η_o) of one point on the contour are known. The equation of such a curve is given by dV=0. In local coordinates, this becomes:

$$0 = (\partial V/\partial \xi)d\xi + (\partial V/\partial \eta)d\eta \qquad (5.9.4)$$

where,

$$d\xi = dL \cos \theta$$

$$d\eta = dL \sin \theta$$

$$\partial V/\partial \xi = [\partial N/\partial \xi]\{V_e\}$$

$$\partial V/\partial \eta = [\partial N/\partial \eta]\{V_e\}$$

where $d\xi$ and $d\eta$ are components of a known contour trace step size dL which is tangential to the contour line, Figure 5.9.6. Thus, given a starting points on an element contour line, all one needs to trace through the element are nodal values of the function, the local coordinate derivatives of the shape functions, and assumed step increment dL. Using this assumption, the formulas which predict the position of the contour line's new location with respect to the old location are:

$$\nabla = \sqrt{[(\partial V/\partial \xi)^2 + (\partial V/\partial \eta)^2]}$$

$$\xi_{new} = \xi_{old} + (dL/\nabla)(\partial V/\partial \xi) \qquad (5.9.5)$$

$$\eta_{new} = \eta_{old} + (dL/\nabla)(\partial V/\partial \eta)$$

The above procedure can be further improved to make the accumulated error acceptably small without excessive increase in computational cost. This is in the form of a simple correction step normal to the contour line, thus the corrected local coordinates may be calculated from the following set of equations:

$$\xi_{cor} = \xi_{new} - (1/\nabla)^2(\partial V/\partial \xi)[V(\xi_{new},\eta_{new}) - V_{cor}] \qquad (5.9.6)$$

$$\eta_{cor} = \eta_{new} - (1/\nabla)^2(\partial V/\partial \eta)[V(\xi_{new},\eta_{new}) - V_{cor}]$$

where V_{cor} is the correct contour value. To terminate the contour, one checks the coordinates at end of each segment to see if they remain within the element. Once a contour inside an element has been completely traced in local coordinates, all points on the contour are converted to the corresponding global coordinates.

The contour tracing process repeats for every element and all stress values desired. A global picture of stress variations which aids the analyst to identify problem areas is thus obtained.

5.9.8 Program flow

The program is modular in nature. Its operation maybe considered in distinct phases and they are illustrated diagrammatically in Figures 5.9.7 and 5.9.8. Further details of VPCREEP will be found in separate reports (vide Appendix C).

5.10 Economic Assessment of the Algorithm

In the previous chapter (vide section 4.9), it has been shown that the conventional step-by-step approaches is very expensive, in terms of computer times, using England's classical restrained beam as an example, see Figures 4.8.4 and 4.8.4. It is found that the computer time required was 0.2 seconds per increment on an IBM 3081 KX3 mainframe computer. The transient creep solutions were obtained up to c=4.0E-06 and it took 58 increments. The arithmatic progression type of incremental strategy coupled with a initial coarse time step was used.

The same beam was analysed using the VPCREEP as a plane stress problem, Figure 5.10.1. A total of six 8-nodes isoparametric elements were used for comparable accuracies. Two self-equilibrating stress distributions, namely the thermal type and the steady-state type, were used and six sets of stresses were sought. The computer time required per transient creep solution was approximately 0.13 seconds on the same computer. The self-equilibrating stress distributions generating phase of the analysis took approximately 2 seconds.

The results from the two analyses were shown in Figure 5.10.2. The relative cost in computer time between the step-by-step approach and the power minimisation procedure is:

$$\frac{0.2 \times 58}{2 + 6 \times 0.13} = 4.2$$

From this comparison, it can be safely concluded that the minimisation procedure is much more economical with respect to computer time in relation to conventional step-by-step approaches.

5.11 Benchmark Problems - Elastic Analysis

Three elastic analyses were carried out to verify that the VPCREEP program is capable of performing plane stress, axisymmetric and three dimensional problems. The solutions obtained were compared with known analytical ones.

(a) Plane stress analysis of a cantilever beam under tip load

The cantilever beam and its idealisation are shown in Figure 5.11.1(a). Ten 8-nodes elements and the 3rd order integration rule were used. The elastic modulus, Poisson's ratio, thickness were taken as 1.0E5 MN/m^2, 0.3 and 1 m respectively. The theoretical and numerical solutions were found to be exact, Figure 5.11.1(b).

(b) Axisymmetric analysis of a cylinder subjected to internal pressure

The cylinder under investigation and its idealisation are shown in Figure 5.11.2. The cylinder was subjected to an internal pressure of magnitude 10.0 MN/m^2. The elastic modulus and Poisson's ratio were assumed to be 0.34E5 MN/m^2 and 0.2 respectively. The results obtained were compared with analytical solutions, Table 5.11.1. The agreement was very good.

(c) Three dimensional analysis of a cantilever beam

The beam analysed in section (a) above was analysed as an three dimensional model, Figure 5.11.3. Two load cases were analysed:

Case 1: The beam analysed in section (a) above was subjected to an end moment. The results obtained were compared with analytical and solutions from a general purpose finite element program called ANSYS, Table 5.11.2(a).

Case 2: The beam analysed in section (a) above was subjected to an end shear. The results obtained were compared with analytical and solutions from a general purpose finite element program called ANSYS, Table 5.11.2(b).

5.12 Benchmark Problems - One Dimensional Creep Analysis

England's prestressed restrained beam was solved by the Power Minimisation Procedure as a one dimensional structure and compared with the stresses obtained by the step-by-step rate of creep method (vide section 4.8). Details of boundary conditions and loadings are shown in Figure 5.12.1. Two types of temperature variations were investigated:

(a) Sustained temperature field, see Figure 5.12.1(b).
(b) Unidirectional cyclic temperature field, see Figure 5.12.1(c).

Four types of self-equilibrating stress distributions were studied:

(I) Thermal distribution, $\sigma_1 = X$.

(II) The parabolic distribution, $\sigma_2 = X_2 - 1/3$

(III) The difference between the thermo-elastic and the steady-state stresses, $\sigma_3 = \sigma_o - \sigma_{ss}$ for sustained temperature and $\sigma_3 = \sigma_o - \sigma_{ssc}$ for unidirectional cyclic temperature. σ_o is the thermo-elastic stresses.

(IV) The rectangular distributions, Figure 5.12.2.

Results of the investigation are presented in Figures 5.12.4 to 5.12.9. It is observed that for practical purposes, the results gave acceptable approximate solutions.

5.13 Benchmark Problems - Finite Element Creep Analysis

5.13.1 England's restrained beam problem

The flexurally restrained beam was used as a benchmark problem and solved as two and three dimensional models, Figure 5.13.1 shows the details of boundary conditions and loadings. The sustained temperature field was considered.

Young's modulus, Poisson's ratio and coefficient of thermal expansion were taken as 34500 MN/m^2, 0.3 and 0.12xE-04 per ^oC respectively. Stresses are expressed in MN/m^2.

a. Two-dimensional analysis

The prestresses restrained beam is solved as a two-dimensional plane stress problem. A mesh of 12 iso-parametric elements was used to represent the beam, Figure 5.13.2.

The stresses presented in Table 5.13.1 to 5.13.3 are evaluated at the Gauss integration points. The 3x3 Gauss Quadratic rule were used. It is observed that no more improvement on stress results for using more than four self-equilibrating stress distributions.

b. Three-dimensional analysis

Although strictly unnecessary for solving the problem, a three dimensional version of the beam was considered in order to test the ability of VPCREEP for solving three dimensional problems. The beam was modeled using 12 elements, Figures 5.13.3 and 5.13.4.

Results for the above analyses are given in Tables 5.13.4 to 5.13.5 for sustained temperature problems.

5.13.2 Allen's rectangular plate with parabolic edge loading

A finite element solution to a rectangular plate of aspect ratio of 3 was obtained by Allen (England et al 1971). The plate is subjected to a sustained temperature gradient and an inplane edge parabolic loading. A quarter of the plate was modeled using a finite element mesh of 25x9 rectangular elements. An analytical solution was also dervied based on a minimization principle approach.

The same problem was analysed utilising VPCREEP using a 12 8-nodes element mesh,Figure 5.13.5. The following data was used (Smith 1981):

Young's modulus	= 41400 MN/m^2
Poisson's ratio	= 0.2
Coefficient of thermal expansion	= 0.0000135 per ^oC
Reference temperature	= 20.0 ^oC

The logitudinal stresses at x=0 for inner and outer faces obtained was compared with those given by Allen and Smith, Figure 5.13.6 It is observed that a close match of solutions was obtained.

More detailed pictures of the transient longitudinal stresses distribution, in the form of stress contour diagrams over the structure, are shown in Figures 5.13.7 to 5.13.9. The stresses plotted were obtained by first extrapolating Gaussian stresses to nodal points using a stress transformation technique and then interpolated inside the element using a predictor-corrector contour tracing algorithm as described in section 5.9.

5.11 Conclusions

The Complementary Power Theory presented permits stresses to be evaluated in both the transient creep phase and in the limiting steady-state condition from a Power Minimisation Procedure in conjunction with a Ritz process. This process has the advantage that it maybe used in the form of exact or approximate analysis and is more economic than the conventional time-step algorithms.

Extension of the procedure to general two and three dimensional continua utilising the finite element technique is described in detail and a computer program, VPCREEP, is developed for elastic and creep analysis of structures subjected to (i) sustained loads and sustained temperature and (ii) sustained loads and cyclically varying temperatures between any two states. VPCREEP has the ability to generate the self-equilibrating stress distributions (for Ritz's expression) automatically and this reduces the effort required in solving general problems and allows the stress analyst to concentrate on the interpretation of the analysis results.

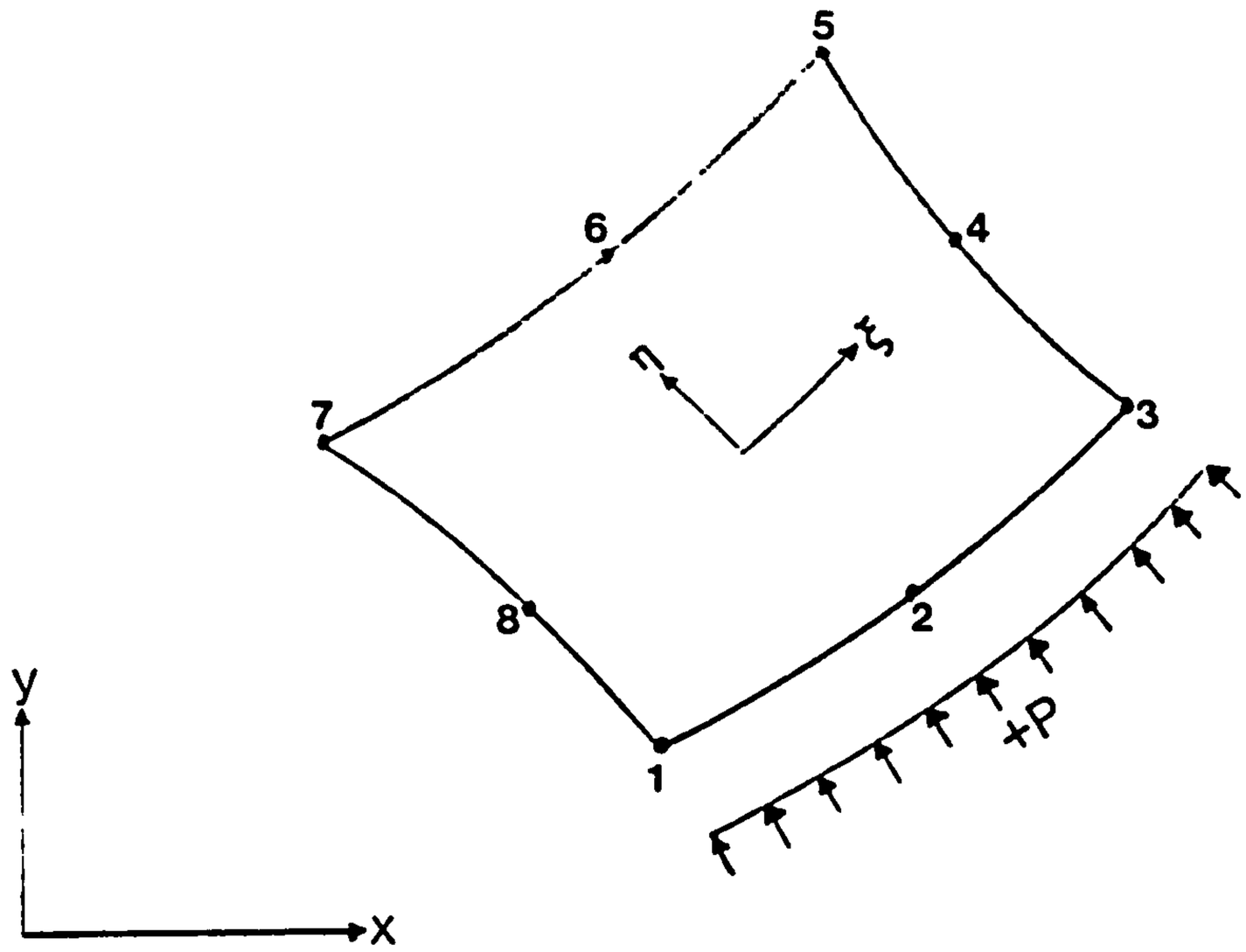

(a) Node numbers & direction of positive pressure

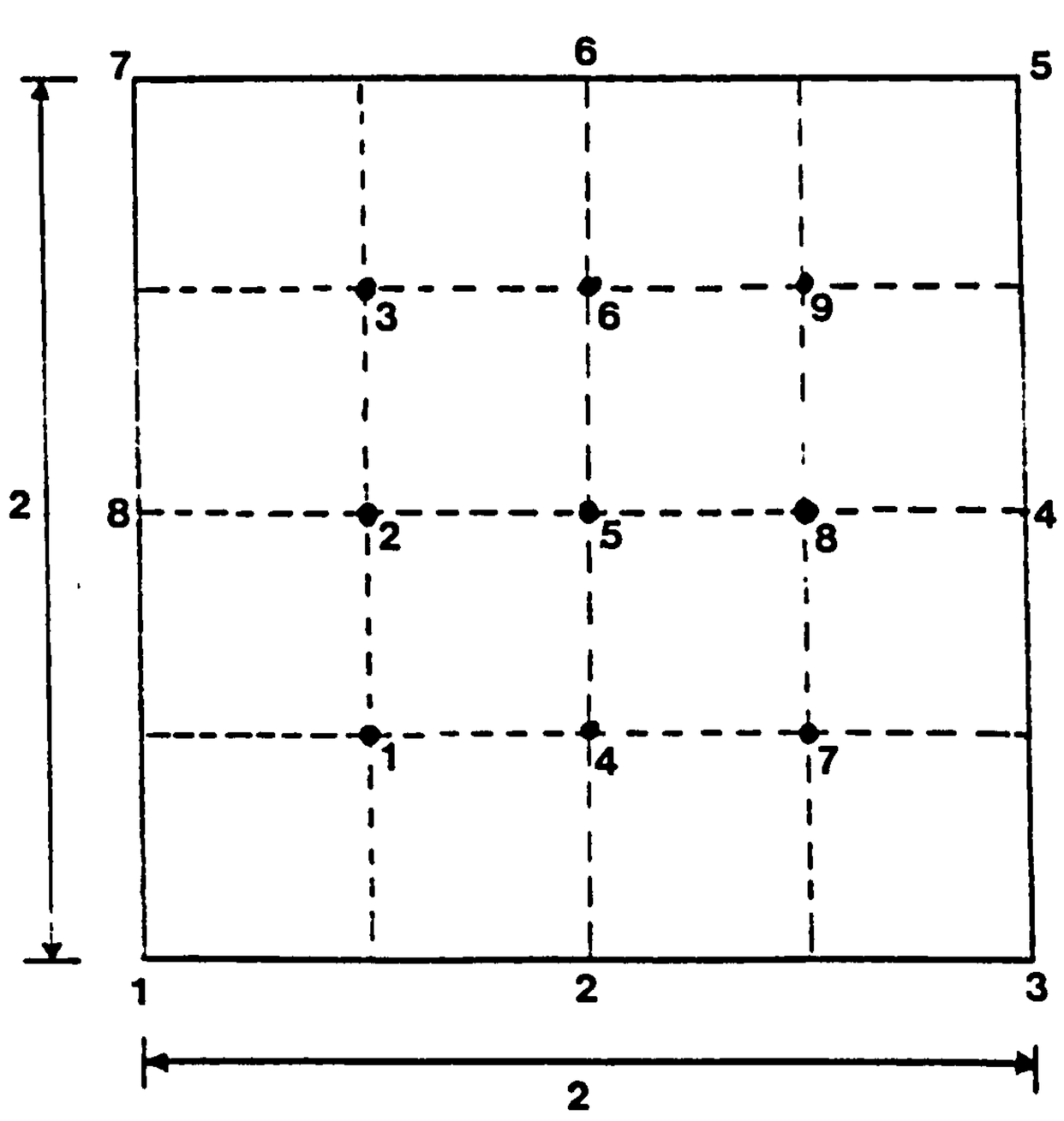

(b) Gauss integration points

Figure 5.2.1: The 8-node iso-parametric plane element

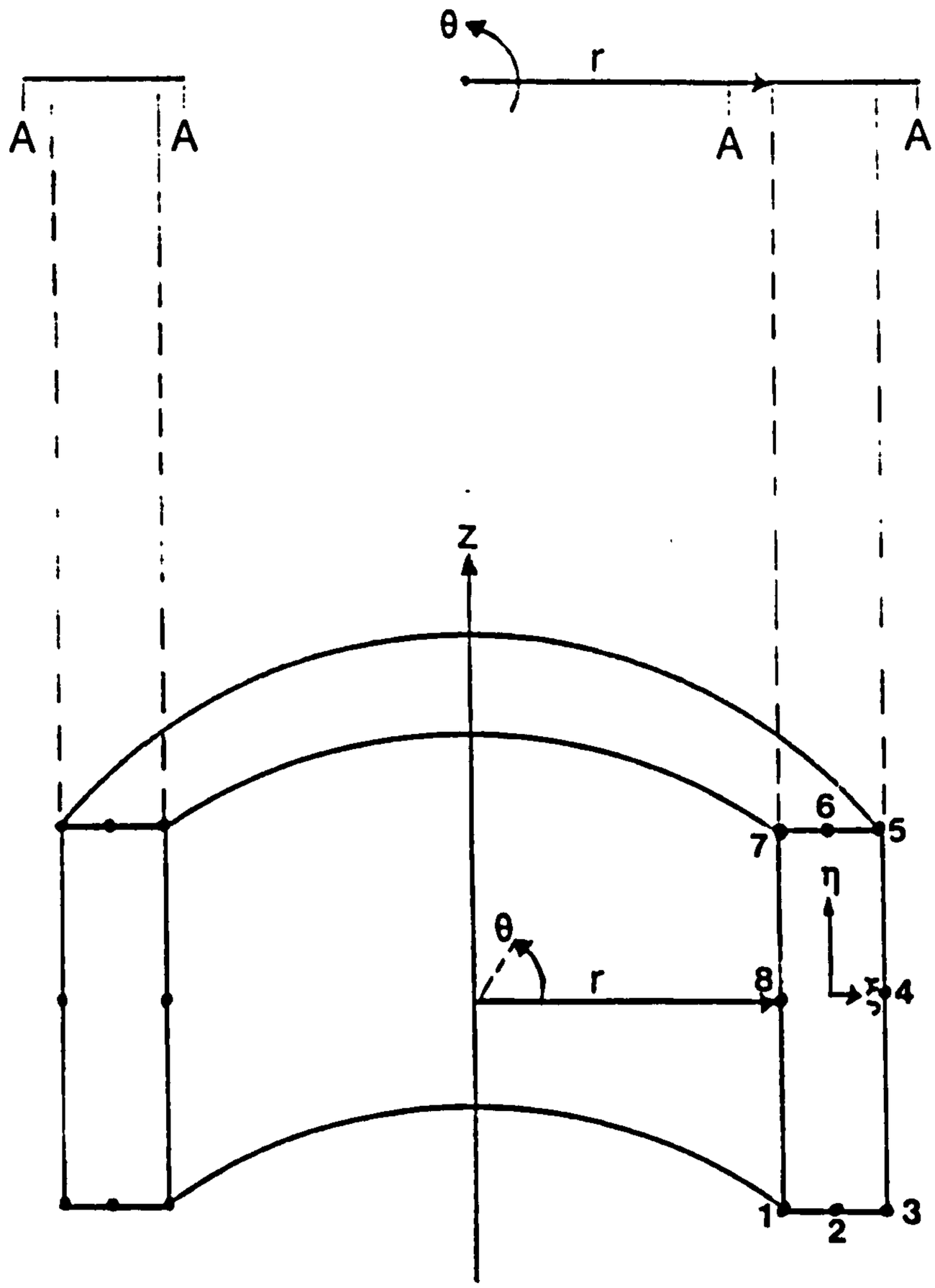

Figure 5.2.2: The 8-node iso-parametric axisymmetric ring element

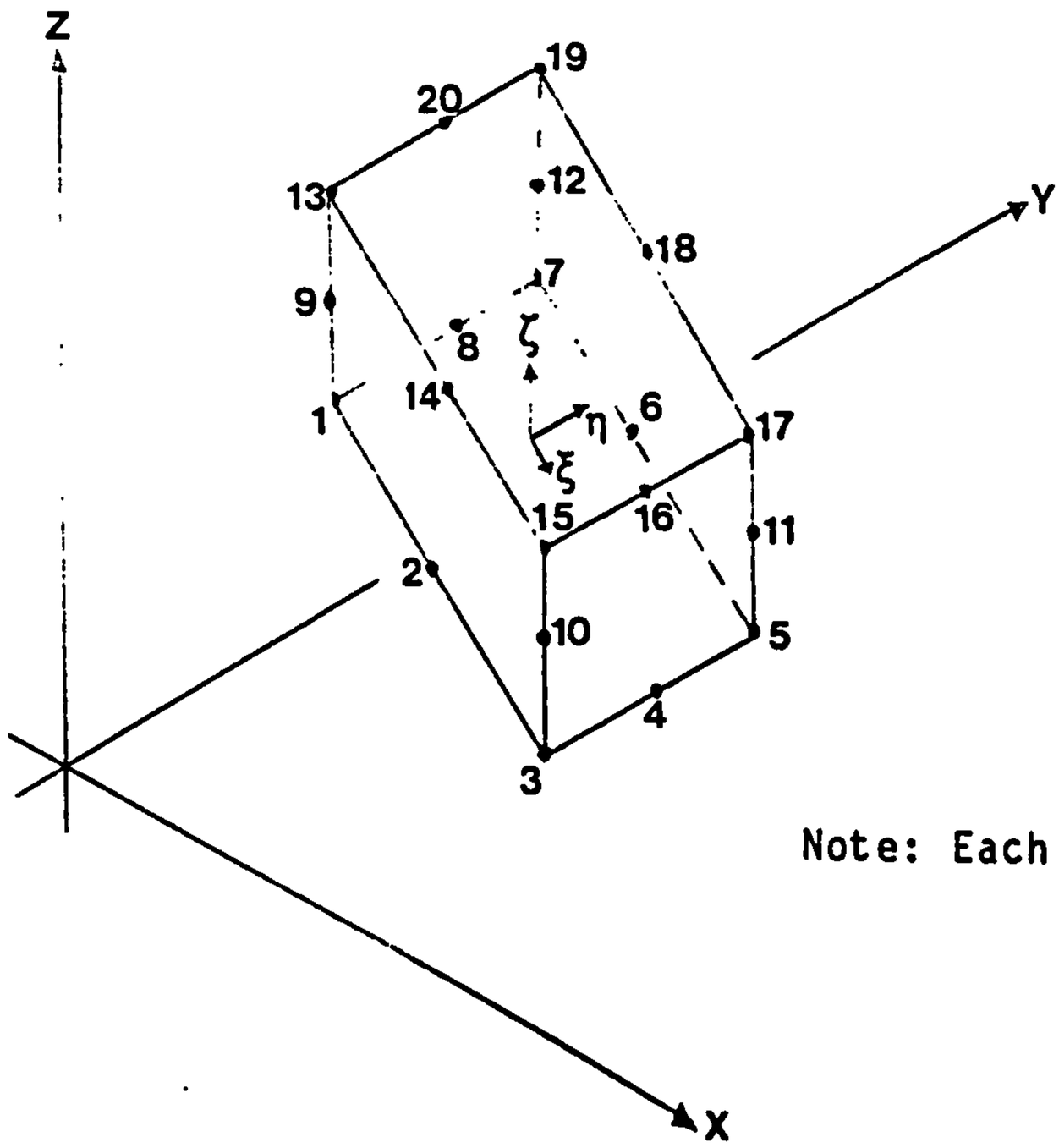

Note: Each edge may be parabolic

(a) Node numbers

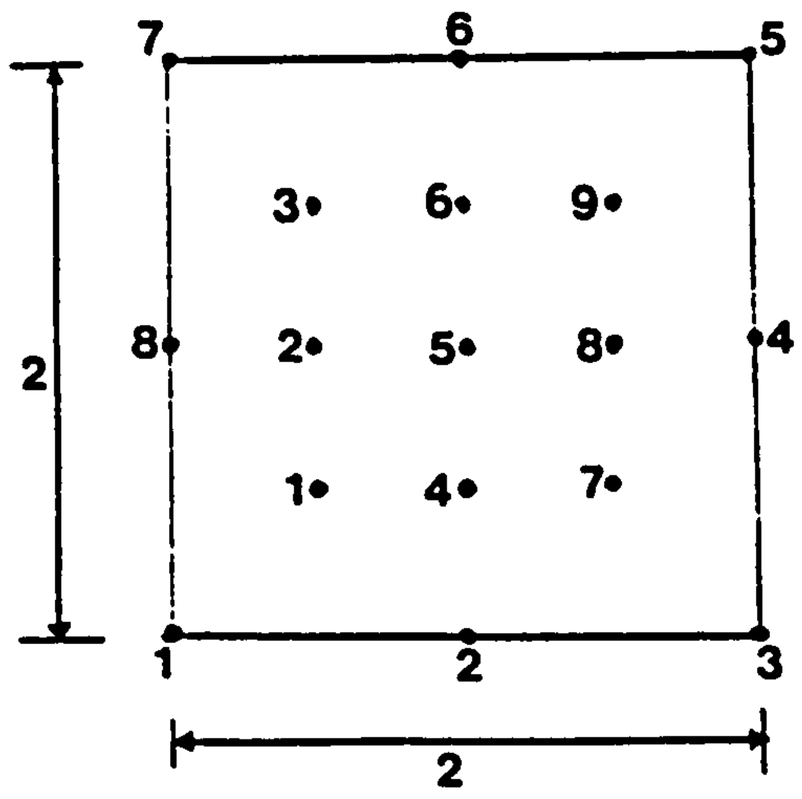

(b) The Gauss integration points for ζ_m = - 0.775.

Figure 5.2.3: The 20-node iso-parametric brick element

$$\int_{-1}^{1} f(x)\,dx = \sum_{j=1}^{n} H_j f(a_j),$$

$\pm a$	H
$n = 1$	
0	2·00000 00000 00000
$n = 2$	
0·57735 02691 89626	1·00000 00000 00000
$n = 3$	
0·77459 66692 41483	0·55555 55555 55556
0·00000 00000 00000	0·88888 88888 88889
$n = 4$	
0·86113 63115 94053	0·34785 48451 37454
0·33998 10435 84856	0·65214 51548 62546
$n = 5$	
0·90617 98459 38664	0·23692 68850 56189
0·53846 93101 05683	0·47862 86704 99366
0·00000 00000 00000	0·56888 88888 88889
$n = 6$	
0·93246 95142 03152	0·17132 44923 79170
0·66120 93864 66265	0·36076 15730 48139
0·23861 91860 83197	0·46791 39345 72691
$n = 7$	
0·94910 79123 42759	0·12948 49661 68870
0·74153 11855 99394	0·27970 53914 89277
0·40584 51513 77397	0·38183 00505 05119
0·00000 00000 00000	0·41795 91836 73469
$n = 8$	
0·96028 98564 97536	0·10122 85362 90376
0·79666 64774 13627	0·22238 10344 53374
0·52553 24099 16329	0·31370 66458 77887
0·18343 46424 95650	0·36268 37833 78362
$n = 9$	
0·96816 02395 07626	0·08127 43883 61574
0·83603 11073 26636	0·18064 81606 94857
0·61337 14327 00590	0·26061 06964 02935
0·32425 34234 03809	0·31234 70770 40003
0·00000 00000 00000	0·33023 93550 01260
$n = 10$	
0·97390 65285 17172	0·06667 13443 08688
0·86506 33666 88985	0·14945 13491 50581
0·67940 95682 99024	0·21908 63625 15982
0·43339 53941 29247	0·26926 67193 09996
0·14887 43389 81631	0·29552 42247 14753

Table 5.3.1: Abscissae and weight coefficients of the Gaussian Quadrature formula

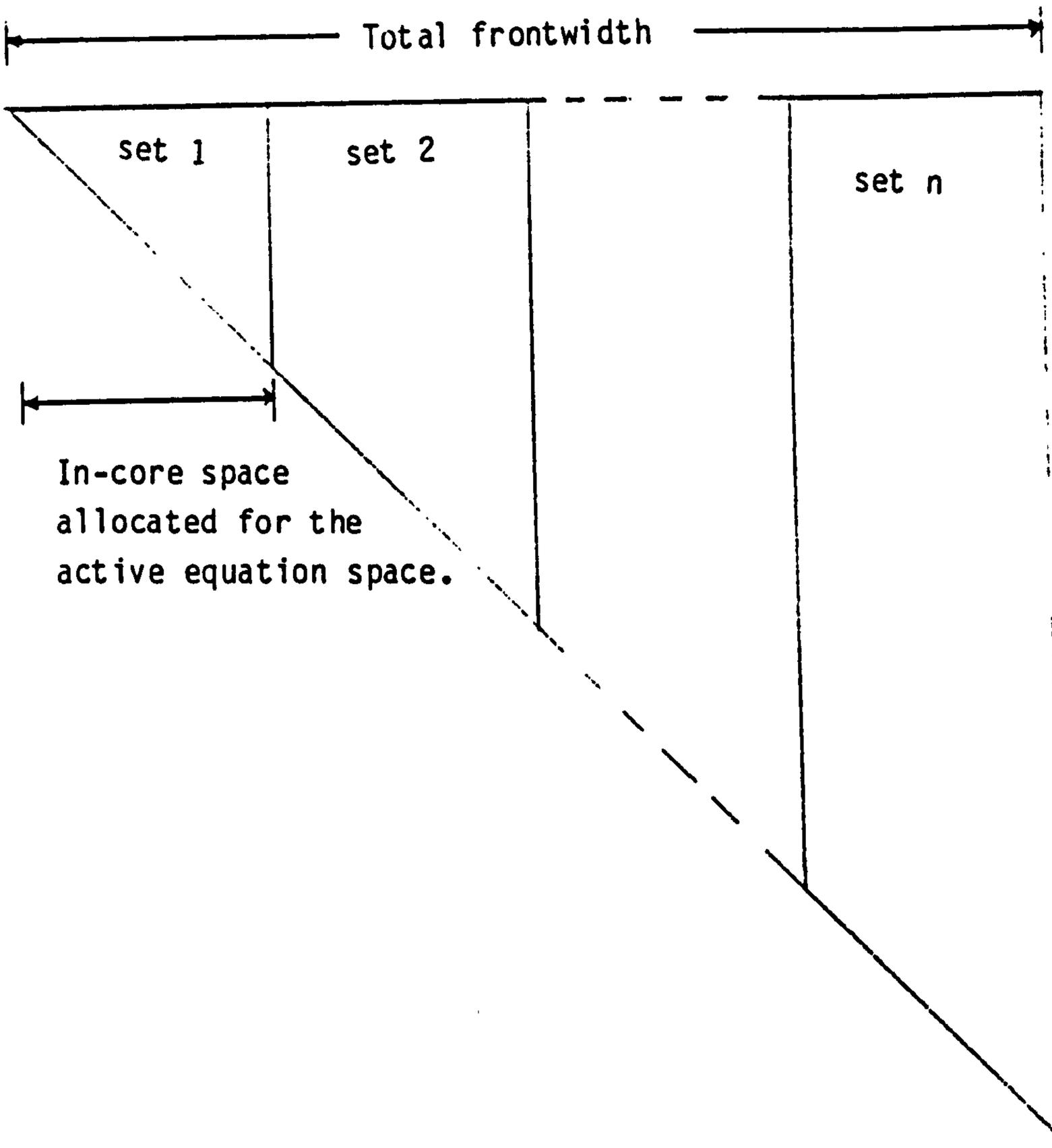

Figure 5.6.1: Partition of the front

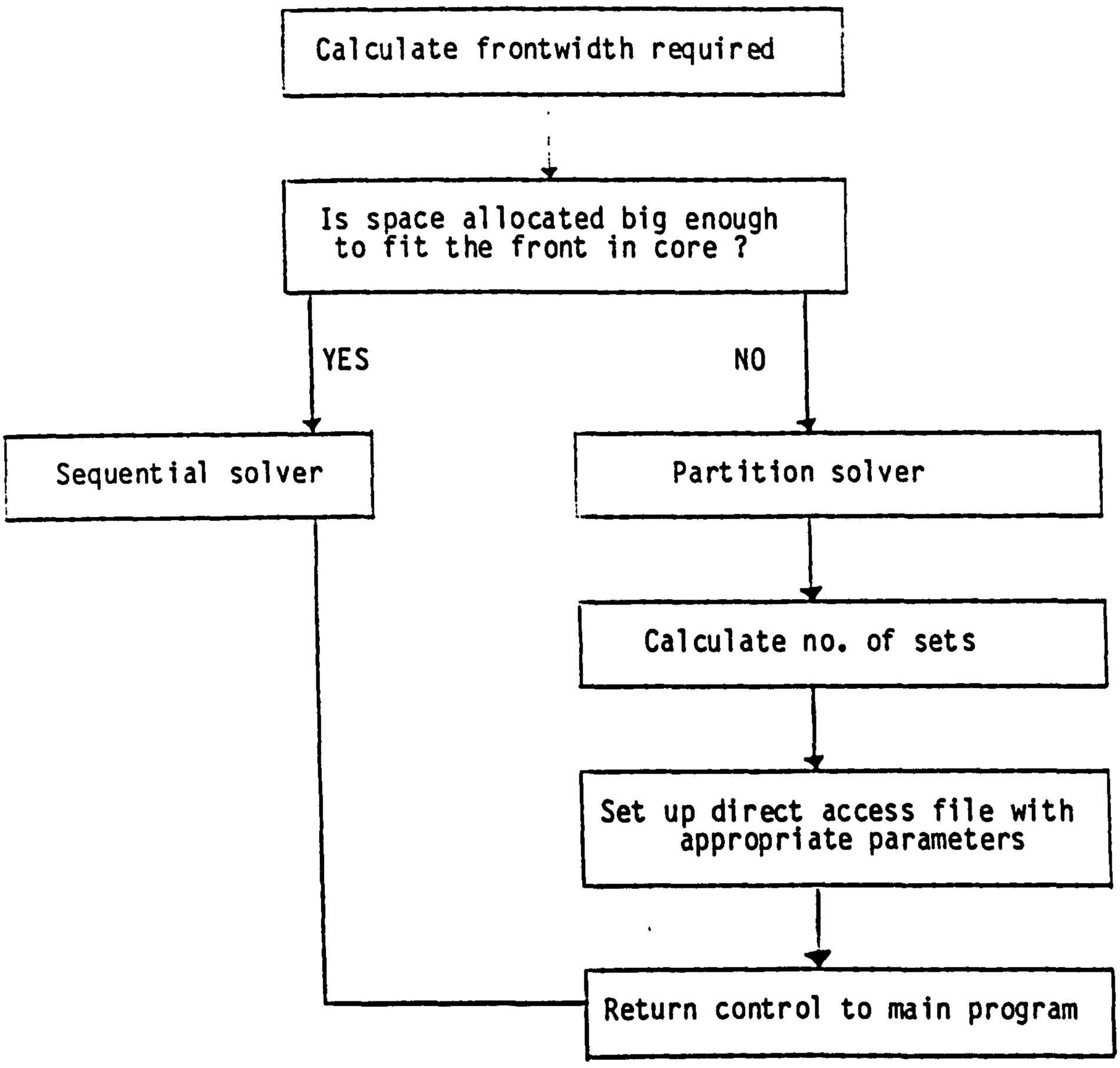

Figure 5.6.2: The frontal partition process

Package	Company
FEGS	Fegs Ltd., U.K.
SOLVIA	Solvia Engineering, Sweden.
PATRAN	PDA Engineering, U.S.A.
SUPERTAB	Structural Dynamics Research Corporation, U.S.A.
MEMTAT	MARC Research Analyis Corporation, U.S.A.
AGS/AIM	Application Inc., U.S.A.
FASTDRAW	McDonnell Douglas Automation Co., U.S.A.
FEM 181	Tektronix Inc., U.S.A.
FEMGEN	Lund University Computing Centre, Sweden.
INGA	University of Stuttgart, W. Germany.
HEL	National Engineering Laboratory, U.K.
PLANIT	University of Pittsburg, U.S.A.
SIGS	Sandia Laboratories, U.S.A.
SUPERNET	Brown, Boveri & Cie AG, West Germany.
UNISTRUC	Control Data Corporation, U.S.A.
PREP	Swanson Analysis Systems, U.S.A.
ASDIS	Atkins Research & Development, U.K.
BERMESH	BERSAFE, Central Electricity Generating Board, U.K.
COCO	Nuclear Research Centre, Scalay, France.
GIFTS	University of Arizona, U.S.A.
MISA	Mitsui Engineering & Shipbuilding, Japan.
MSGMESH	The MacNeal-Schwendler Co., U.S.A.
PIGS	PAFEC Ltd., U.K.
SESAM-69	A.S. Computas, Norway.

Table 5.9.1: Some CAD packages

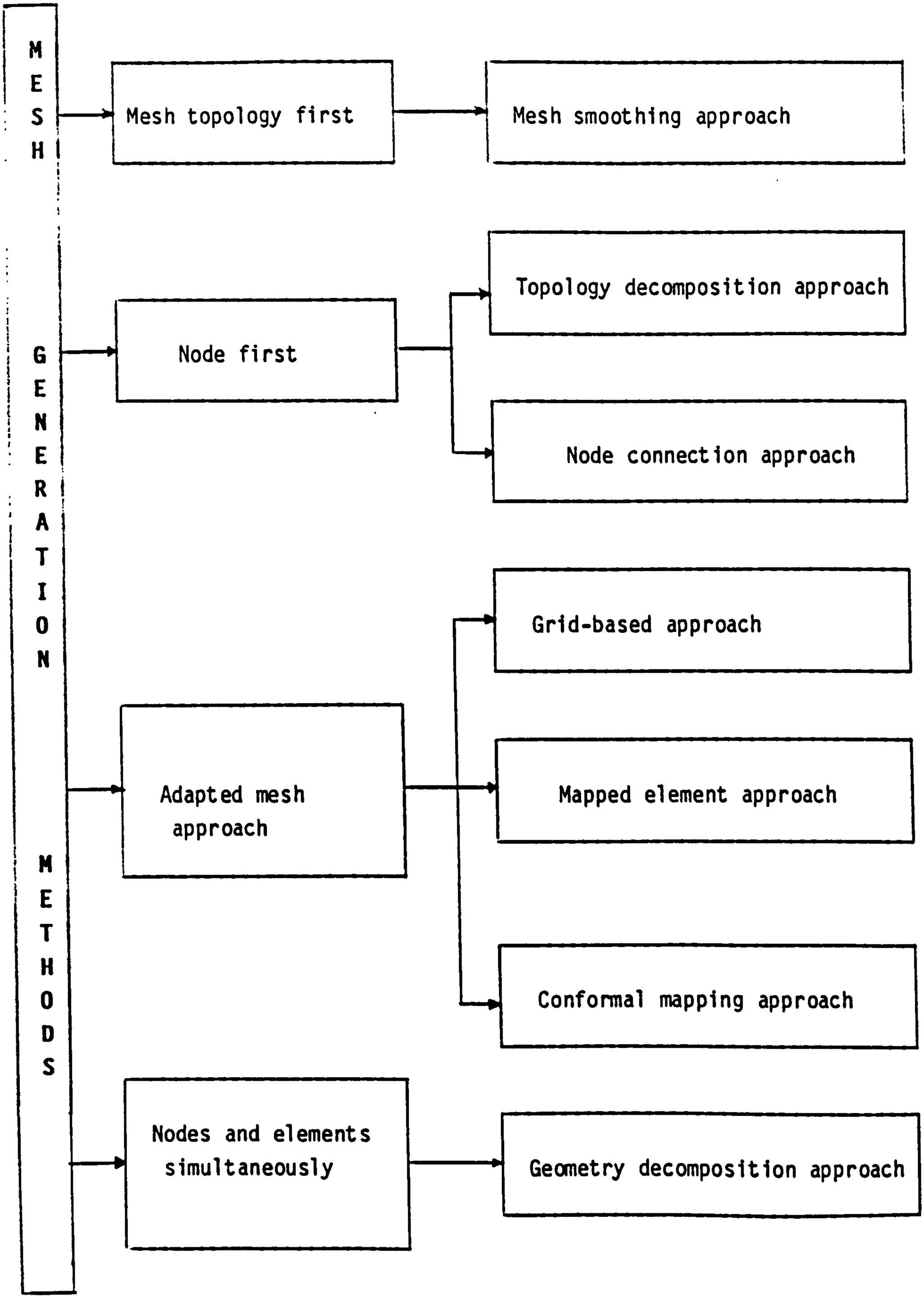

Figure 5.9.1: Classification scheme for mesh generation methods

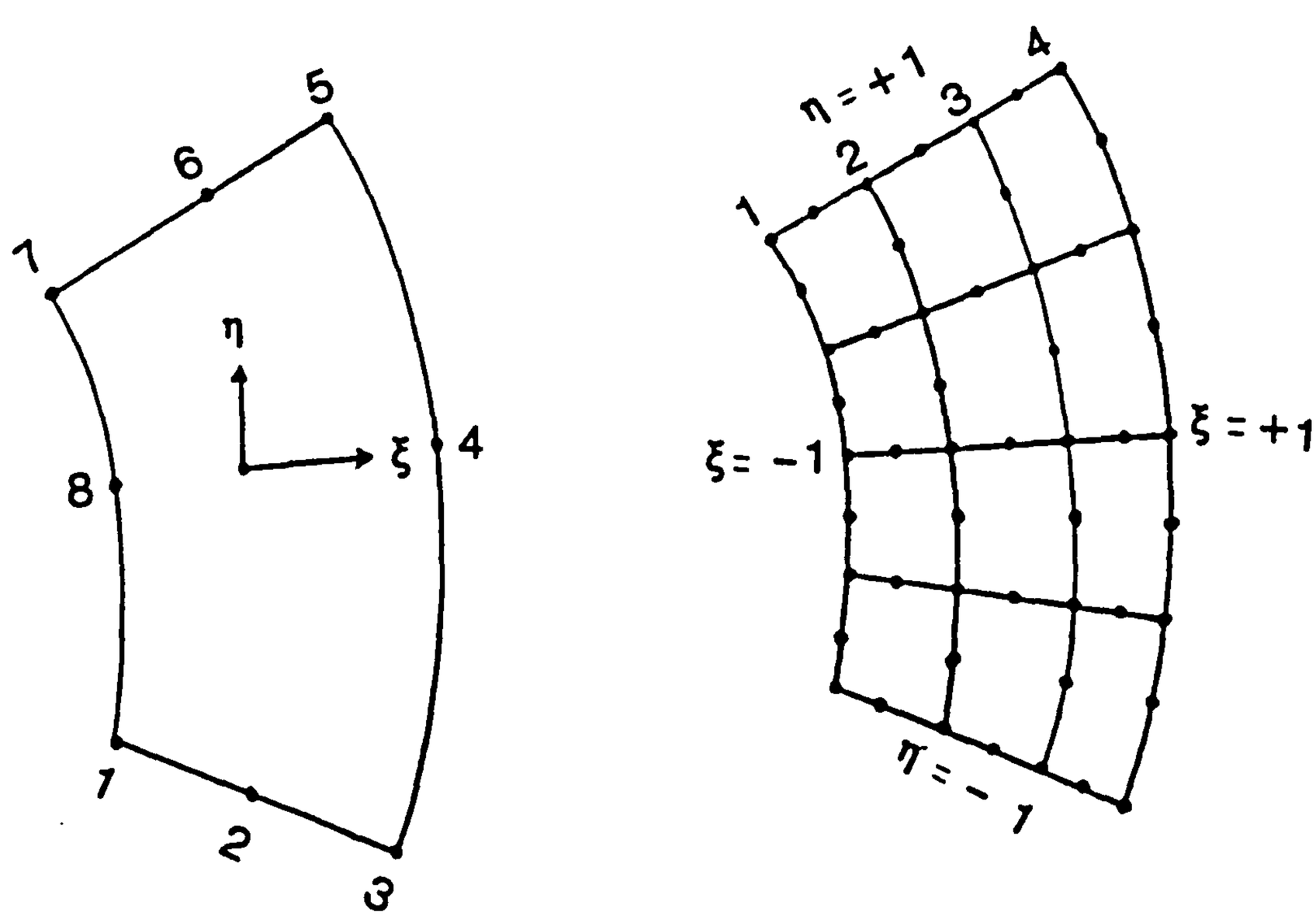

(a) Input master mesh

(b) Output generated mesh

Figure 5.9.2: A mesh generation example

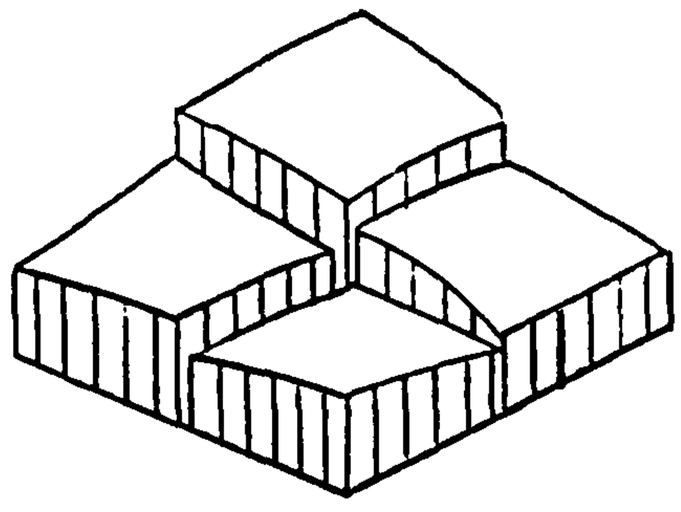

unsmoothed stresses

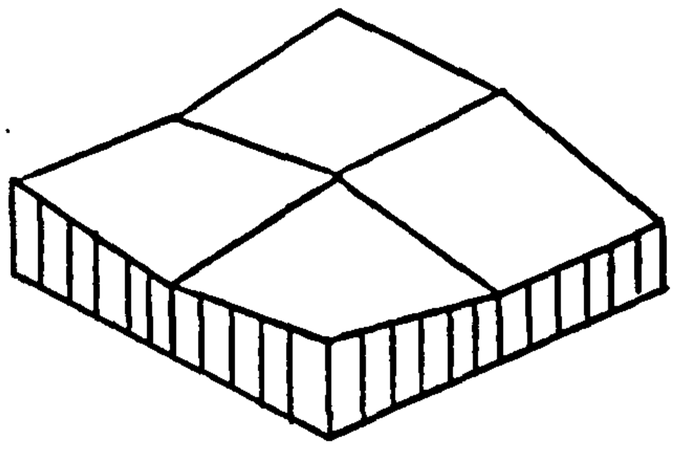

Globally smoothed stresses

Figure 5.9.3: Smoothed and unsmoothed stresses

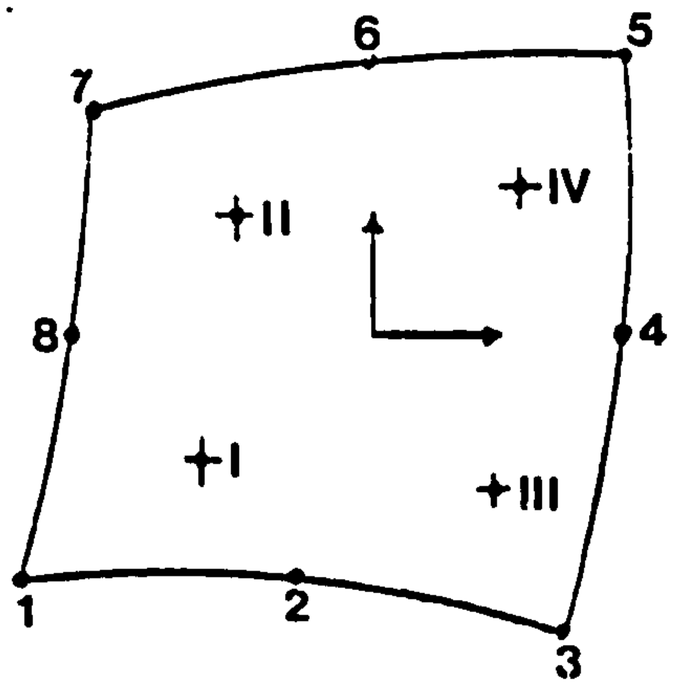

$$\sigma_1 = a\sigma_I + b\sigma_{II} + c\sigma_{III} + b\sigma_{IV}$$
$$\sigma_3 = b\sigma_I + c\sigma_{II} + b\sigma_{III} + a\sigma_{IV}$$
$$\sigma_5 = b\sigma_I + a\sigma_{II} + b\sigma_{III} + c\sigma_{IV}$$
$$\sigma_7 = c\sigma_I + b\sigma_{II} + a\sigma_{III} + b\sigma_{IV}$$

Where $a = 1 + \frac{1}{2}\sqrt{3}$

$b = -\frac{1}{2}$

$c = 1 - \frac{1}{2}\sqrt{3}$

Figure 5.9.4: Local stress smoothing for an isoparametric element using a least squares method

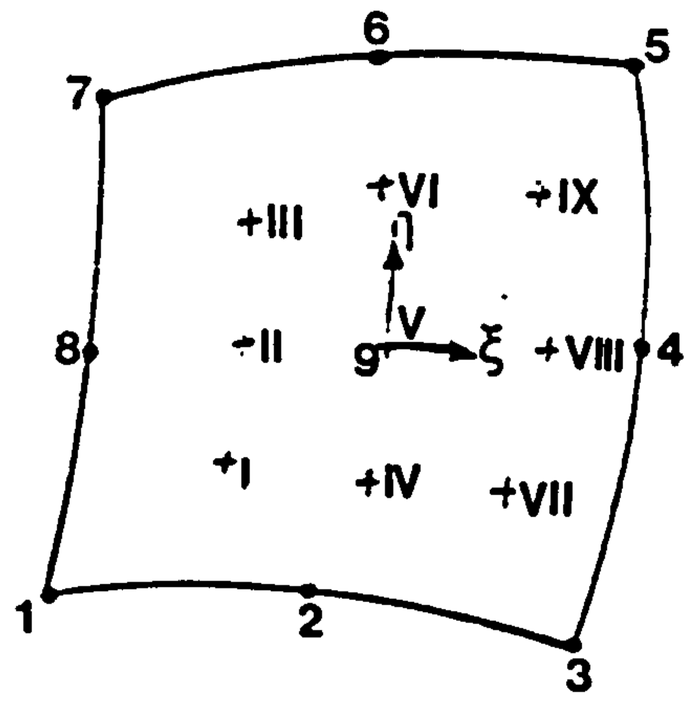

$$G = \begin{bmatrix} \sigma_I & \sigma_{IV} & \sigma_{VII} \\ \sigma_{II} & \sigma_V & \sigma_{VIII} \\ \sigma_{III} & \sigma_{VI} & \sigma_{IX} \end{bmatrix}$$

$$Q = \begin{bmatrix} 3.33333325 & -4.62432766 & 1.47883058 \\ -6.66666651 & 6.66666651 & -0.66666663 \\ 3.33333325 & -2.04233885 & 0.18783610 \end{bmatrix}$$

$T_1 = \{\ 0.0 \quad 0.0 \quad 1.0\ \}$; $S_1 = \{\ 0.0 \quad 0.0 \quad 1.0\ \}$

$T_2 = \{\ 0.25 \quad 0.5 \quad 1.0\ \}$; $S_2 = \{\ 0.25 \quad 0.5 \quad 1.0\ \}$

$T_3 = \{\ 1.0 \quad 1.0 \quad 1.0\ \}$; $S_3 = \{\ 1.0 \quad 1.0 \quad 1.0\ \}$

$$[R] = [Q][G][Q]^T$$

$\sigma_1 = \{S_1\}[R]\{T_1\}^T$; $\sigma_8 = \{S_2\}[R]\{T_1\}^T$

$\sigma_2 = \{S_1\}[R]\{T_2\}^T$; $\sigma_9 = \{S_2\}[R]\{T_2\}^T$

$\sigma_3 = \{S_1\}[R]\{T_3\}^T$; $\sigma_4 = \{S_3\}[R]\{T_3\}^T$

$\sigma_7 = \{S_3\}[R]\{T_1\}^T$; $\sigma_6 = \{S_3\}[R]\{T_2\}^T$

$\sigma_5 = \{S_3\}[R]\{T_3\}^T$

Figure 5.9.5: Local stress smoothing for an isoparametric element using a blending functions technique

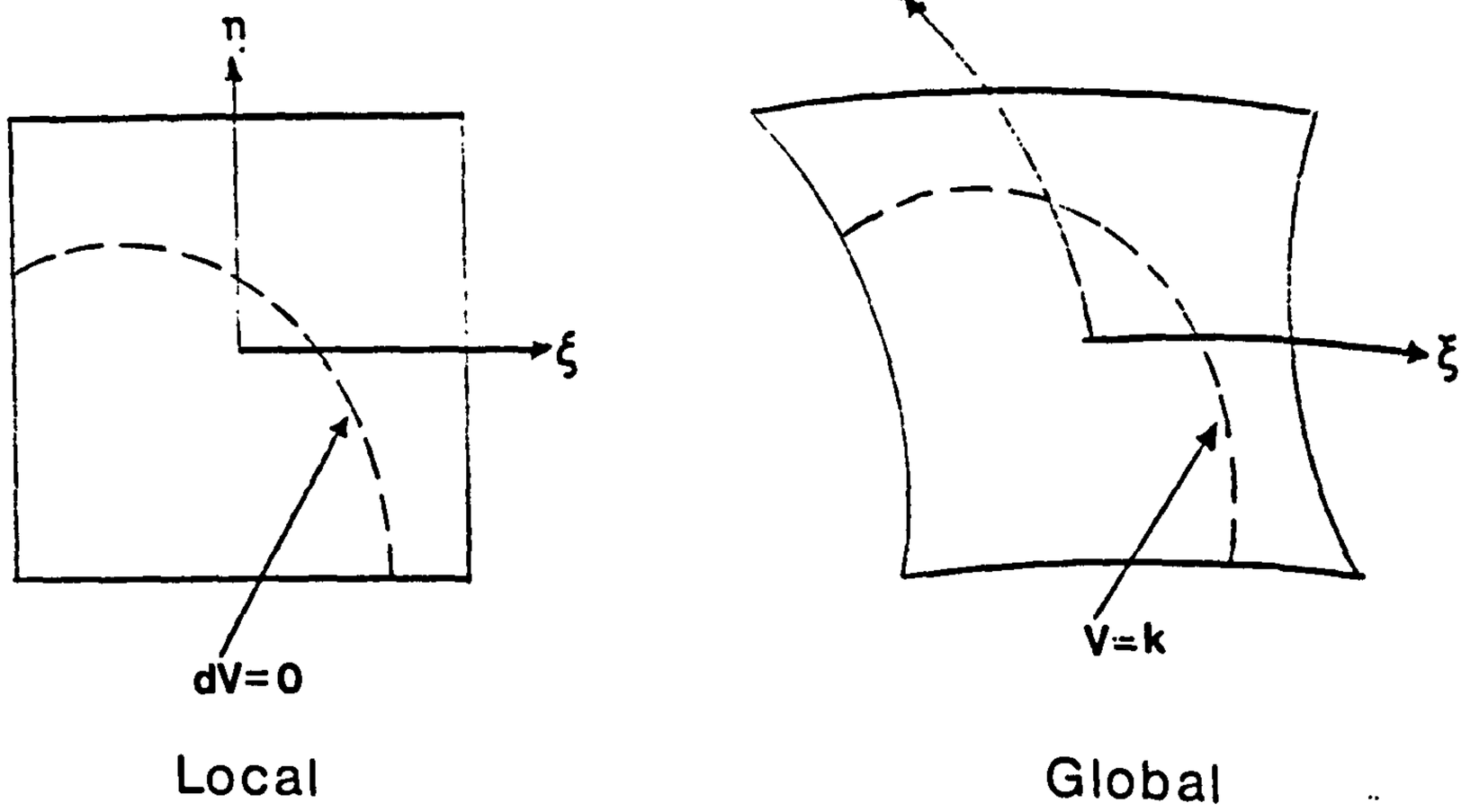

(a) Typical element contours

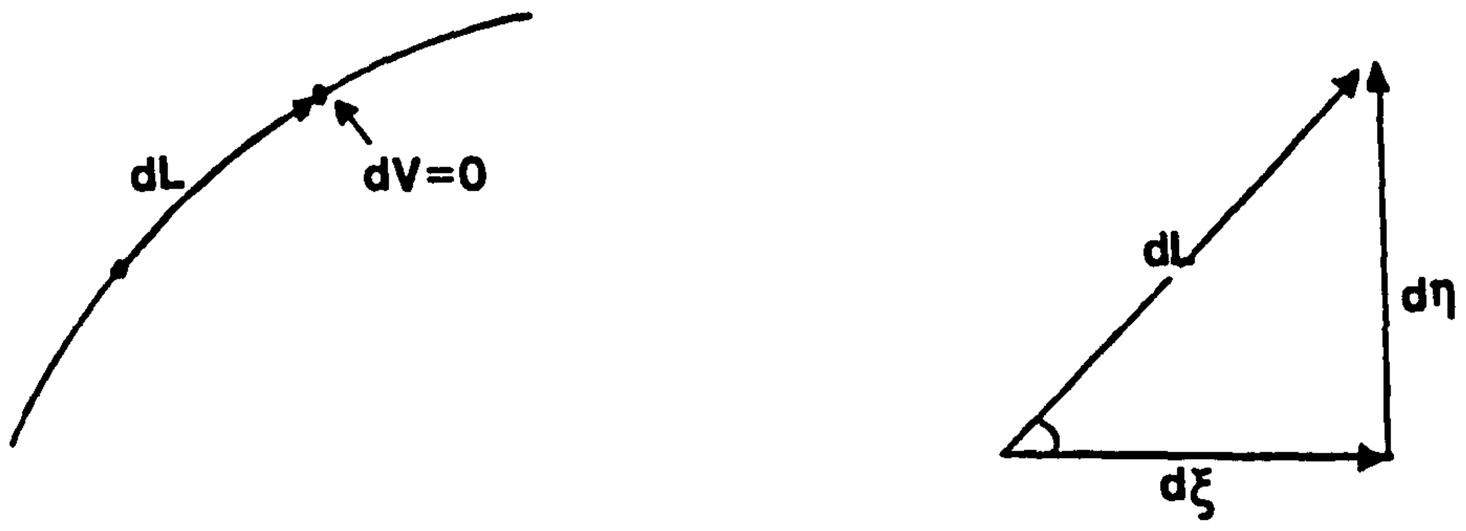

(b) Marching along a contour

Figure 5.9.6 Contouring on an isoparametric surface

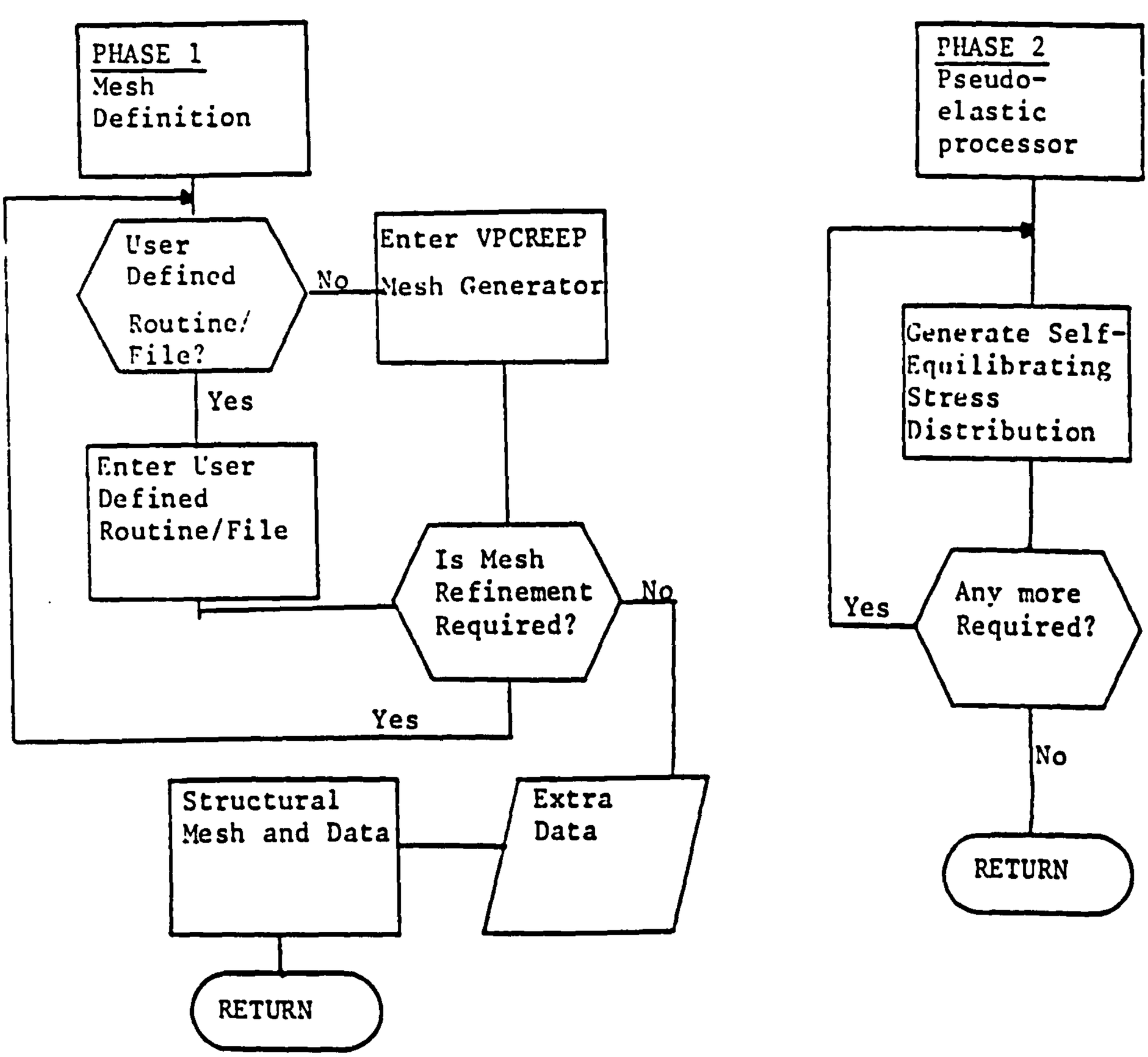

Figure 5.9.7: Macro flow chart for VPCREEP - phases 1 & 2

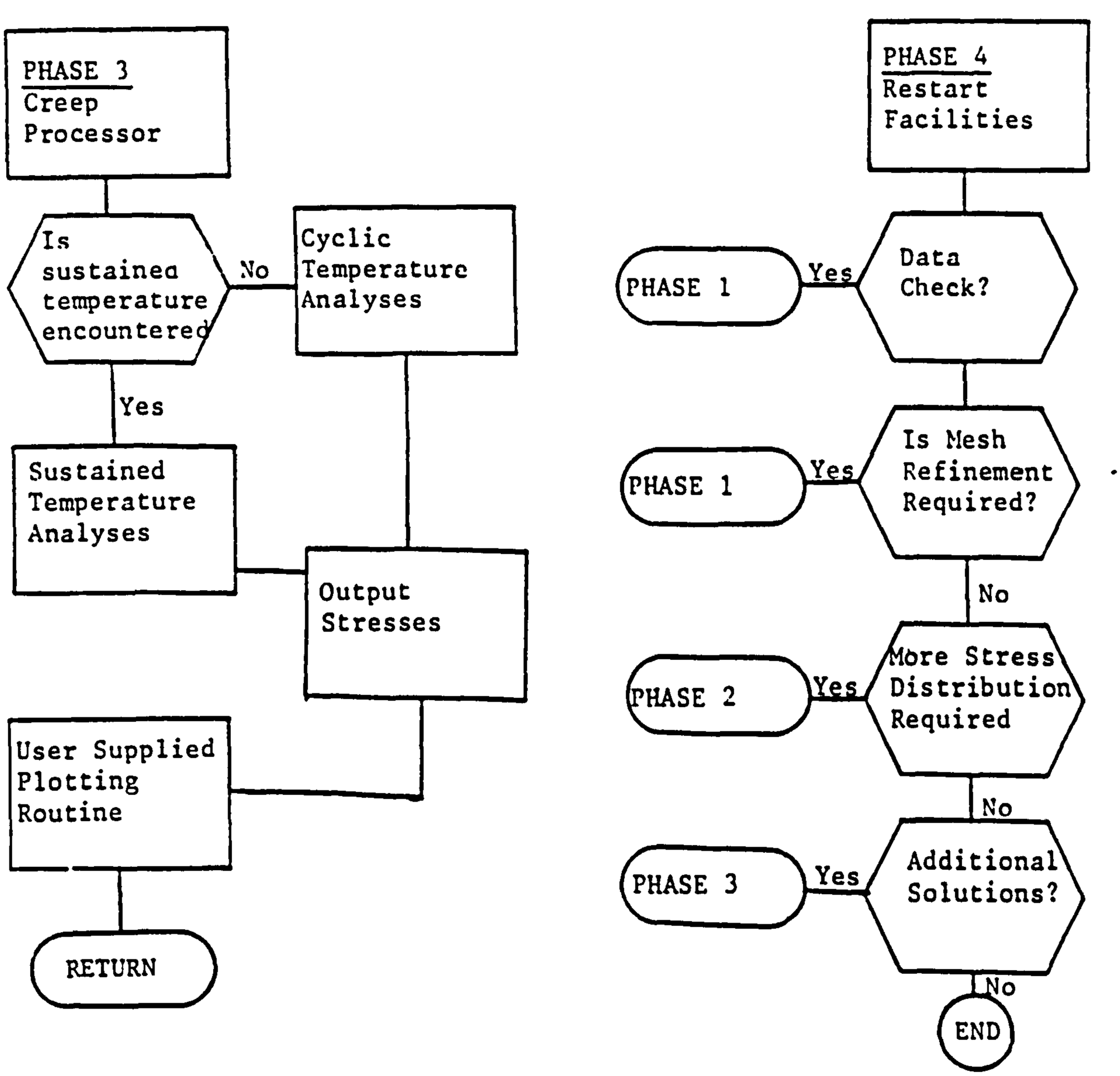

Figure 5.9.8: Macro flow chart for VPCREEP - phases 3 & 4

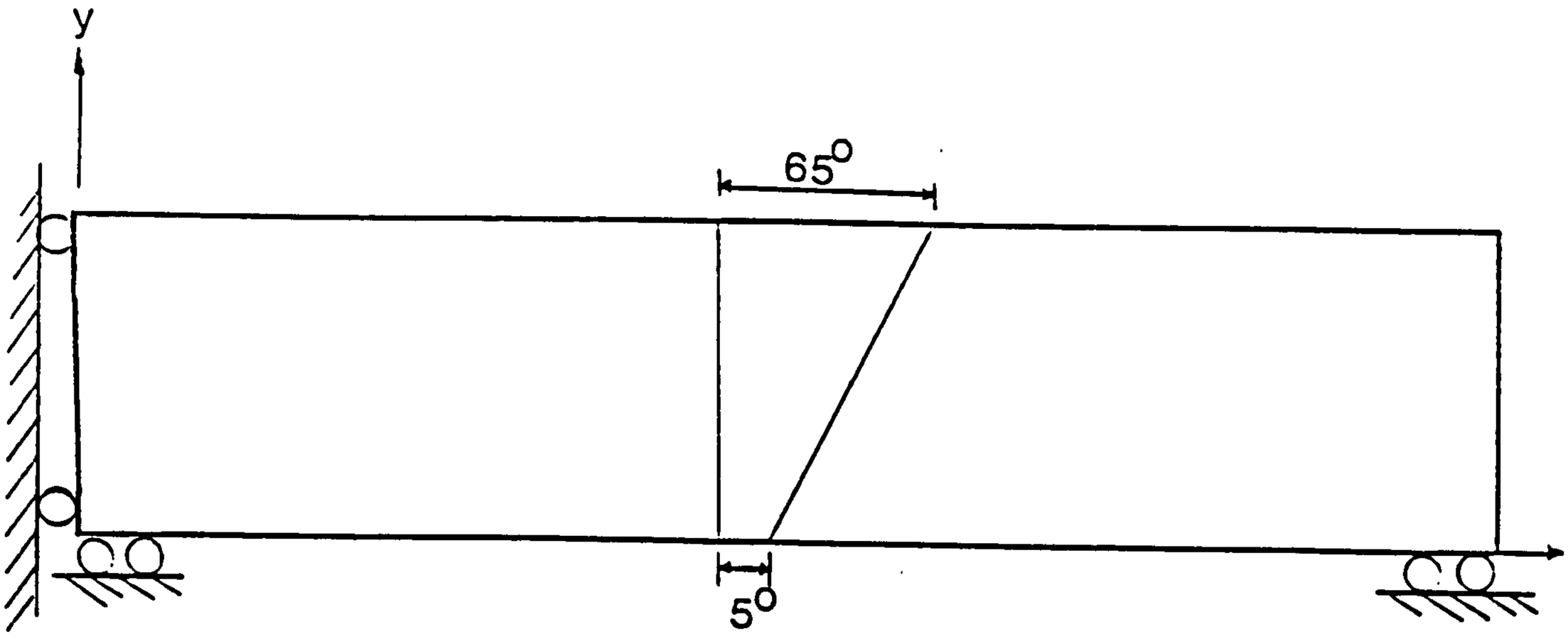

(a) The beam model

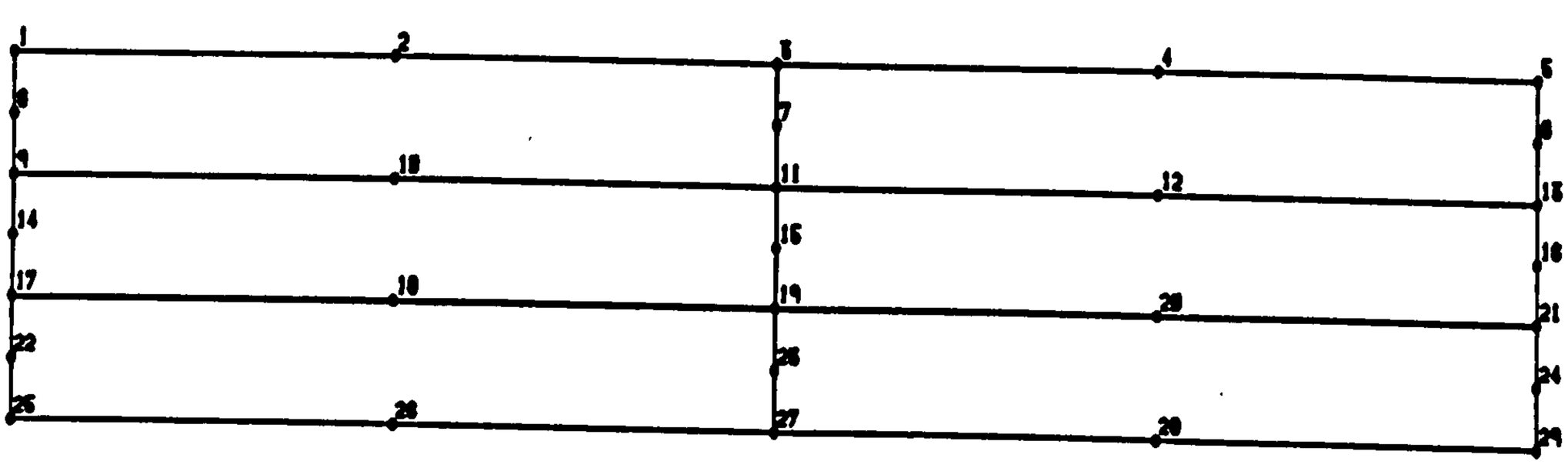

(b) Finite element idealisation

Figure 5.10.1 The finite element model for the flexurally restrained beam problem

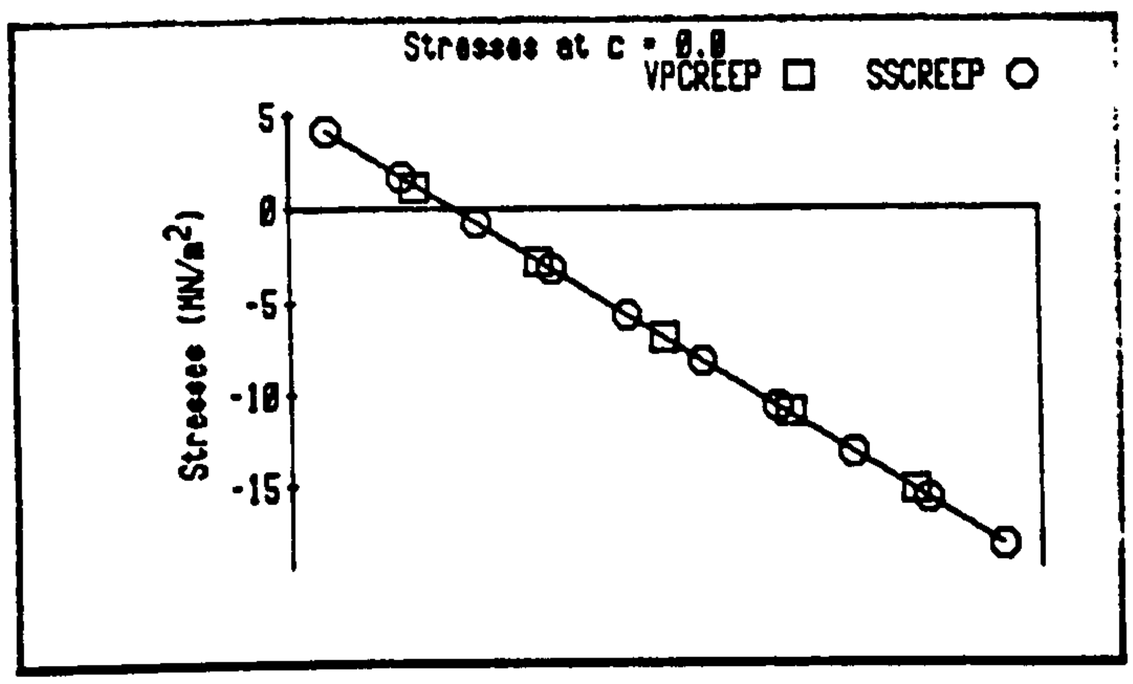

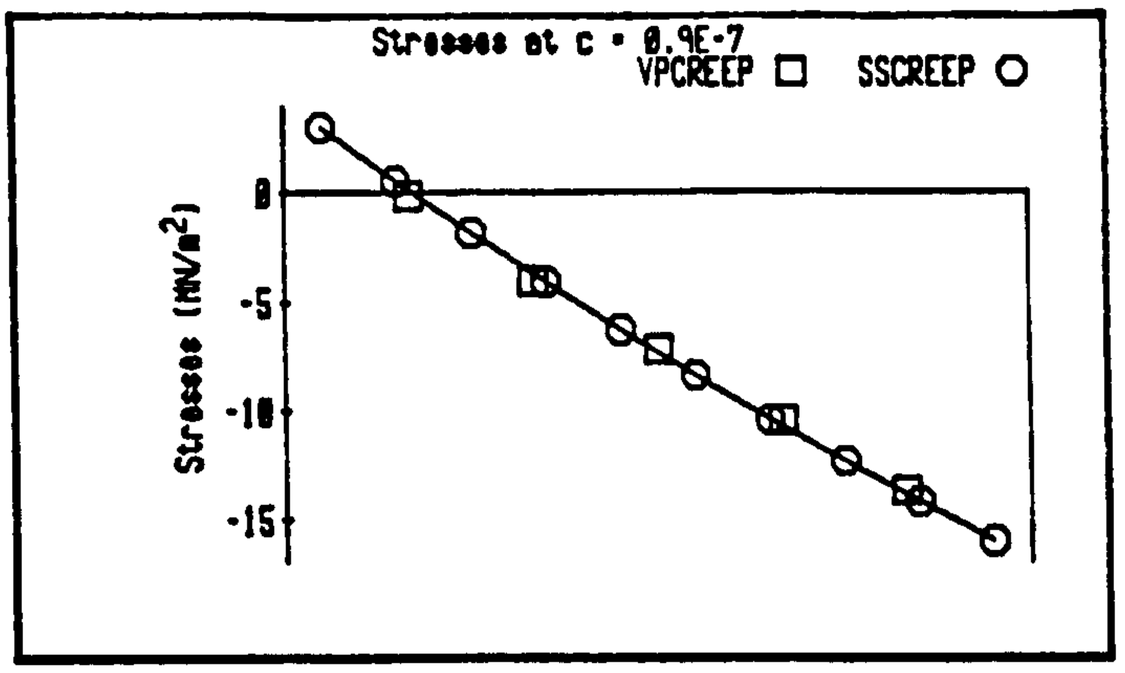

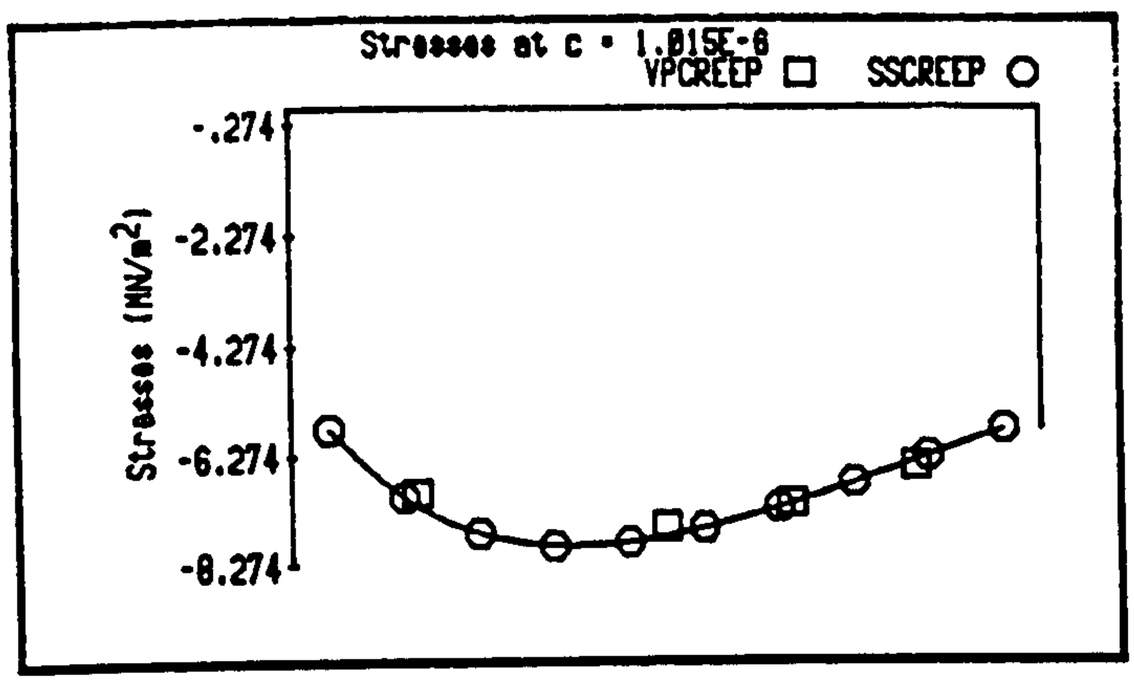

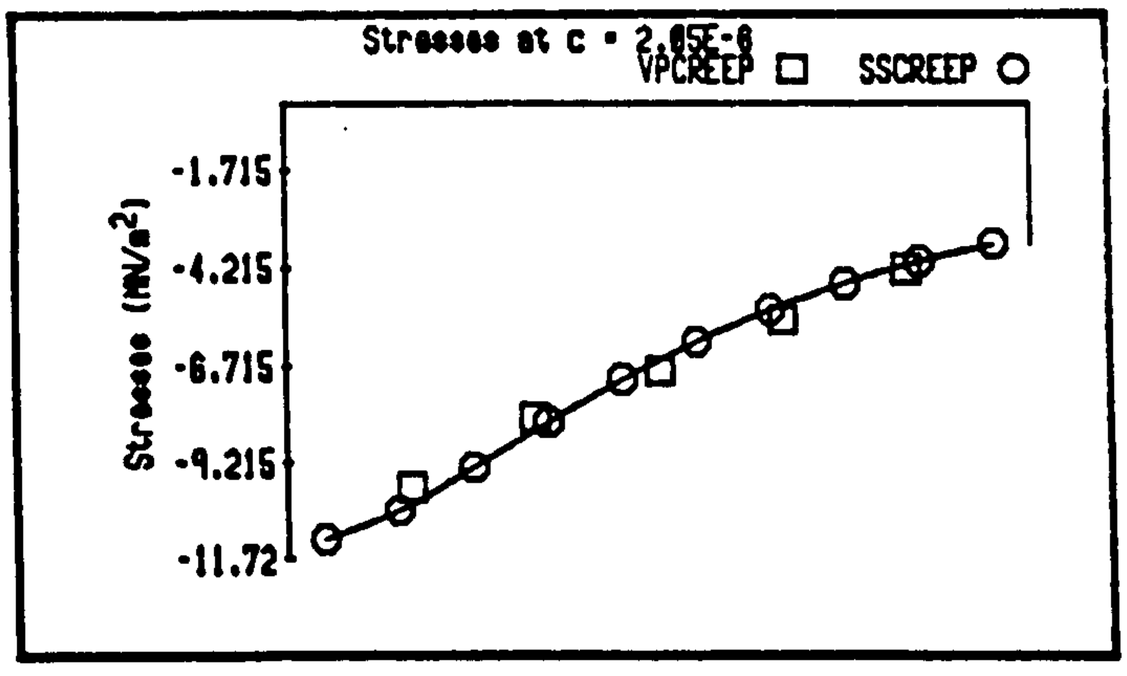

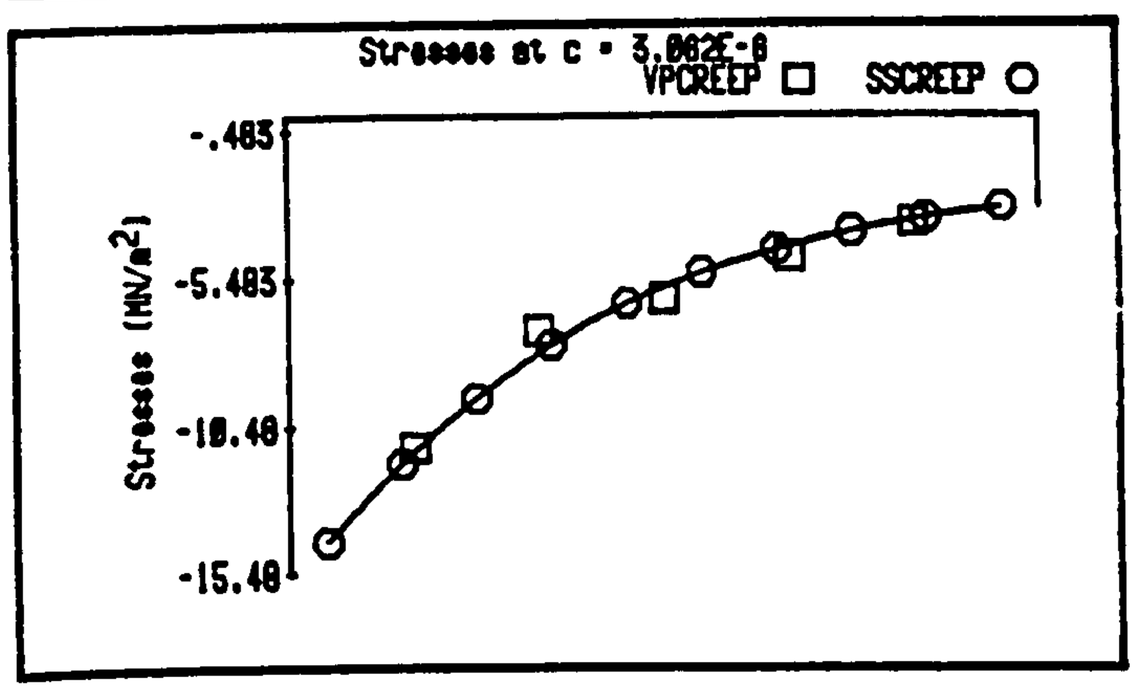

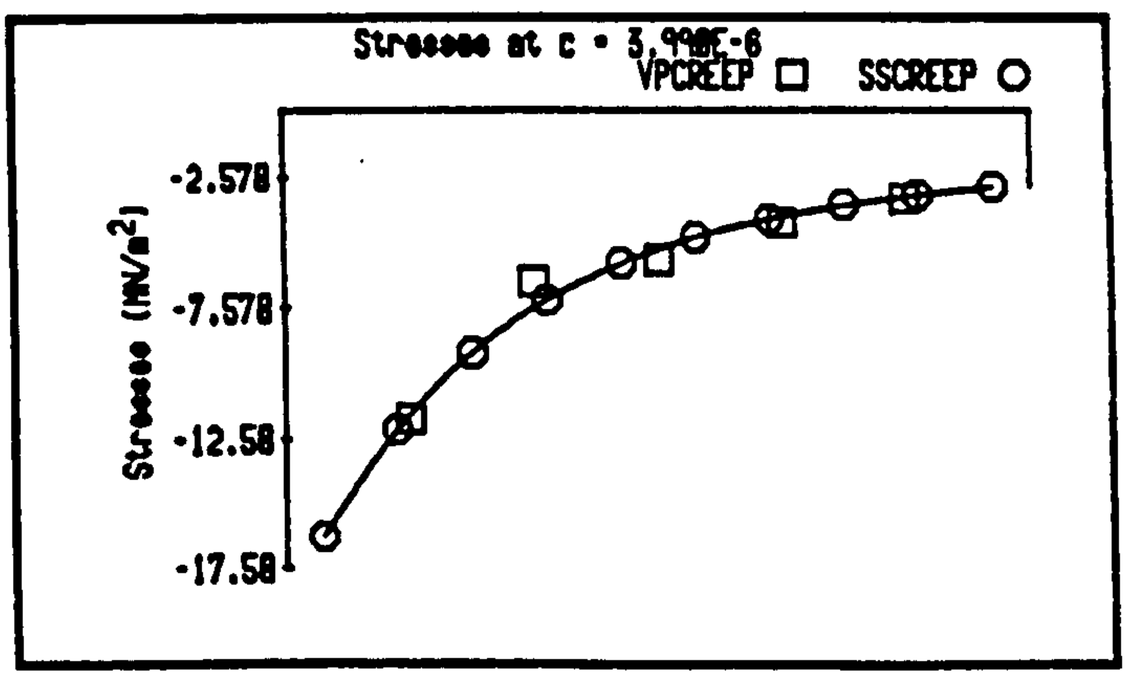

Figure 5.10.2 Comparison between SSCREEP & VPCREEP results

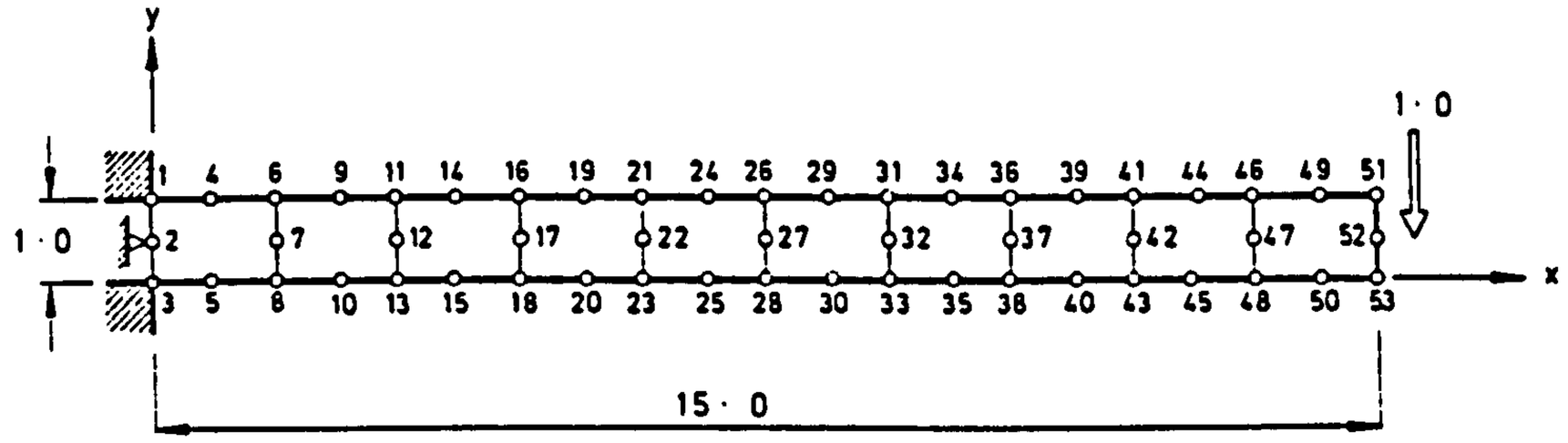

ELASTIC MODULUS , E = 100 000·0
POISSONS RATIO , ν = 0·3
THICKNESS , t = 1·0
MASS DENSITY , ρ = 0·1

PLANE STRESS CONDITIONS

(a) The finite element model

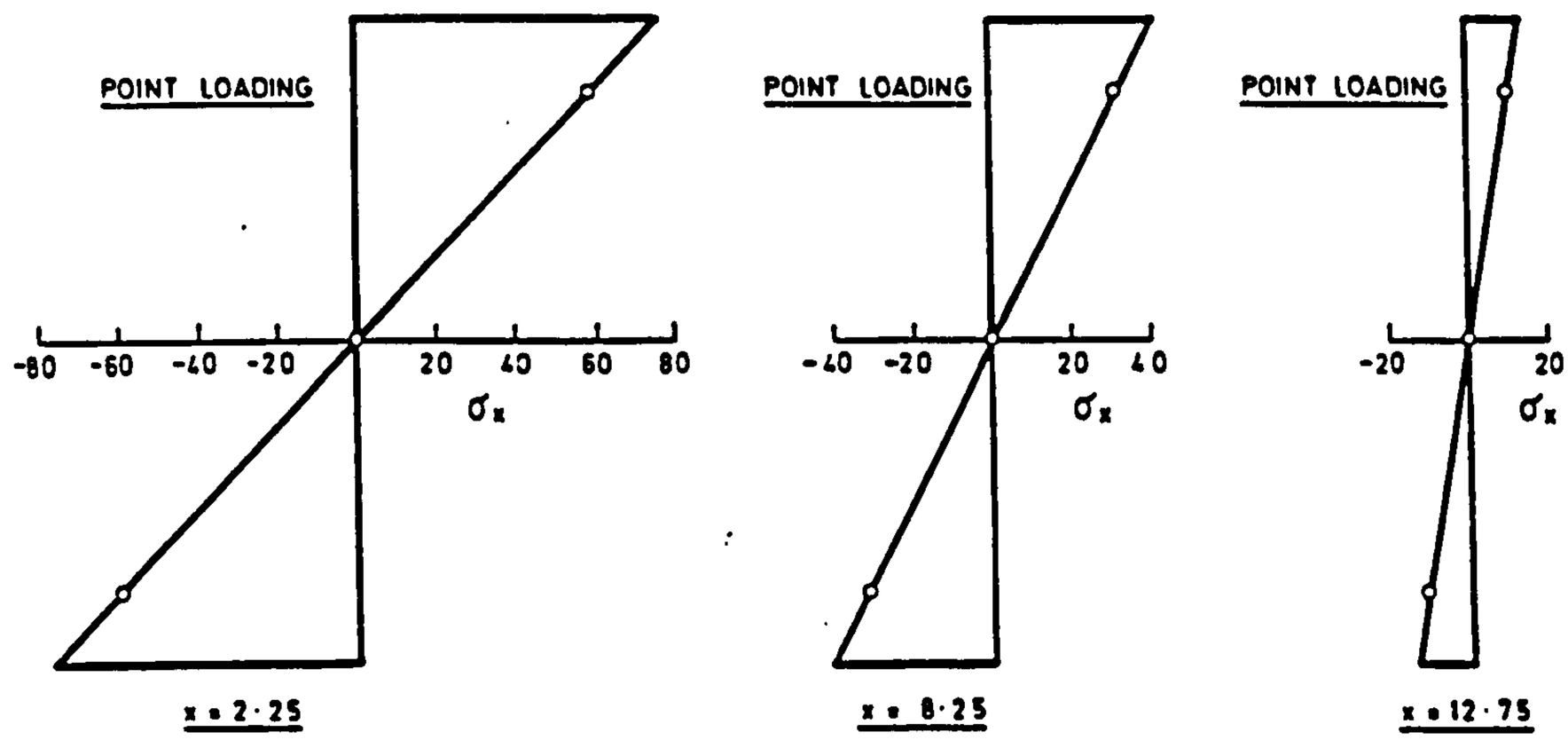

Numerical end deflection = 0.134546 mm

Analytical end deflection = 0.135000 mm

(b) Axial stress distribution and deflections

Figure 5.11.1: Plane stress elastic analysis of a cantilever beam under tip load

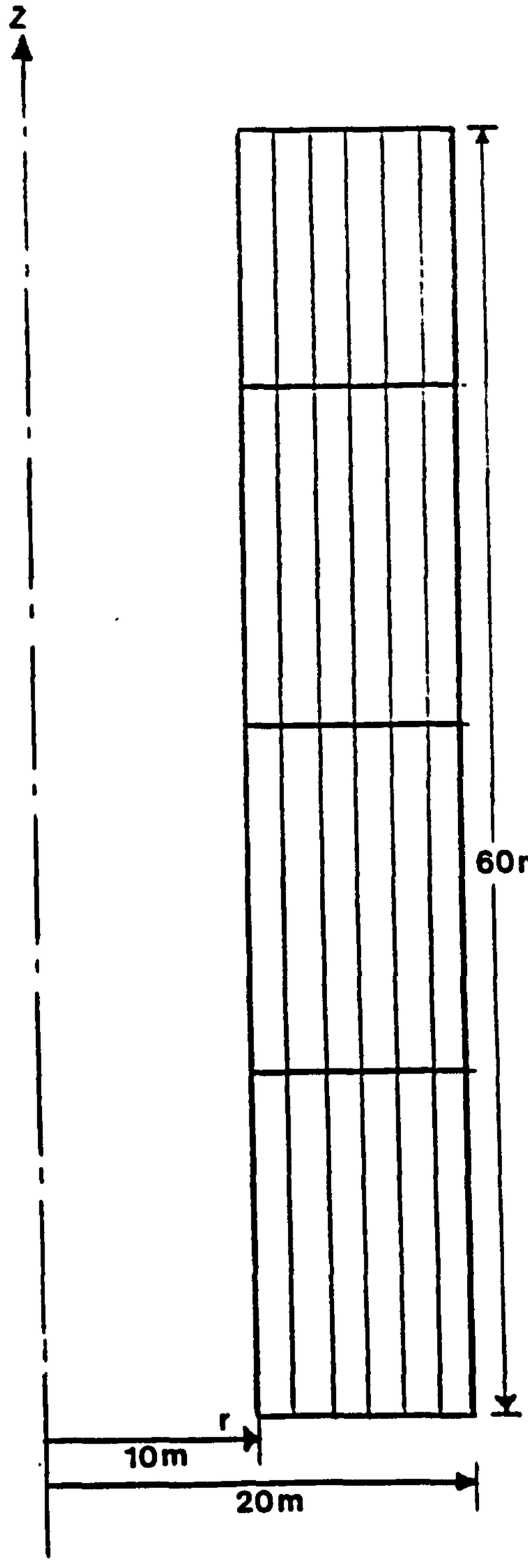

Figure 5.11.2: Axisymmetric elastic analysis of a cylinder subjected to internal pressure

r	σ_r		σ_θ	
	Analytical	Numerical	Analytical	Numerical
10.19	-9.507	-9.440	16.174	16.200
10.83	-8.035	-8.120	14.701	14.670
11.48	-6.784	-6.718	13.450	13.470
11.85	-6.162	-6.111	12.829	12.830
12.50	-5.200	-5.250	11.867	11.850
13.15	-4.377	-4.344	11.044	11.060
13.52	-3.961	-3.934	10.628	10.630
14.17	-3.307	-3.341	9.974	9.969
14.81	-2.745	-2.720	9.412	9.416
15.19	-2.445	-2.430	9.112	9.118
15.83	-1.988	-2.005	8.654	8.647
16.48	-1.576	-1.562	8.243	8.247
16.85	-1.363	-1.349	8.030	8.030
17.50	-1.020	-1.034	7.687	7.684
18.15	-0.714	-0.706	7.381	7.385
18.52	-0.554	-0.546	7.221	7.222
19.17	-0.295	-0.305	6.962	6.960
19.81	-0.064	-0.056	6.731	6.732

Table 5.11.1 Comparison between stresses obtained from numerical and analytical elatsic analysis of a long cylinder

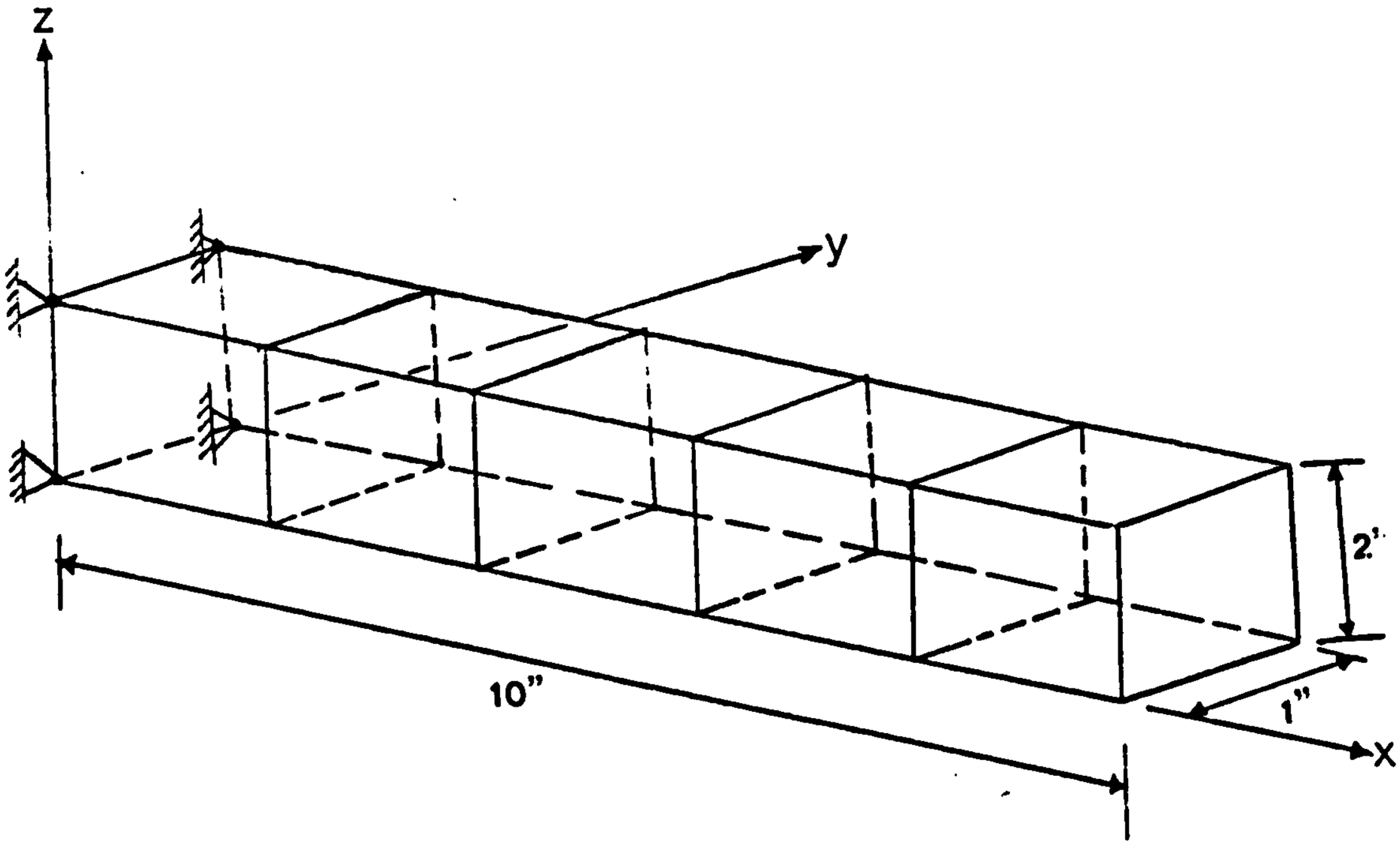

Note: (1) Node and element numbers not shown.
(2) Imperial units were used here.
(3) The following material constants were used:

Young's modulus = 0.3×10^8 p.s.i.
Poisson's ratio = 0.2
End moment applied = 2000 in-lb.
End shear applied = 300 lb.

Figure 5.11.3: Three dimensional elastic analysis of a cantilever beam subjected to end moment and end shear

	Tip deflection (in)	Bending stressses (psi)
Theory	0.00500	3000.0
ANSYS	0.00500	3000.0
VPCREEP	0.00500	3006.0

(a) Results for case 1

	Tip deflection (in)	Bending stressses (psi)
Theory	0.00500	4050.0
ANSYS	0.00505	4050.0
VPCREEP	0.00506	4050.0

(b) Results for case 2

Table 5.11.2 Comparison between results obtained from numerical and analytical elatsic analysis of a three dimensional beam

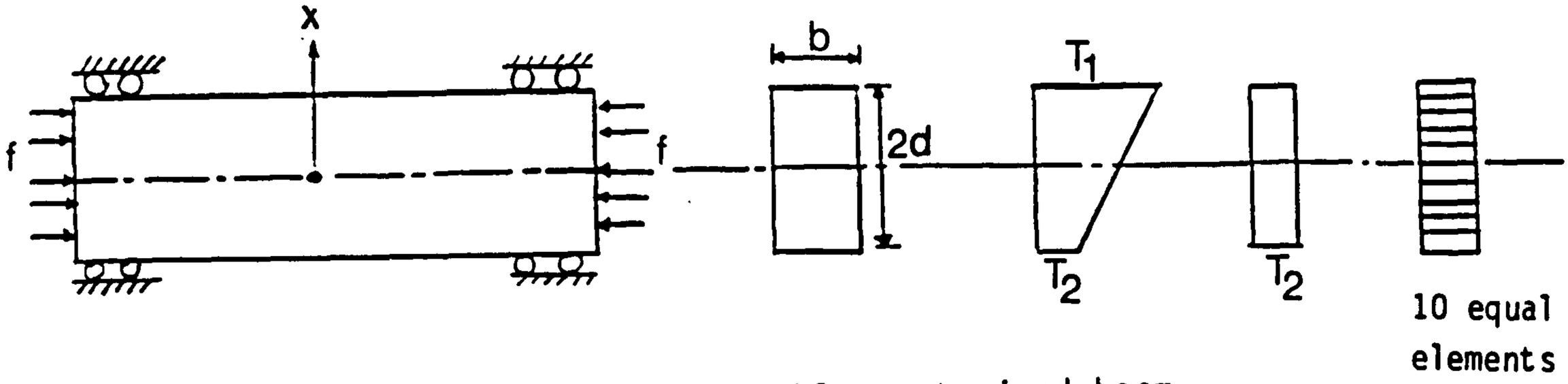

(a) Prestressed flexurally restrained beam

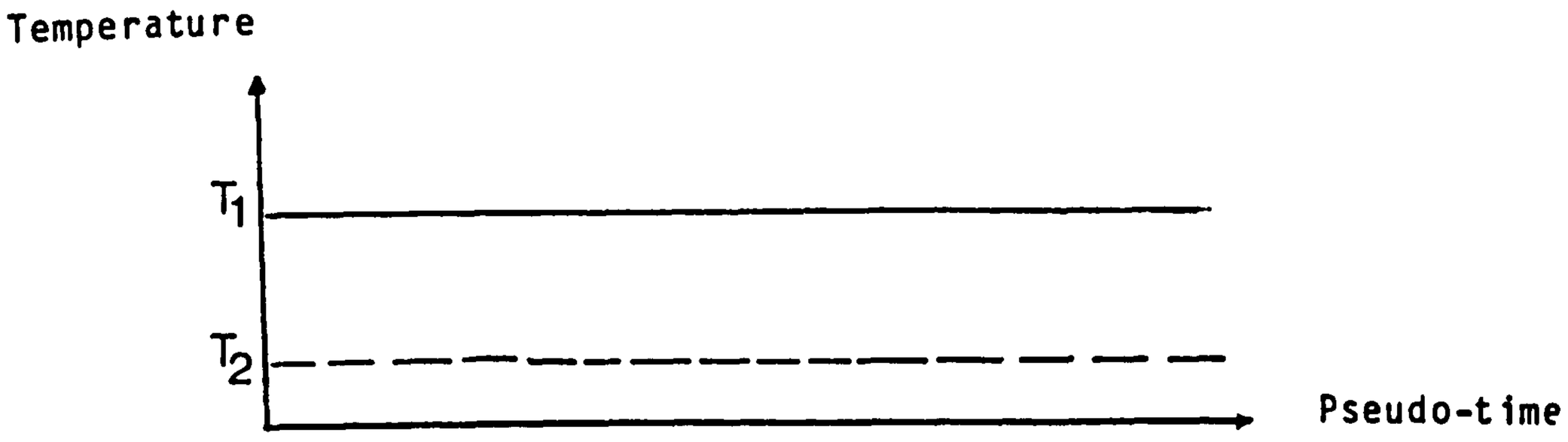

(b) Sustained temperatue field

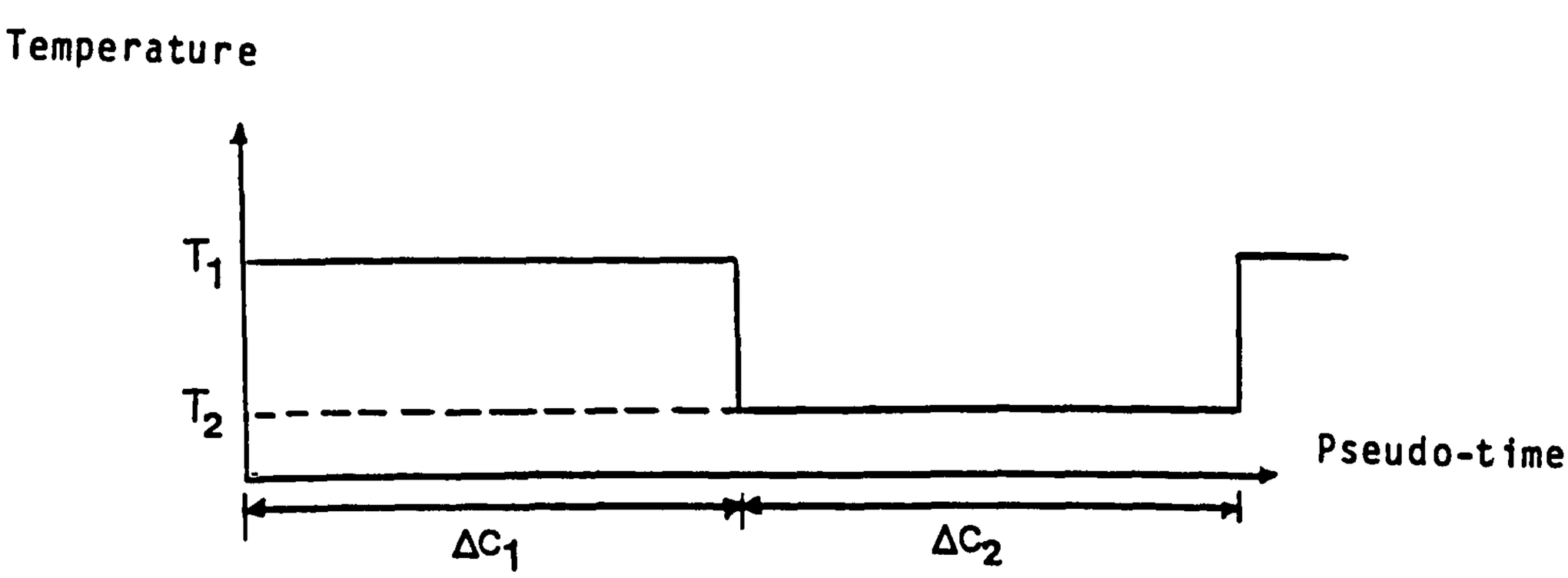

(c) Unidirectional cyclic temperature field,k=1

Figure 5.12.1: The beam and nature of temperature fields

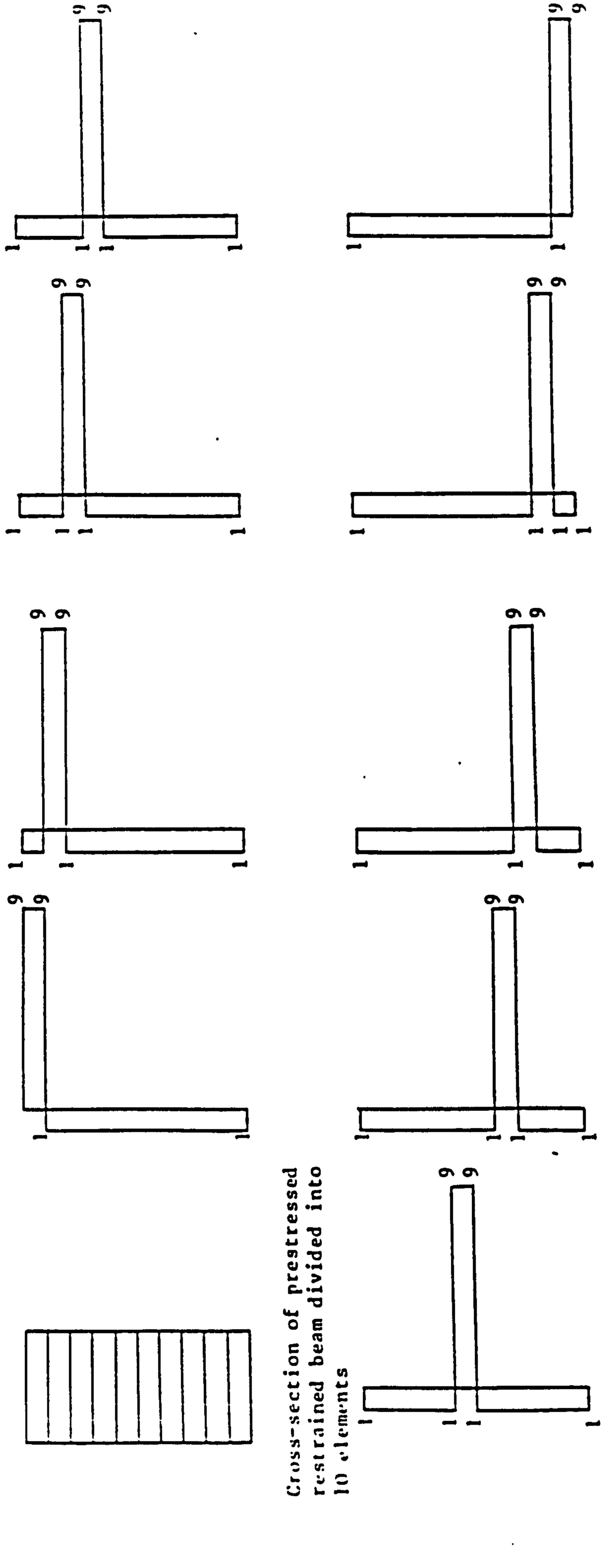

Figure 5.12.2: Group of self-equilibrating stresses used

Cross-section of prestressed restrained beam divided into 10 elements

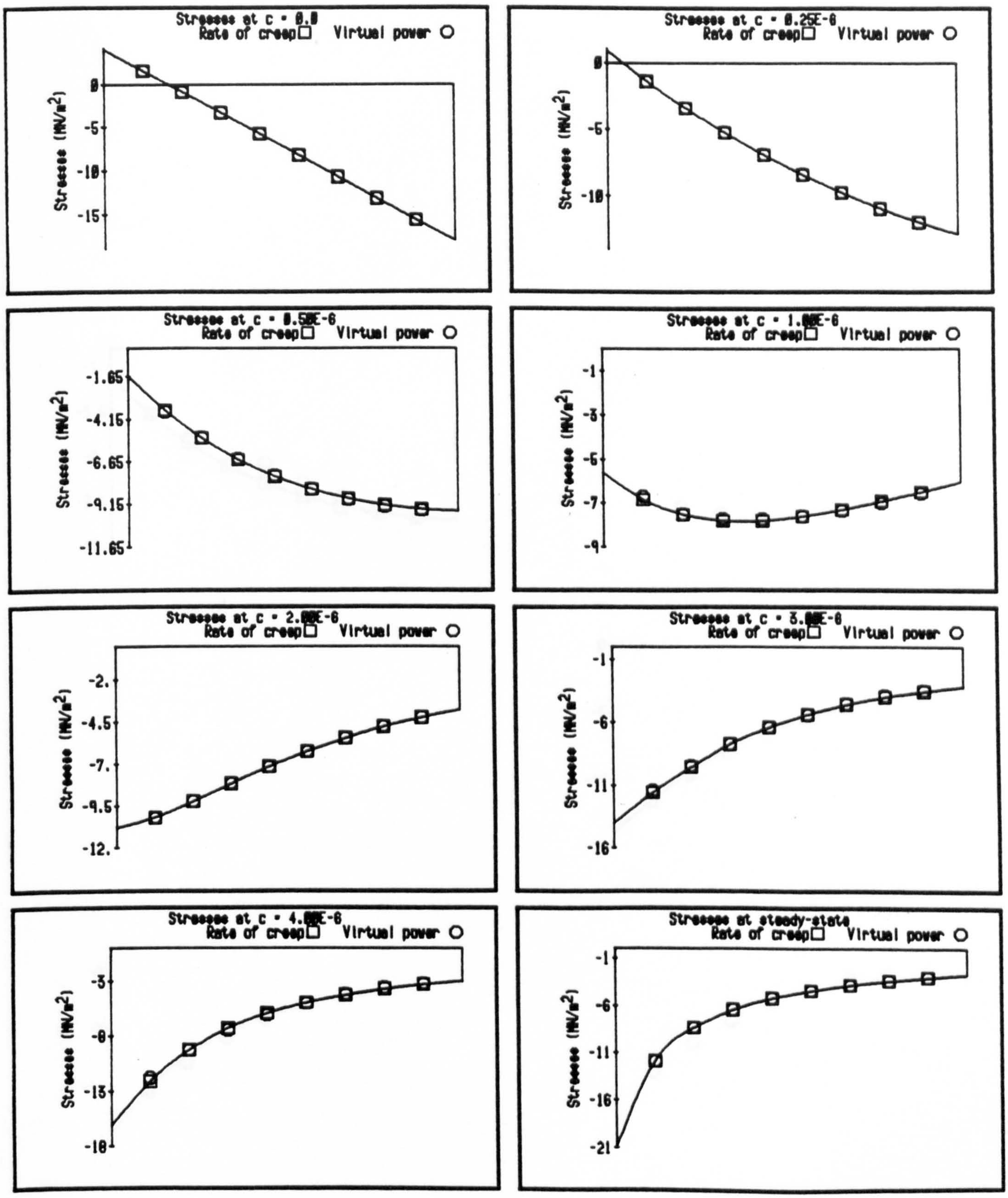

Note: Type (I), (II), & (III) distributions were used

Figure 5.12.3: Comparison between stresses obtained from the rate of creep method and the power method for a sustained temperature cross-fall

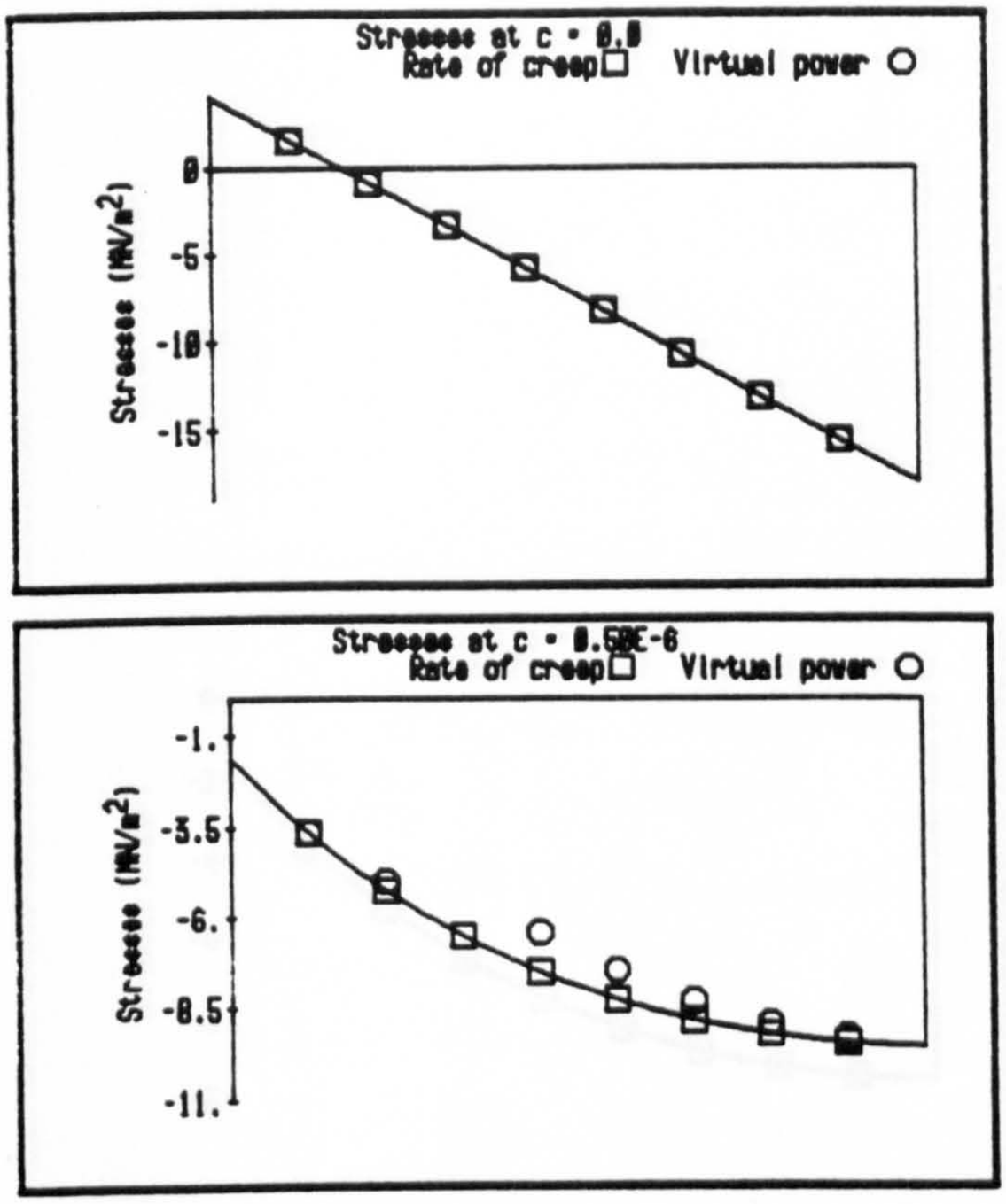

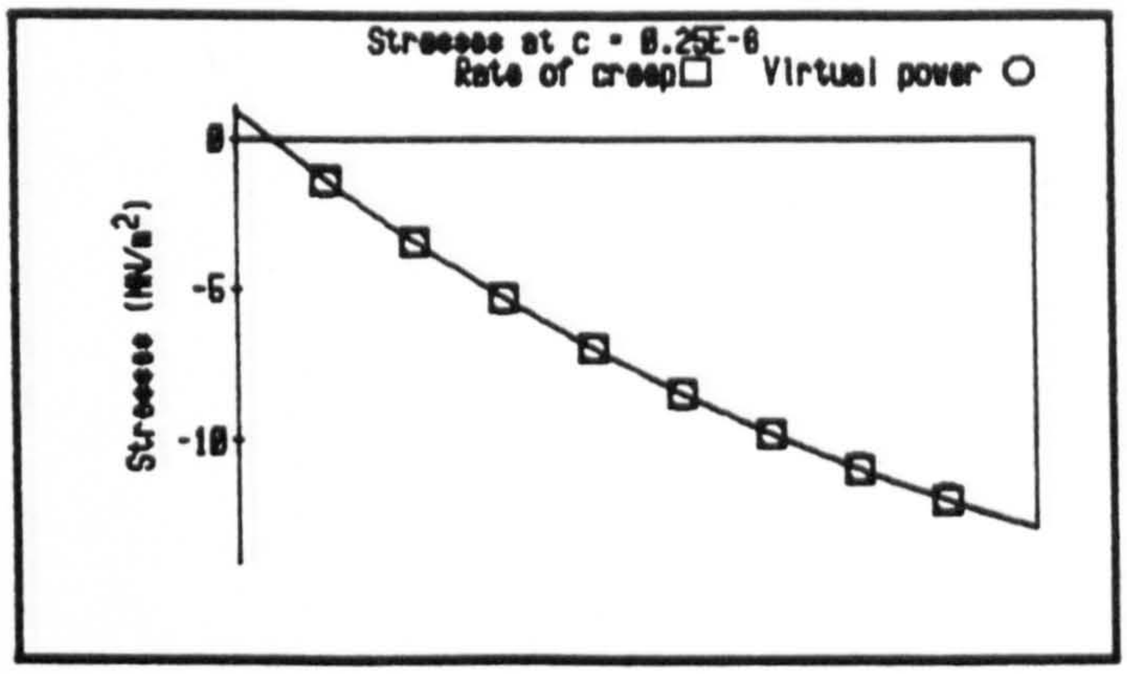

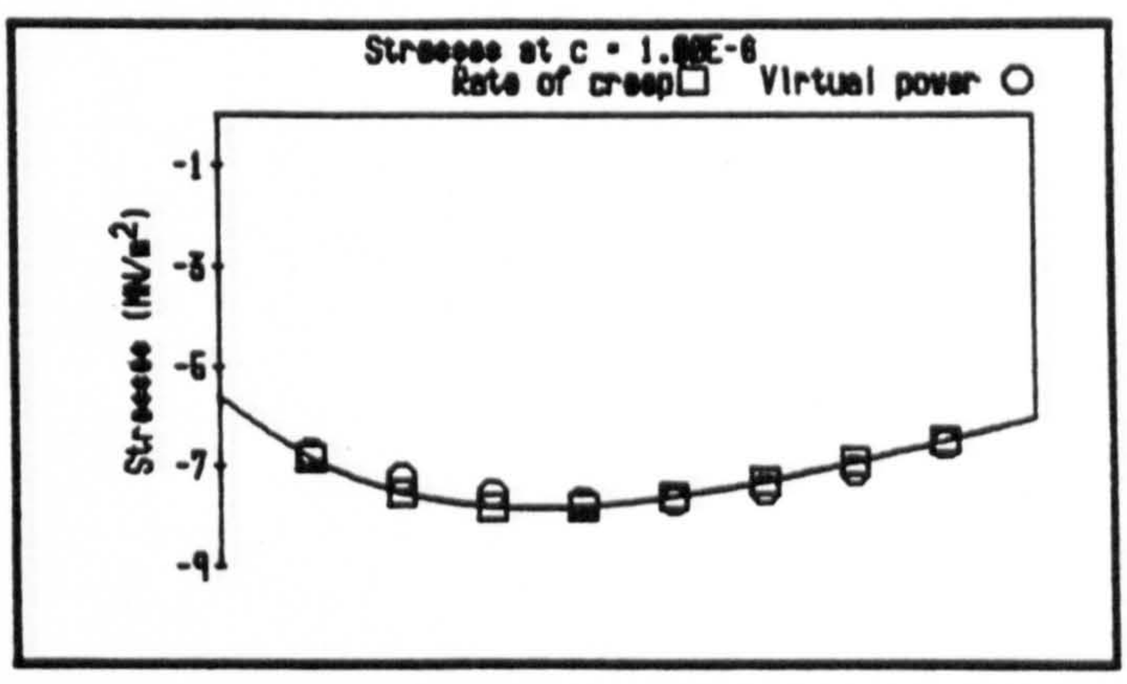

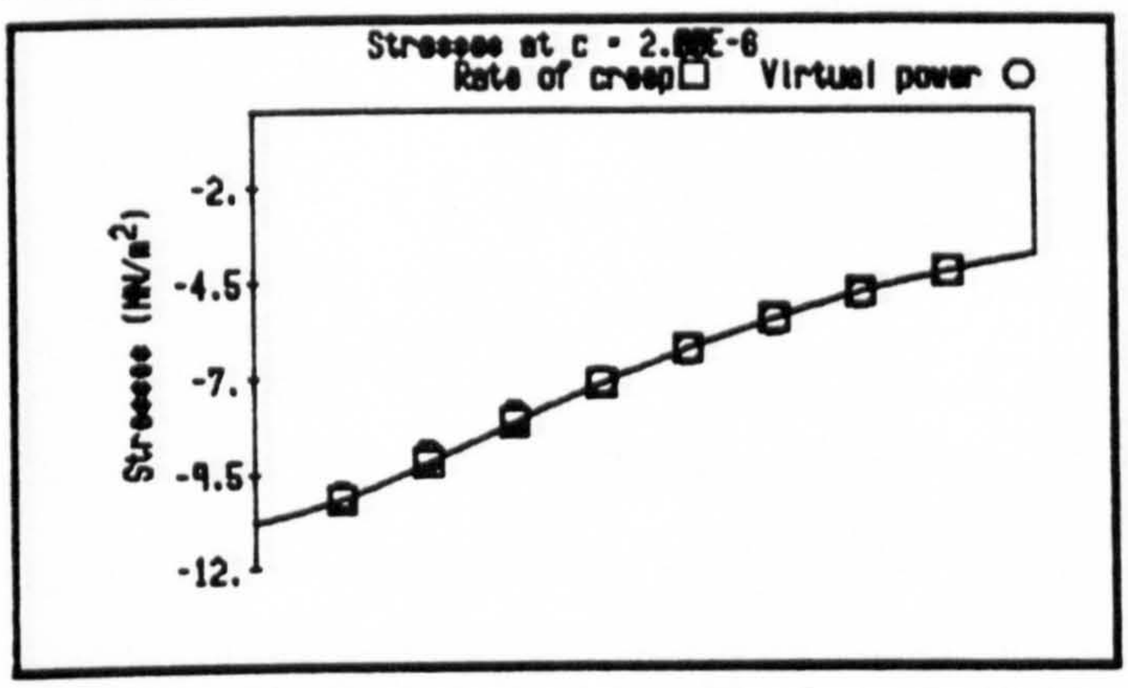

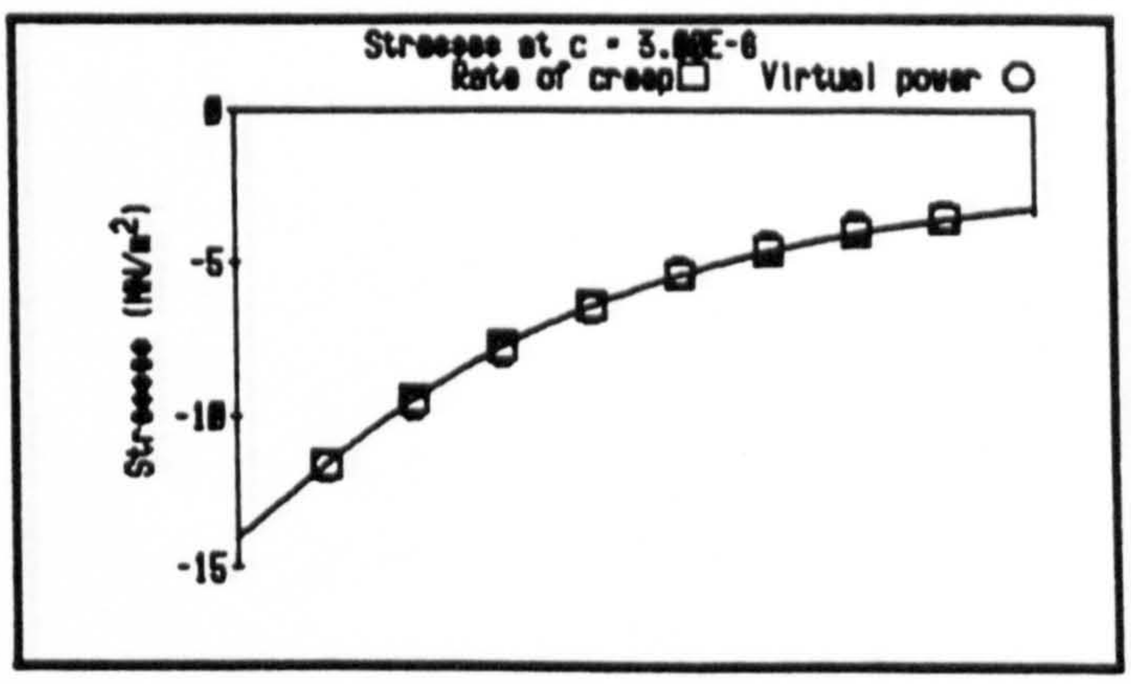

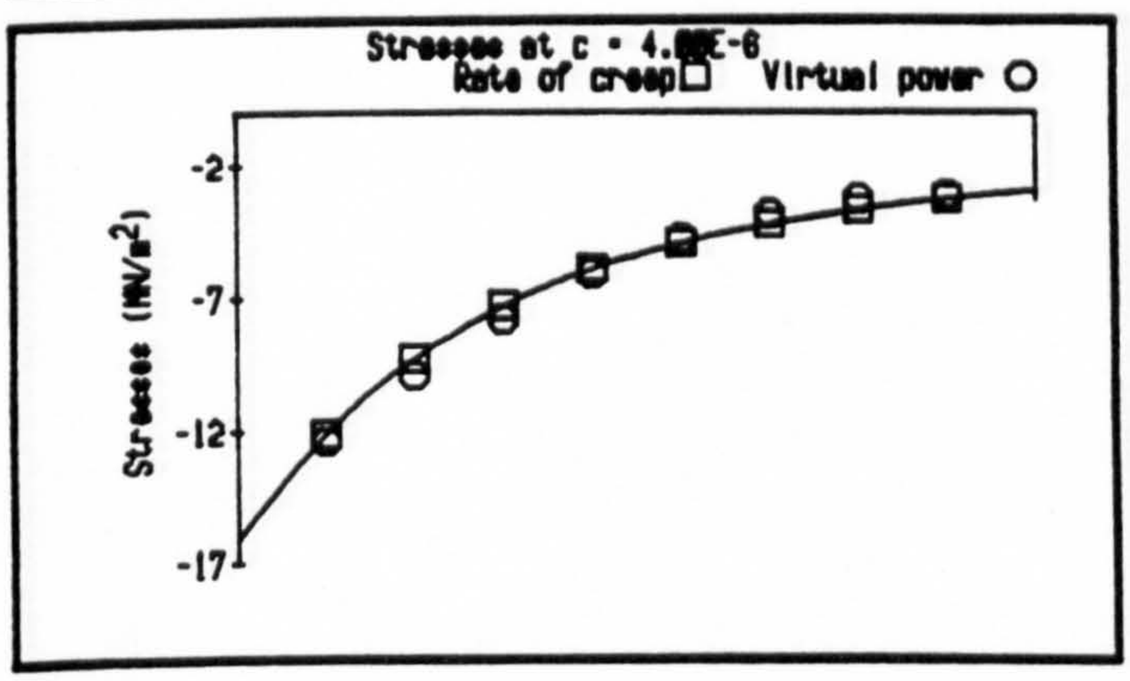

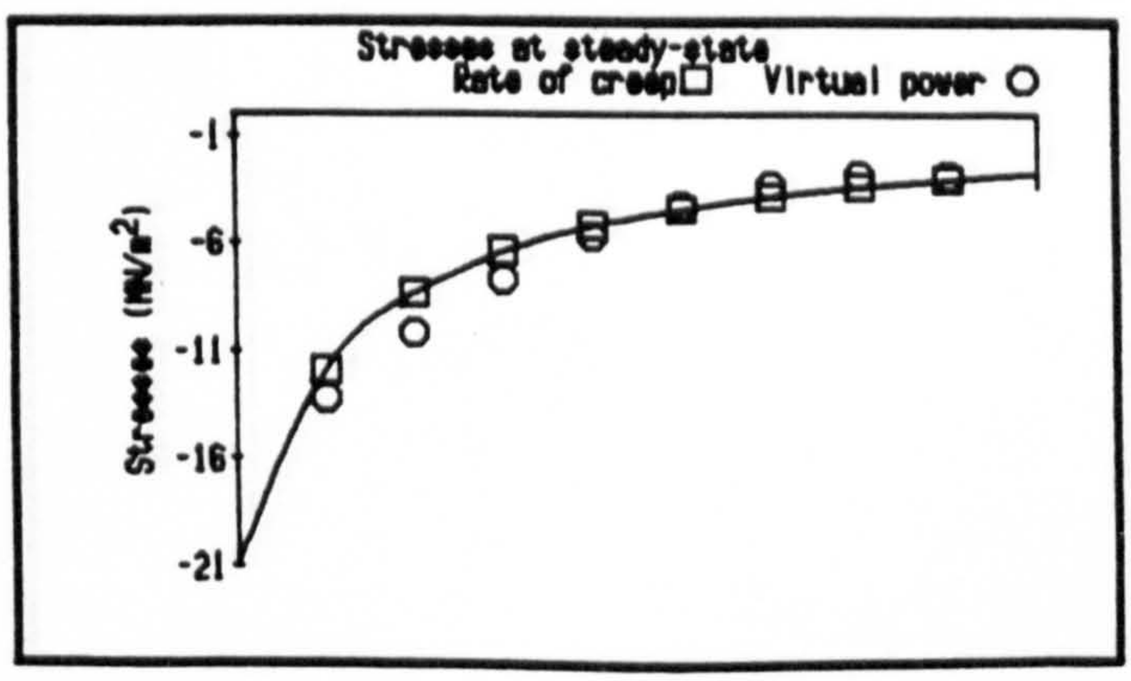

Note: Type (I) & (II) distributions were used

Figure 5.12.4: Comparison between stresses obtained from the rate of creep method and the power method for a sustained temperature cross-fall

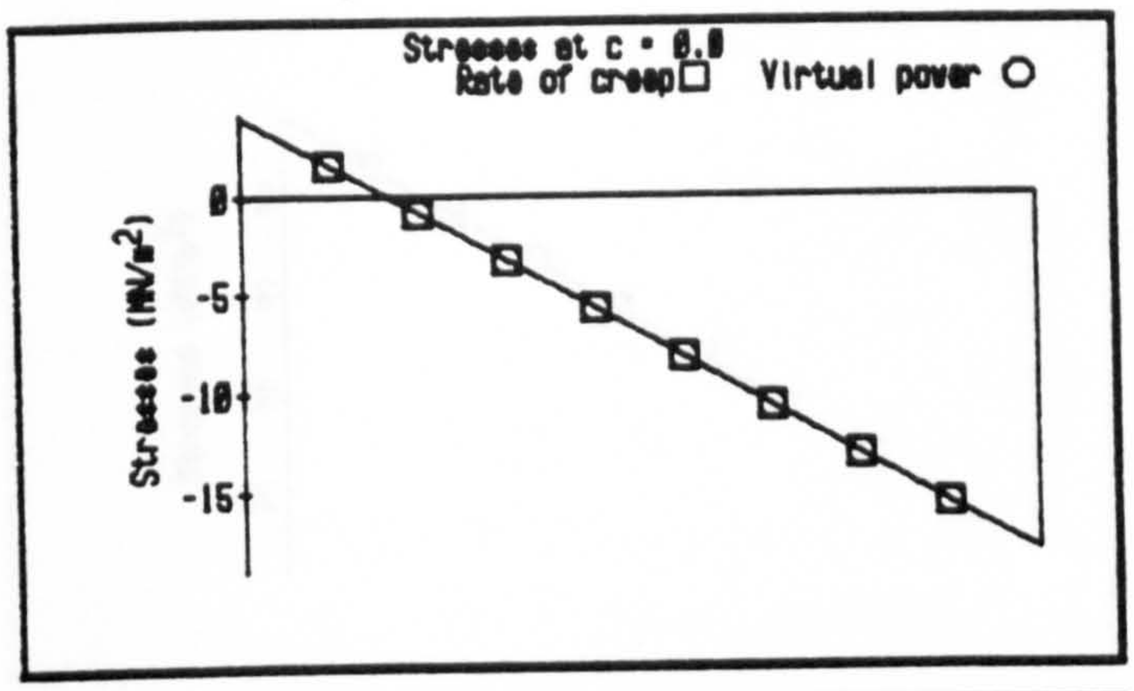

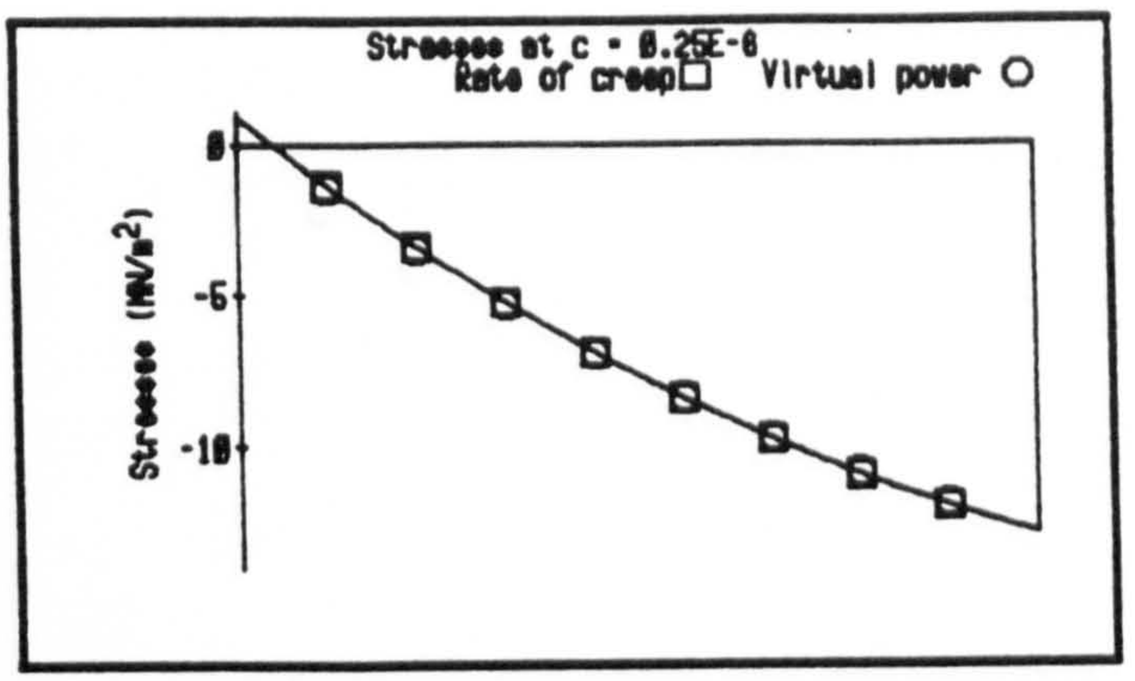

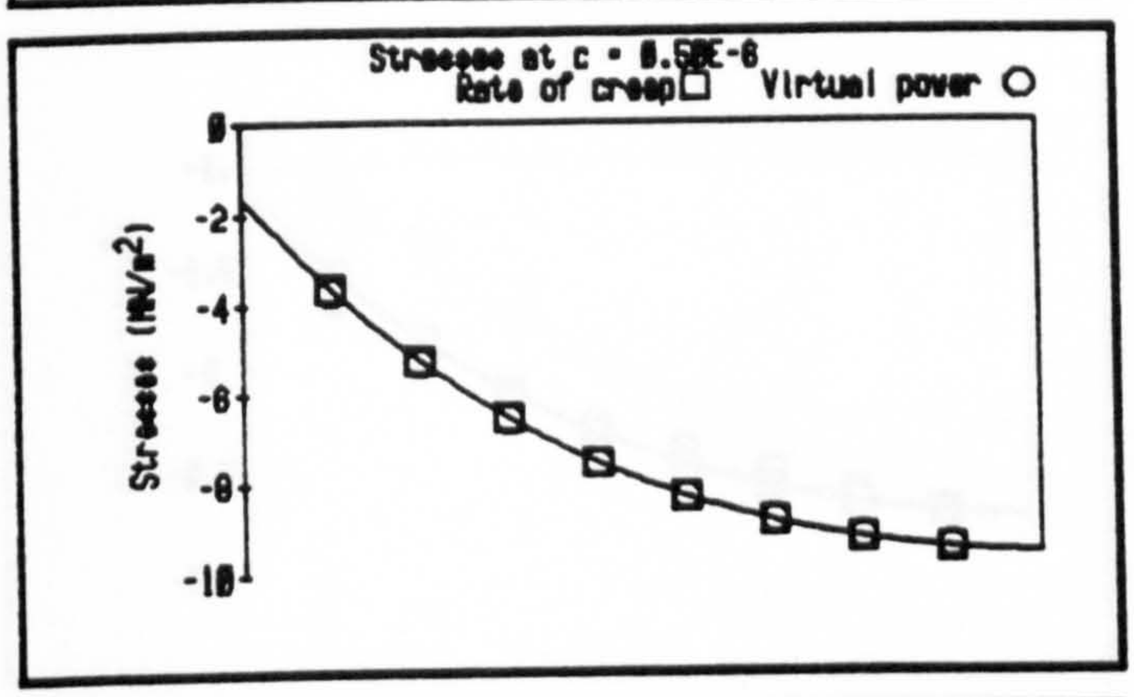

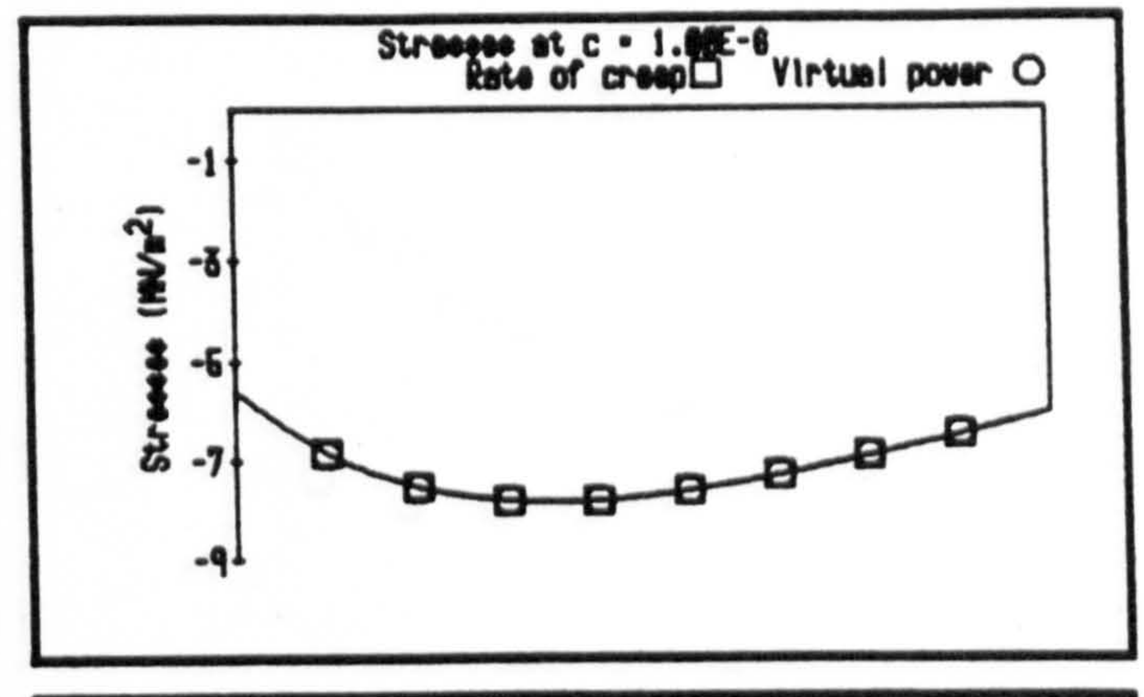

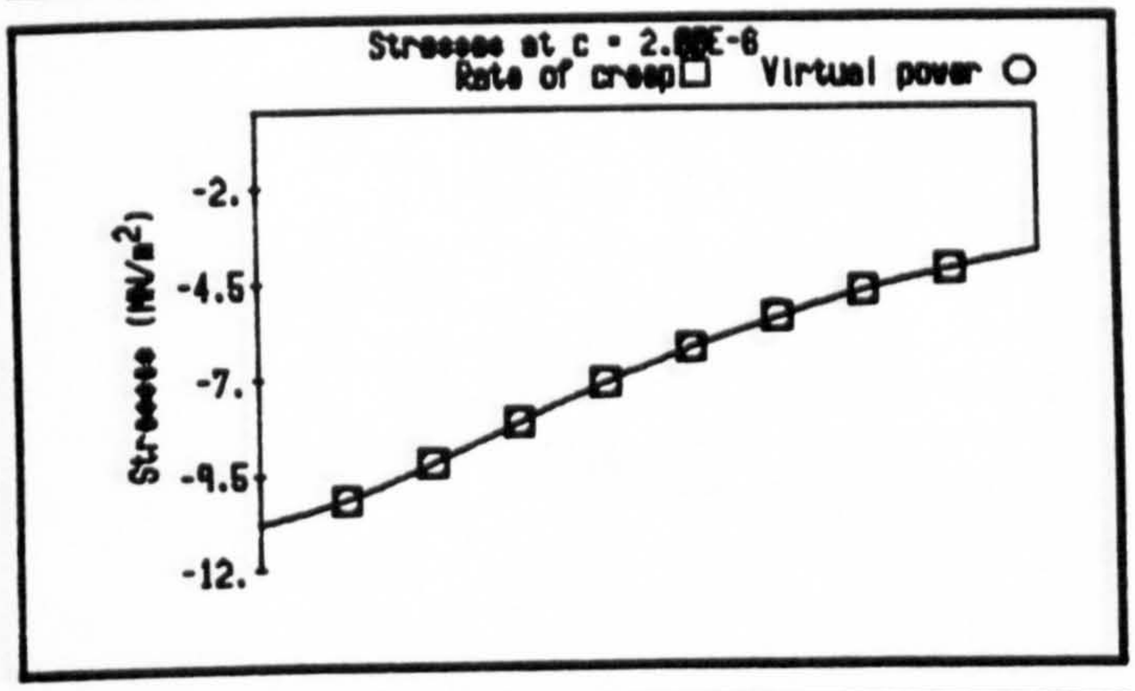

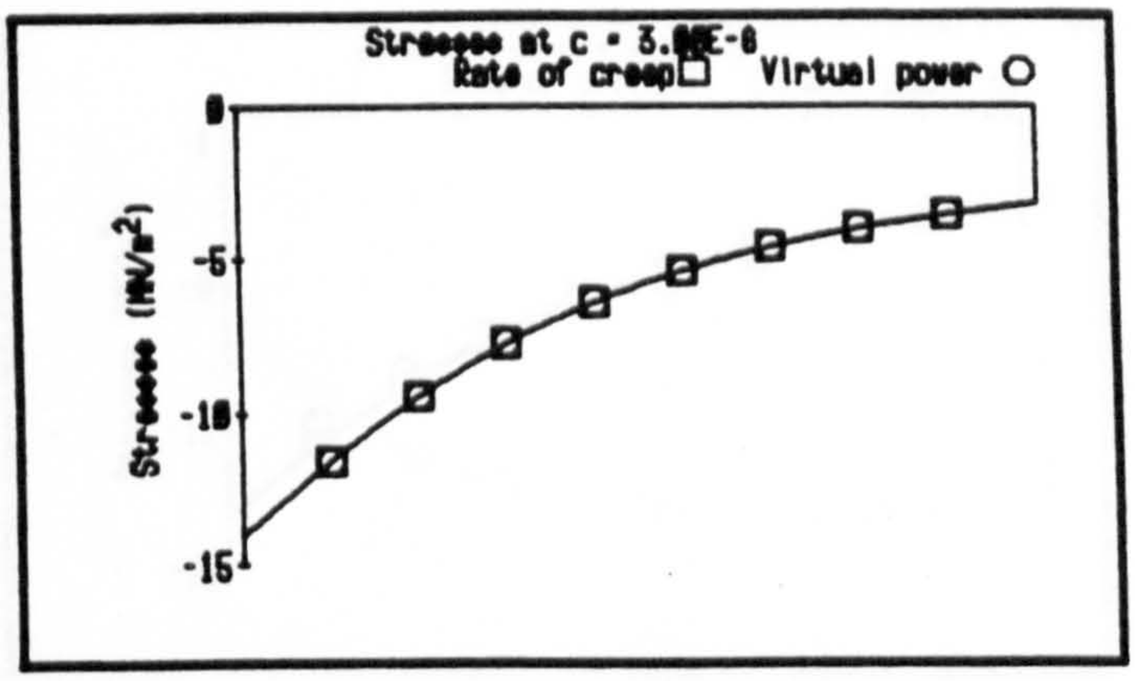

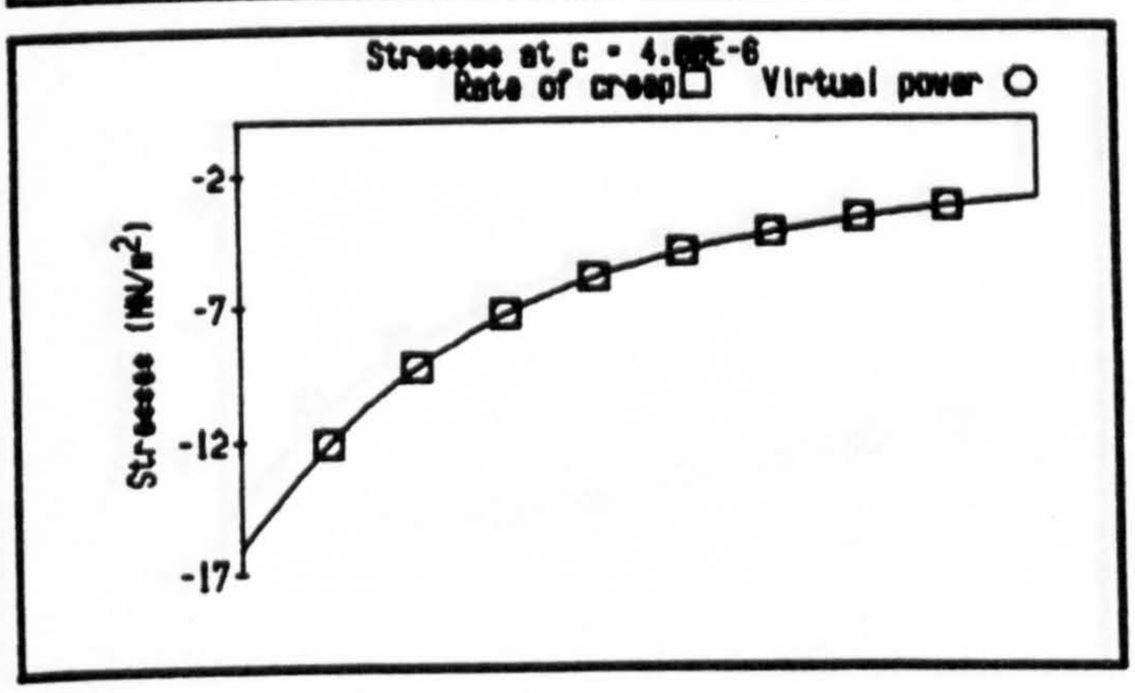

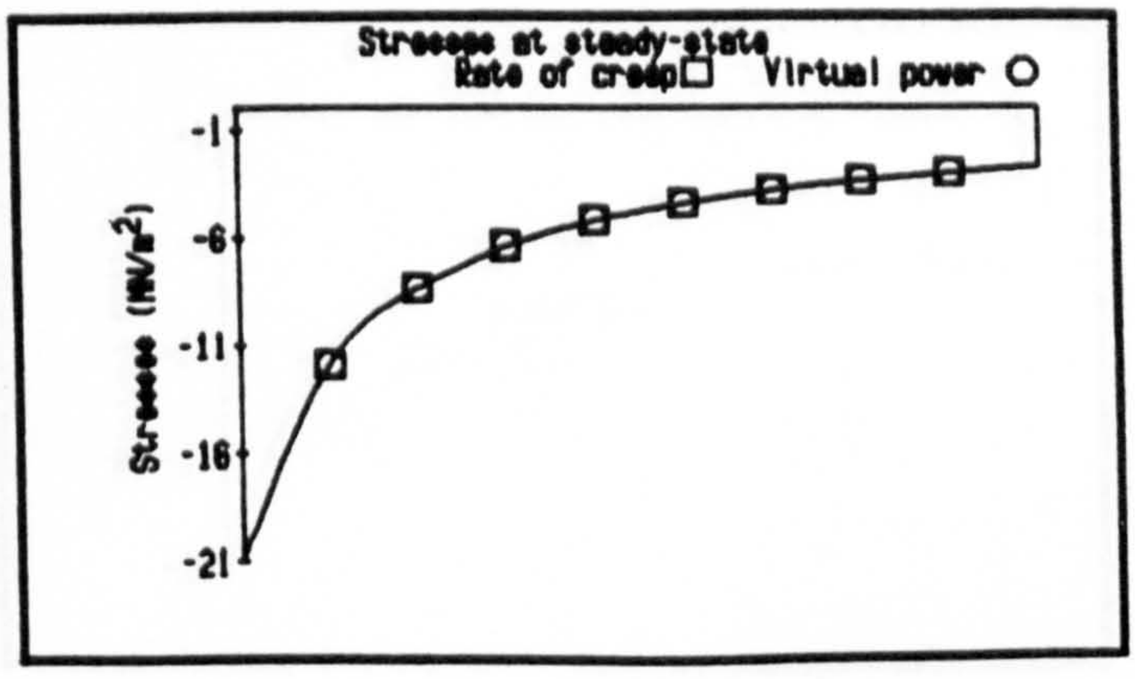

Note: Type (I) & (III) distributions were used

Figure 5.12.5: Comparison between stresses obtained from the rate of creep method and the power method for a sustained temperature cross-fall

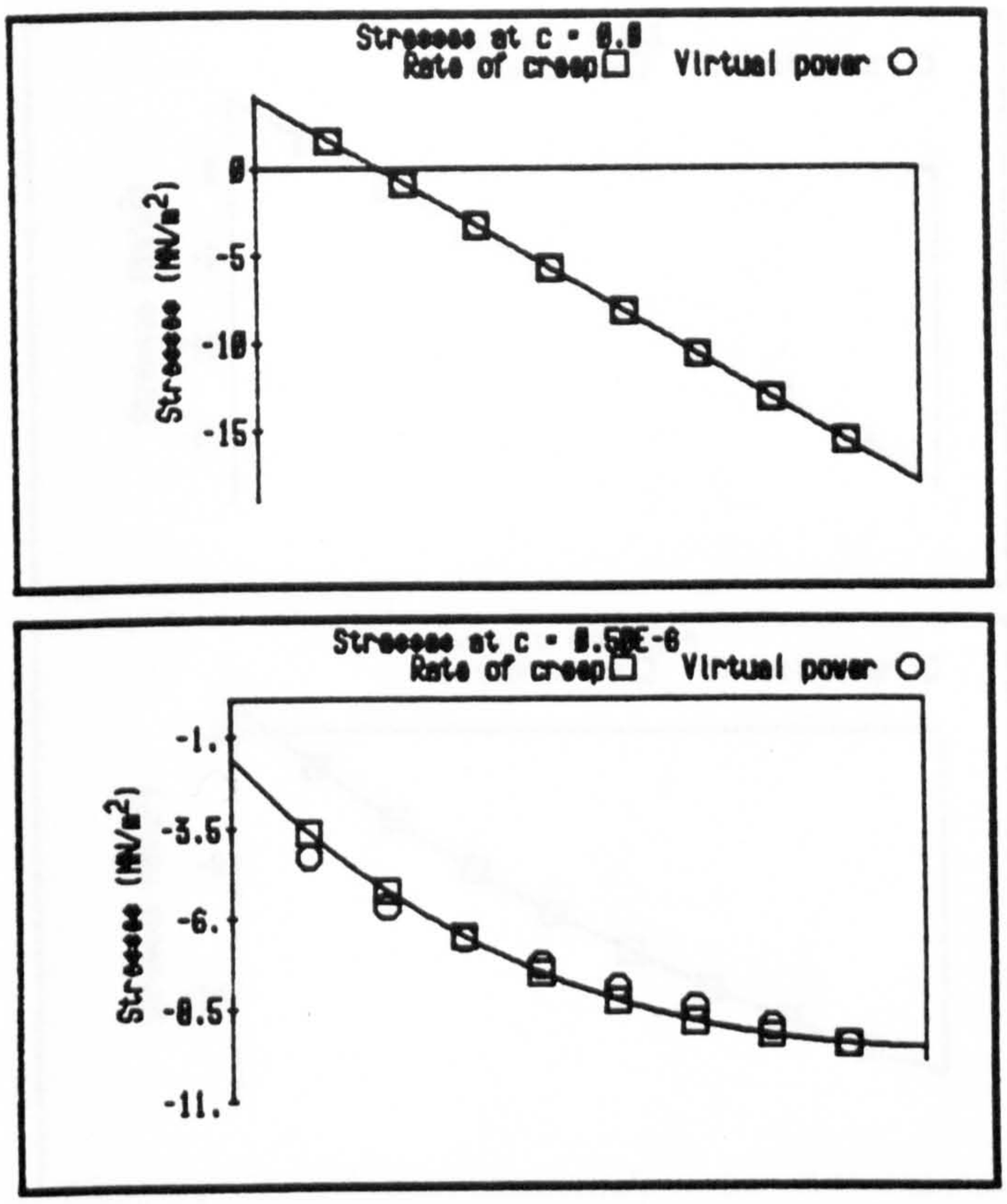

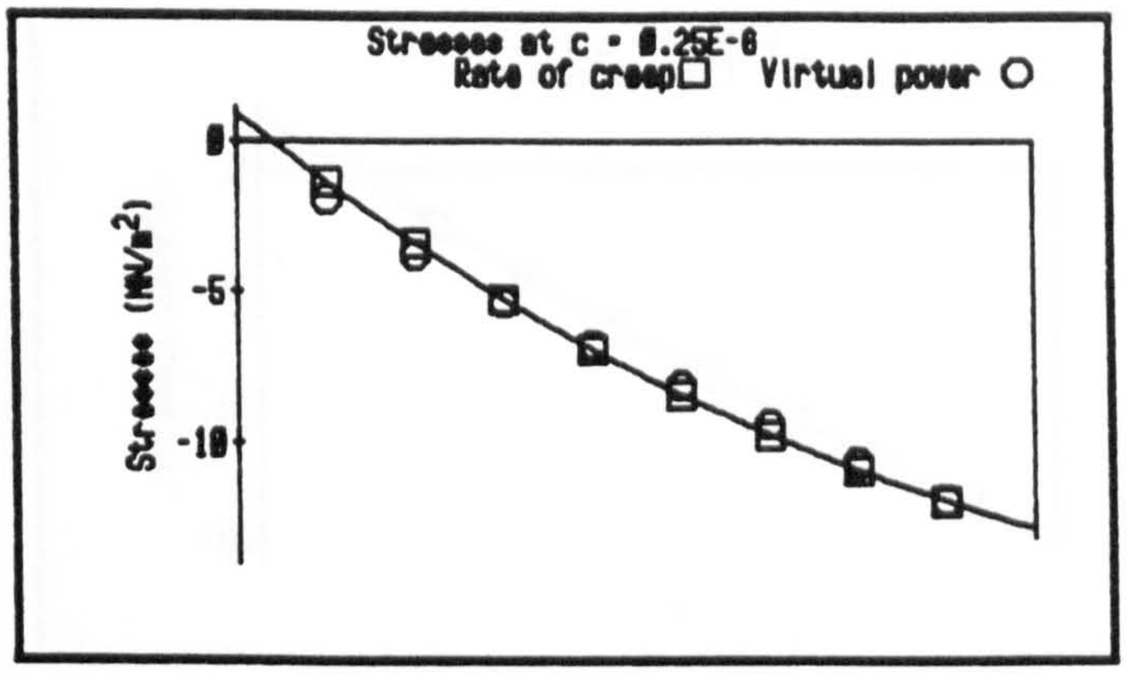

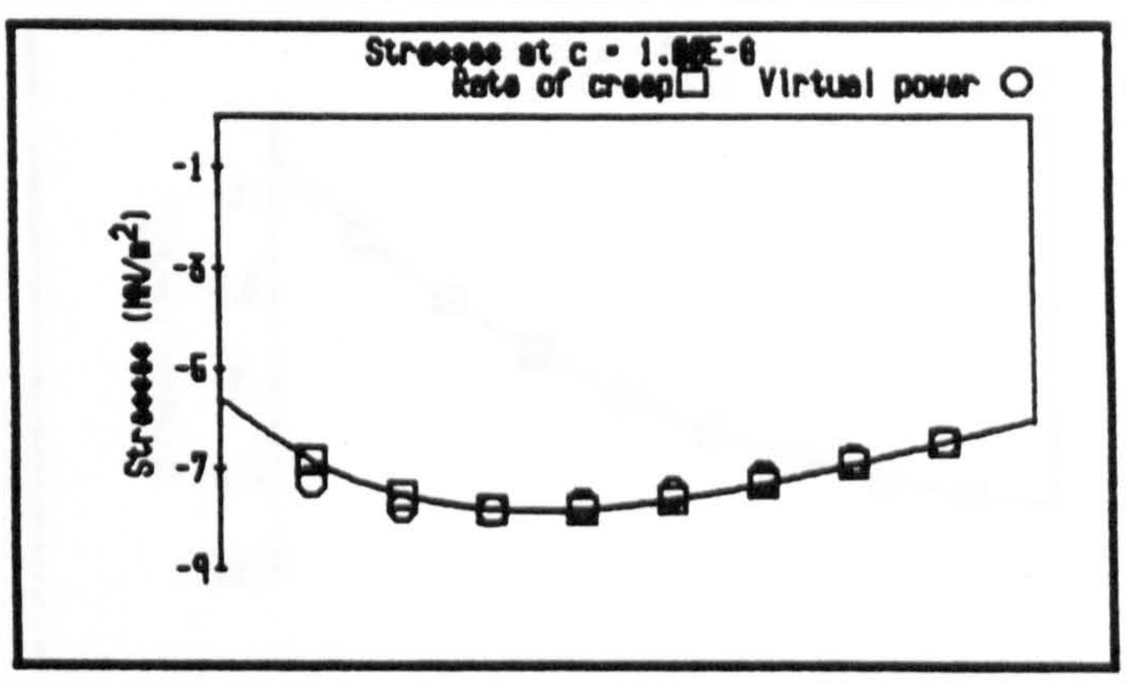

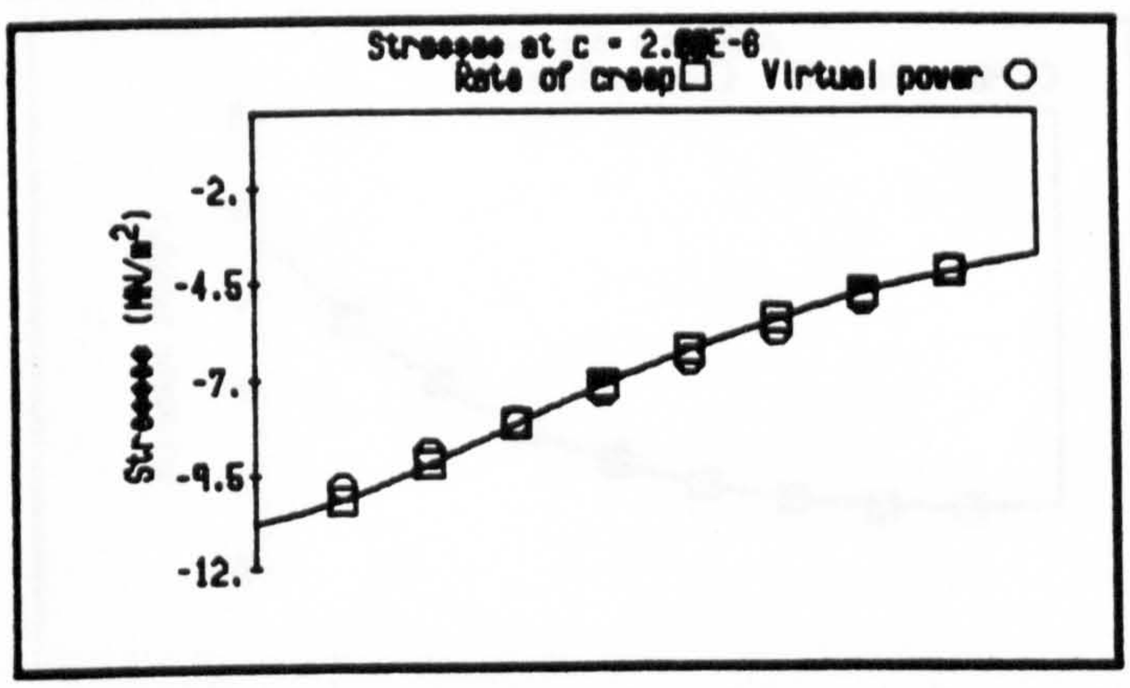

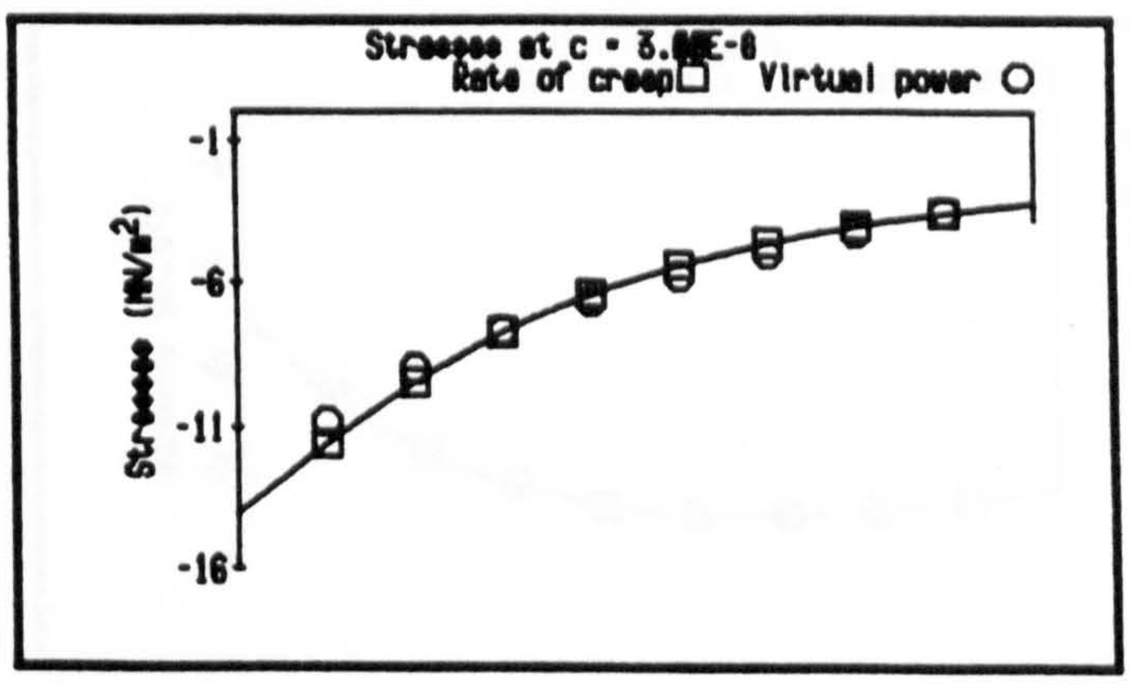

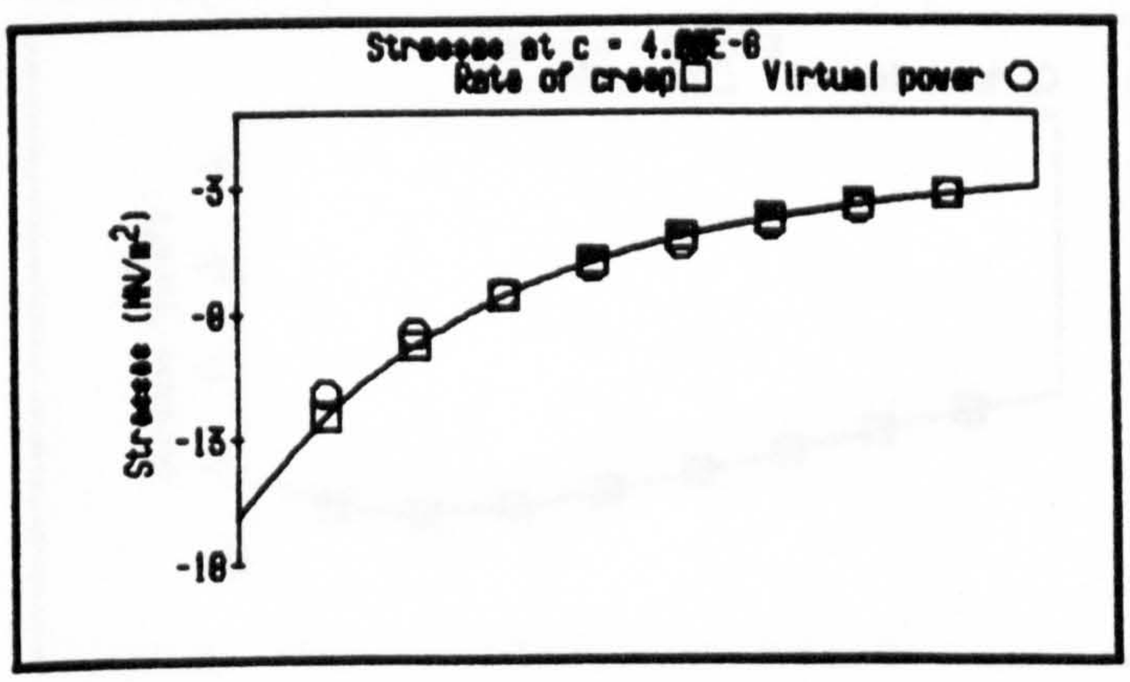

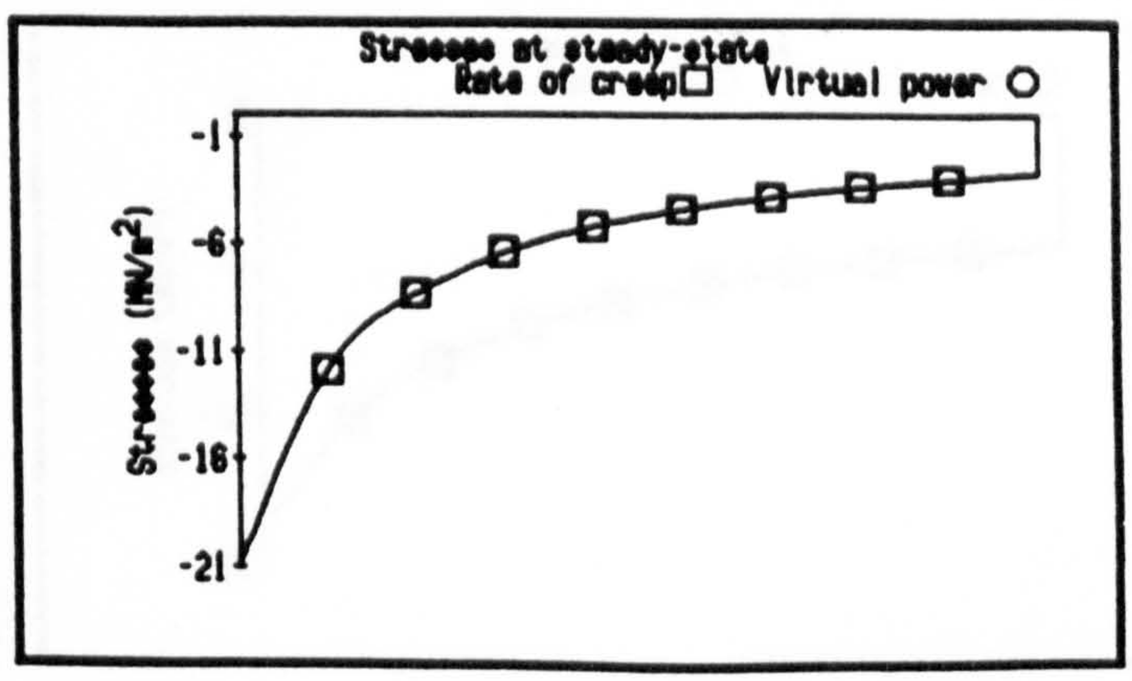

Note: Type (IV) distributions were used

Figure 5.12.6: Comparison between stresses obtained from the rate of creep method and the power method for a sustained temperature cross-fall

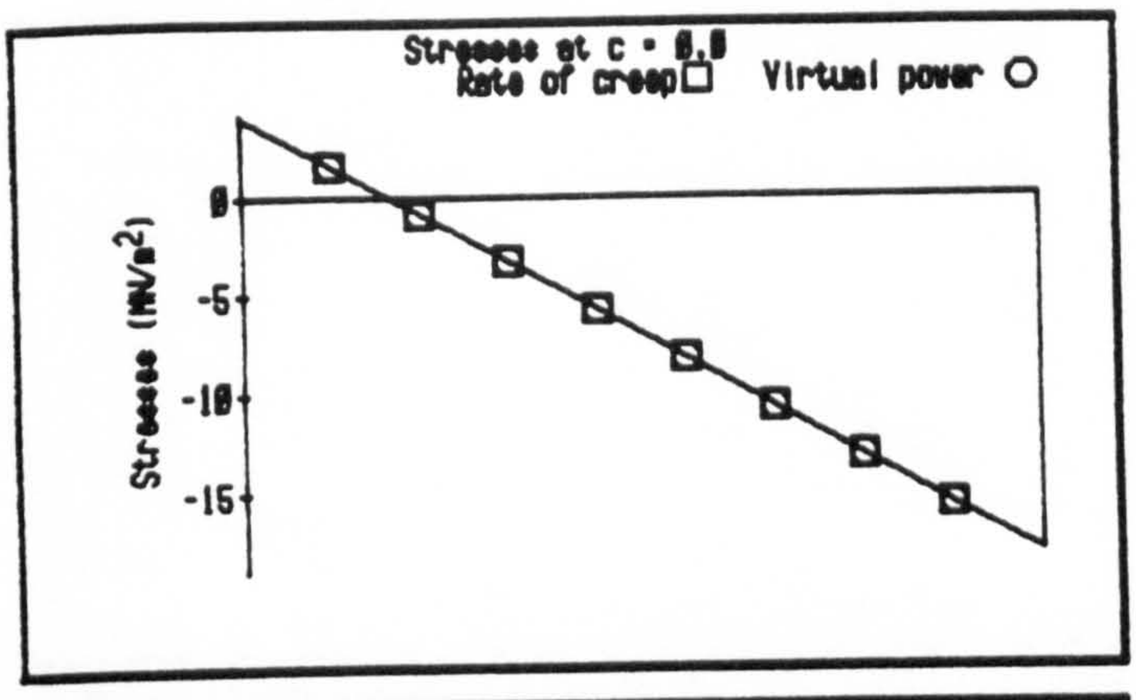

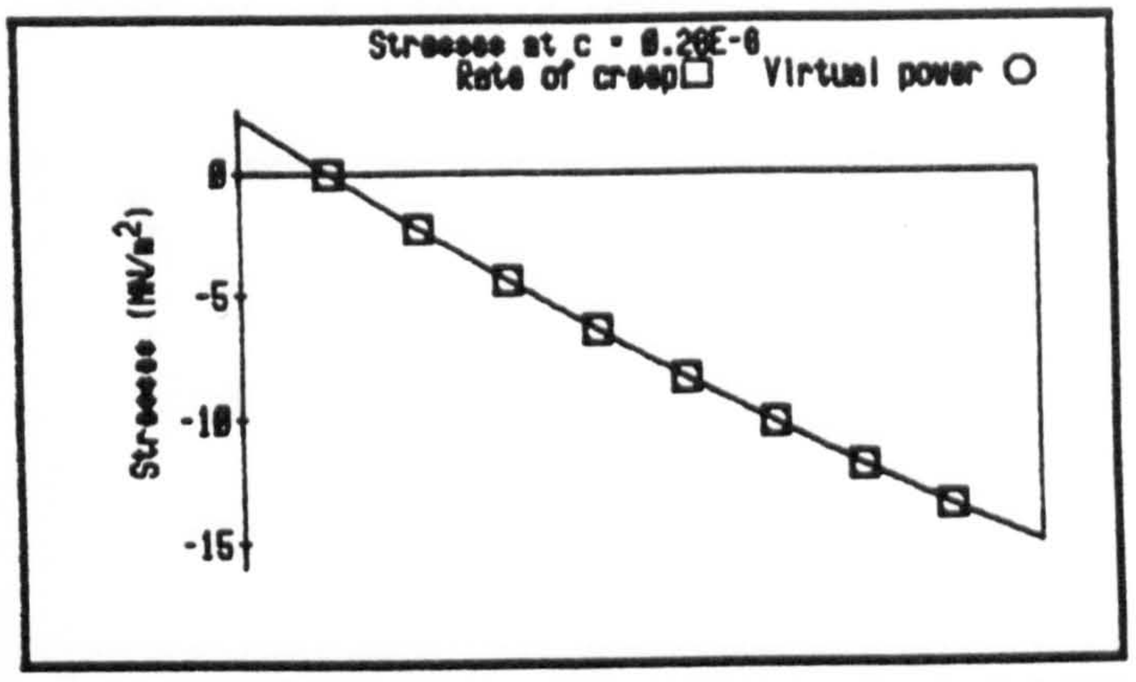

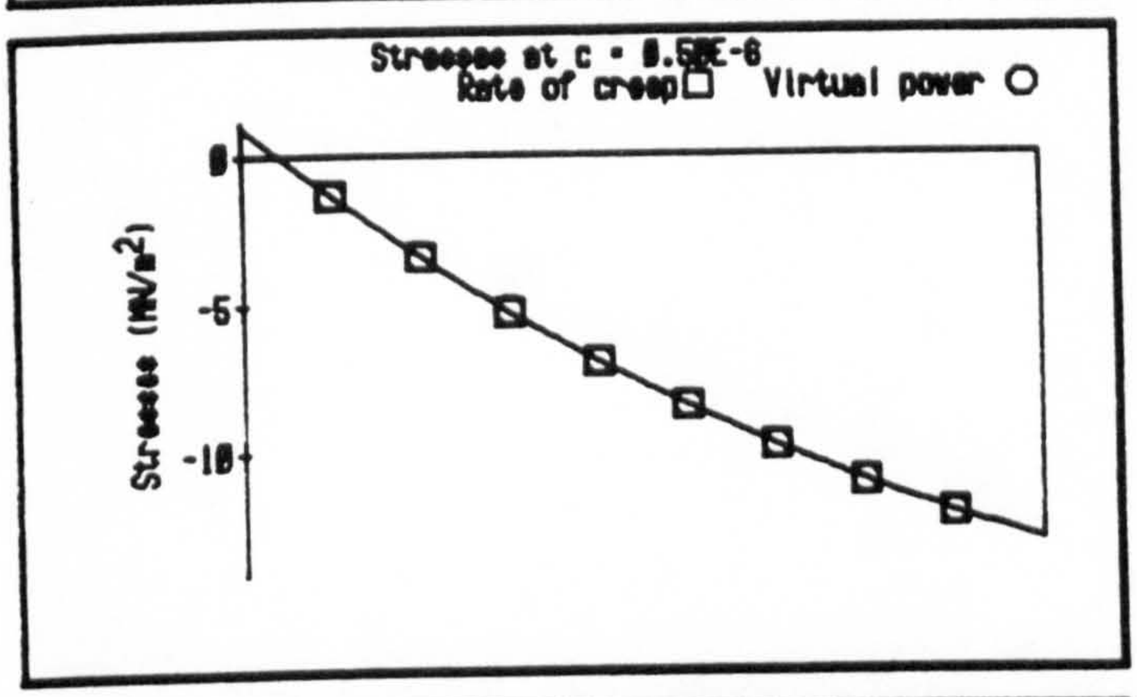

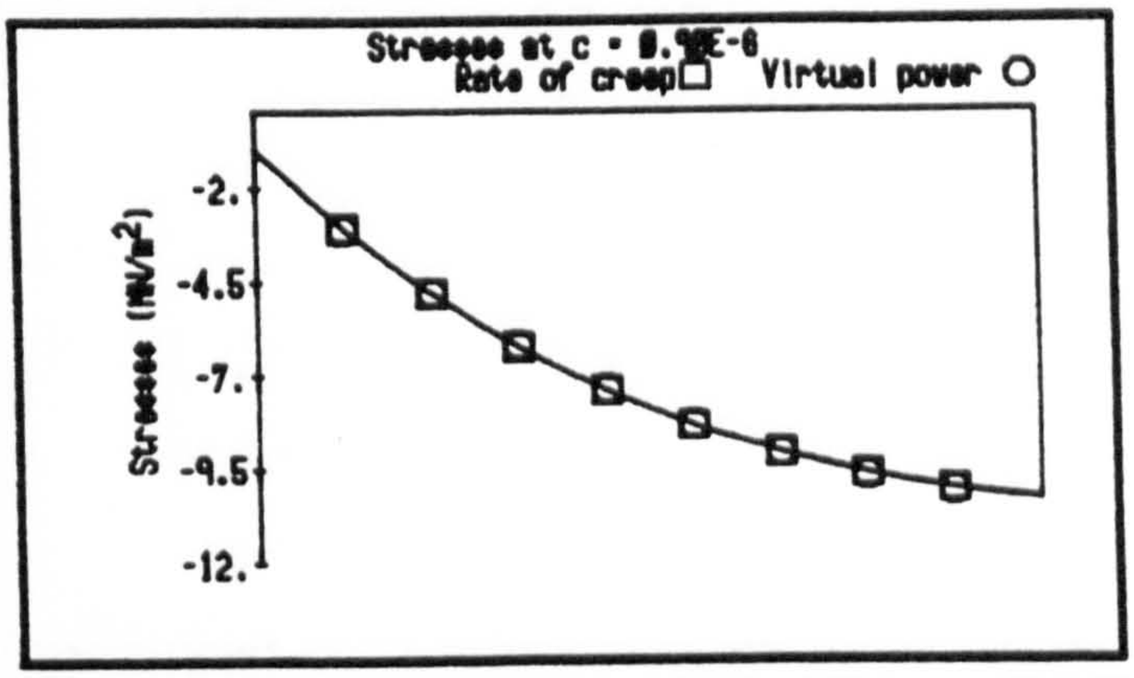

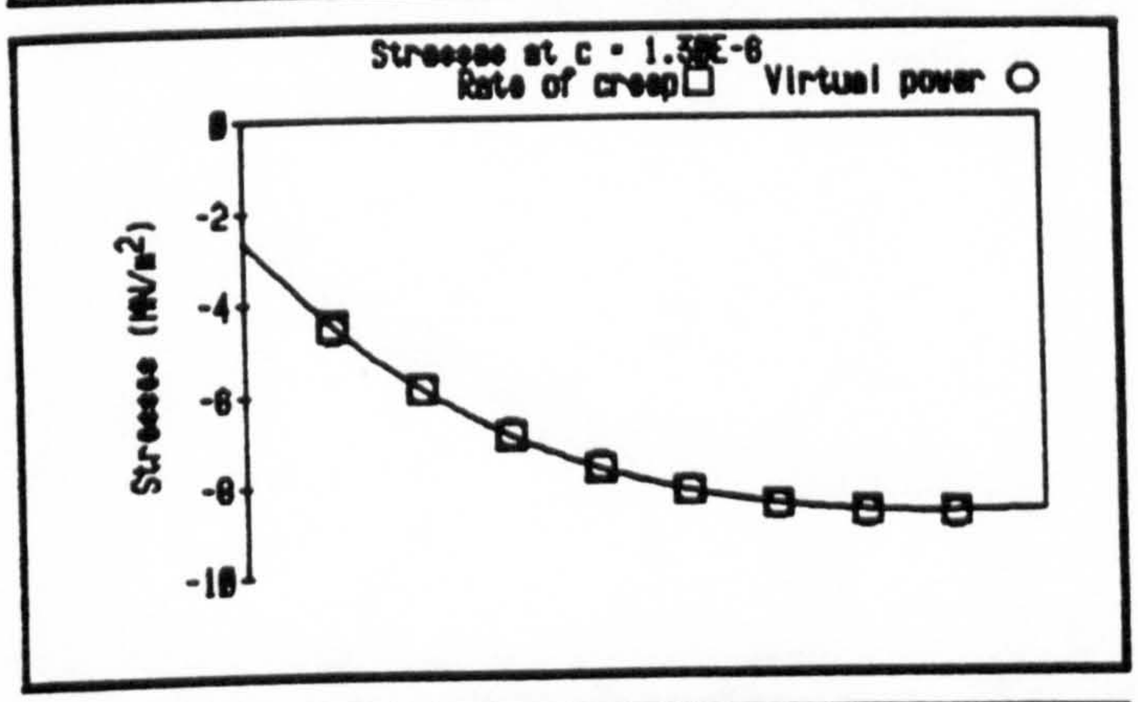

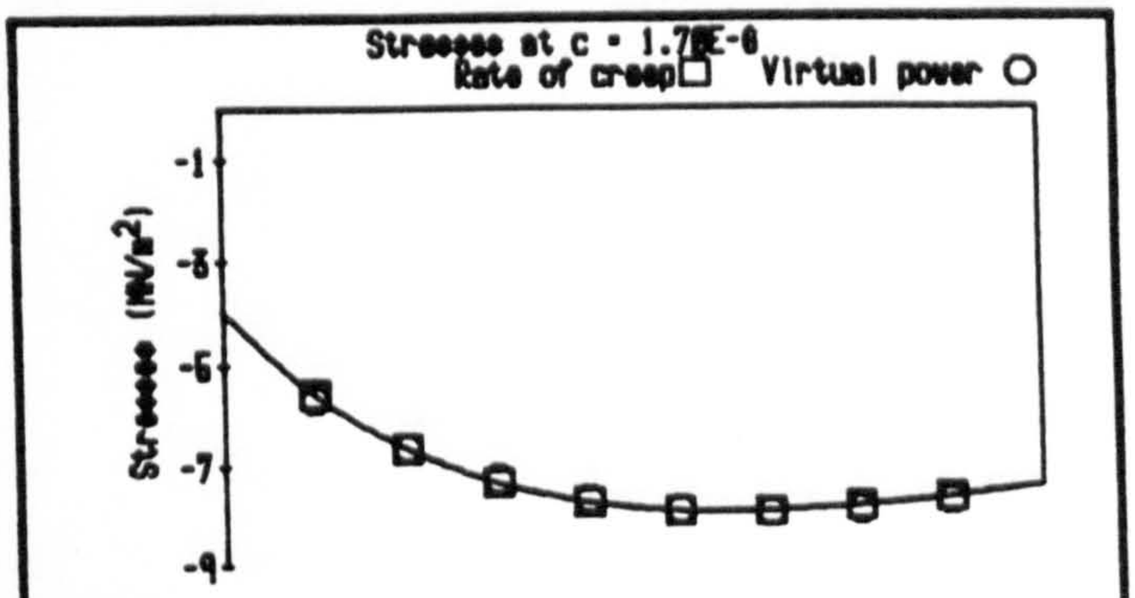

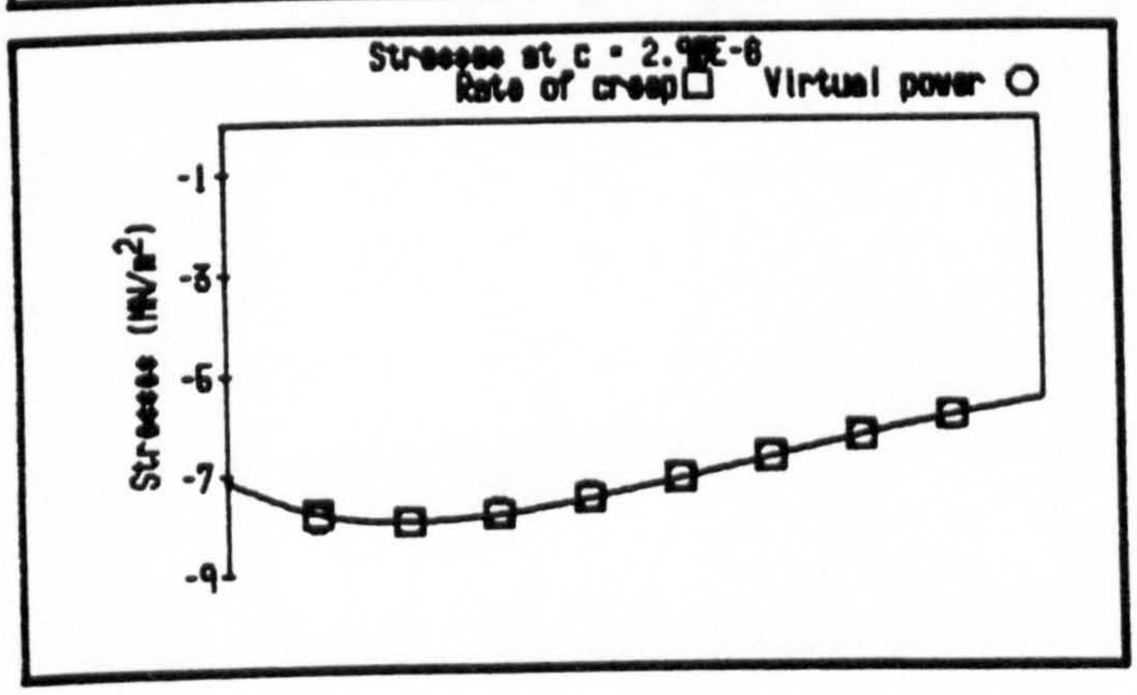

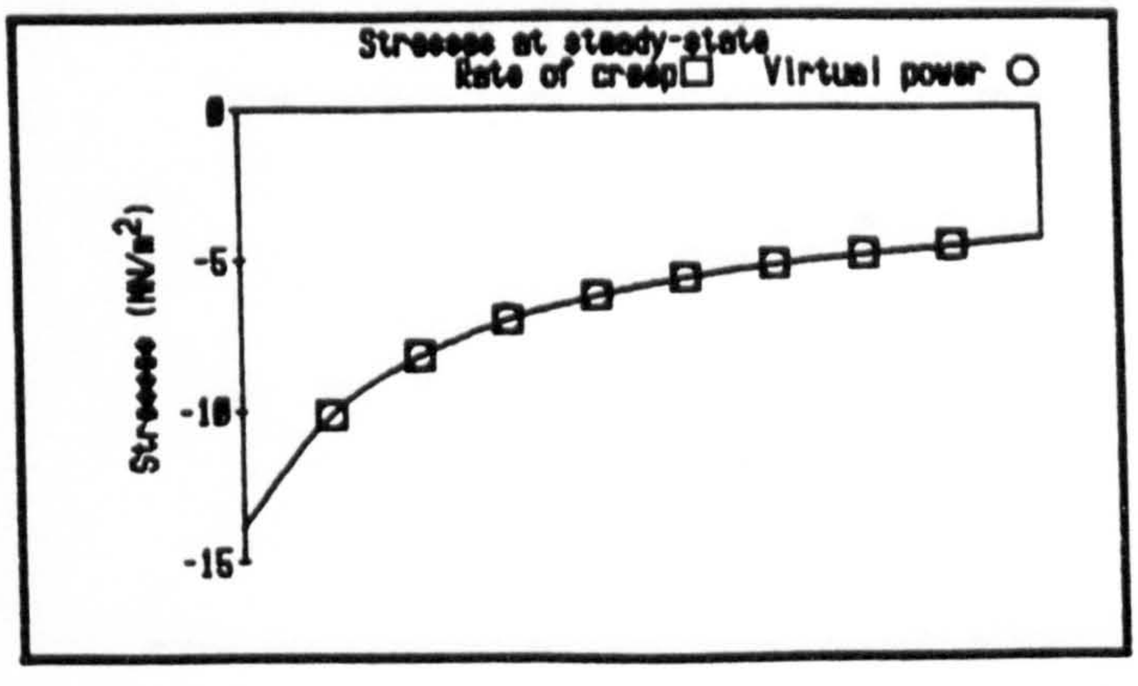

Note: Type (I), (II), & (III) distributions were used

Figure 5.12.7: Comparison between stresses obtained from the rate of creep method and the power method for unidirectional cyclic temperature states

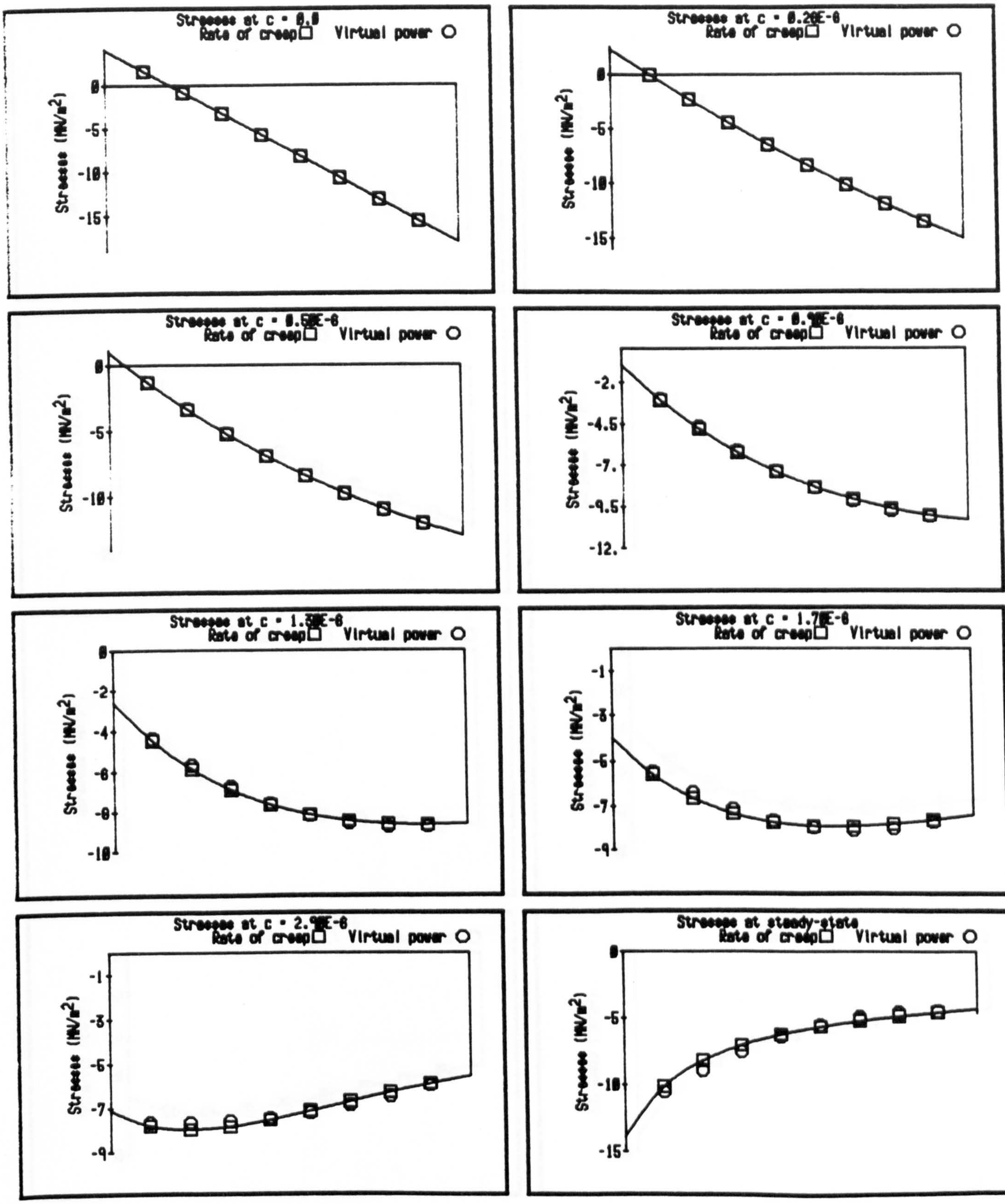

Note: Type (I) & (II) distributions were used

Figure 5.12.8: Comparison between stresses obtained from the rate of creep method and the power method for unidirectional cyclic temperature states

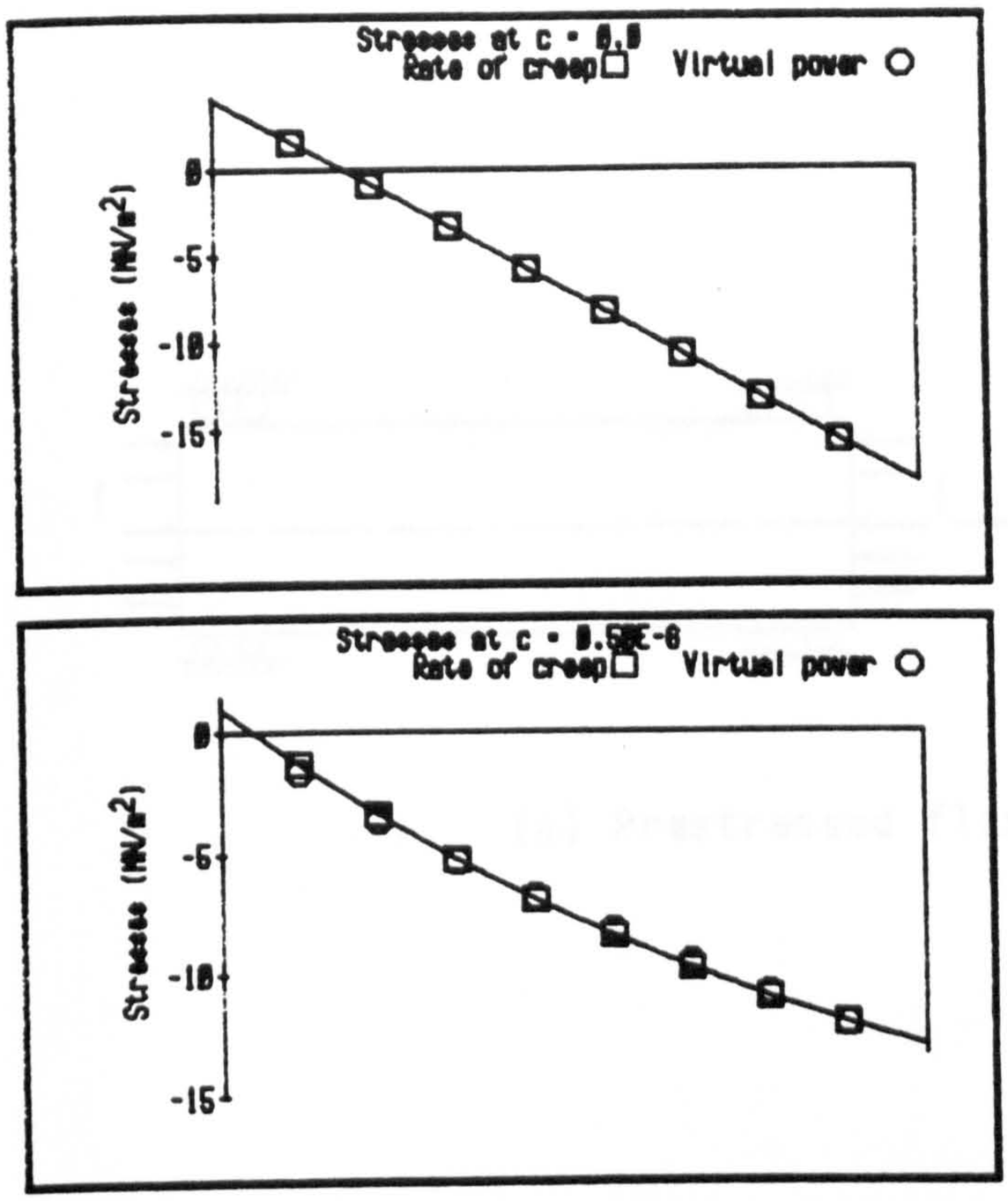

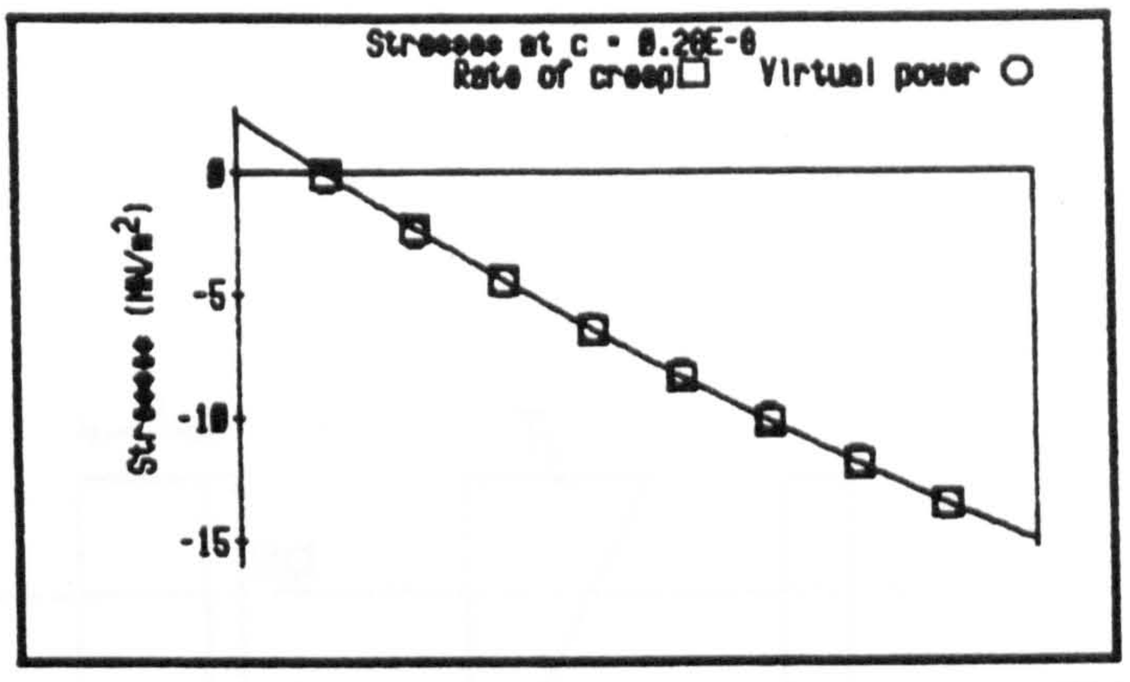

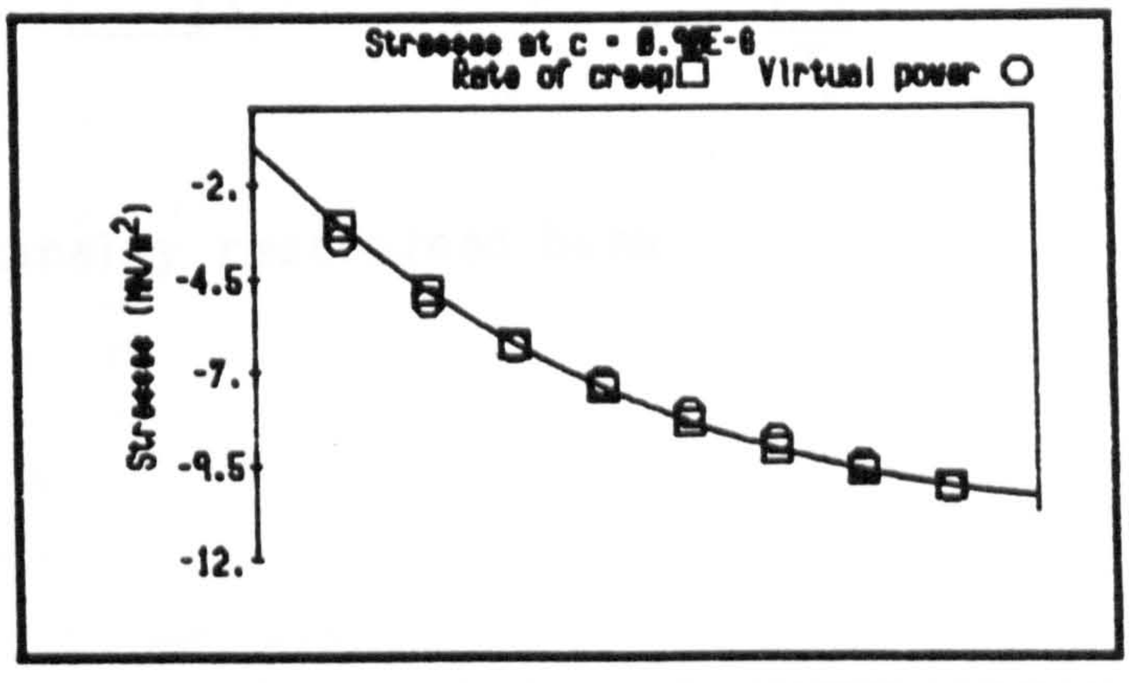

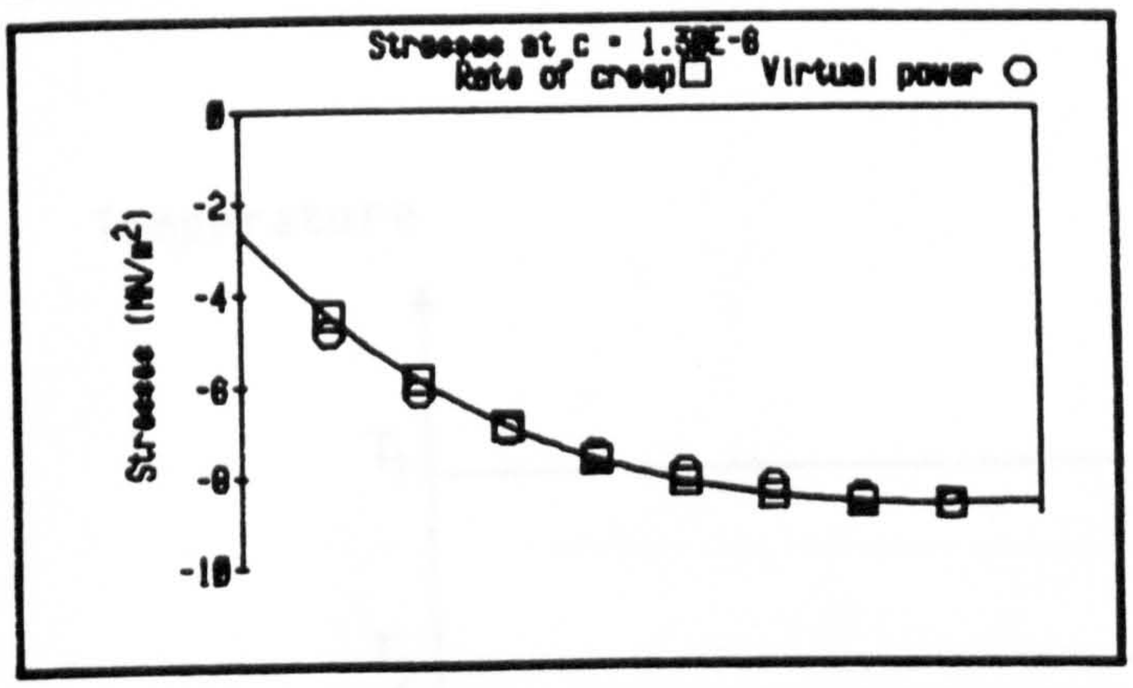

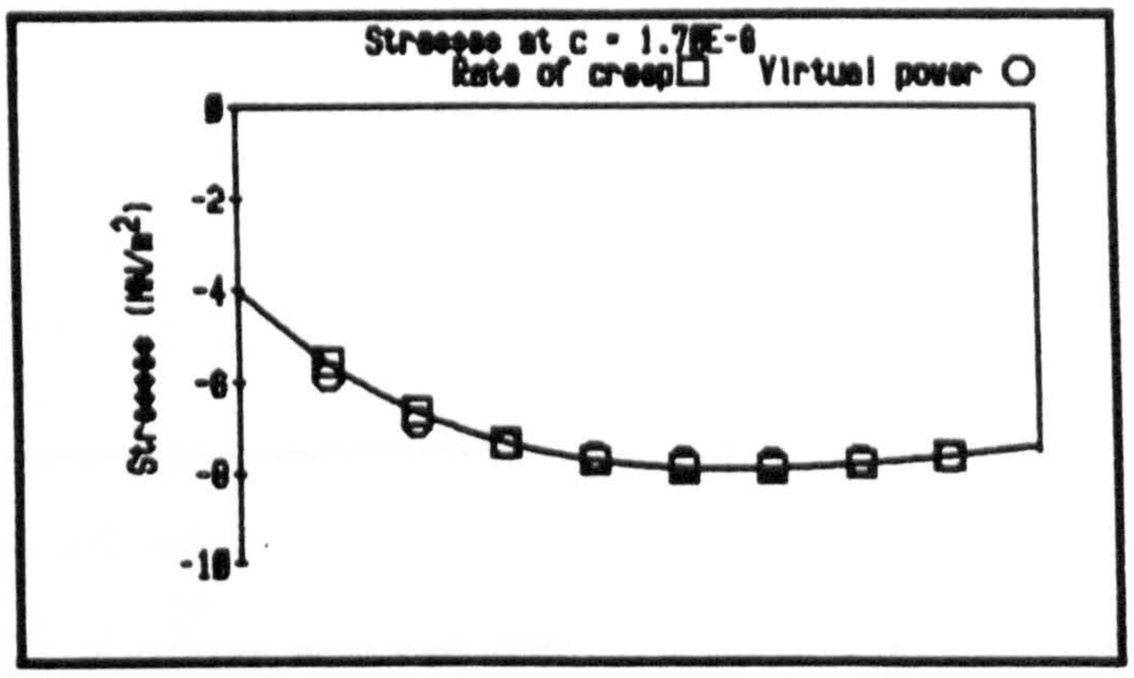

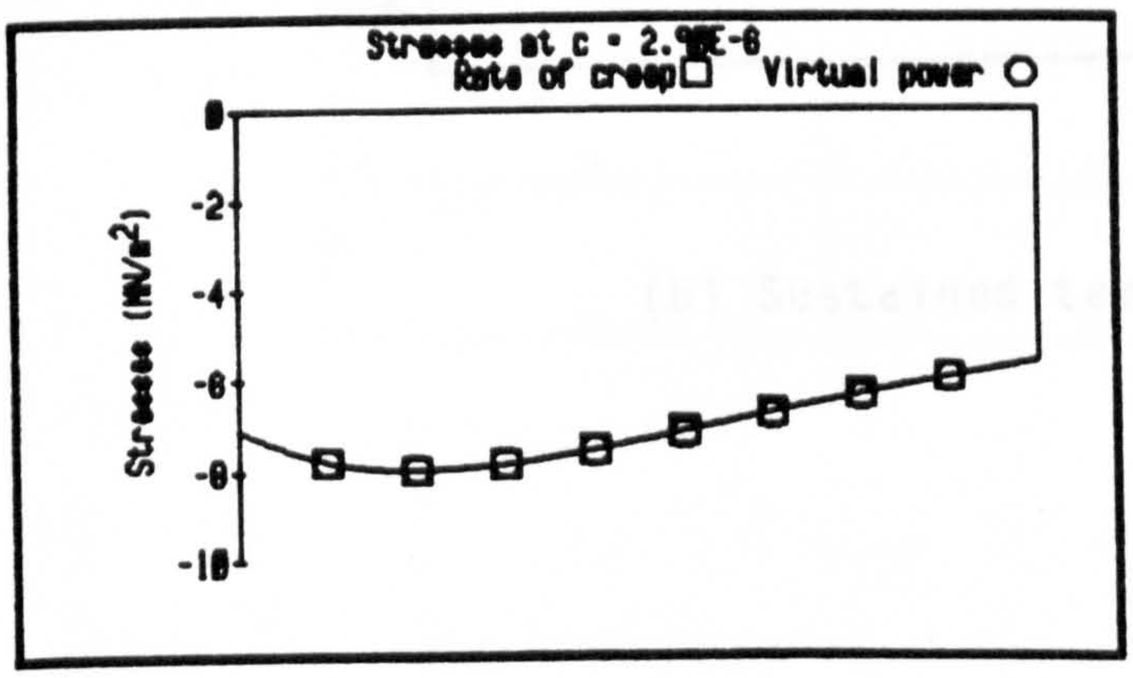

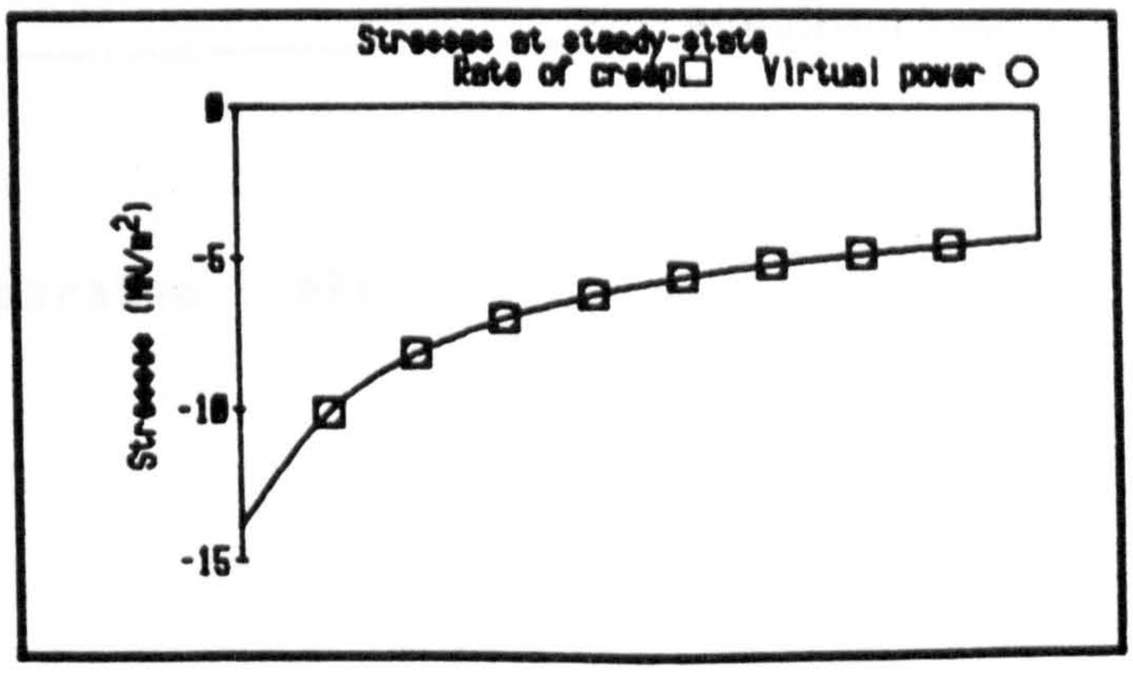

Note: Type (I) & (III) distributions were used

Figure 5.12.9: Comparison between stresses obtained from the rate of creep method and the power method for unidirectional cyclic temperature states

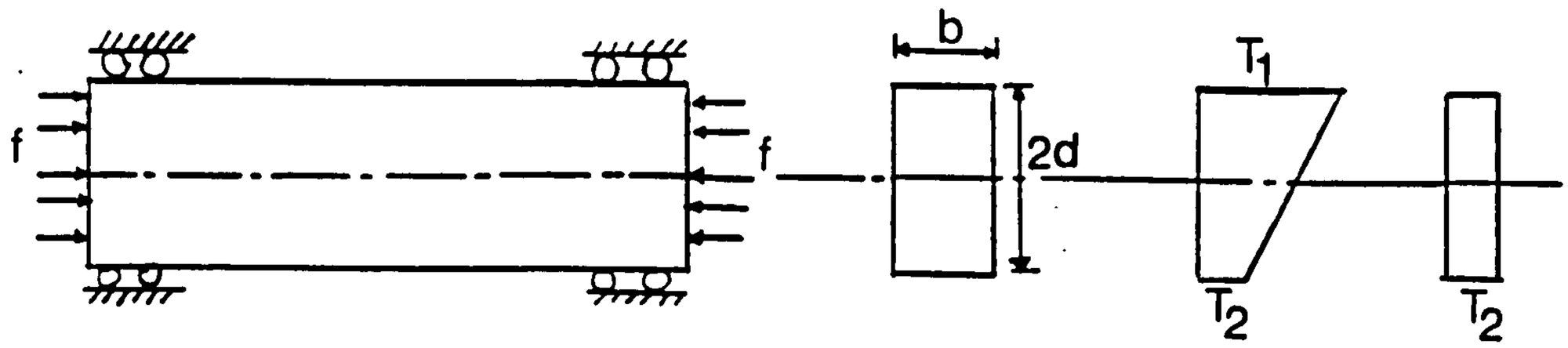

(a) Prestressed flexurally restrained beam

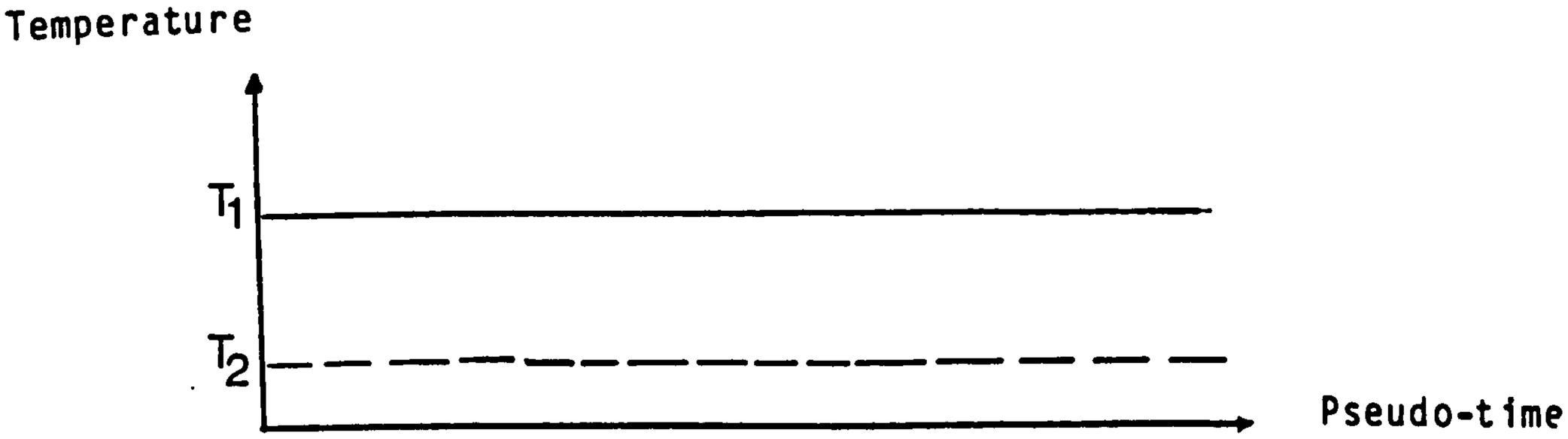

(b) Sustained temperatue field

Figure 5.13.1: The beam and nature of temperature fields

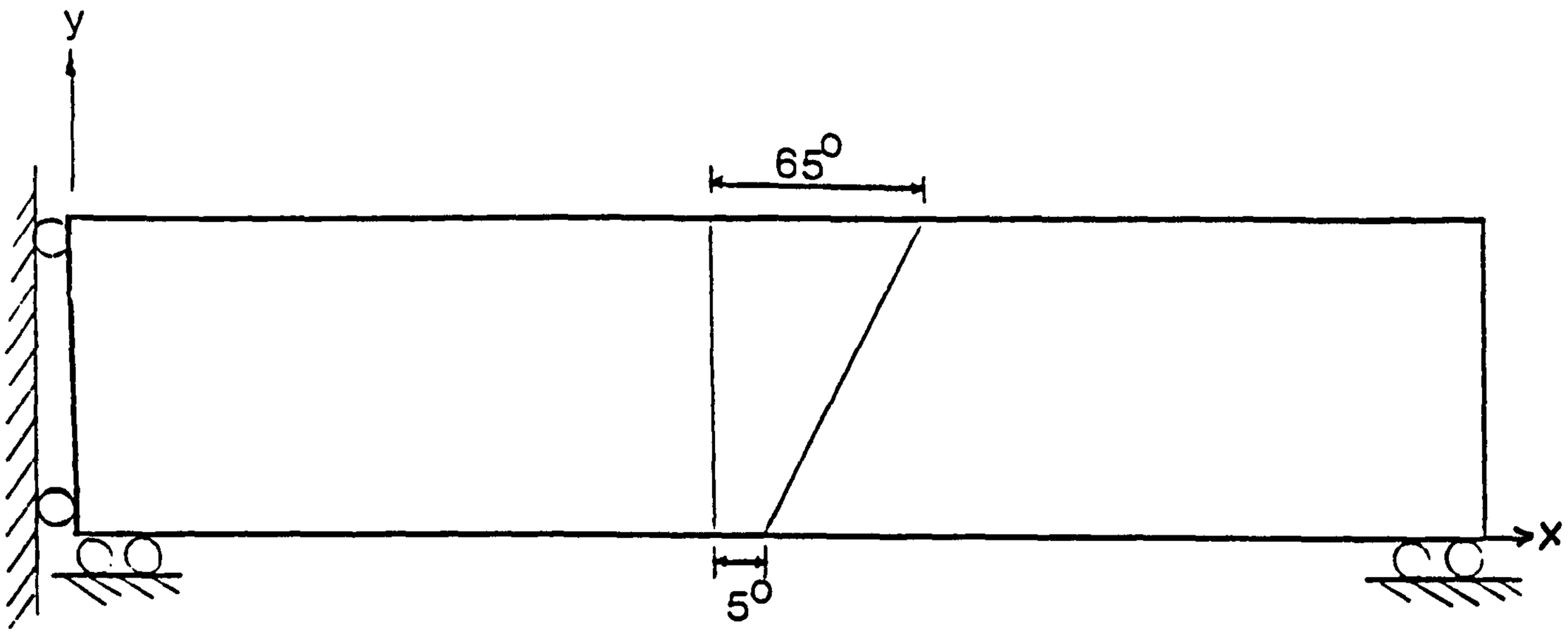

Applied prestress is 7 MN/m^2

(a) The beam model

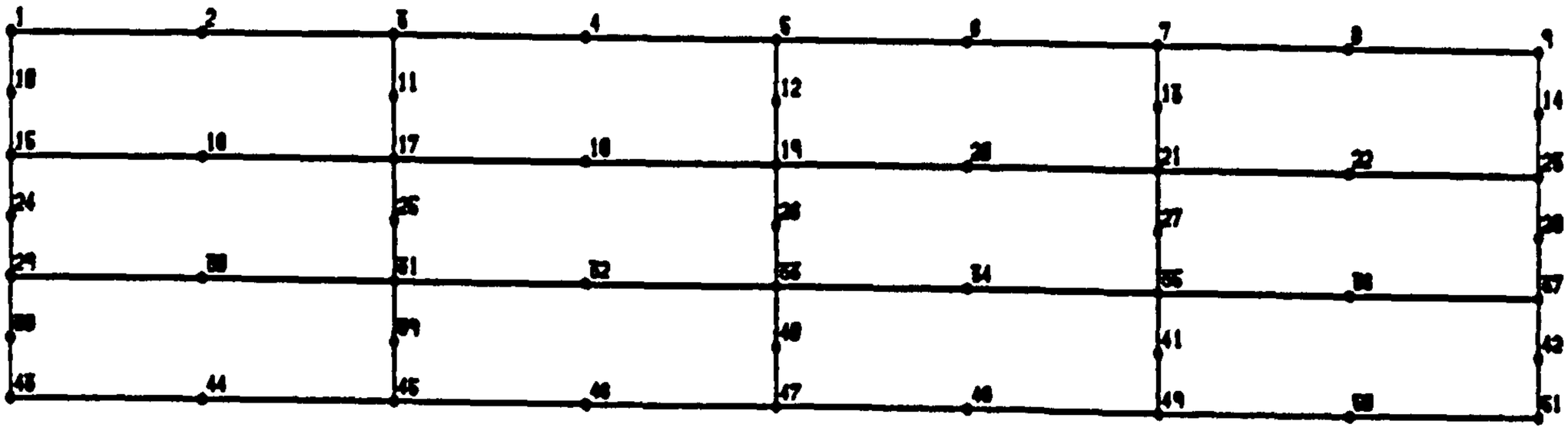

(b) Finite element idealisation

Figure 5.13.2: The two dimensional finite element model for the flexurally restrained beam problem

Gauss Pt.	s=2	s=3	s=4	s=5	Exact
1	3.159	3.017	3.016	3.016	3.016
2	-0.325	-0.081	-0.812	-0.812	-0.812
3	-3.103	-3.107	-3.108	-3.108	-3.108
4	-4.638	-4.660	-4.660	-4.660	-4.660
5	-7.204	-7.358	-7.358	-7.358	-7.358
6	-9.728	-9.913	-9.918	-9.918	-9.918
7	-11.190	-11.340	-11.340	-11.340	-11.340
8	-13.680	-13.680	-13.680	-13.680	-13.680
9	-16.160	-15.890	-15.890	-15.890	-15.890

(a) Stresses at $c = 0.1 \times 10^{-6}$
$x = 0$

Gauss Pt.	s=2	s=3	s=4	s=5	Exact
1	-5.059	-5.354	-5.401	-5.400	-5.401
2	-7.432	-7.100	-7.000	-7.000	-7.000
3	-7.815	-7.634	-7.700	-7.700	-7.700
4	-7.794	-7.735	-7.835	-7.835	-7.835
5	-7.577	-7.690	-7.740	-7.740	-7.740
6	-7.241	-7.425	-7.400	-7.400	-7.400
7	-7.012	-7.188	-7.120	-7.120	-7.120
8	-6.590	-6.647	-6.590	-6.590	-6.590
9	-6.128	-6.052	-6.020	-6.020	-6.020

(b) Stresses at $c = 0.1 \times 10^{-5}$
$x = 0$

Note: s - Number of self-equilibrating stresses used.

Table 5.13.1: Comparison of stresses obtained using different number of self-equilibrating stresses

Gauss Pt.	s=2	s=3	s=4	s=5	Exact
1	-10.990	-10.830	-10.850	-10.900	-10.900
2	-9.673	-10.080	-10.050	-10.050	-10.050
3	-8.578	-8.713	-8.710	-8.710	-8.710
4	-7.970	-7.921	-7.925	-7.940	-7.940
5	-6.940	-6.674	-6.670	-6.670	-6.670
6	-5.920	-6.610	-6.610	-6.600	-6.610
7	-5.330	-5.070	-5.070	-5.070	-5.070
8	-4.324	-4.313	-4.310	-4.310	-4.310
9	-3.320	-3.750	-3.740	-3.740	-3.740

(c) Stresses at $c = 0.2\times10^{-5}$
$x = o$

Gauss Pt.	s=2	s=3	s=4	s=5	Exact
1	-14.880	-14.370	-14.300	-14.300	-14.300
2	-10.350	-11.060	-11.200	-11.200	-11.200
3	-8.353	-8.680	-8.600	-8.600	-8.600
4	-7.499	-7.544	-7.414	-7.410	-7.410
5	-6.266	-5.940	-5.870	-5.860	-5.860
6	-5.190	-4.720	-4.770	-4.770	-4.770
7	-4.596	-4.200	-4.270	-4.270	-4.270
8	-3.630	-3.543	-3.610	-3.620	-3.620
9	-2.702	-3.241	-3.142	-3.132	-3.132

(d) Stresses at $c = 0.3\times10^{-5}$
$x = o$

Note: s - Number of self-equilibrating stresses used.

Table 5.13.2: Comparison of stresses obtained using different number of self-equilibrating stresses

Gauss Pt.	s=2	s=3	s=4	s=5	Exact
1	-17.450	-16.800	-16.680	-16.680	-16.680
2	-10.600	-11.310	-11.500	-11.500	-11.500
3	-8.030	-8.409	-8.270	-8.270	-8.270
4	-7.052	-7.158	-6.964	-6.960	-6.960
5	-5.761	-5.495	-5.390	-5.390	-5.390
6	-4.730	-4.312	-4.360	-4.360	-4.360
7	-4.196	-3.811	-3.920	-3.920	-3.920
8	-3.357	-3.250	-3.350	-3.350	-3.350
9	-2.584	-3.030	-2.910	-2.920	-2.920

(e) Stresses at $c = 0.4 \times 10^{-5}$
$x = o$

Gauss Pt.	s=2	s=3	s=4	s=5	Exact
1	-19.170	-18.480	-18.330	-18.300	-18.300
2	-10.730	-11.310	-11.610	-11.610	-11.610
3	-7.774	-8.123	-7.950	-7.950	-7.950
4	-6.720	-6.850	-6.652	-6.650	-6.650
5	-5.410	-5.230	-5.110	-5.110	-5.110
6	-4.433	-4.115	-4.200	-4.200	-4.200
7	-3.950	-3.650	-3.800	-3.800	-3.800
8	-3.220	-3.130	-3.200	-3.200	-3.200
9	-2.574	-2.920	-2.800	-2.820	-2.820

(f) Stresses at $c = 0.5 \times 10^{-5}$
$x = o$

Note: s - Number of self-equilibrating stresses used.

Table 5.13.3: Comparison of stresses obtained using different number of self-equilibrating stresses

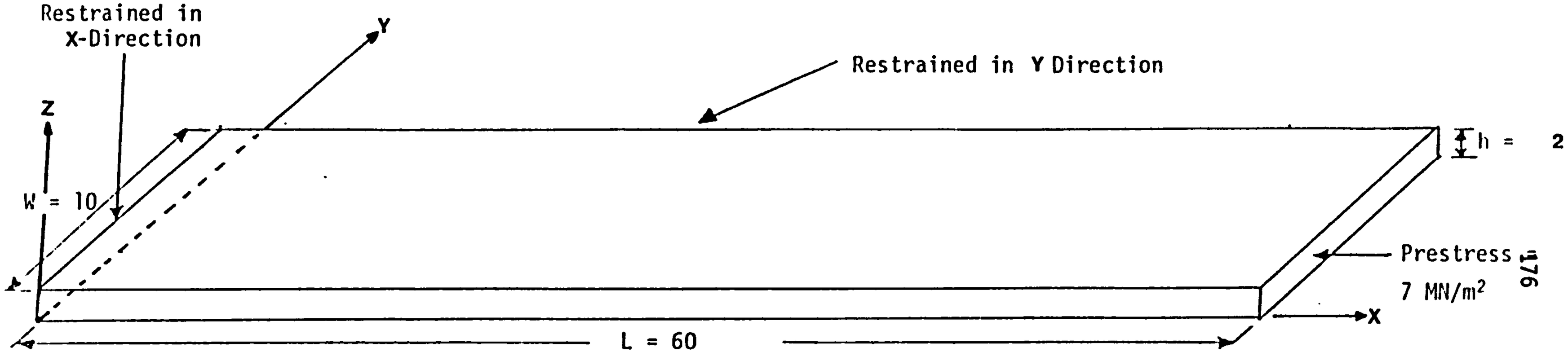

Datum Temperature = $5^{o}C$

Raised Sustained Temperature, $T = (5 + 6Y)^{o}C$

Figure 5.13.3: The three dimensional finite element model for the flexurally restrained beam problem

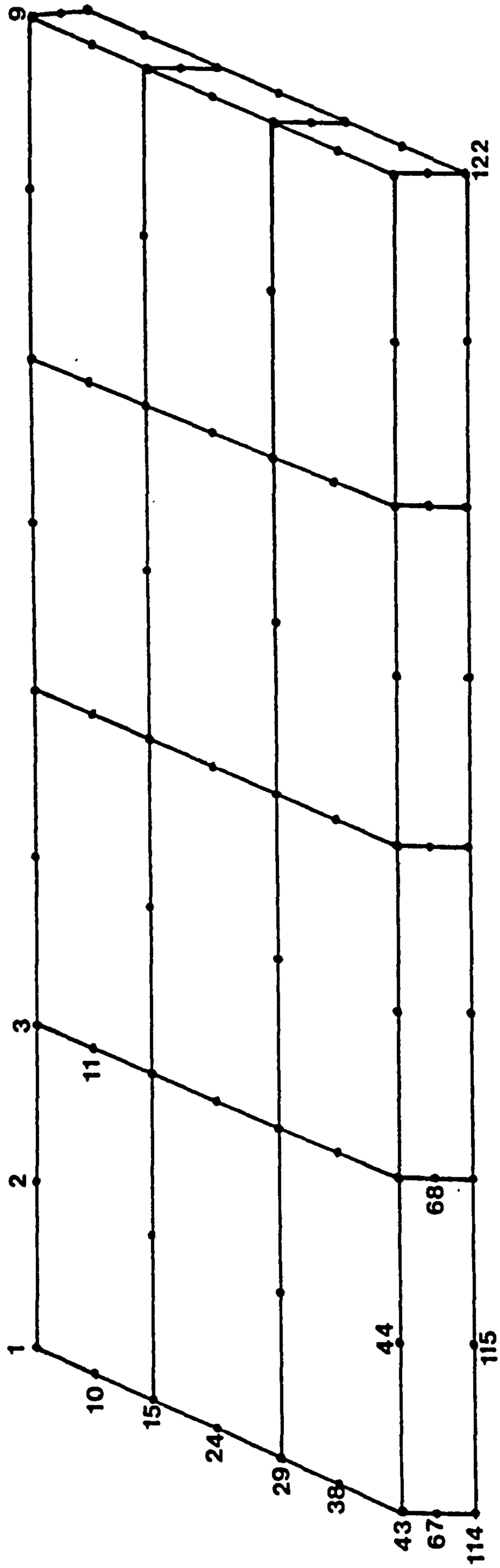

Figure 5.13.4: The three dimensional finite element mesh for the flexurally restrained beam problem

Gauss Point	c = 0.1×10^{-6}	c = 0.1×10^{-5}	c = 0.2×10^{-5}
1	3.017	-6.016	-12.250
2	-0.078	-6.299	-8.700
3	-3.017	-7.183	-7.862
4	-4.658	-7.586	-7.571
5	-7.359	-7.959	-7.044
6	-9.916	-7.885	-6.326
7	-11.340	-7.629	-5.789
8	-13.680	-6.825	-4.639
9	-15.890	-5.567	-3.191

Note:

(a) 3D stresses are extracted at z=0.01 and x=1.691.
(b) Three self-equilibrating stresses are used.

Table 5.13.4: Three dimensional results

Gauss Point	c = 0.3×10^{-5}	c = 0.4×10^{-5}	steady-state
1	-16.120	-18.540	-20.070
2	-9.699	-10.200	-10.490
3	-7.767	-7.596	-7.463
4	-7.108	-6.728	-6.471
5	-6.213	-5.652	-5.294
6	-5.371	-4.789	-4.432
7	-4.851	-4.317	-3.997
8	-3.866	-3.504	-3.302
9	-2.740	-2.650	-2.628

Note:

(a) 3D stresses are extracted at z=0.01 and x=1.691.
(b) Three self-equilibrating stresses are used.

Table 5.13.5: Three dimensional results

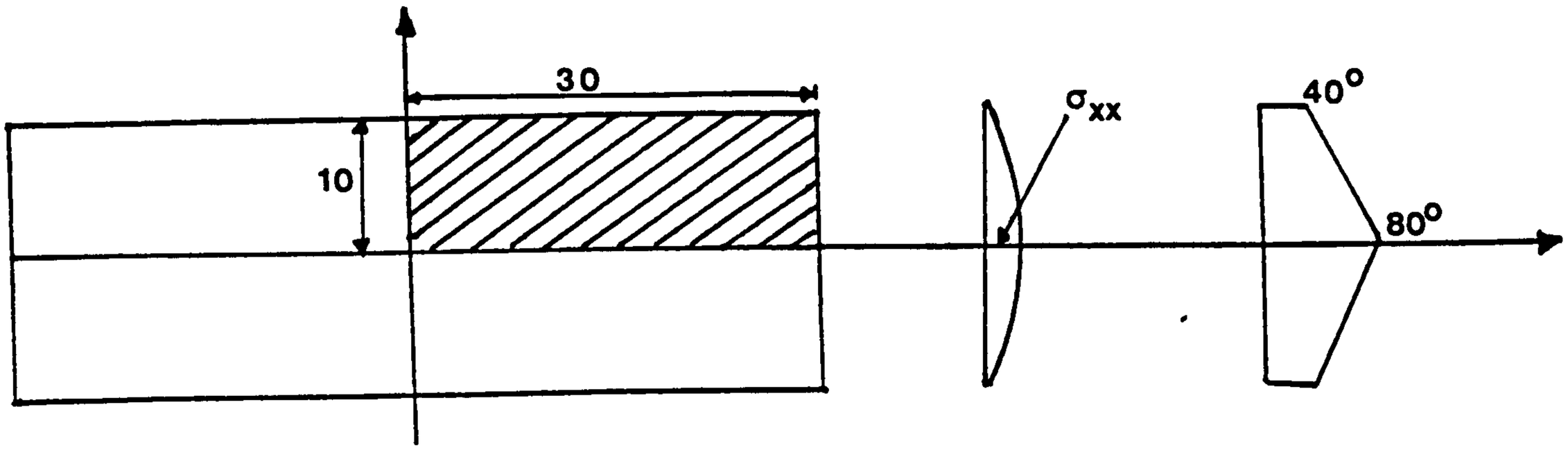

Aspect ratio = 3

Compressive edge pressure
$\sigma_{xx}=13.79(1-y^2)$

Temperature
T=T(y)

(a) Allen's plate subjected to parabolic edge loading

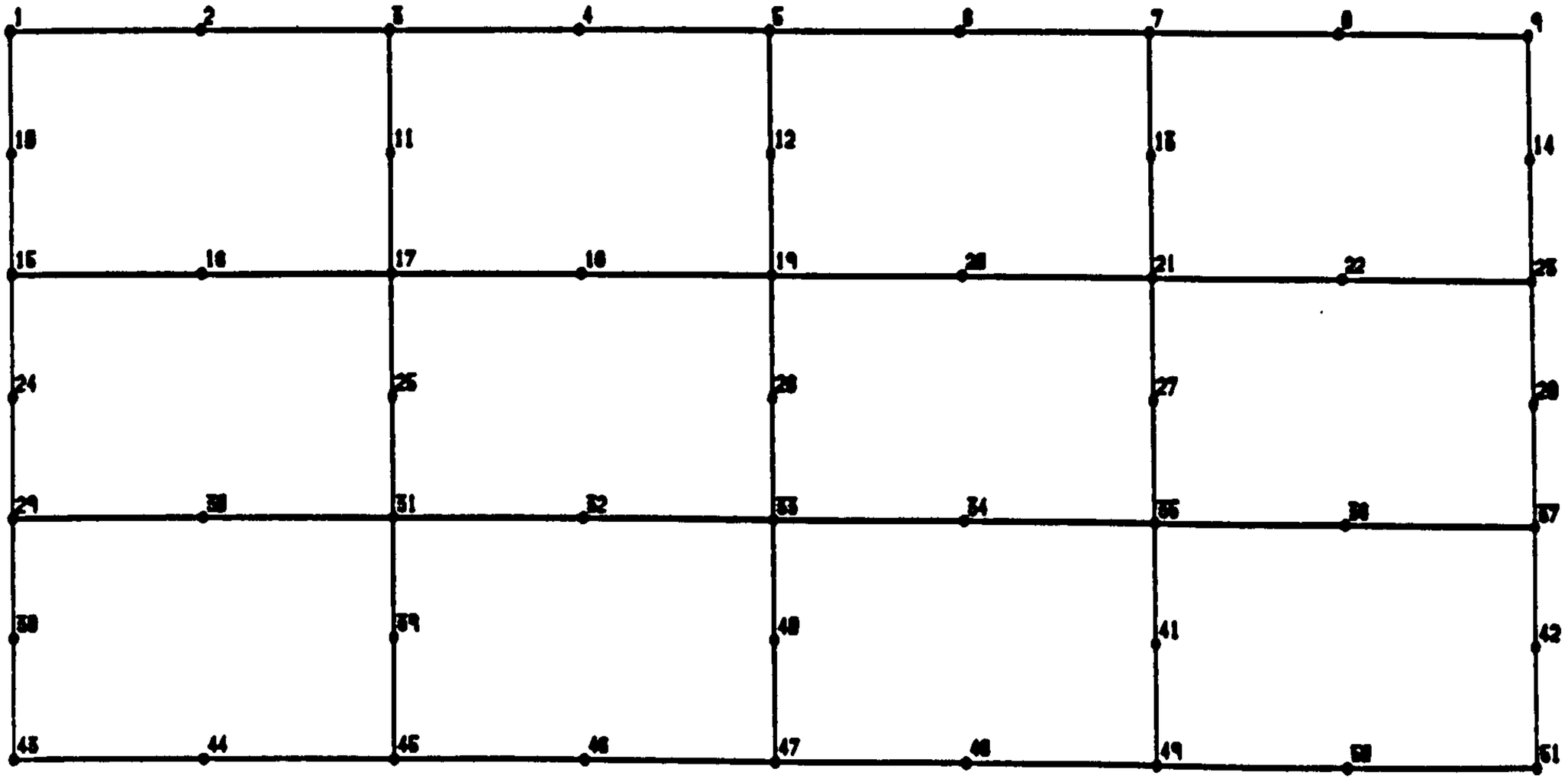

(b) Finite element mesh

Figure 5.13.5: The Allen's plate analysed as a plane stress problem

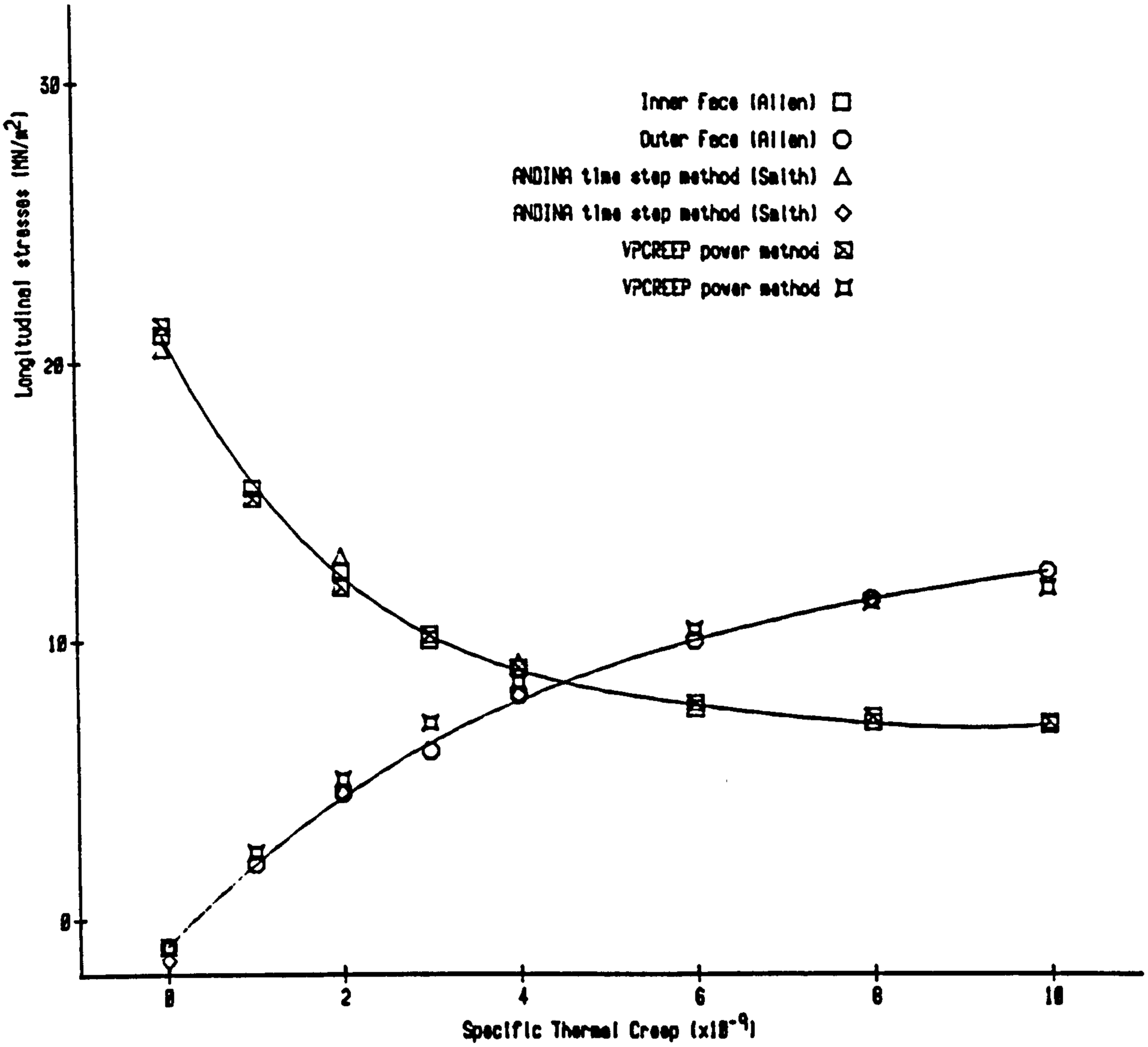

Note:

(a) Units for specific thermal creep is microstrain per lb/in^2 per ^oC.

(b) Allen's results were obtained using an analytical approach.

(c) Smith's results were obtained using a general purpose finite element program called ADINA.

Figure 5.13.6: Stress comparisons for Allen's plate problem

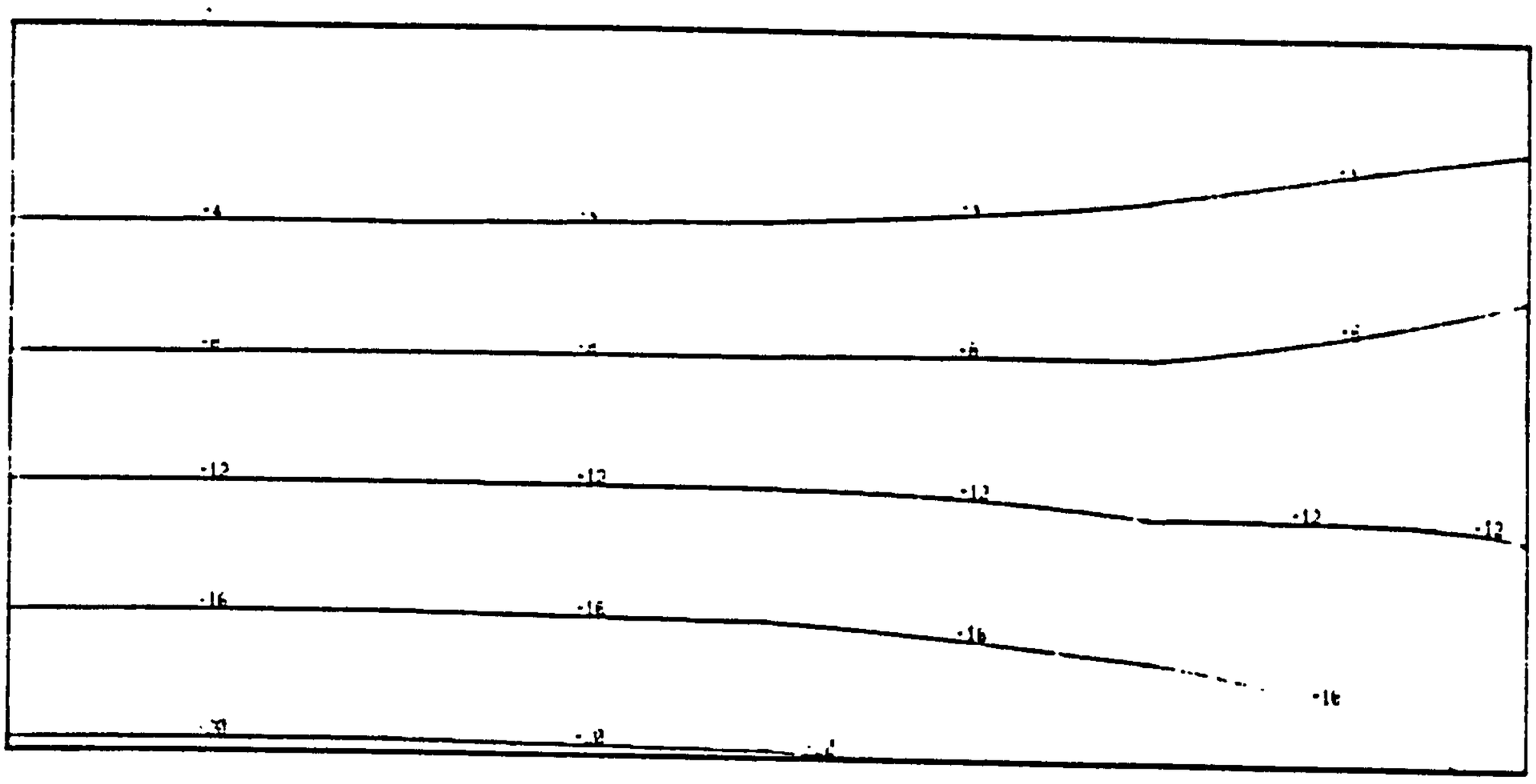

(a) σ_{xx} (x10) at c = 0.0

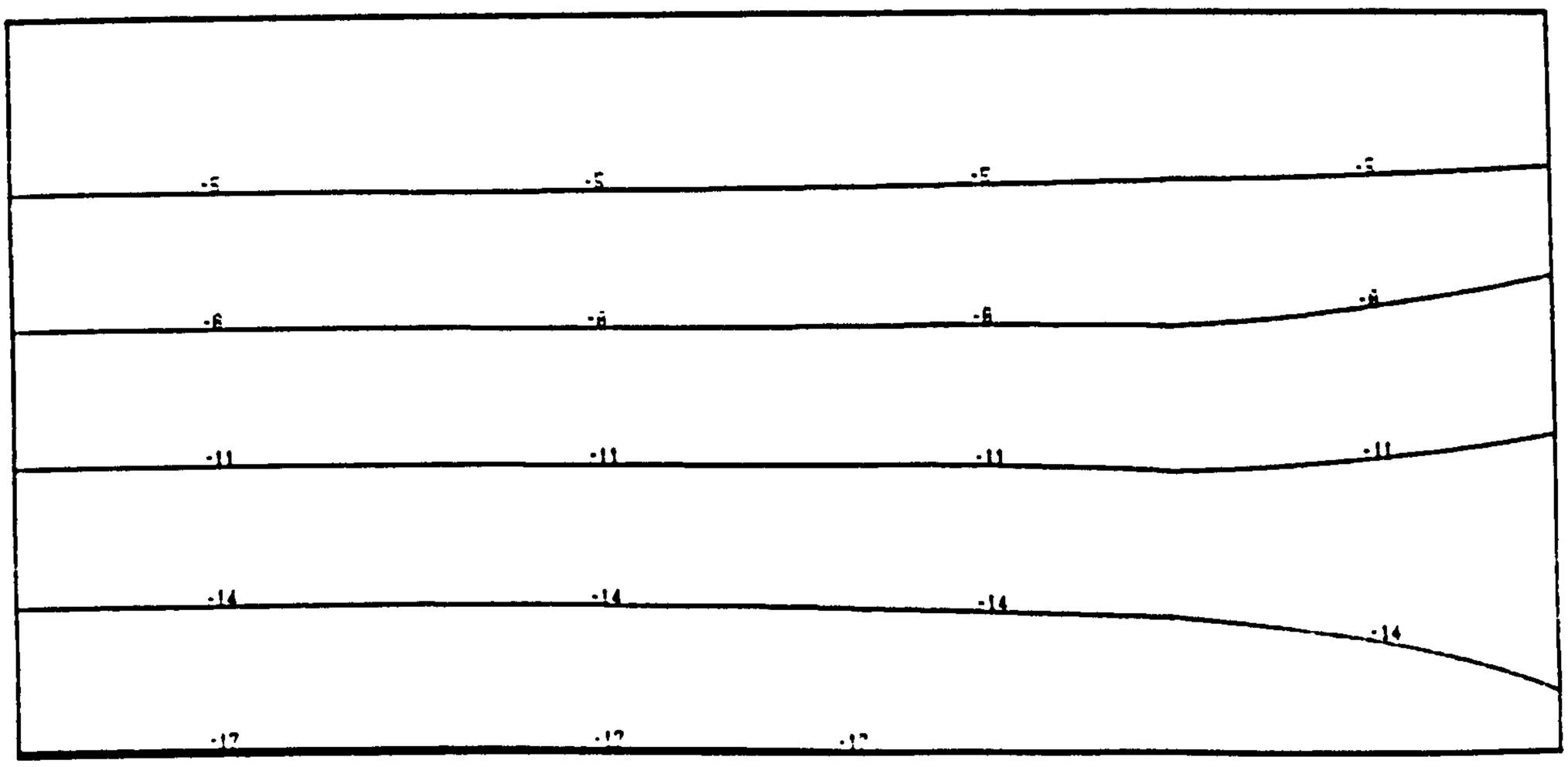

(b) σ_{xx} (x10) at c = 0.9E-07

Figure 5.13.7: Stress contour for Allen's plate problem

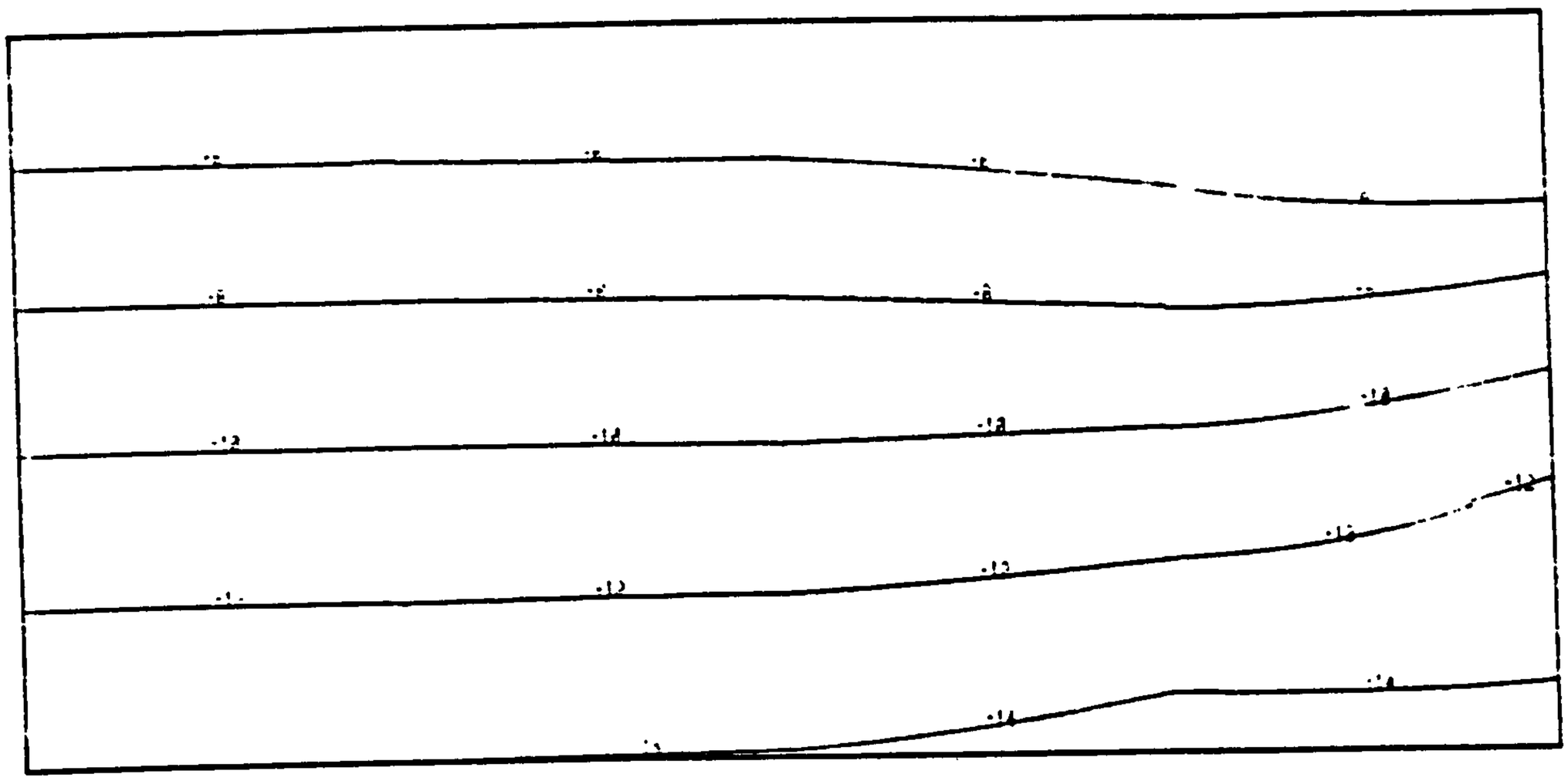

(a) σ_{xx} (x10) at c = 0.2275E-06

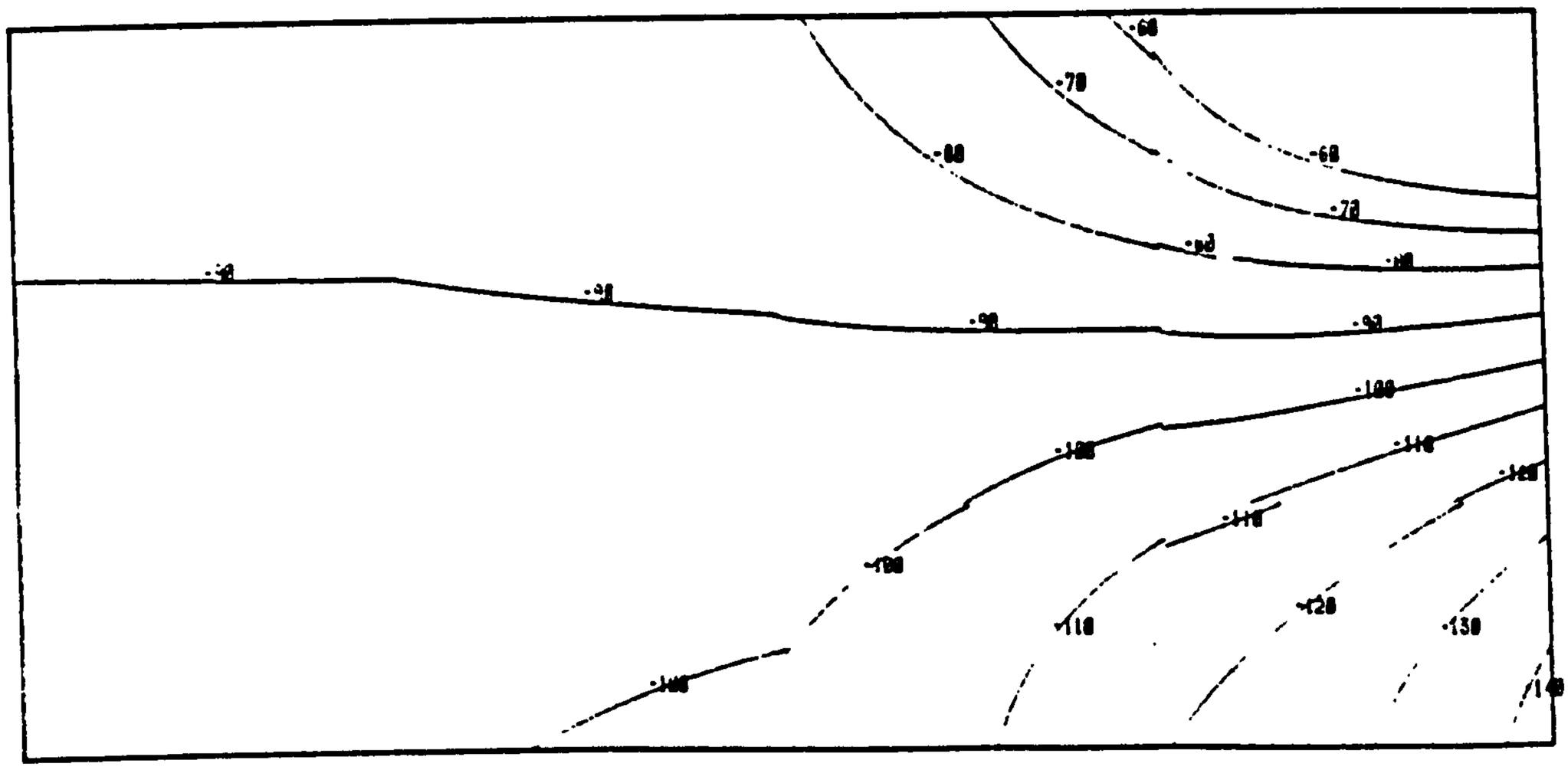

(b) σ_{xx} (x10) at c=0.525E-06

Figure 5.13.8: Stress contour for Allen's plate problem

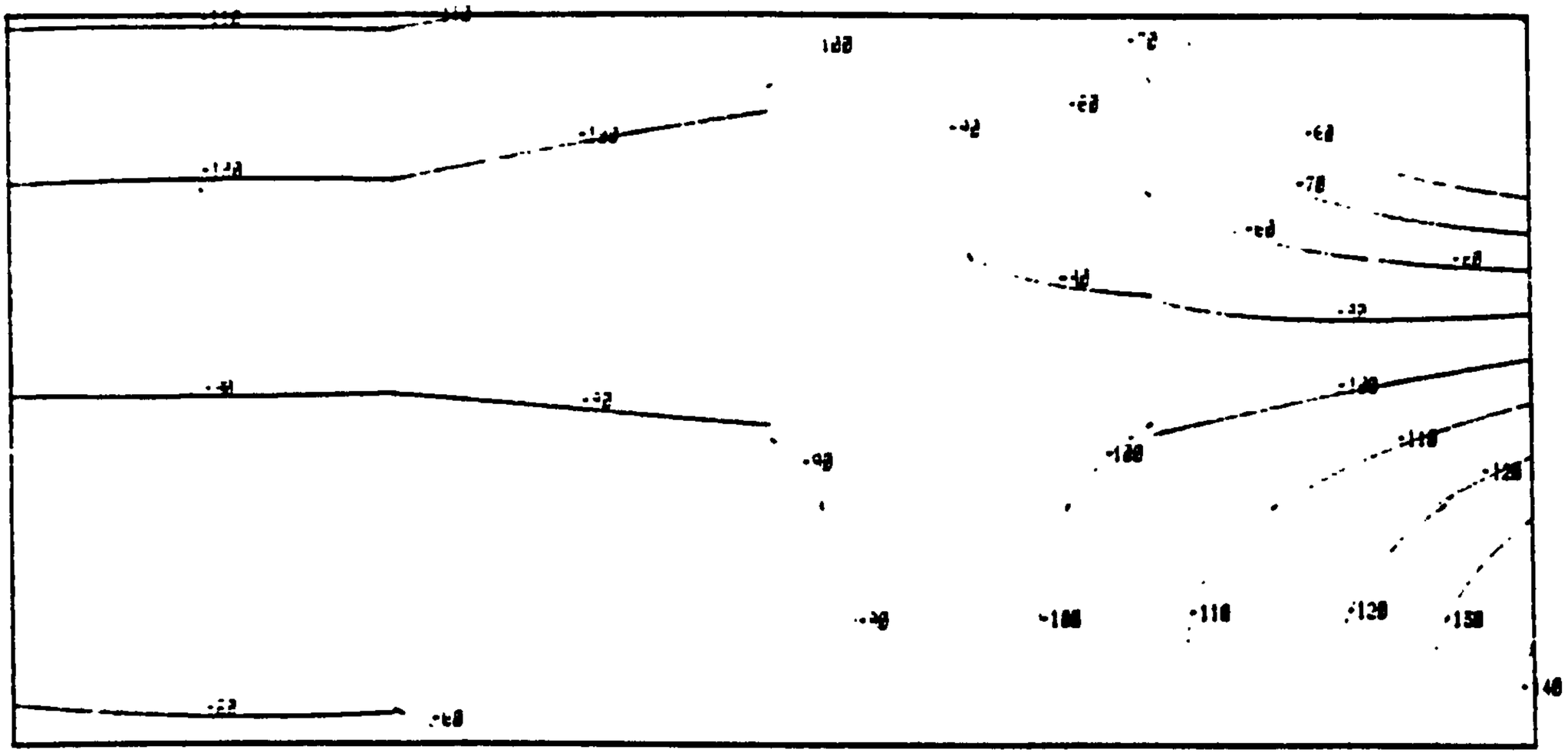

(a) σ_{xx} (x10) at c = 0.8775E-06

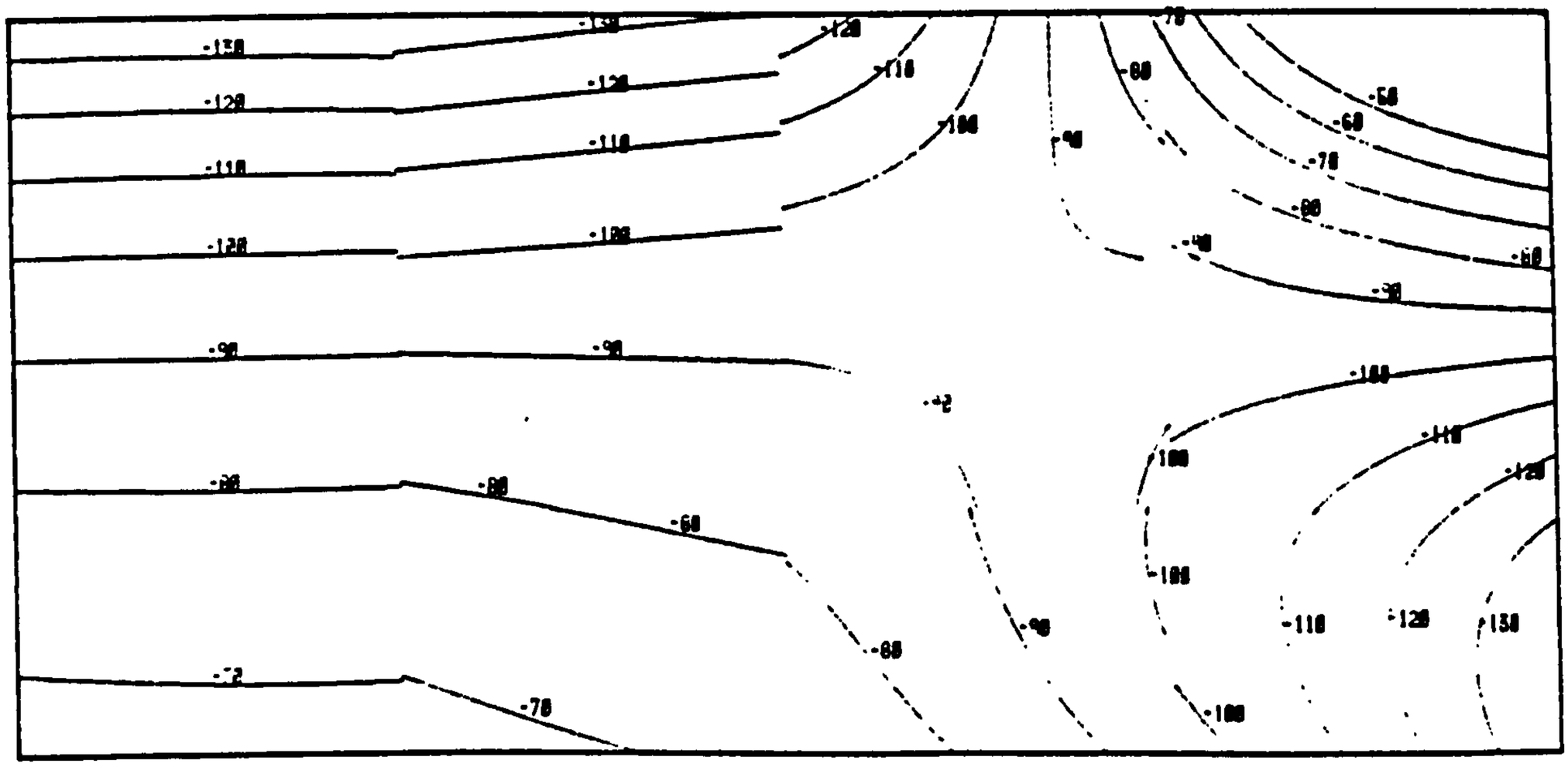

(b) σ_{xx} (x10) at c=0.25E-04

Figure 5.13.9: Stress contour for Allen's plate problem

CHAPTER SIX

EXTENSION OF COMPLEMENTARY POWER THEORY TO INCLUDE DELAYED ELASTIC STRAIN - BURGERS MODEL REPRESENTATION

Summary

Extension of the Power Minimisation Procedure to include delayed elastic strain, namely the analogous Burgers Model which is able to describe the concrete material behaviour more closely, is investigated. A second order matrix differential equation is obtained and methods of solving it are discussed. It is found that no new Ritz expression is necessary to approximate the time-dependent stress distributions throughout the structural continuum.

6.1 Extension of the Complementary Power Principle

Assuming a structure is at all times in equilibrium with the specified loading and compatible with respect to both internal strain and geometrical constraint and the supports are rigid, the Complementary Power Principle states (vide section 2.7):

$$\int \{\dot{\varepsilon}\}^T\{\delta\sigma\}\, dV = 0 \qquad (6.1.1)$$

An extension of the Complementary Power principle of equation 6.1.1 leads to a similar statement (England et al 1975) involving the second derivative of the strains $\{\ddot{\varepsilon}\}$ viz:

$$\int \{\ddot{\varepsilon}\}^T\{\delta\sigma\}\, dV = 0 \qquad (6.1.2)$$

Equation 6.1.2 does not have any appropriate physical interpretation.

6.2 The Analogous Burgers Model

The analogous Burgers Model, shown in Figure 2.5.2, has the following uniaxial constitutive relationship (vide section 2.5):

$$\ddot{\varepsilon} + \{\frac{E_k}{\eta_k}\}\dot{\varepsilon} = \{\frac{(E_m + E_k)}{\eta_k E_m} + \Phi(T)\}\dot{\sigma} + \frac{\ddot{\sigma}}{E_m} + \{\frac{E_k \Phi(T)}{\eta_k}\}\sigma \qquad (6.2.1)$$

Here E_k and η_k refer to the elastic and viscous parameters of the Kelvin component, E_m refers to the elastic modulus of the Maxwell component, $\Phi(T)$ is the temperature normalisation function. Again the differentiation is with respect to pseudo-time.

The creep behaviour of the Burgers model under constant uniaxial stress, σ_o, can be obtained from solving equation 6.2.1 using Laplace transformation (Findley et al 1976) with two initial conditions:

$$\varepsilon = \varepsilon_1 = \sigma_o/E_m \; ; \; \varepsilon_2 = 0, \; c = 0 \qquad (6.2.2)$$

$$\dot{\varepsilon} = (\frac{1}{\eta_k} + \Phi(T))\sigma_o \quad , \; c = 0 \qquad (6.2.3)$$

Thus the creep behaviour is given as:

$$\varepsilon(c) = (\frac{1}{E_m} + \frac{1}{E_k}(1-T(-c)) + \Phi(T)c)\sigma_o \qquad (6.2.4)$$

Where $T(-c) = EXP(-E_k c/\eta_k)$.

Equation 6.2.4 indicates the creep behaviour of the analogous Burgers Model is the sum of the creep behaviour of the analogous Maxwell and Kelvin models. The first two terms in the right hand side of equation 6.2.4 represent instantaneous elastic strain and viscous flow, and the last term represents delayed elasticity of the Kelvin model.

Differentiate equation 6.2.4 yields the creep strain rate $\dot{\varepsilon}$ viz:

$$\dot{\varepsilon} = \Phi(T)\sigma_o + \frac{\sigma_o}{\eta_k} T(-c) \qquad (6.2.5)$$

Thus the creep rate at c = 0+ with a finite value,

$$\dot{\varepsilon}(0+) = (\Phi(T) + 1/\eta_k)\sigma_o \qquad (6.2.6)$$

and approaches asymtotically to the value:

$$\dot{\varepsilon}(\infty) = \Phi(T)\sigma_o \qquad (6.2.7)$$

If the stress σ_o is removed at time c_1, the recovery behaviour of the analogous Burgers model can be obtained from equation 6.2.4 and the superposition principle by considering that at $c = c_1$ a constant stress $\sigma = -\sigma_o$ is added. According to the superposition principle the recovery strain $\varepsilon(c)$, $c > c_1$, is the sum of these two independent actions:

$$\varepsilon(c) = \left(\frac{1}{E_m} + \Phi(T)c + \frac{1}{E_k}(1-T(-c))\right)\sigma_o$$

$$-\left(\frac{1}{E_m} + \Phi(T)(c-c_1) + \frac{1}{E_k}(1-T(c-c_1))\right)\sigma_o \qquad (6.2.8)$$

$$= \Phi(T)\sigma_o c_1 + \frac{\sigma_o}{E_k}(T(c_1)-1)T(-c) \qquad (6.2.9)$$

Where $T(c-c_1) = EXP(-E_k(c-c_1)/\eta_k)$.
$T(c_1) = EXP(E_k c_1/\eta_k)$.

Thus the recovery has an instantaneous elastic recovery followed by creep recovery at a decreasing rate. The second term decreases toward zero for large times, while the first term represents a permanent strain due to the viscous flow of $\Phi(T)$. The creep strain rate $\dot{\varepsilon}(c)$, $c > c_1$ is given as:

$$\dot{\varepsilon}(c) = -\frac{\sigma_o}{\eta_k}(T(c_1) - 1)T(-c) \qquad (6.2.10)$$

The general three dimensional constitutive law of the analogous Burgers model can be written in matrix form as:

$$(\nabla^2 + \frac{E_k}{\eta_k}\nabla)\{\varepsilon\} = (\frac{\nabla^2}{E_m} + (\frac{1}{\eta_k} + \frac{E_k}{E_k E_m} + \Phi(T))\nabla + \frac{E_k\Phi(T)}{\eta_k})[V]\{\sigma\} \quad (6.2.11)$$

where ∇ is the differential operator viz:

$$\nabla = d(\ )/dc \quad ; \quad \nabla^2 = d^2(\ )/dc^2 \quad (6.2.12)$$

Again it is assumed that the creep Poisson ratio is the same as its elastic counterpart (vide section 5.1).

6.3 The Minimisation Procedure

Again, assuming a Ritz type stress representation (vide section 5.1) viz:

$$\{\sigma\} = \{\sigma_o\} + a_1\{\sigma_1\} + a_2\{\sigma_2\} + \ldots + a_n\{\sigma_n\}$$

$$= \{\sigma_o\} + \{a\}^T[\sigma] \quad (6.3.1)$$

And combination of equation 6.1.1 and equation 6.1.2 gives:

$$\int \{\dot{\varepsilon}\}^T\{\delta\sigma\}\, dV + \frac{E_k}{\eta_k}\int\{\ddot{\varepsilon}\}^T\{\delta\sigma\}\, dV = 0 \quad (6.3.2)$$

After substitution of $\{\dot{\varepsilon}\}$ and $\{\ddot{\varepsilon}\}$ of equation 6.2.11, equation 6.3. into equation 6.3.2 and noting that

$$\{\delta\sigma\} = \frac{\partial\{\sigma\}}{\partial a_i}\delta a_i = \{\sigma_i\}\delta a_i \quad (6.3.3)$$

leads to the following second order matrix differential equation for the time function $\{a\}$, thus:

$$[P_b]\{\ddot{a}\} + [Q_b]\{\dot{a}\} + [R_b]\{a\} + \{s_b\} = \{0\} \quad (6.3.4)$$

where

$$[P_b] = \int \frac{1}{E_m}[\sigma]^T[V][\sigma]\ dV \qquad (6.3.5)$$

$$[Q_b] = \int (\frac{1}{\eta_k} + \chi_m + \Phi(T))[\sigma]^T[V][\sigma] \qquad 6.3.6)$$

$$[R_b] = \chi_k \int \Phi(T)[\sigma]^T[V][\sigma]\ dV \qquad (6.3.7)$$

$$\{s_b\} = \chi_k \int \Phi(T)[\sigma]^T[V]\{\sigma_o\}\ dV \qquad (6.3.8)$$

Where $\chi_k = E_k/\eta_k$ and $\chi_m = \chi_k/E_m$.

6.4 Finite Element Model and Numerical Integration

Again iso-parametric finite elements of the serendipity family (vide chapter 5) are used. The matrices of equation 6.3.5 to 6.3.8 need to be evaluated numerically using the Gauss-Legendre Quadrature (vide section 5.4) and let,

$$\Psi(\sigma) = ([\sigma]^T[V][\sigma] \det [J])$$

and $$\Psi(\sigma_o) = ([\sigma]^T[V]\{\sigma_o\} \det [J])$$

Thus,

$$[P_b] = \Sigma\Sigma\Sigma\Sigma\ H_i H_j H_m(\Psi(\sigma)/E_m) \qquad (6.4.1)$$

where $\Sigma\Sigma\Sigma\Sigma$ is the summation over the body volume and $[\sigma]$ was evaluate at the sampling points (ξ_i, η_j, ζ_k). Similarly,

$$[Q_b] = \Sigma\Sigma\Sigma\Sigma\ H_i H_j H_m(1/\eta_k + \chi_m + \Phi(T))\Psi(\sigma) \qquad (6.4.2)$$

$$[R_b] = \Sigma\Sigma\Sigma\Sigma\ H_i H_j H_m(\chi_k \Phi(T))\Psi(\sigma) \qquad (6.4.3)$$

$$\{s_b\} = \Sigma\Sigma\Sigma\Sigma\ H_i H_j H_m(\chi_k \Phi(T))\Psi(\sigma_o) \qquad (6.4.4)$$

Where $\chi_k = E_k/\eta_k$ and $\chi_m = \chi_k/E_m$.

Also [J] is the Jacobian matrix (vide section 5.3) and again $\Phi(T)$ is evaluated at the sampling points (ξ_i, η_j, ζ_m).

6.5 Solution of Differential Equation

a. Scalar differential equation

If the number of self-equilibrating stress used is one, viz:

$$\{\sigma\} = \{\sigma_o\} + a_1\{\sigma_1\} \qquad (6.5.1)$$

Equation 6.3.4 reduces to a scalar differential equation. Writing the auxiliary equation as:

$$\kappa^2 + \kappa e + f = 0 \qquad (6.5.2)$$

Completing squares gives:

$$\kappa_{1,2} = -\tfrac{1}{2}e \pm \tfrac{1}{2}(e^2 - 4f)^{\frac{1}{2}} \qquad (6.5.3)$$

Because equation 6.5.3 arises from a power principle and its extension, it is natural to conjecture that:

$$e^2 - 4f > 0 \qquad (6.5.4)$$

is always assured. Thus equation 6.3.5 has the trivial solution,

$$a = C_1\exp(-\kappa_1 c) + C_2\exp(-\kappa_2 c) \qquad (6.5.5)$$

where C_1 and C_2 are arbitrary constants to be determined from initial conditions.

b. Matrix differential equation

If the number of self-equilibrating stress distributions used is greater than one viz:

$$\{\sigma\} = \{\sigma_o\} + a_1\{\sigma_1\} + a_2\{\sigma_2\} + \ldots + a_n\{\sigma_n\} \qquad (6.5.6)$$

then the coefficient matrices $[P_b],[Q_b],[R_b]$ will be of the size nxn, and $\{s_b\}$ is a nx1 vector. Hence solution 6.5.4 cannot be extended to include matrix differential equations because in general $[\kappa]$ and [e] matrices are not commutable, i.e.

$$[\kappa][e] \neq [e][\kappa] \tag{6.5.7}$$

Let $\Theta = [P_b]^{-1}$ and rewriting equation 6.3.4 as:

$$\{\ddot{a}\}=-(\Theta[Q_b]\{\dot{a}\}+\Theta[R_b]\{a\}+\Theta\{s_b\}) \tag{6.5.8}$$

and let

$$\{Y'\} = \{\dot{a}\}$$
$$\{\dot{Y}'\} = \{\ddot{a}\} \tag{6.5.9}$$

Equation 6.5.8 maybe reduced to a system of 2n equations of the form:

$$\{C'\} = \begin{Bmatrix}\{Y'\}\\ \{\dot{Y}'\}\end{Bmatrix} \tag{6.5.10}$$

At c = 0, the initial condition is given by the vector {X'(0)} viz:

$$\{X'(0)\} = \begin{Bmatrix}\{a(0)\}\\ \{\dot{a}(0)\}\end{Bmatrix} \tag{6.5.11}$$

Equation 6.5.10 can be solved by any of the numerical methods like Runge-Kutta, Adams-Bashforth and Hamming (Ralston 1965).

In the fourth order Runge-Kutta method, starting from the known initial vector {X'(0)} at c= 0, the vector $\{X'(c + \Delta c)\}$ after time Δc maybe computed as:

$$\{X'(c+\Delta c)\} = \{X'(c)\} + (\{K'_1\} + 2\{K'_2\} + 2\{K'_3\} + \{K'_4\})/6 \tag{6.5.12}$$

where,

$$\{K'_1\} = \Delta c\{C'(\{X'(c)\}), c+\tfrac{1}{2}\Delta c\}$$

$$\{K'_2\} = \Delta c\{C'(\{X'(c) + \tfrac{1}{2}K'_1\}), c+\tfrac{1}{2}\Delta c\}$$

$$\{K'_3\} = \Delta c\{C'(\{X'(c) + \tfrac{1}{2}K'_2\})\}, c+\tfrac{1}{2}\Delta c\} \qquad (6.5.13)$$

$$\{K'_4\} = \Delta c\{C'(\{X'(c) + K'_3\}), c+\tfrac{1}{2}\Delta c\}$$

6.6 Computation of Initial Conditions

If $\{\sigma_o\}$ in equation 6.5.6 is chosen as the thermo-elastic solution, then:

$$\{\dot{a}(0)\} = \{0\} \qquad (6.6.1)$$

The second initial condition concerns the initial rate of change of the time dependent coefficient $\{a(0)\}$. They maybe evaluated by considering the initial creep rates of the analogous Burgers and Maxwell model.

The creep rate of the analogous Burgers model at $c = 0+$ is given as (vide section 6.2):

$$\dot{\varepsilon}(0+) = (\Phi(T) + 1/\eta_k)\sigma_o \qquad (6.6.2)$$

The creep rate of the analogous Maxwell model at 0+ is simply:

$$\dot{\varepsilon}(0+) = \Phi(T)\sigma_o \qquad (6.6.3)$$

From the analogous Maxwell solution (vide section 5.1),

$$\{\dot{a}(0)\} = -[Q]^{-1}\{s\} \qquad (6.6.4)$$

where,

$$[Q] = \int [\sigma]^T[V][\sigma]/E_m \, dV \qquad (6.6.5)$$

$$\{s\} = \int \Phi(T)[\sigma]^T[V]\{\sigma_o\} \, dV \qquad (6.6.6)$$

Comparison between equation 6.6.1 and 6.6.2 suggests that the $\{\dot{a}(0)\}$

vector for the analogous Burgers model is given simply as:

$$\{\dot{a}(0)\} = -[Q]^{-1}\{s'_b\} \tag{6.6.7}$$

where,

$$\{s'_b\} = \int (\Phi(T) + 1/\eta_k)[\sigma]^T[V]\{\sigma_o\}\, dV \tag{6.6.8}$$

6.7 Illustrative Problem

The prestressed restrained beam was solved as a two-dimensional plane stress problem. Figure 6.7.1 shows details of boundary conditions and loadings. The sustained temperature field was considered. A mesh of 12 iso-parametric elements was used to represent the beam. Length to depth ratio is 6:1. The stresses derived also represent those of a plate with an aspect ratio (length to width ratio) of 3, see Figure 5.13.2.

Young's modulus, Poisson's ratio and coefficient of thermal expansion are taken as 34000 MN/m^2, 0.2 and 0.12xE-04 per ^oC respectively. Stresses are expressed in MN/m^2. It is assumed that the temperature normalisation function is $\Phi(T) = T$.

The stresses presented in Table 6.7.1 were evaluated at the Gauss integration points. The 3x3 Gauss Quadratic rule were used. Comparisons are made between the analogous Maxwell and Burgers solutions. It can be observed that at long term, both models give identical solutions.

6.8 Concluding Remarks

The Complementary Power Theory described in Chapter 5 has been extended to include delayed elastic strain using the analogous Burgers Model representation. Solutions of the second order matrix differential equations resulted together with initial conditions have been presented. It is found that no new Ritz expression is necessary to approximate the time-dependent stress distributions.The Burgers Model has also been incorporated into the VPCREEP computer program.

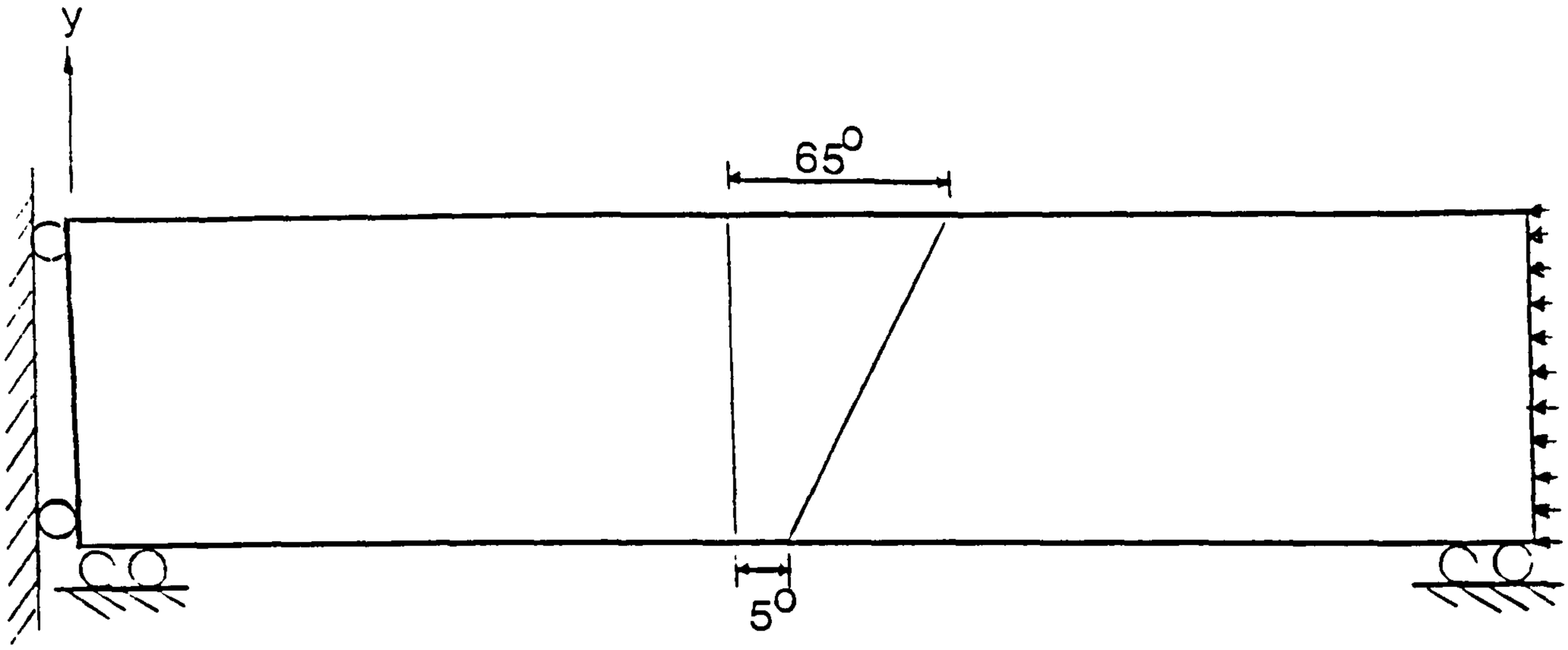

Axial force applied = 7 MN/m^2

(a) The beam model

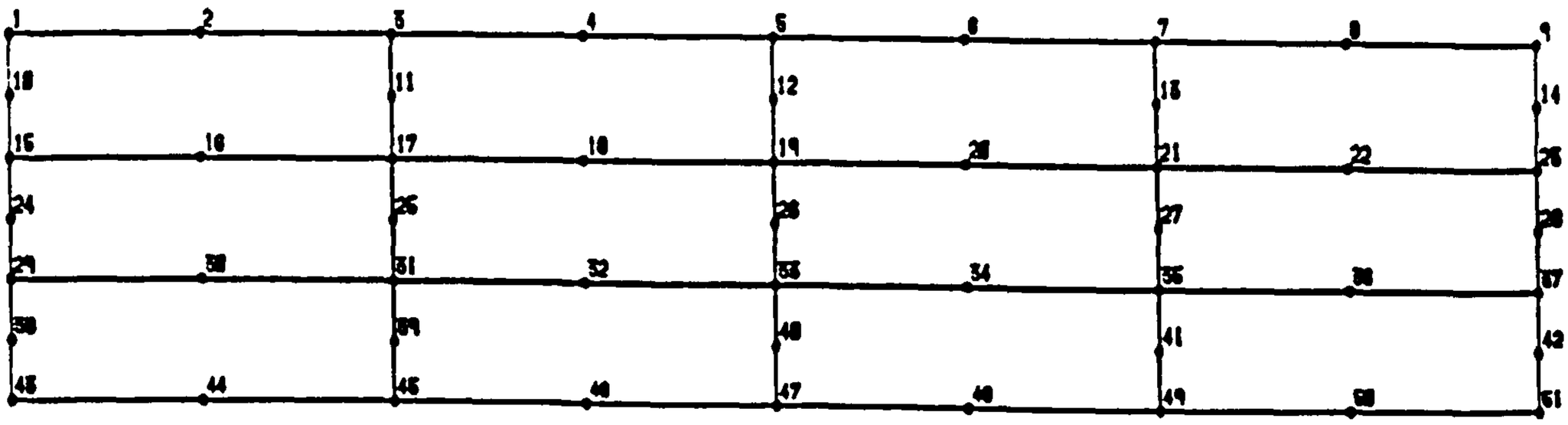

(b) Finite element idealisation

Figure 6.7.1: The two dimensional finite element model for the flexurally restrained beam problem

c ($x10^{-6}$)	0.0		0.1		1.0		2.0	
Y	Maxwell	Burgers	Maxwell	Burgers	Maxwell	Burgers	Maxwell	Burgers
9.25	18.32	18.32	16.16	15.20	6.13	6.55	3.32	3.94
6.67	15.16	15.16	13.68	12.98	6.58	6.82	4.32	4.80
4.08	12.00	12.00	11.19	10.75	7.01	7.08	5.33	5.66
2.58	10.16	10.16	9.73	9.44	7.24	7.21	5.92	6.16
0.00	7.00	7.00	7.20	7.18	7.58	7.40	6.94	7.02
-2.58	3.84	3.84	4.64	4.88	7.79	7.51	7.96	7.87
-4.08	2.00	2.00	3.10	3.51	7.81	7.50	8.58	8.36
-6.67	-1.16	-1.16	0.32	1.02	7.43	7.19	9.67	9.20
-9.25	-4.32	-4.32	-3.16	-2.09	5.06	5.48	10.99	9.97

c ($x10^{-6}$)	3.0		4.0		5.0		Steady-state	
Y	Maxwell	Burgers	Maxwell	Burgers	Maxwell	Burgers	Maxwell	Burgers
9.25	2.70	3.02	2.58	2.70	2.57	2.60	2.62	2.62
6.67	3.63	3.96	3.36	3.57	3.22	3.37	2.99	2.99
4.08	4.60	4.92	4.20	4.49	3.95	4.21	3.47	3.48
2.58	5.19	5.50	4.73	5.06	4.43	4.74	3.84	3.85
0.00	6.27	6.54	5.76	6.11	5.41	5.77	4.69	4.70
-2.58	7.50	7.67	7.05	7.36	6.72	7.06	6.02	6.04
-4.08	8.35	8.42	8.03	8.24	7.77	8.03	7.22	7.23
-6.67	10.35	10.03	10.60	10.40	10.73	10.59	10.94	10.94
-9.25	14.88	13.23	17.45	15.63	19.17	17.42	22.63	22.57

Note: (a) All stresses are in MN/m^2

(b) Both Maxwell & Burgers model are assumed to have the same temperature normalisation function $\phi(T) = T$

Table 6.7.1: Maxwell and Burgers Models compared for various pseudo-time c

CHAPTER SEVEN

STEP-BY-STEP FINITE ELEMENT NON-LINEAR CREEP ANALYSIS FOR CONTINUUM PROBLEMS

Summary

Attention in this chapter is concentrated on the analysis of structures which exhibit non-linear creep behaviour using a step-by-step approach and non-linear creep law, together with an analogous von Mises flow rule. This development is particularly applicable to the non-linear finite element analysis of two and three dimensional continua influenced by creep and temperature.

The SSCREEP program developed in chapter four is modified to include the non-linear power creep law. Criteria for pseudo-time step-size are also deduced.

7.1 Preliminary

Creep effects under variable stress and varying temperature are observed in other materials, too, and are especially prominent in metals. The detailed studies of metallurgical engineering and materials science present metals so complex and individual that formal mathematical expression for the behaviour of even a simple metal under the simplest loading can be regarded only as an approximation tenable in a limited range over which a single structural mechanism predominates. There is little agreement on the correct mathematical expression to adopt for the uniaxial relationship (vide chapter 2).

However, the apparent difficulties are resolved if the many differences of metallurgical details average out on an engineering scale of magnitude. On these grounds, together with the grounds that predictions need only be accurate to within certain factor of safety, stress analyst would claim a freedom to disregard the multitudinous factors to which attention is directed in other disciplines. The freedom claimed tends to be supported by families of curves which represent σ, ε, c, T relationships as measured for each metal in various standard types of test (vide chapter 2). Between families of

curves measured for different well developed metals in any one type of test, a distinct family likeness may usually be recognised. The feature is witnessed by the various phenomenological formulae which have been advocated for general use (Dorn 1961, Johnson et al 1961-1964, Snedden 1972, Henderson 1974-1979 and also vide chapter 2). England (1983) suggested that for metallic structures subjected to sustained raised non-uniform temperatures the following uniaxial relationship is appropriate (vide chapter 2) viz:

$$\varepsilon_c = \Phi(T)c\sigma^{\mu} \quad \text{for } \mu > 1 \qquad (7.1.1)$$

7.2 Multiaxial Creep Formulation

Creep experiments under multiaxial stresses are much more difficult to perform than uniaxial creep and mathematical representation is much more involved for combined stresses. Since creep deformation shows some similarities to plastic deformation, an analogous flow rule, similar to von Mises flow rule (Mendelson 1968), maybe derived from the following assumptions:

1. The area of study is concerned with primary creep and the corresponding manifestations of creep behaviour common to that stage (Figure 7.2.1).

2. The multiaxial formulation must reduce to non-linear uniaxial creep law (vide equation 7.1.1) when it is appropriate.

3. The formulation should express material incompressibility that has been observed experimentally during creep process.

4. The creep rate is independent of superimposed hydrostatic pressure.

5. Coaxiality of principal directions of stress and strain rate.

Thus the creep strain rate tensors can be written in terms of the stress deviator tensor, as follows, in a three dimensional Cartesian coordinate system $x_i = x_1, x_2, x_3$:

$$\dot{\varepsilon}_{ij,c} = \lambda S_{ij} \quad , \; i,j = 1,2,3. \qquad (7.2.1)$$

λ is a factor of proportionality to be determined. The stress deviator tensor S_{ij} is determined from the stress tensor σ_{ij} viz:

$$S_{ij} = \sigma_{ij} - \frac{1}{3}\sigma_{kk}\delta_{ij} \qquad (7.2.2)$$

where δ_{ij} is the Kronecker delta. The stress deviator represents the distortional component of the stress since it is formed by subtracting the hydrostatic or volumetric portion of the stress from the stress tensor and it satisfies the fourth basic requirement that the formulation be independent of hydrostatic pressure.

The overwhelming evidence (vide chapter 2 and section 7.1) of tests at various temperatures indicated that von Mises effective stress or second order invariant stress criterion controls the creep rate for practical conditions of stress and temperature. The effective stress σ_e is defined as:

$$\sigma_e = (3J_2)^{\frac{1}{2}} \quad ; \quad J_2 = \tfrac{1}{2}S_{ij}S_{ij} \qquad (7.2.3)$$

Here J_2 is the second invariant of the stress deviator tensor. Similarly, the effective creep strain rate can be defined as:

$$\dot{\varepsilon}_e = (\frac{4}{3}I_2)^{\frac{1}{2}} \quad ; \quad I_2 = \tfrac{1}{2}\dot{\varepsilon}_{ij,c}\dot{\varepsilon}_{ij,c} \qquad (7.2.4)$$

where I_2 is the second invariant of the strain rate tensor. The use of the effective quantities is intended to satisfy the second requirement that multiaxial formulation must reduce to the correct uniaxial formulation. Indeed, in uniaxial case, $\sigma_{11} \neq 0$ and the other stress components all equal to zero, then equation 7.2.3 reduces to:

$$\sigma_e = \sigma_{11} \qquad (7.2.5)$$

Furthermore in the uniaxial case $\varepsilon_{11,c} \neq 0$, $\varepsilon_{22,c} = \varepsilon_{33,c}$, the rest of the creep rates being zero. Then by constancy of volume in creep, we have:

$$\dot{\varepsilon}_{kk,c} = 0 \qquad (7.2.6)$$

from which,

$$\dot{\varepsilon}_{22,c} = \dot{\varepsilon}_{33,c} = -\tfrac{1}{2}\dot{\varepsilon}_{11,c} \qquad (7.2.7)$$

Substitution of equation 7.2.7 into equation 7.2.4 gives:

$$\dot{\varepsilon}_e = \dot{\varepsilon}_{11,c} \qquad (7.2.8)$$

Finally,

$$\lambda S_{kk} = \dot{\varepsilon}_{kk,c} = 0 \qquad (7.2.9)$$

which satisfies third requirement on material incompressibility.

If we substitute the creep flow rule, equation 7.2.1 into equation 7.2.4 for the effective creep strain rate and using equation 7.2.3, it can be shown that,

$$\lambda = \frac{3}{2\sigma_e}\frac{d\varepsilon_e}{dc} \qquad (7.2.10)$$

Non-linear uniaxial creep law (vide section 7.1) states that,

$$\varepsilon_c = \Phi(T)c\sigma^{\mu} \quad \text{for } \mu > 1 \qquad (7.2.11)$$

Utilising equation 7.2.10, one obtains:

$$\lambda = \frac{3}{2\sigma_e}\frac{d\varepsilon_e}{dc}$$

$$= 1.5\ \Phi(T)\sigma_e{}^{\mu-1} \qquad (7.2.12)$$

From equation 7.2.1, the multiaxial creep flow rule is thus:

$$\dot{\varepsilon}_{ij,c} = 1.5\ \Phi(T)\sigma_e^{\mu-1}S_{ij} \qquad (7.2.13)$$

The elastic (time independent) part of the total strain rate is obtained from Hooke's law.

7.3 The Time-Step Strategy

The step-by-step procedure utilised in chapter four has been used here because it is more easily adapted to the SSCREEP program. The fundamental assumption in the step-by-step creep solution technique is that the time can be subdivided into sufficiently small time intervals such that the stress can be assumed to be constant within each time interval. Therefore the non-linear creep problem can be solved as a series of linear problems for each time interval treating the incremental creep strains from the last time interval as initial strains for the current time interval. Thus the creep strain increment $\Delta\varepsilon_{ij,c}$ for a small pseudo-time interval Δc is given as:

$$\Delta\varepsilon_{ij,c} = 1.5\ \Phi(T)\sigma_e^{\mu-1}\Delta c S_{ij} \qquad (7.3.1)$$

The success of the step-by-step procedure for solving creep problems depends upon the ability to select appropriate time intervals because if the time interval is too large, instability may occur. Thus it is necessary for,

$$\Delta c < \Delta c_{critical} \qquad (7.3.2)$$

where $\Delta c_{critical}$ depends on the type of creep law used. A rule of thumb (Zienkiewicz 1982) which proves quite effective in practice is that the increment of creep strain should not exceed a fraction, γ, of the total elastic strain, in that:

$$\Delta c_{critical}\Phi(T)\sigma_e^{\mu} < \gamma\varepsilon_{elastic} = \gamma\sigma_e/E_m \qquad (7.3.3)$$

i.e. $$\Delta c_{critical} = \gamma/(E_m\Phi(T)\sigma_e^{\mu-1}) \qquad (7.3.4)$$

for uniaxial case. E_m is the Young's modulus.

From the author's own experience,

$$\gamma = 0.05 \tag{7.3.5}$$

A time-step strategy is used in which the time increment is increased by a power of 2, at each step, viz:

$$\Delta c = 2^{k-1}\Delta c_{critical} \tag{7.3.6}$$

where k = 1, 2, ... n.

7.4 Illustrative Problem

England's (England 1962) classical flexurally restrained beam was solved as a two-dimensional plane stress problem. Figure 7.4.1 shows details of boundary conditions and loadings. The sustained temperature field was considered. A total of 60 triangular elements was used to model the beam. Young's modulus, Poisson's ratio and coefficient of thermal expansion are taken as 34500 MN/m^2, 0.3 and 0.12xE-04 per ^oC respectively. Stresses are expressed in MN/m^2. The temperature normalisation function is taken as $\Phi(T)= T$. Stresses for the case where $\mu=3$ are presented in Table 7.4.1.

7.5 Concluding Remarks

The finite element computer program 'SSCREEP' has been extended to incorporate the power creep law derived in this chapter as an option for the purpose of performing non-linear creep analysis for plane, stress plane strain, axisymmetric and three dimensional continuum problems.

It has been found that numerical instability occurs as the creep component increases, this has been caused by the decrease of the time-step size which approaches the machine word-size limit. As the current version of the SSCREEP program supports only single precision 32-bit arithmetic, it is concluded that while the algorithm is useful in general, further study into the time-stepping strategy should be carried out and the SSCREEP program should be converted into 64-bit double precision arithmetic and be tested on machines such as Cray 2

before a full evaluation of the usefulness of the theory proposed here be ascertained.

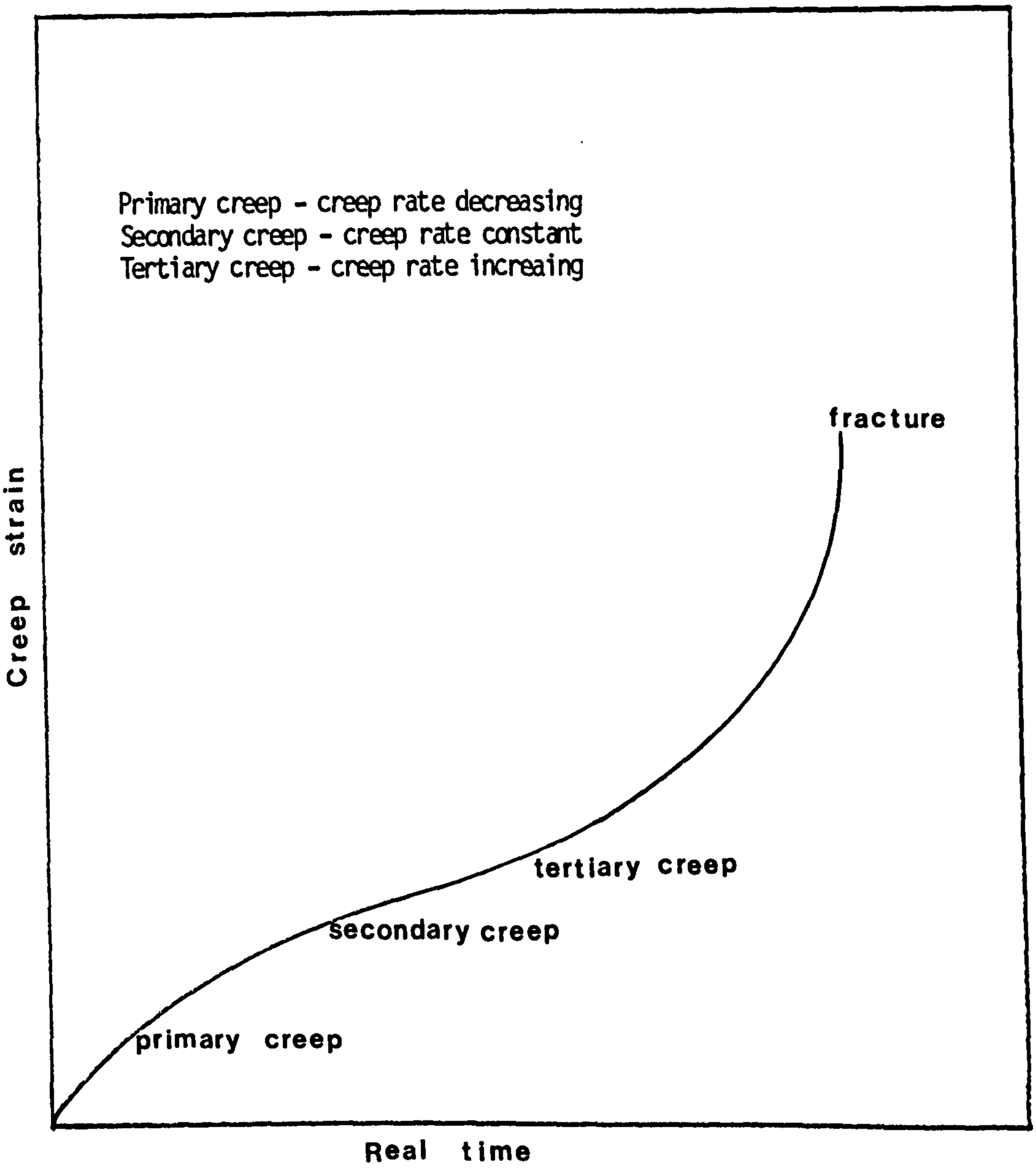

Figure 7.2.1: Typical creep curve

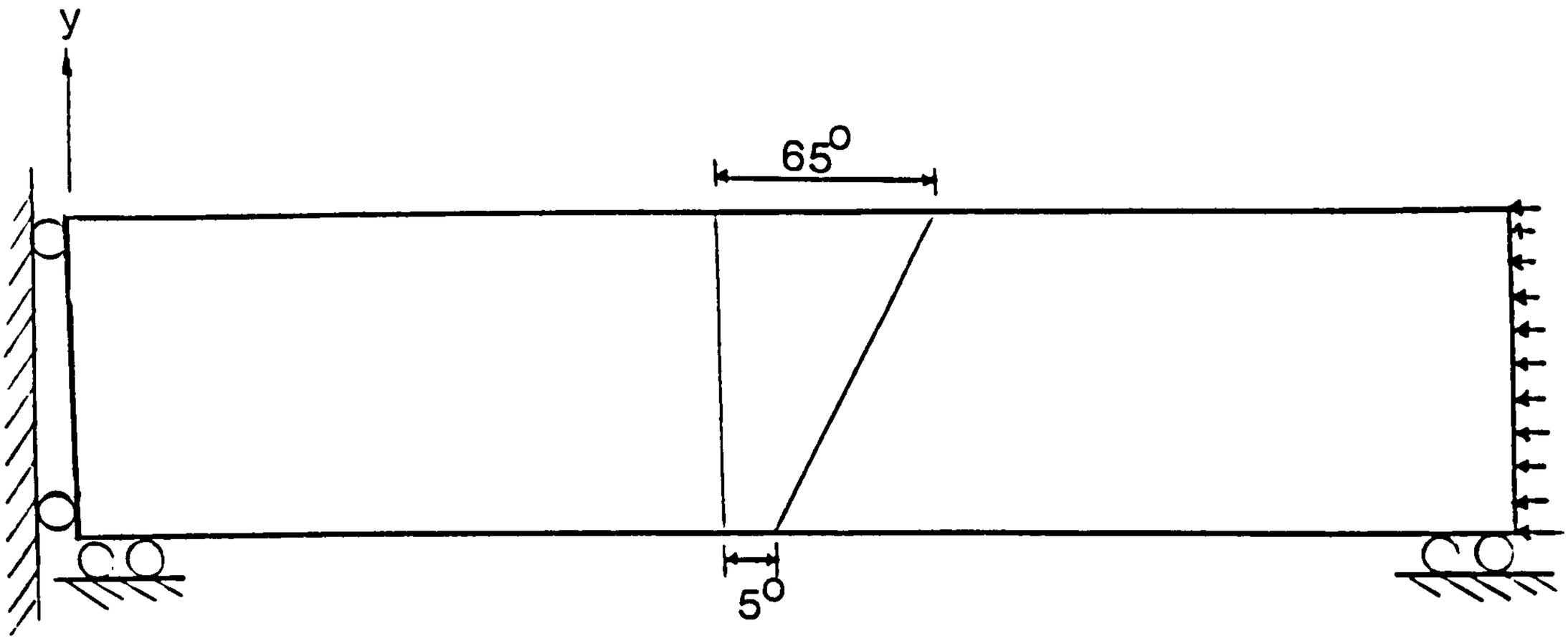

Axial force applied = 7 MN/m^2

(a) The beam model

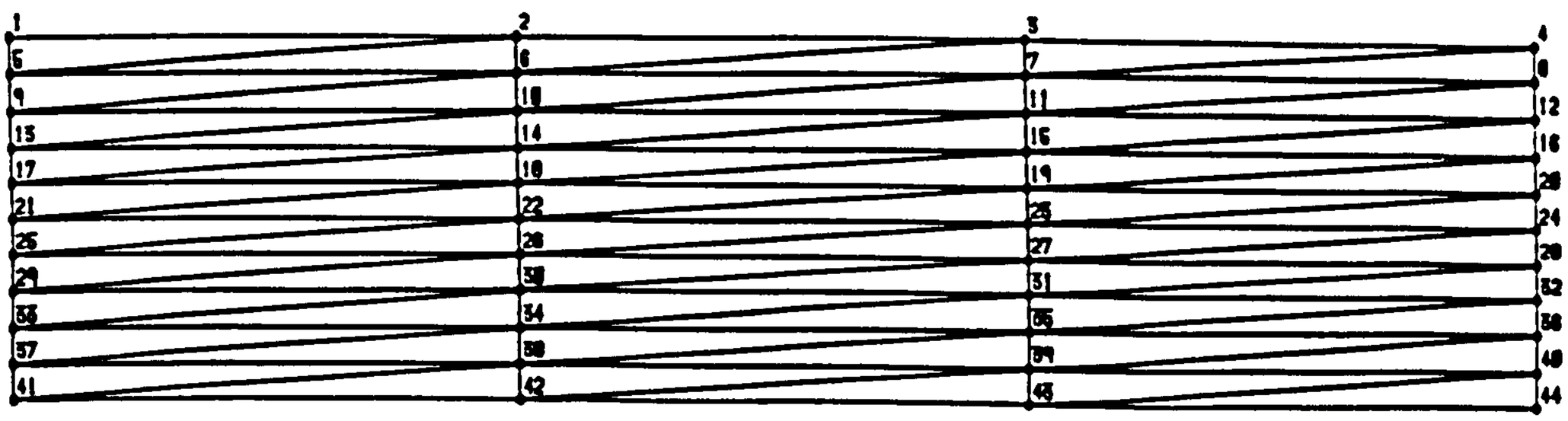

(b) Finite element idealisation

Figure 7.4.1: The finite element model for the flexurally restrained beam problem

c ($\times 10^{-9}$) / Y	0.0	1.0	2.0	4.0	8.0	16.0	32.0	steady-state
9.67	4.19	2.01	0.80	-0.89	-3.26	-6.46	-9.56	-10.60
8.67	1.70	-0.47	-1.67	-3.35	-5.56	-7.79	-8.77	-8.80
7.67	-0.78	-2.95	-4.13	-5.67	-7.29	-8.11	-7.97	-7.81
6.67	-3.27	-5.38	-6.42	-7.52	-8.14	-7.86	-7.33	-7.16
5.67	-5.76	-7.63	-8.30	-8.65	-8.29	-7.46	-6.84	-6.68
4.67	-8.24	-9.53	-9.58	-9.09	-8.10	-7.06	-6.45	-6.31
3.67	-10.73	-10.91	-10.23	-9.09	-7.79	-6.72	-6.13	-6.01
2.67	-13.21	-11.68	-10.37	-8.87	-7.47	-6.42	-5.87	-5.76
1.67	-15.70	-11.86	-10.20	-8.57	-7.17	-6.16	-5.65	-5.54
0.67	-18.18	-11.52	-9.84	-8.24	-6.90	-5.94	-5.46	-5.36

All stresses are in MN/m^2

Table 7.4.1: Beam Stresses for $\mu = 3$ at x=0 at various pseudo-time c

CHAPTER EIGHT

CONCLUSIONS AND SUGGESTIONS

8.1 Preliminary

Research reported in this thesis led to several conclusions, and these have already been incorporated in the appropriate discussions. The main points are summarised in the first part of this chapter, while the second part contains suggestions for further studies.

8.2 Conclusions

8.2.1 Material Models

The effects of temperature and stress on creep have been reviewed in this thesis. The concept of pseudo-time has been justified based on the creep curves similarity hypothesis which has been well-supported in the literature for problems involving moderate strains and temperatures.

Constitutive equations for concrete and non-concrete materials in which creep-temperature plays an essential role have been formulated as differential equations utilizing the pseudo-time concept. The emphasis is on an engineering theory of creep for structures with a strong reliance on experimental data and on practicality. In connexion with the differential equation approach advocated in this thesis, rheological models have been used to enable the mechanisms of creep to be appreciated.

As far as concrete is concerned, it has been shown that for situations where recovery of strains is not important, the analogous Maxwell rheological body is an appropriate material model. If allowance is made for recovery of strains when stresses decline, the analogous Burgers model is more suitable. It has the advantage over the simpler Maxwell model in that it is capable of predicting, with good engineering accuracy, the major strain features associated with stressed concrete.

As far as non-concrete material is concerned, a multi-axial creep law has been derived from an analogous flow rule approach.

8.2.2 Methods of Structural Analysis

8.2.2.1 Beam Analysis

A flexibility method of creep analysis for steady-state stresses in continuous prestressed concrete beam structures subjected to cyclically varying temperatures has been derived based on England's steady-state theory. The method has been shown to be analogous to a beam theory of non-homogeneous elasticity. Use is then made of elastic analysis procedures to generate creep solutions. A Fortran program 'FCREEP' has been developed based on the theory and it maybe utilised, with minimal cost, for design or analysis. FCREEP maybe run on microcomputers, minicomputers or mainframes.

Based on some realistic temperature data supplied by the Transport and Road Laboratory, the study concluded that the combined influences of creep and cyclic temperatures cause significant changes to the working stresses of bridges which should be accounted for in design. It is also recommended that the Codes of Practice BS 5400 should include explicit information relating to temperature for different seasons and different times of day, together with theory and information on temperature-dependence of creep to enable designers to perform creep temperature calculations.

8.2.2.2 Finite Element Analysis

A step-by-step three dimensional finite element algorithm for linear creep continuum problems has been developed. A computer code 'SSCREEP' has been written utilising the algorithm and applied to some benchmark problems. It is revealed that while the algorithm itself is easy to implement, it is very expensive to use even for a small problem. A greater disadvantage is the large amount of information generated from such an analysis and consequently the large human resources which maybe required

for the interpretation of results. In the case of sustained temperature problems, the situation maybe improved by using a variable pseudo-time step increment approach albeit solution accuracy is sacrificed. In the case of cyclic temperature problems, the choice of pseudo-time step increment is restricted because it must not be bigger than the largest temperature phase length within a cycle. It is concluded that while the algorithm is useful in general, it can be extremely expensive and overtax even the most powerful modern computers.

The Complementary Power Theory presented in this thesis permits stresses to be evaluated in both the transient creep phase and in the limiting steady-state condition from a Power Minimisation Procedure in conjunction with a Ritz process. This Procedure has the advantage that it maybe used in the form of exact or approximate analysis and is more economic than the step-by-step algorithms. The nature of the Ritz's expression together with its automatic generation has been explored in detail. The Power Minimisation Procedure has been extended to general two and three dimensional continua utilising the finite element technique. A computer program 'VPCREEP' has been developed for elastic and creep analysis of structures subjected to (i) sustained loads and sustained temperature and (ii) sustained loads and cyclically varying temperatures between any two states. VPCREEP has the ability to generate the self-equilibrating stress distributions (for Ritz's expression) automatically and this reduces the effort required in solving general problems and allows the stress analyst to concentrate on the interpretation of the analysis results.

Extension of the Power Minimisation Procedure to include delayed elastic strain, namely the analogous Burgers Model which is able to describe the concrete material behaviour more closely, has been derived. Solutions of the resulting second order matrix differential equation have been obtained. It has been extended to general two and three dimensional continua utilising the finite element technique and has been incorporated into the 'VPCREEP'

program. It is found that no new Ritz expression is necessary to approximate the time-dependent stress distributions throughout the structural continuum and that the increase in computer time is small in comparison with the finite element solution phase of the program, especially for three dimensional problems.

The finite element computer program 'SSCREEP' has been extended to include the multi-axial non-linear creep law as an option for the purpose of performing non-linear creep analysis for general two and three dimensional problems. It has been found that numerical instability can occur as the creep exponent increases. It is concluded that further study into the time-stepping strategy should be carried out and the 'SSCREEP' program should be converted into 64-bit double precision arithmetic and be tested on machines such as Cray 2 before a full evaluation of the usefulness of the multi-axial non-linear creep theory proposed in this thesis be ascertained.

8.2.3 Finite Element Solution Techniques

The frontal solver with partitioned variable space developed in this thesis and used in the 'SSCREEP' and 'VPCREEP' computer programs has been shown to be a reasonable and natural method for obtaining the solution of large structural systems using the finite element method within computing environments with small in-core storage restrictions. This memory requirement reduction is at the expense of longer processing time as the number of active variable space increases. This increase in computer time is entirely due to additional transfer of data to and from auxiliary storage. Therefore any further hardware improvements in this direction would improve the efficiency of partition frontal solver.

The partition method implemented is completely internal to the solver and required no user intervention. This implementation is further enhanced by the dynamic memory management technique used in these two programs in that the solver will automatically allocate maximum in-core storage available and try to minimise the amount of disk accesses.

8.2.4 Finite Element Preprocessing and Postprocessing

The finite element mesh generations method implemented in 'SSCREEP' and 'VPCREEP' should be adequate for two dimensional and small three dimensional problems. The contouring algorithm used in the programs is also adequate for two dimensional problems.

8.3 Suggestions For Further Studies

8.3.1 Experimental Works

Further experimental studies into the effect of temperature cycling on the properties and structural performance of concrete will be beneficial for the fundamental understanding of the physics of creep and the validation of the analysis methods proposed in this thesis. Experimental data is also required to test the multi-axial non-linear creep theory proposed in this thesis.

8.3.2 Theoretical Investigations

Further investigation into the multi-axial non-linear creep theory will be a worthwhile project.

8.3.3 Software Development

8.3.3.1 Partition Frontal Solver Enhancements

(a) Some form of frontwidth minimisation algorithm should be implemented in 'SSCREEP' and 'VPCREEP' to further enhance the efficiency of the partition frontal solver developed.

(b) The re-writing of the core of the partition frontal solver using assembly language will greatly speed up the solution phase of the programs.

With the wide acceptance of personal computers running DOS or OS/2, the above enhancement will no doubt enable the

programs to be run on these machines.

8.3.3.2 SSCREEP Program Enhancements

The SSCREEP programs should be converted into 64-bit arithmetic and double precision should be used to perform extensive test on the non-linear portion of the program.

8.3.3.3 Preprocessing And Postprocessing Aspects

Further enhancement to the two and three dimensional mesh generation aspects of the programs should be carried out. Likewise, enhancements to the two and three dimensional contouring capabilities, which is a vast subject and is still under intense development at present, should be carried out.

Alternatively, translators which interface with some of the major CAD packages in the software industry should be developed to perform pre-processing and post-processing.

APPENDIX A

REFERENCES

Abbas, S.F. (1980) 'Some novel application of the frontal concept.' Int. J. Num. Meth. Engng. Vol. 15, pp. 519-536.

Andrade, E.N. da C. (1910) 'The viscous flow in metals and allied phenomena.' Proc. Roy. Soc. A, 84, (I).

Arthanar, S. and Yu, C.W. (1967) 'Creep of concrete under uniaxial and biaxial stresses at elevated temperature.' Magazine of concrete research(MCR), Vol. 19, No. 60.

Aruthunyan, N. Kh. (1966) Some Problems in The Theory of Creep in Concrete Structures. Pergamon Press, London.

Barlow, J. (1976) 'Optimal stress locations in finite element models.' Int. J. Num. Meth. Engng., 10, pp.243-251.

Barsoum, R.S., Loomis, R.W. and Steward, B.D. (1976) ASME-MPS Symposium on Creep-Fatigue Interaction. ASME, N.Y. pp.57.

Boley, B.A. and Weiner, J.A. (1967) Theory of Thermal Stresses. John Wiley and Sons, N.Y.

Boley, B.A. (1968) Thermoinelasticity. IUTAM Symposium, East Kilbride, Scotland, Springer-Verlag Wien, N.Y.

Boltzmann, L. (1974) Sber. Akad. Wiss. Wien 70; Wiss. Abn. 1, pp.616.

Boyle, J. and Spence, J. (1983) Stress Analysis for Creep. Butterworths, London.

British Standards Institution (1978), BS 5400: Steel, Concrete and Composite Bridges, London.

Browne, R.D. (1968) 'Properties of concrete in reactor vessels.' Conf. on Prestressed Concrete Pressure Vessels, ICE Proc, London.

Bryant, A.H., Buckle, I.G. and Lanigan, A.G. (1974) 'Prediction of temperatures in box-girder bridges.' Proc. of Australian Road Research Board, Vol. 7, part 7, pp. 296-308.

Buell, W.R. and Bush, B.A. (1973) 'Mesh generation - A survey.' J. Engng. for Industry, Trans. of ASME Series B, Vol. 95, No. 1, Feb., pp. 332-338.

Burrow, R.E.D. (1978) 'The future of prestressed concrete pressure vessels.' Proc. of FIP 78 Congress, London.

CEB-FIP (1978) Internal System of Unified Standard Code of Practice for Structures.

CEB-FIP (1978) Model Code for Concrete Structures.

CEB-FIP (1970) International Recommendations for the Design and Construction of Concrete Structures. London, Cement and Concrete Assoc., June.

Churchward, A. and Sokal, Y.T. (1981) 'Prediction of temperatures in concrete bridges.' J. ASCE, Vol. 107, No. ST11, Nov.

Clarke, J.L. 'Thermal stress problems in offshore structures.' Ocean-ology Int. 78, Offshore Structures Conf. Brighton, March.

Derrington, J.A. (1978) Chairman's Report on 'Concrete sea Structures.' Proc. FIP Congress, London, May.

Deutsche Normen (1953) Prestressed Concrete -Rules for Design and Manufacture. Berlin and Koln, German Design Standard DIN 4227.

Dhalla, A.K. and Gallagher, R.H. (1980) 'Computational methods for structural analysis.' J. ASME.

Dhalla, A.K. and Roche, R.V. (1975) Advance in Design for Elevated Temperature Environment. ASME, pp.83, N.Y.

Dorn, J.E. (1955) 'Some fundamental experiments on high-temperature creep.' J. Mech. Phys. Solids 3, No. 2, Jan.

Dorn, J.E. (1961) Behaviour of Materials at Elevated Temperatures. McGraw-Hill, London.

Emerson, M. (1966-67) Digest of Report: LR672, LR696, LR744, LR748, LR765, LR783, TRRL Report, U.K.

England, G.L. (1961) Study of the Time-dependent Strains in Concrete Maintained at Elevated Temperatures and Their Effects in Reinforced Concrete. Ph.D Thesis, University of London.

England, G.L. and Ross, A.D. (1962) 'Reinforced concrete under thermal gradients.' Mag. Conc. Res. 14 (40) 5.

England, G.L. (1966) 'Steady-state stresses in concrete structures subjected to sustained loads and temperatures. Part I and II.' Nucl. Eng. Des. 3, 54, 246.

England, G.L. (1967) 'Numerical creep analyses applied to concrete structures.' J. Am. Conc. Inst. Proc. 64(6), pp.301.

England, G.L. (1968) 'Long term thermal stresses in prestressed concrete structures.' Proc. ICE Conf. Prestressed Concrete Pressure Vessels, p.349, London.

England, G.L. (1968) 'Time-dependent stresses in creep elastic materials - a general method of calculation.' JBCSA Conf. Recent Advances in Stress Analtsis: New Concepts and their Practical Application, London.

England, G.L. and Allen, S.J. (1971) 'The calculation of time-dependent stresses in PCPV's by an approximate method.' Proc. 1st SMIRT Conf., Berlin, Vol. 4, part H, pp. 289-313, North Holland, Amsterdam.

England, G.L. and Jordaan, I.J. (1975)'Time-dependent and steady-state stresses in concrete structures with steel reinforcement, at normal and raised temperatures.' Mag. Conc. Res. 27(92) 131.

England, G.L., Labib, G. and Moharram, A. (1977) 'The influence of

time and temperature on behaviour of concrete structures.' Cement and Conc. Assoc. Report No. 48.

England, G.L., Macleod, J.S. and Moharram, A. (1978) 'Design for creep and temperature in concrete offshore structures.' Oceanology Int. 78 Offshore Structures Conf., Brighton, pp.25-32.

England, G.L. (1979) 'Calculation of stresses in concrete ocean structures subjected to steady and time-varying temperatures, as influenced by creep.' Applied Ocean Research Vol. 1, No. 1.

England, G.L., Andrews, K.R.F. (1981) 'Cyclic temperatures and creep in continuous prestressed concrete beam structures.' Proc. Eighth Canadian Congress of Applied Mechanics, Moncton.

England, G.L. (1983), Private Communication.

Ferry, J.D. (1961) Viscoelasticity Properties of Polymers. John Wiley and Sons, N.Y.

Findley, W.N., Lai, J.S. and Onaran, K. (1976) Creep and Relaxation of Non-linear Viscoelastic Materials. North-Holland Pub. Co., Amsterdam.

Finnie, I. and Heller, W.R. (1959) Creep of Engineering Materials. McGraw Hill, N.Y.

Fluck, P.G. and Washa, G.W. (1958) 'Creep of plain and reinforced concrete.' J. ACI, April.

Freudental, A.M. and Roll, F. (1958) 'Creep and creep recovery of concrete under high compressive stress.' J. ACI, June.

Gallagher, R.H., Padlog, J. and Sijlarrd, P.D. (1962) 'Stress analysis of heated complex shapes.' ARS Journal 32.

Gallagher, R.H. (1975) 'Enhancements of the finite element method through multidisciplinary applications.' CANCAM, Proc. University of New Brunswick, Fredericton, May 26-30, pp. G35-G47.

Gittus, J. (1975) Creep, Viscoelasticity and Creep Fracture in Solids.

Applied Science Pub. Co., London.

Gordon, W.J. and Hall, C.A. (1973) 'Construction of curvilinear coordinates systems and application to mesh generation.' Int. J. Num. Meth. Engng. 7, pp.461-477.

Gray, W.H. and Akin, J.E. (1979) 'An improved method for contouring on isoparametric surfaces.' Int. J. Num. Meth. Engng. 14 pp.451-472.

Greenbaum, G.A. and Rubenstein (1968) 'Creep analysis of axisymmetric bodies using finite elements.' Nuclear Engng. Design Vol. 7.

Griffiths, W.T. (1948) Proc. Roy. Aero. Soc. 52(I).

Gross, B. (1953) Mathematical Structure of the Theories of Viscoelasticity. Hermann et Cie, Paris.

Haisler, W.E. and Sanders, D.R. (1979) 'Elastic-plastic-creep-large strain analysis at elevated temperatures by the finite element method.' Computer and Structures, Vol. 10.

Hannah, I.W. (1961) 'Thermal stress in concrete.' Nucl. Engng. Design, pp. 69-74.

Hannant, D.J. (1967) 'The strain behaviour of concrete under compressive stress under elevated temperatures.' CERL Report RD/L/N 67/66.

Hannant, D.J. (1968) 'Strain behaviour of concrete up to 95^{o}C under compressive stress.' Proc. ICE Conf. Prestressed Concrete Pressure Vessels pp. 171-191, London.

Hansen, T.C. (1960) 'Creep and stress relaxation of concrete: a theoretical and experimental investigation.' Proc. Swedish Cement and Concrete Institute, Stockholm, pp. 98-102.

Hansen, T.C. and Erikson, L. (1966) 'Temeprature change effect on behaviour of cement paste, mortar and concrete under load.' J. ACI, Vol. 38, No. 63, pp. 489-502.

Henderson, J. (1974) 'Complex-stress relaxation of metals at elevated

temperatures.' 2nd Int. Conf. on Structural Mechanics in Reactor Technology. Berlin 1973 and Metals Technology 1974, Vol. 1, No. 7, pp. 338-342.

Henderson, J. (1979) 'An investigation of multi-axial creep characteristics of metals.' J. of Engng. Materials and Technology, Vol. 101, Oct.

Hilton, H.H. and Clements, J.R. (1964) Proc. Conf. on Thermal Loading and Creep. 6-17, Institution of Mechanaical Engineers, London.

Hilton, E. and Campbell, J.S. (1974) 'Local and gobal smoothing of discontinuous finite elem,ent functions using a least squares method.' Int. J. Num. Meth. Engng. 8, pp.461-480.

Hinton, E. and Owen, D.R.J. (1977) Finite Element Programming. Academic Press, London.

Hoff, N.J. (1954) 'Approximate analysis of structures in the presence of moderately large creep deformation.' Quarterly J. Appl. Math., Vol. 12, pp. 49-55.

Ho-Le, K. (1988) 'Finite element mesh generation methods: a review and classification.' CAD, Vol. 20, number 1, pp. 27-38.

Hult, J.A.H. (1966) Creep in Engineering Structures. Blaisdell Pub. Co., Waltham, Mass. U.S.A.

Illston, J.M. (1965) 'The component of strain in concrete under sustained compressive stress.' Magazine of concrete research, Vol. 17, No. 50, pp. 21-28.

Illston, J.M. and Sanders, P.D. (1973) 'The effect of temperature change upon the creep of mortar, under torsional loading.' MCR, Vol. 25, No.48, pp.136-144.

Irons, B.M. (1970) 'A frontal solution program for finite element analysis.' Int. J. Meth. Engng, 2, pp.5-32.

Ivanova, G.M. (1958) 'Creep of alloy EI-437B at variable temperature.' Izv. AN SSSR, OTN, No. 4.

Jennings, A. (1966) 'A compact storage scheme for the solution of symmetric simultaneous equations.' Comp. J., 9, pp.281-5.

Johnson, A.E., Henderson, J. and Khan, B. (1961) 'The behaviour of metallic thick-walled cylindrical vessels or tubes subjected to high internal or external pressures at elevated temperatures.' Proc. Instn. Mech. Engrs., Vol. 175, No. 25, pp. 1043-1069.

Johnson, A.E., Henderson, J. and Khan, B. (1962) 'Creep of solid metallic bar or thick-walled tube or circular section, at elevated temperatures, when subjected to various combinations of uniform bending moment, torque and axial load.' Int. J. Mech. Sci., Vol. 4, pp. 195-203.

Johnson, A.E., Henderson, J. and Khan, B. (1964) 'Stress and strain rate distribution in thick-walled spherical pressure vessels of various metallic materials under internal and external pressures at elevated temperatures.' Enginner, London, Vol. 217, No. 5648, pp. 729-739.

Johnson, A. (1973) 'An alternative definition of reference stress for creep.' Int. Conf. on Creep and Fatigue in Elevated Temperature Applications, Inst. Mech. Engrs. Conf. Pub. No. 13, Paper C205/73, Philadelphia, U.S.A.

Jordaan, I.J. and Illston, J.M. (1969) 'The creep of sealed concrete under multiaxial compressive stresses.' MCR, Vol. 21, No. 66, Mar., pp. 195-204.

Jordaan, I.J. (1969) The Time-dependent Strains of Concrete under Multiaxial Systems of Stress. Ph.D. Thesis, London University.

Jordaan, I.J., England, G.L. and Khalifa, M.M.A. (1977) 'Creep of concrete: a consistent engineering approach.' J.ASCE Structural Division, ST3, pp. 475-491.

Kovalenko, A.D. (1969) ThermoelasticityBasic Theory and Applications.

Wolters-Noordhoft Pub. Co., Netherlands.

Kraus, H. (1981) Creep and Creep Buckling. McGraw Hill, London.

Krishnamarthy, N. (1971) 'Temperature effects on a continuous reinforced concrete bridge.' Montgomery, Alabama State Highway Dept., July, HRR58 78P.

Lee, E.H. and Hulbert, L.E. (1973) 'Continuum description: deformation and fracture of high temperature polymers.' Ed. H.H. Kausch, J.A. Hassell and R.I. Jaffee, New York, Plenum Publ. Corp., pp. 443-464.

Leonhardt, F., Kelbe, G. and Peter, T. (1965) 'Temperature differences endanger prestressed concrete bridges.' Beton-und stahlbetonbau, Vol. 60, No. 7, July, pp. 231-244. Germany.

L'Hermite, R.G. (1969) 'What do we know about the plastic deformation and creep of concrete.' RILEM Bull, No. 1, March.

Lorman, W.R. (1940) 'Theory of concrete creep.' ASTM Proc. Vol. 40, pp.1082-1102.

Mendelson, A. and Manson, S.S. (1959) 'A general approach to the practical solution of creep problems.' J. of Basic Engng., Dec.

Mendelson, A. (1968) Plasticity: Theory and Application. Macmillan Co., N.Y.

McVetty, P.G. (1943) Trans. Amer. Soc. Mech. Engrs. 65 (761).

Nasser, W.N. and Neville, A.M. 'Creep of old concrete beam under thermal gradients.' MCR, Vol. 64, No. 64-9, pp.97-103.

Naruoka, M., Hirai, I. and Yamaguti, T. (1957) 'The measurement of the temperature of the interior of the reinforced concrete slab of the Shigita Bridge and the pressumption of the thermal stress.' Proc. of the Symp. on Stress Measurements for Bridges and Structures. Tokyo, Japanese Society for the Promotion of Science, pp.106-116.

Nickell, R.E. (1974) 'Thermal stress and creep.' Structural Mechanics

Computer Programs, editors W. Pilkey, K. Saczalski and H. Schaeffer, University Press of Virginia, pp. 103-122.

Nishihara, T., Taira, S., Tanaka, K. and Ohnami, M. (1958) 'Creep of low carbon steel under varying temperatures.' Proc. 1st Japan Congr. Testing Mater. Kyoto.

Odqvist, F.K.G. (1974) Mathematical Theory of Creep and Creep Rupture. McGraw Hill, Oxford.

Padlog, J., Huff, R.D. and Holloway, G.F. (1960) 'Unelastic behaviour of structures subjected to cyclic, thermal and mechanical stressing conditions.' WADD Technical Report 60-271.

Penny, R.K. and Marriott, D.L. (1971) Design for Creep. McGraw Hill, London.

Priestley, M.J.N. (1972) 'Model study of a prestressed concrete box-girder bridge under thermal thermal loading.' Proc. 9th Congr. of the Int. Asso. for Bridge and Structural Engineering, Zurich, pp.737-746.

Ralston, A. (1965) First Course in Numerical Analysis. McGraw Hill, New York.

Richmond, B. and England, G.L. (1977) 'The design of concrete structures for the containment of hot oil.' Int. Conf. in Offshore Structures Engineering, Rio de Janeiro, Sept.

Roll, F. (1964) 'Long-time recovery of highly stresses concrete cylinders.' ACI Special Publications SP-9.

Ross, R.D. (1958) 'Creep of concrete under variable stress.' J.Am. Conc. Inst. Proc. 54(9), 739.

Ross, A.D., Illston, A.M. and England, G.L. (1965) 'Short and long term deformations of concrete as influenced by its physical structure and state.' Paper HI, Int. Conf. in Structure of Concrete,London.

Sanders, P.D. (1973) The Effect of Temperature Change on the Creep of Mortar under Torsional Loading. Ph.D. Thesis, University of London,

1973.

Schapery, R.A. (1969) 'On the characteristic of non-linear viscoelastic materials.' J. Polymer. Engng. and Science 9, pp. 295-310.

Smith, A.I. and Nicolson, A.M. (1971) Advances in Creep Design. Applied Science Pub., London.

Smith, I.G. (1981) 'Application of ADINA and ADINAT in creep analysis of heated concrete structures.' Computer and Structures, Vol. 13, pp. 717-725.

Snedden, J.D. (1972) 'Primary creep of anisotropic RR58 aluminum alloy at 180^{o}C.' NEL Report No. 531, National Eng. Lab., East Kilbride, Glasgow.

Sully, A.H. (1949) Metallic Creep and Creep Resistant Alloys. Butterworths Scientific Publ. London.

Taira, S. and Ohnami, M. (1960) 'Creep under rapid cycling temperatures.' Proc. 3rd Japan Congr. testing mater. Kyoto.

Thacker, W.C. (1980) 'A brief review of techniques for generating irregular computational grids.' Int. J. Num. Meth. Engng., Vol. 15, pp. 1335-1341.

Theuer, A.U. 'Effect of temperature on the stress deformation of concrete.' J. Research, National Bureau of Standards, No. 18, U.S.A., pp. 195-204.

Volterra, V. (1930) Theory of Fundamentals, Chapter 6, Blackie, London.

Vyas, N.C., Kalani, M. and Limaye, R.G. (1979) 'Creep of concrete at different temperatures.' The Indian Concrete J., Vol. 53, pp.190-195, July.

Wittman, F.H. (1982) Fundamental Research on Creep and Shrinkage of Concrete. Martinus Hijhoff Pub., Hague, Netherlands.

Yamada, Y. and Nagato, K. (1979) First Report of Japanese Coorporation in International Benchmark Project of Subcommittee on Elevated Temperature Design of the U.S. Pressure Vessel Committee, March.

Zienkiewicz, O.C., Watson, M. and King, I.P. (1968) 'A numerical method of visco-elastic satress analysis.' Int. J. Mech. Sc.

Zienkiewicz, O.C. and Phillips, D.V. (1971) 'An automatic mesh generation scheme for plane and curved surfaces by iso-parametric coordinates.' Int. J. Num. Meth. Engng., Vol. 3, pp.519-529.

Zienkiewicz, O.C. (1982) The Finite Element Method. McGraw Hill, London.

BIBLIOGRAPHY

(1) Finite element preprocessing and post processing

Akin, J.E. and Gray, W.H. (1977) 'Contouring on isoparametric surfaces.' Int. J. Num. Meth. Engng. Vol. 11, pp. 1893-1897.

Cohen, H.D. (1980) 'A method for the automatic generation of triangular elements on a surface.' Int. J. Num. Meth. Engng. Vol. 11, pp. 470-476.

Cook, R.D. (1977) 'Discussion of a paper by B.M.R. Irons and T.K. Hellen.' Int. J. Num. Meth. Engng. Vol. 13, pp. 1631-1632.

Corradi, L. (1986) 'On stress computation in displacement finite element models.' Computer methods in Appl. Mech. & Engng. 54, pp.325-339, North-Holland.

Barlow, J. (1976) 'Optimal stress locations in finite element models.' Int. J. Num. Meth. Engng. Vol. 10, pp. 243-251.

Fong, H.H. (1982) 'An evaluation of eight U.S. general purpose finite element computer programs.' The 23rd AIAA/ASME/ASCE/AHS Structures, Structural Dynamics and Materials Conference, May 10-12, pp. 1-16.

Fredriksson, B., Mackerle, J. and Allan-Persson, B.G. (1981) 'Finite element programs in integrated software for structural mechanics and CAD.' CAD, Vol. 13, number 1, pp. 27-39.

Gordon, W.J. (1971) 'Blending function methods of bivariate and multivariate interpolation and approximation.' J. Num. Anal., Vol. 8, pp. 158-177.

Gordon, W.J. and Hall, C.A. (1973) 'Transfinite element methods blending function interpolation over arbitrary curved element domains.' J. Num. Math., Vol. 21, pp. 109-129.

Gordon, W.J. and Hall, C.A. (1973) 'Construction of curvilinear co-

ordinate systems and applications to mesh generation.' Int. J. Num. Meth. Engng. Vol. 7, pp. 461-477.

Hinton, E. and Campbell, J.S. (1974) 'Local and global smoothing of discontinuous finite element functions using a least squares method.' Int. J. Num. Meth. Engng. Vol. 8, pp. 461-480.

Hinton, E., Scott and Ricketts, R.E. (1975) 'Local least squares stress smoothing for parabolic isoparametric elements.' Int. J. Num. Meth. Engng. Vol. 9, pp. 235-256.

Imafuku, I., Kodera, Y. and Sayawaki, M. (1980) 'A generalised automatic mesh scheme for finite element method.' Int. J. Num. Meth. Engng. Vol. 15, pp. 713-731.

Kleinstreuer, C. and Holdeman, J.T. (1980) 'A triangular finite element mesh generator for fluid dynamic systems of arbitrary geometry.' Int. J. Num. Meth. Engng. Vol. 15, pp. 1325-1334.

Kontopidis, G.D. and Limbert, D.E. 'A predictor-corrector contouring algorithm for isoparametric 3D elements.' Int. J. Num. Meth. Engng. Vol. 19, pp. 995-1004.

Leone, J.M., Gresho, P.M., Chan, S.T. and Lee, R.L. (1979) 'A note on the accuracy of Gauss-Legendre quadrature in the finite element method.' Int. J. Num. Meth. Engng. Vol. 14, pp. 769-784.

Lo, S.H. (1987) 'A hidden-line algorithm using picture subdivision technique.' Computers & Structures, Vol.28, No.1, pp. 37-45.

Meek, J.L. and Beer, G. (1975) 'Contour plotting of data using isoparametric element representation.' Int. J. Num. Meth. Engng. Vol. 10, pp. 954-957.

Pitter, J. and Hartl, H. (1980) 'Improved stress evaluation under thermal load for simple finite elements.' Int. J. Num. Meth. Engng. Vol. 15, pp. 1507-1515.

Nielson, G.M. (1980) 'A first order blending method for triangles based upon cubic interpolation.' Int. J. Num. Meth. Engng. Vol. 15,

pp. 308-318.

Stelzer, J.F. and Welzel, R. (1987) 'Plotting of contours in a natural way.' Int. J. Num. Meth. Engng. Vol. 24, pp. 1757-1769.

(2) Linear equations solution algorithms

Attard, M., Lawther, R. and Kabaila (1980) 'Assemly condesation algorithm.' UNICIV Report no. R-197, University of New South Wales, Australia.

Cantin, G. (1971) 'An equation solver of very large capacity.' Int. J. Num. Meth. Engng., Vol. 3, pp.379-388.

Cedolin, L. and Gallagher, R. (1978) 'A frontal-base solver for frequency analysis.' Int. J. Num. Meth. Engng., Vol. 12, pp.1659-1666.

Collins, R.J. (1978) 'Dynamic destinations: a method for removing redundant operations in the front algorithm.' Int. J. Num. Meth. Engng., Vol. 12, pp.1042-1043.

Elwi, A.E. and Murray, D.W. (1985) 'Skyline algorithms for multilevel substructural analysis.' Int. J. Num. Meth. Engng., Vol. 21, pp.465-479.

Furuike, T. (1972) 'Computerized multiple level substructuring analysis.' Computers & Structures, Vol. 2, pp. 1063-1073.

Kascic, M.J. (1979) 'Vector processing on the cyber 200.' Control Data Corporation, St. Paul, MN.

Mondkar, D.P. and Powell, G.H. (1974) 'Large capacity equation solver for structural analysis.' Computers & Structures, Vol. 4, pp.699-728.

Recuero, A. and Gutierrez, J.P. (1979) 'A direct linear system solver with small core requirements.' Int. J. Num. Meth. Engng., Vol. 14, pp.633-645.

Stabrowski, M.M. (1981) 'An algorithm for the solution of very large

banded unsymmetric linear equation systems.' Int. J. Num. Meth. Engng., Vol. 24, pp. 289-300.

Stabrowski, M.M. (1987) 'A block equation solver for large unsymmetric linear equation systems with dense coefficient matrices.' Int. J. Num. Meth. Engng., Vol. 24, pp. 289-300.

Thomson, E. and Shimazki, Y. (1980) 'A frontal procedure using skyline storage.' Int. J. Num. Meth. Engng., Vol. 15, pp. 889-910.

Wilson, E.L., Bathe, K. and Doherty, W.P. (1974) 'Direct solution of large systems of linear equations.' Computers & Structures, Vol. 4, pp. 363-372.

Yeo, M. F. (1973) 'A more efficient front solution: allocating assembly locations by longevity considerations.' Int. J. Num. Meth. Engng., Vol. 9, pp. 570-573.

(3) Matrix bandwidth and frontwidth minimization algorithm

Akhras, G. and Dhatt, G. (1976) 'An automatic node relabelling scheme for minimizing a matrix or network bandwidth.' Int. J. Num. Meth. Engng., Vol. 10, pp. 787-797.

Akin, J.E. and Pardue, R.M. (1975) 'Element resequencing for frontal solutions.' The mathematics of finite elements and applications II, editor J.R. Whiteman, Academic Press, N.Y., pp.535-541.

Alway, G.G. and Martin, D.W. (965) 'An algorithm for reducing the bandwidth of a matrix of symmetrical configuration.' Computer J., Vol. 8, pp. 264-272.

Bykat, A. (1977) 'A note on an element ordering scheme.' Int. J. Num. Meth. Engng., Vol. 11, pp. 194-198.

Collins, R.J. (1973) 'Bandwidth reduction by automatic renumbering.' Int. J. Num. Meth. Engng., Vol. 6, pp. 345-356.

Cuthill, E. and McKee, J. (1969) 'Reducing the bandwidth of sparse

symmteric matrices.' Proc. National Conference of the Association for Computing Machinery, San Francisco, U.S.A.

Everstine, G.C. (1979) 'A comparison of three resequencing algorithms for the reduction of matrix profile and wavefront.' Int. J. Num. Meth. Engng., Vol. 14, pp. 837-853.

Webb, J.P. and Froncioni, A. (1986) 'A time memory trade-off frontwidth reduction algorithm for finite element analysis.' Int. J. Num. Meth. Engng., Vol. 23, pp. 1905-1914.

Grooms, H.R. (1972) 'Algorithm for matrix bandwidth reduction.' Proc. ASCE, ST1, pp. 8636-8638.

Pina, H.L.G. (1981) 'An algorithm for frontwidth reduction.' Int. J. Num. Meth. Engng., Vol. 17, pp. 1539-1546.

Razzaqus, A. (1980) 'Automatic reduction of frontwidth for finite element analysis.' Int. J. Num. Meth. Engng., Vol. 15, pp. 1315-1324.

Sloan, S.W. (1983) 'Automatic element reordering for finite element analysis with frontal solution schemes.' Int. J. Num. Meth. Engng., Vol. 19, pp. 1153-1181.

Sloan, S.W. (1986) 'An algorithm for profile and wavefront reduction of sparse matrices.' Int. J. Num. Meth. Engng., Vol. 23, pp. 239-251.

(4) Finite element element creep analysis: General

Argyris, J.H., Buck K.E., Scharpf, D.W. and Willian, K.J. (1972) 'Non-linear methods of structural analysis.' Nuclear Engng. Design 19, pp.169-197.

Argyris, J.H. and William, K.J. (1974) 'Some considerations for the evaluation of finite element models.' Nuclear Engng. Design 27, pp.79-96.

Clough, R.W. (1969) 'Comparison of three dimensional finite elements.' Proc. of the Symp. on Applications of Finite Element Methods for

Civil Engineering, U.S.A., Editor Brown W.H. and Hackett R.M.

Melosh, R.J. (1974) 'A status report on computational techniques for finite element analysis.' Nuclear Engng. Design 27, pp.274-285.

Batoz, J. (1979) 'Incremental displacement algorithms for nonlinear problems.' Int. J. Num. Meth. Engng., Vol. 14, pp. 1262-1267.

Keramidas, G.A. and Ting, E.C. (1976) 'A finite element formulation for thermal stress analysis. Part I: Variational formulation.' Nucl. Engng. Design 39, pp. 267-275.

Keramidas, G.A. and Ting, E.C. (1976) 'A finite element formulation for thermal stress analysis. Part I: Finite element formulation.' Nucl. Engng. Design 39, pp. 277-287.

Robinson, J. (1985) 'The mode and amplitude technique and hierarchical stress elements-a simplified and natural approach.' Int. J. Num. Meth. Engng., Vol. 21, pp. 487-507.

Sutherland, W.H. (1970) 'AXICRP - Finite element computer code for creep analysis of plane stress, plane strain and axisymmetric bodies.' Nucl. Engng. Design 11, pp. 269-285.

(5) Finite element analysis: Pressure vessels

Argyris, J.H., Faust, G. Szimmat, J., Warnke, E.P. and William, K.J. 'Recent developments in the finite element analysis of prestreesed concrete reactor vessels.' Nucl. Engng. Design 28, pp. 42-75.

Barrett, N.T. and Murray, J.T. (1967) 'Creep in pressure vessels at elevated temperatures.' Proc. ICE Conf. Prestressed Concrete Pressure Vessels, London, pp. 153-166.

Bathe, K.J. and Ramswamy, S. (1979) 'On three dimensional nonlinear analysis of concrete structures.' Nucl. Engng. Design 52, pp. 385-409.

Cederberg, H. and David, M. (1969) 'Computation of creep effects in

prestressed concrete vessels using dynamic relaxation.' Nucl. Engng. Design 9, pp. 439-448.

Lewis, D.J., Bye, G.P. and Crisp, R.J. (1967) 'Long term thermal creep effects in pressure vessels.' Proc. ICE Conf. Prestressed Concrete Pressure Vessels, London, pp. 329-337.

Rashid, Y.R. and Rockenhauser, W. (1967) 'Pressure vessels by finite element techniques.' Proc. ICE Conf. Prestressed Concrete Pressure Vessels, London, pp. 375-383.

Saugy, B., Zimmermann, Th. and Hussain, M. (1974) 'Three dimensional rupture analysis of a prestressed concrete pressure vessel including creep effects.' Nucl. Engng. Design 28, pp. 97-120.

Wade, M.J., Henrywood, R.K. and Jategaonkar, R. (1977) 'Experience in the application of a finite element system to the analysis of complex prestressed concrete pressure vessels.' Nucl. Engng. Design 40, pp. 347-368.

(6) Creep of structures: General principles

Herivel, J.W. (1954) 'A general variational principle for dissipative systems: I & II.' Proc. R.I.A, Vol. 56, Sect. A, pp. 37-75.

Hill, R. (1956) 'New horizons in mechanics of solids.' J. Mech. & Phy. of Solids, Vol. 5, pp. 66-74.

Marc, M. (1982) 'Checking the principle of superposition by testing.' Fundamental Research on Creep and Shrinkage of Concrete, Edited by Wittmann, F.H., Martinus Nijhoff Publishers, London.

Sanders, J.L., McComb, H.J. and Schlechte, F.R. (1957) 'A variational theorm for creep with applications to plates and columns.' Technical report 4003, NACA, Langley Aero. Lab.

Wang, A.J. and Prager, W. (1954) 'Thermal and creep effects in work-hardening elastic-plastic solids.' J. Aero. Sciences, Vol. 21, pp. 343-344.

(7) Creep of structures: Constitutive relationships

Bazant, Z.P. and Najjar, L.J. (1973) 'Comparison of approximate linear methods for concrete creep.' J. Structural Divison ST9, ASCE.

Lubliner, J. (1966) 'Rheological models for time-variable materials.' Nucl. Engng. Design 4, pp. 287-291.

Reiner, M. (1968) 'Dynamical strength of an ideal solid with definite constitutive equation.' Mechanical Behaviour of Materials under Dynamic Loads, Edited by Lindholm, U.S, Springer-Verlag, N.Y.

Zienkiewicz, O.C. (1961) 'Analysis of visco-elastic behaviour of concrete structures with particular reference to thermal stress.' J. ACI, Vol. 58, pp. 383-394.

(8) Creep of concrete: Design implications

Fraas, A.P. 'Foreseeable thermal, mechanical, and materials engineering problems of fusion reactor power plants.' Nucl. Engng. Design 29, pp. 295-310.

Griffin, D.S. (1978) 'Inelastic structural analysis: Design implications and experience.' Nucl. Engng. Design 51, pp. 11-21.

Tomkins, B. (1978) 'Elevated temperature codes - New directions on life prediction.' Nucl. Engng. Design 51, pp. 3-10.

Townley, C.H.A. (1972) 'Design methods for structures operating at high temperature.' Nucl. Engng. Design 19, pp. 99-117.

Wright, W.B. (1972) 'linear and nonlinear thermal gradients - An interpretation of the nuclear componenets code - Section III.' Nucl. Engng. Design 23, pp. 179-181.

(9) Creep of structures: Experimental results

Altmann, K. (1982) 'shrinkage of concrete in extreme climate.' Foundamental Research on Creep and Shrinkage of Concrete, Edited by Wittmann, F.H., London.

Ho, D. and Liu, C.H. (1989) 'Extreme loadings in highway bridges.' J. of Structural Engineering, ASCE, Volume 115, No. 7, pp.1681-1696.

Johansen, R. and Best, C.H. (1962) 'Creep of concrete with and without ice in the system.' RILEM Bulletin No. 16.

Kruml, F. (1982) 'A contribution to the problem of reversible and irreversible creep of compact structural concretes.' Foundamental Research on Creep and Shrinkage of Concrete, Edited by Wittmann, F.H., London.

Moncrieff, M.L.A. and Waggott, J.G. (1967) 'Time, temperature, creep and shrinkage in concrete in concrete.' Proc. ICE Conf. Prestressed Concrete Pressure Vessels, London, pp. 123-130.

Nasser, K.W. & Neville, A.M. (1965) 'Creep at elevated temperatures.' J. American Concrete Institute (ACI), pp. 1567-1579.

Nasser, K.W. & Mazouk, H.M. (1981) 'Creep of concrete at temperatures from 70 to 450 F under atmospheric pressure.' J. ACI,title no. 78-13, pp. 147-150.

Walther, R. and Pareth, T. (1982) 'Rheologoical properties at high temperature of a concrete with a crushed limestone aggregate and blast furance cement.' Foundamental Research on Creep and Shrinkage of Concrete, Edited by Wittmann, F.H., London.

Washa, G.W. & Wendt, K.F. (1975) 'Fifty year properties of concrete.' J. ACI, title no. 71-4, pp. 20-28.

(10) Creep of concrete structures: Bridge and roof structures

M.J.S. Hirst (1984) 'Thermal loading of concrete roofs.' J. Structural

Division, Vol. 110, No. 8, ASCE.

Gamble, W.L. (1982) 'Creep of concrete in variable enviroments.' J. Structural Division, Vol. 108, ST10, ASCE.

White, I.G. (1979) 'Non-linear differential temperature distributions in concrete bridge structures: a review of the current literature.' Cement & Concrete Association, Technical Report No. 525.

Priestley, M.J.N (1978) 'Design of concrete bridges for temperature gradients.' J. ACI, title no. 75-23, pp. 209-217.

Javor, T. (1982) 'Creep observation of prestressed concrete bridges.' Foundamental Research on Creep and Shrinkage of Concrete, Edited by Wittmann, F.H., London.

PAGE/PAGES EXCLUDED UNDER INSTRUCTION FROM UNIVERSITY